

PART I. SYNTHESSES AND NMR ANALYSES OF SELECTED
 ω -(2-ANTHRYL)SUBSTITUTED FATTY ESTERS
PART II. SYNTHESSES AND CHARACTERIZATIONS OF
SELECTED HETEROAROTINOIDS

By

KRISTY MARIE WAUGH

Bachelor of Science

Cameron University

Lawton, Oklahoma

1978

Submitted to the Faculty of the Graduate College
of the Oklahoma State University
in partial fulfillment of the requirements
for the Degree of
DOCTOR OF PHILOSOPHY
July, 1983

Thesis
1983D
W354s
cop. 2



PART I. SYNTHESSES AND NMR ANALYSES OF SELECTED
 ω -(2-ANTHRYL)SUBSTITUTED FATTY ESTERS
PART II. SYNTHESSES AND CHARACTERIZATIONS OF
SELECTED HETEROAROTINOLDS

Thesis Approved:

K D Berlin

Thesis Adviser

Eldon C Nelson

Will Purditt

J G Rockley

Norman D. Durbin

Dean of the Graduate College

1172861

ACKNOWLEDGMENTS

I would like to express my gratitude to those who have made my graduate work at Oklahoma State University much easier and more enjoyable. I am grateful to the members of the support staff at O.S.U. for their help and understanding. In particular, I am especially grateful to Stan Sigle for teaching me to operate the Varian XL-100 NMR and for the many enjoyable conversations we have had during the last four years.

I gratefully acknowledge the financial support provided by the Skinner Fellowship, the Johnston Foundation, and the Phillips Petroleum Company Summer Fellowship.

I sincerely appreciate the encouragement provided by my brothers and their families throughout the course of my graduate work. I am especially thankful to Bruce Bailey, whose love, understanding, and moral support have made the good times so much better and the bad times a lot more bearable.

Finally, I am especially grateful to my parents, Mr. and Mrs. Bud Waugh, for their constant love, understanding, and encouragement. With great pride and pleasure, I wish to dedicate this work to them.

TABLE OF CONTENTS

Chapter	Page
INTRODUCTION	1
PART I. SYNTHESSES AND NMR ANALYSES OF SELECTED ω -(2-ANTHRYL)SUBSTITUTED FATTY ESTERS	
I. HISTORICAL	3
Introduction	3
Biological Membranes	3
Fluorescent Probes of Biological Membranes	6
Carbon-13 Spin Lattice Relaxation Times	16
II. RESULTS AND DISCUSSION	28
Suggestions for Future Work	51
III. EXPERIMENTAL SECTION	53
General Information	53
Starting Materials	53
2-(Hydroxymethyl)anthracene (37)	54
3-(Bromomethyl)anthracene (38)	54
(2-Anthrylmethyl)triphenylphosphonium Bromide (33)	54
Methyl 11-Bromoundecanoate (40)	55
Methyl 11-Oxoundecanoate (34a)	55
Methyl 12-(2-Anthryl)-11-dodecenoate (35a)	56
Methyl 12-(2-Anthryl)dodecanoate (25d)	56
Methyl 13-Hydroxytridecanoate (42)	57
Methyl 13-Oxotridecanoate (34b)	58
Methyl 14-(2-Anthryl)-13-tetradecenoate (35b)	59
Methyl 14-(2-Anthryl)tetradecanoate (25e)	59
Methyl 16-Hydroxyhexadecanoate (44)	60
Methyl 16-Oxohexadecanoate (34c)	60
Methyl 17-(2-Anthryl)-16-heptadecenoate (35c)	61
Methyl 17-(2-Anthryl)heptadecanoate (25f)	62
BIBLIOGRAPHY	87

PART II. SYNTHESSES AND CHARACTERIZATIONS
OF SELECTED HETEROAROTINOIDS

I. HISTORICAL	92
Retinoids in the Treatment of Skin Disorders	95
Retinoids in the Prevention and Treatment of Cancer	97
II. RESULTS AND DISCUSSION	107
Synthesis of Heteroarotinooids	108
NMR Analysis of the Heteroarotinooids	117
X-Ray Diffraction Analysis of <u>30c</u>	125
X-Ray Diffraction Analysis of Heteroarotinooid <u>22a</u>	127
Pharmacological Activity of the Heteroarotinooids	127
Suggestions for Future Work	131
III. EXPERIMENTAL SECTION	134
General Information	134
Starting Materials	134
Ethyl 3-(Phenylthio)propionate (<u>26a</u>)	135
2-Methyl-4-(phenylthio)-2-butanol (<u>27a</u>)	135
3-Methyl-1-(phenylthio)-2-butene (<u>28</u>)	136
4,4-Dimethylthiochroman or 3,4-Dihydro-4,4- dimethyl-2H-1-benzothiopyran (<u>29a</u>)	137
Method I	137
Method II	137
4,4-Dimethylthiochroman-6-yl Methyl Ketone or 1-(3,4-Dihydro-4,4-dimethyl-2H-1-benzothio- pyran-6-yl)ethanone (<u>30a</u>)	138
4,4-Dimethylthiochroman-6-yl Methyl Ketone 1,1-Dioxide (<u>30c</u>)	139
α ,4,4-Trimethylthiochroman-6-methanol or 3,4- Dihydro- α ,4,4-trimethyl-2H-1-benzothio- pyran-6-methanol (<u>31a</u>)	139
[1-(4,4-Dimethylthiochroman-6-yl)ethyl]tri- phenylphosphonium Bromide or [1-(3,4-di- hydro-4,4-dimethyl-2H-1-benzothiopyran- 6-yl)ethyl]triphenylphosphonium Bromide (<u>32a</u>)	140
Ethyl (E)-p-[2-(4,4-Dimethylthiochroman- 6-yl)-propenyl]benzoate or Ethyl (E)-4- [2,3-Dimethyl-2H-1-benzothiopyran-6-yl)-1- propenyl]benzoate (<u>22a</u>)	141
Ethyl (E)-p-[2-(4,4-Dimethylthiochroman-1- oxo-6-yl)propenyl]benzoate or Ethyl (E)-4- [2-(3,4-Dihydro-4,4-dimethyl-2H-1-benzothio- pyran-1-oxo-6-yl)-1-propenyl]benzoate (<u>22d</u>)	142

Methyl 3-Phenoxypropionate (26b)	142
2-Methyl-4-phenoxy-2-butanol (27b)	143
4,4-Dimethylchroman or 3,4-Dihydro-4,4-dimethyl-2H-1-benzopyran (29b)	144
4,4-Dimethylchroman-6-yl Methyl Ketone or 1-(3,4-Dihydro-4,4-dimethyl-2H-benzopyran-6-yl)ethanone (30b)	144
α -4,4-Trimethylchroman-6-methanol or 3,4-Dihydro- α ,4,4-trimethyl-2H-1-benzopyran-6-methanol (31b)	145
[1-(4,4-Dimethylchroman-6-yl)ethyl]triphenylphosphonium Bromide or [1-(3,4-Dihydro-4,4-dimethyl-2H-1-benzopyran-6-yl)ethyl]triphenylphosphonium Bromide (32b)	146
Ethyl (E)-p-[2-(4,4-Dimethylchroman-6-yl)propenyl]benzoate or Ethyl (E)-4-[2-(3,4-Dihydro-4,4-dimethyl-2H-1-benzopyran-6-yl)-1-propenyl]benzoate (22b)	147
(E)-p-[2-(4,4-Dimethylchroman-6-yl)propenyl]benzoic Acid or (E)-4-[2-(3,4-Dihydro-4,4-dimethyl-2H-1-benzopyran-6-yl)-1-propenyl]benzoic Acid (22c)	148
Ethyl 4-Formylbenzoate (33)	148
Attempted Preparation of 22a	149
Attempted Preparation of 22a	150
Attempted Preparation of 22a	150
BIBLIOGRAPHY	190

LIST OF TABLES

Table	Page
PART I. SYNTHESSES AND NMR ANALYSES OF SELECTED ω -(2-ANTHRYL)SUBSTITUTED FATTY ESTERS	
I. ^{13}C NMR Chemical Shifts (T_1 Values (SEC)) for the Carbons in the Side Chain of <u>25d-25f</u>	38
II. ^{13}C NMR Chemical Shifts for <u>25d</u> and Selected Model Compounds	39
III. Comparison of ^{13}C NMR Chemical Shifts Reported for <u>25b</u> and <u>25c</u> with Assignments Made for <u>25d</u> Using Model Compounds	40
IV. Corrected ^{13}C NMR Assignments and T_1 Values for <u>25a-25c</u>	45
V. ^{13}C NMR Assignments (T_1 Values) of Aromatic Carbons of <u>25d-25f</u>	48
VI. ^1H NMR Assignments for the Aromatic Protons of <u>25d</u>	50
PART II. SYNTHESSES AND CHARACTERIZATIONS OF SELECTED HETEROAROTINOIDS	
I. Structure and Activity of Ring-Modified Retinoids	102
II. Structure and Activity of Retinoids with Multiple Modifications	104
III. Structure and Activity of Retinoids with Multiple Modifications	105
IV. ^{13}C NMR Data for the Heteroarotinooids	119
V. Bond Angles and Distances of <u>30c</u>	128
VI. Activity of the Heteroarotinooids in the Hamster Tracheal Organ Culture	130

LIST OF FIGURES

Figure	Page
PART I. SYNTHESSES AND NMR ANALYSES OF SELECTED ω -(2-ANTHRYL)SUBSTITUTED FATTY ESTERS	
1. General Structure of a Phospholipid	4
2. Fluid Mosaic Model	5
3. Electronic Transitions Leading to Fluorescence and Other Relaxation Processes	8
4. The Rotating Frame of Reference	18
5. Symmetry Axis in Monosubstituted Benzenes	25
6. Synthesis of <u>25d-25f</u>	30
7. Synthesis of Oxoesters <u>34a-34c</u>	32
8. Synthesis of <u>25a-25c</u>	33
9. HETCOR 2-D Spectrum of <u>25d</u> in the Aliphatic Region	42
10. HETCOR 2-D Spectrum in the Aromatic Region for <u>25d</u>	49
PART II. SYNTHESSES AND CHARACTERIZATIONS OF SELECTED HETEROAROTINOIDS	
1. Biological Importance and Interconversions of Natural Retinoids	93
2. Regions of the Vitamin A Molecule	100
3. Synthesis of Ketone <u>30a</u>	109
4. Synthesis of Ketone <u>30b</u>	110
5. Synthesis of Heteroarotinooids <u>22a</u> and <u>22b</u>	111
6. Preparation of Ethyl 4-Formylbenzoate (<u>33</u>)	115

Figure	Page
7. Contour Plot of HETCOR 2-D Spectrum of <u>22d</u> in the Aliphatic Region	120
8. Contour Plot of HETCOR 2-D Spectrum of <u>22a</u> in the Aromatic Region	122
9. HETCOR 2-D Spectrum of <u>22b</u> in the Aromatic Region	123
10. Contour Plot of HETCOR 2-D Spectrum of <u>22d</u> in the Aromatic Region	124
11. Structure of Ketone <u>30c</u>	127
12. Structure of Heteroarotinoid <u>22a</u>	129

LIST OF PLATES

Plate		Page
PART I. SYNTHESSES AND NMR ANALYSES OF SELECTED ω -(2-ANTHRYL)SUBSTITUTED FATTY ESTERS		
I.	^1H NMR Spectrum of <u>38</u>	63
II.	^1H NMR Spectrum of <u>33</u>	64
III.	^1H NMR Spectrum of <u>40</u>	65
IV.	^{13}C NMR Spectrum of <u>40</u>	66
V.	^1H NMR Spectrum of <u>34a</u>	67
VI.	^1H NMR Spectrum of <u>51</u>	68
VII.	^1H NMR Spectrum of <u>35a</u>	69
VIII.	^1H NMR Spectrum of <u>25d</u>	70
IX.	^{13}C NMR Spectrum of <u>25d</u>	71
X.	^1H NMR Spectrum of <u>42</u>	72
XI.	^{13}C NMR Spectrum of <u>42</u>	73
XII.	^1H NMR Spectrum of <u>34b</u>	74
XIII.	^{13}C NMR Spectrum of <u>34b</u>	75
XIV.	^1H NMR Spectrum of <u>35b</u>	76
XV.	^1H NMR Spectrum of <u>25e</u>	77
XVI.	^{13}C NMR Spectrum of <u>25e</u>	78
XVII.	^1H NMR Spectrum of <u>44</u>	79
XVIII.	^{13}C NMR Spectrum of <u>44</u>	80
XIX.	^1H NMR Spectrum of <u>34c</u>	81
XX.	^{13}C NMR Spectrum of <u>34c</u>	82

Plate		Page
XXI.	^1H NMR Spectrum of <u>35c</u>	83
XXII.	^1H NMR Spectrum of <u>25f</u>	84
XXIII.	^{13}C NMR Spectrum of <u>25f</u>	85
XXIV.	IR Spectrum of <u>25f</u>	86

PART II. SYNTHESSES AND CHARACTERIZATIONS OF
SELECTED HETEROAROTINOIDS

I.	^1H NMR Spectrum of <u>26a</u>	152
II.	^{13}C NMR Spectrum of <u>26a</u>	153
III.	^1H NMR Spectrum of <u>27a</u>	154
IV.	^{13}C NMR Spectrum of <u>27a</u>	155
V.	^1H NMR Spectrum of <u>28</u>	156
VI.	^{13}C NMR Spectrum of <u>28</u>	157
VII.	^1H NMR Spectrum of <u>29a</u>	158
VIII.	^{13}C NMR Spectrum of <u>29a</u>	159
IX.	^1H NMR Spectrum of <u>30a</u>	160
X.	^{13}C NMR Spectrum of <u>30a</u>	161
XI.	^1H NMR Spectrum of <u>30c</u>	162
XII.	^{13}C NMR Spectrum of <u>30c</u>	163
XIII.	^1H NMR Spectrum of <u>31a</u>	164
XIV.	^{13}C NMR Spectrum of <u>31a</u>	165
XV.	^1H NMR Spectrum of <u>32a</u>	166
XVI.	^1H NMR Spectrum of <u>22a</u>	167
XVII.	^{13}C NMR Spectrum of <u>22a</u>	168
XVIII.	^1H NMR Spectrum of <u>22b</u>	169
XIX.	^{13}C NMR Spectrum of <u>22b</u>	170
XX.	IR Spectrum of <u>22a</u>	171

Plate	Page
XXI. IR Spectrum of <u>22d</u>	171
XXII. ¹ H NMR Spectrum of <u>26b</u>	172
XXIII. ¹³ C NMR Spectrum of <u>26b</u>	173
XXIV. ¹ H NMR Spectrum of <u>27b</u>	174
XXV. ¹³ C NMR Spectrum of <u>27b</u>	175
XXVI. ¹ H NMR Spectrum of <u>29b</u>	176
XXVII. ¹³ C NMR Spectrum of <u>29b</u>	177
XXVIII. ¹ H NMR Spectrum of <u>30b</u>	178
XXIX. ¹³ C NMR Spectrum of <u>30b</u>	179
XXX. ¹ H NMR Spectrum of <u>31b</u>	180
XXXI. ¹³ C NMR Spectrum of <u>31b</u>	181
XXXII. ¹ H NMR Spectrum of <u>32b</u>	182
XXXIII. ¹ H NMR Spectrum of <u>22b</u>	183
XXXIV. ¹³ C NMR Spectrum of <u>22b</u>	184
XXXV. ¹ H NMR Spectrum of <u>22c</u>	185
XXXVI. ¹³ C NMR Spectrum of <u>22c</u>	186
XXXVII. IR Spectrum of <u>22b</u>	187
XXXVIII. IR Spectrum of <u>22c</u>	187
XXXIX. ¹ H NMR Spectrum of <u>33</u>	188
XXXX. ¹³ C NMR Spectrum of <u>33</u>	189

INTRODUCTION

Due to the difference in the major objective of the two investigations reported herein, this dissertation has been divided into two parts. Each is complete and independent of the other and contains its own Historical, Results and Discussion, Experimental Section, and Bibliography.

PART I

SYNTHESES AND NMR ANALYSES OF SELECTED
 ω -(2-ANTHRYL)SUBSTITUTED FATTY ESTERS

CHAPTER I

HISTORICAL

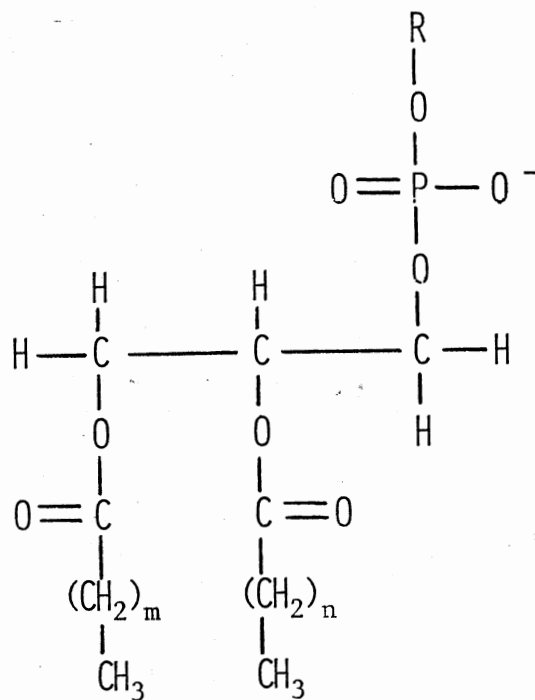
Introduction

Biological membranes serve a number of important functions in all living organisms. In general, membranes function in (1) the regulation of the identity and rate at which materials are transported into or out of a cell or cellular organelle, (2) the recognition of cellular regulators, (3) nerve impulse conduction, and (4) certain metabolic processes such as biosynthesis, electron transport, and photosynthesis.²⁴ Although biological membranes have been the subjects of many investigations in recent years, much remains to be learned about the relationship between membrane structure and function. For example, how does membrane structure affect the selective transport of materials across a cell or organelle membrane? What role does membrane structure play in the biosynthesis of macromolecules such as cell wall polymers, glycoproteins, and DNA? Why is the presence of water and inorganic cations essential to the maintenance of membrane structure? A complete understanding of the answers to these questions and many others will come only as a result of a more thorough knowledge of membrane structure.

Biological Membranes

Before examining the methods that can be used to study membrane structure, a discussion of the features of membrane structure that are

presently known is appropriate. The major components of all biological membranes are lipids (ca. 40% dry weight), proteins (ca. 60% dry weight), carbohydrates (ca. 1-10% total dry weight), and water (ca. 20% total weight).²⁴ Although a variety of different types of lipids can be found in membranes, the most common one is the phospholipid. The general structure for this lipid is shown (Figure 1). A phospholipid consists of a polar "head" and two nonpolar "tails". The aliphatic chains comprising the phospholipid "tails" are of varying lengths and degrees of saturation and unsaturation



$m, n = 10-22$ (14, 16 most common)

$\text{R} = \text{CH}_2\text{CH}_2\text{NH}_3, \text{CH}_2\text{CH}_2\text{N}(\text{CH}_3), \text{CH}_2\underset{\text{NH}_2}{\text{CHCO}_2\text{H}}$

Figure 1. General Structure of a Phospholipid.

A large number of structural models have been proposed to explain the manner in which the components of a membrane are associated with each other. Currently, the most widely accepted model of membrane structure is the Fluid Mosaic Model (Figure 2).⁵² In this model the phospholipids are arranged in a bilayer with the hydrophilic "heads" (represented by the circles) on the outer surfaces and the hydrophobic "tails" (represented by the zigzag lines) on the inside. The membrane proteins are associated with the bilayer in two different ways. Most of the globular proteins are embedded in the lipid matrix and extend either partially or completely through the lipid bilayer. The remainder of the proteins (not shown in Figure 2) is associated strictly with the polar "heads" on the bilayer surface. Although supported by most experimental data, this model still does not adequately explain many of the membrane structure-function relationships.

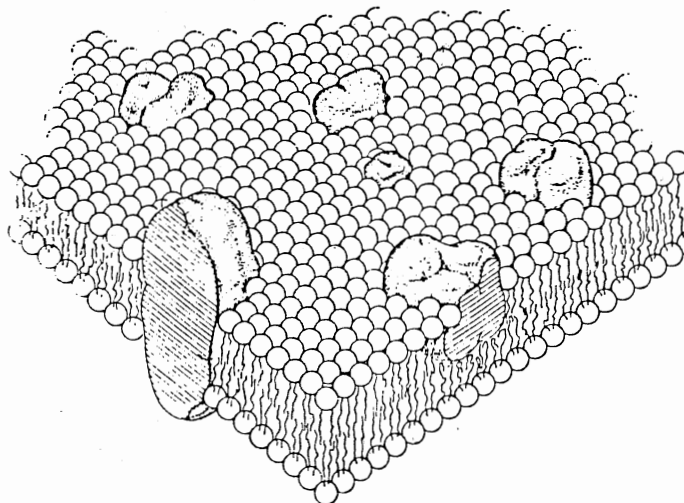
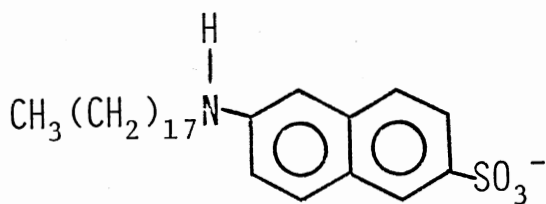


Figure 2. Fluid Mosaic Model.⁵²

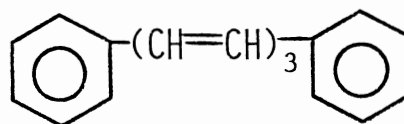
Fluorescent Probes of Biological Membranes

A variety of methods can be used to study membrane structure and its relationship to its various functions. Among the most common methods are freeze-fracture electron microscopy,^{9,60} X-ray diffraction,²⁷ electron spin resonance (ESR),³² nuclear magnetic resonance (NMR),^{26,45,48,35} and fluorescence spectroscopy.^{5,8} X-Ray diffraction studies of phospholipid vesicles have been used to verify the existence of a lipid bilayer structure²¹ while freeze-fracture techniques have been used to examine the internal anatomy of biological membranes.^{9,60} ESR has been used to study the mobility of a free-radical probe incorporated into an artificial or biological membrane and the polarity of its environment. NMR has been used to study not only the mobility of the lipids in the membrane but also the location of an incorporated probe and the amount of perturbation induced by its incorporation.^{26,45}

One of the most versatile and widely used techniques, however, involves the incorporation of a fluorescent probe such as 1 or 2 into an artificial or biological membrane followed by an appropriate fluorescence experiment. Since this technique is so important in the study of membrane structure and function, it will be discussed in some detail beginning first with a short discussion of the fluorescence phenomenon itself.



1



2

In most molecules, the overall electronic energy state can be classified as either a singlet (S) or a triplet (T) state.⁶² In the singlet state, the spins of all electrons in a molecule are paired, whereas in the triplet state the spins of one set of electrons are unpaired. At room temperature most molecules are in the ground state, S_0 . Absorption of ultraviolet or visible light with a frequency, ν , raises the molecules from the ground state to an excited singlet electronic state such as S_1 or S_2 (Figure 3).⁶² The identity of the excited state depends upon the energy ($E = h\nu$) of the incident radiation. Generally, the molecule quickly returns to the lowest excited state, S_1 , by transferring its excess energy to other molecules through collisions or by other nonradiative modes. The molecule can return to the ground state by a number of methods. First, the return to S_0 may occur as a result of a nonradiative transition known as internal conversion. Second, the molecule can return to the ground state through a radiative transition ($S_1 \rightarrow S_0$) known as fluorescence. The frequency and energy of the emitted light are lower than those of the incident or exciting radiation. Thus, fluorescence occurs at a longer wavelength than absorption. Third, the molecule can undergo intersystem crossing from the excited singlet state to the lowest triplet state ($S_1 \rightarrow T_1$). The molecule can return to the ground state from the triplet state by a radiative process known as phosphorescence or by collisional deactivation. The efficiency with which fluorescence competes with the other electronic relaxation mechanisms is described by the fluorescence quantum yield, ϕ_F . Thus,

$$\phi_F = \frac{\text{quanta emitted as fluorescence}}{\text{quanta absorbed from incident light}} = \frac{k_F}{k_F + k_{NR}} \quad (1)$$

where k_F is the rate constant for fluorescence and k_{NR} is the rate constant for nonradiative decay from S_1 .⁸ The rate constant, k_{NR} , is the sum of the rate constants for intersystem crossing and internal conversion.

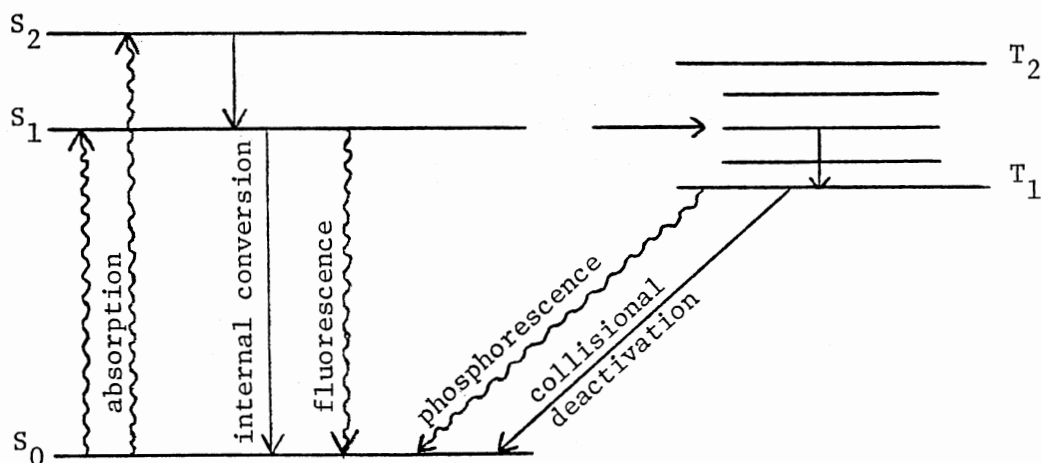


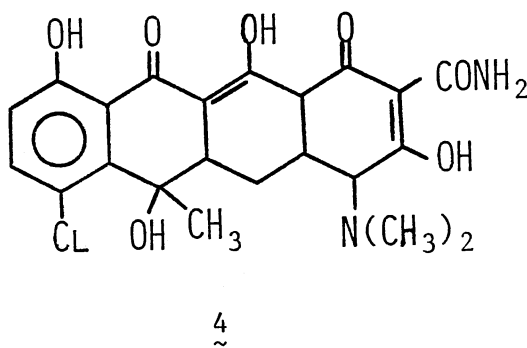
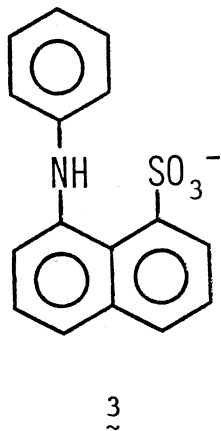
Figure 3. Electronic Transitions Leading to Fluorescence and Other Relaxation Processes. Straight arrows denote nonradiative transitions. Wavy arrows denote the absorption or emission of radiation.

Fluorescent probes are small molecules (relative to the system being studied) that can provide information about the limited volumes in which they are located.⁸ In general, probes can be classified as either intrinsic or extrinsic. Intrinsic probes are those such as tryptophan that occur naturally in the system being studied. Extrinsic probes are those that are artificially incorporated into the system being studied. In order for an extrinsic probe to be useful, there are several criteria that it must meet, namely that (1) the probe must be

sensitive to the properties of the systems that are being studied; (2) the absorption spectrum of the probe should lie at lower frequency than the absorption spectra of any intrinsic probes commonly found in the system; (3) perturbation of the system resulting from incorporation of the probe should be minimal; (4) the location of the probe within the system should be known; and (5) the probe should be stable under the conditions used to study a given system.

Fluorescence experiments using extrinsic probes have been useful in studying various aspects of membrane structure. Some of the properties of biological membranes that have been investigated using this technique are polarity, rotational mobility or microviscosity, distances between selected membrane components or sites,^{4,11,61} and conformational changes in membrane structure. It is important to note, however, that this information on the biological system is obtained indirectly. These experiments provide direct information only about the probe itself.

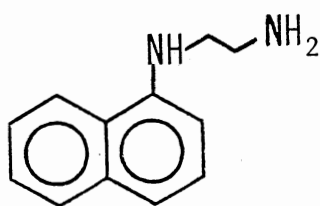
Many of the fluorescent probes used today are sensitive to the polarity of their immediate environments. In many cases, a change in the polarity of the surrounding medium results in a change in the wavelength of the emission maximum and the fluorescence quantum yield of the probe. For example, the probe, 1-anilinonaphthalene-8-sulphonate or ANS (3), shows a large increase in ϕ_F and a shift of its fluorescence maximum to shorter wavelength when transferred from a polar to a non-polar medium.²⁴ The fluorescent chelate probe, chlorotetracycline (4), also shows a large dependence on the polarity of its surroundings. The fluorescence of chlorotetracycline complexed to a divalent cation such as Mg^{2+} is 2.9 times as intense in 50% methanol as in H_2O .¹⁶



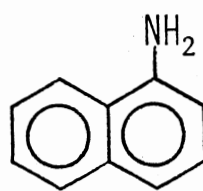
Fluorescent probes have also been used to monitor changes that occur in membranes during various biological processes. Caswell and Warren used chlorotetracycline (4) to monitor ATP-induced Ca^{2+} uptake and binding in skeletal and cardiac muscle microsomes.¹⁷ Jasaitis and co-workers studied changes in ANS fluorescence induced by a membrane potential in mitochondria and submitochondrial particles.²⁸ They found that ANS fluorescence decreased as the membrane interior became more negative and increased as it became more positive. Schuldiner and co-workers have used a variety of probes, 5 through 9, to continuously monitor the changes in ΔpH in chloroplasts.⁵¹

A large number of different probes have been used to determine the gel-liquid crystalline transition temperature of various artificial and biological membranes. Dansylphosphatidylethanolamine (10), 9-methylanthracene (11), and ANS were used to study order-disorder transitions of the aliphatic chains of phospholipids in bilayer systems. The probes 10 and 11 gave the expected transition temperatures for dimyristoylphosphatidylcholine and dipalmitoylphosphatidylcholine bilayers. In contrast ANS showed no phase transition presumably due to its location in the polar region of the lipid bilayer. The probe, N-phenyl-

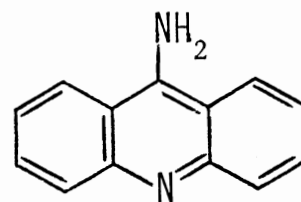
1-naphthylamine (12), was used to detect phase transitions in cells, membranes, and lipids of Escherichia coli.⁴⁴ At concentrations less than 10^{-5} M, the probe did not affect the transition temperature. At concentrations between 10^{-5} and 5×10^{-4} M, the transition temperature was lowered by 3° - 7° C. This suggested that the probe penetrated the nonpolar region of the membrane and interfered with the orderly packing of the lipid chains at higher concentrations.



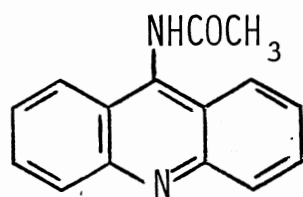
5



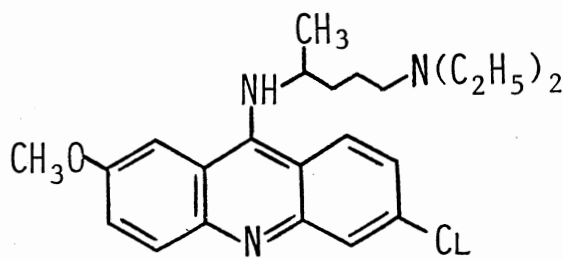
6



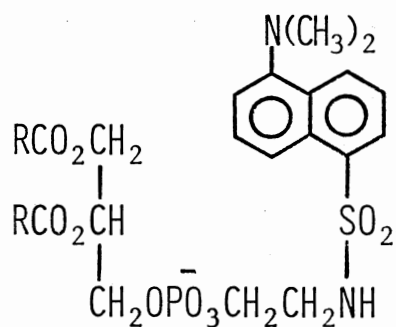
7



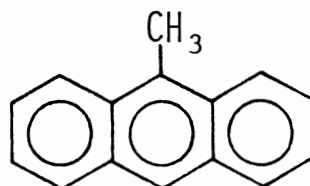
8



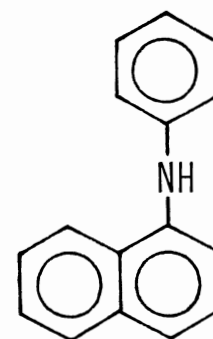
9



10

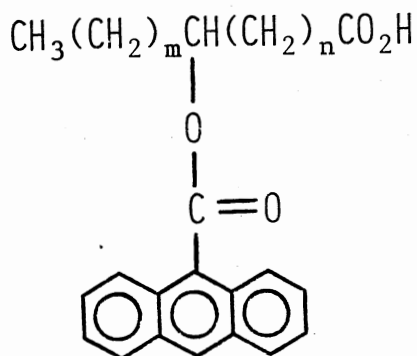


11

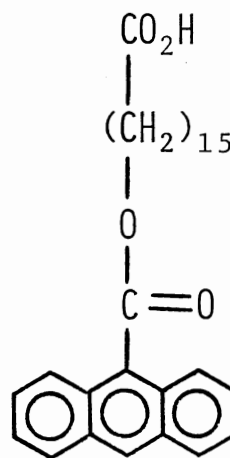


12

Several different research groups have used (9-anthroyl)-substituted fatty acids to detect phase transitions of lipid bilayers. Radda and co-workers⁴² used 12-(9-anthroyl)stearic acid (12-AS) (13) to study the gel-liquid crystalline transition of an oriented lipid bilayer. Using photobleaching experiments, they concluded that 12-AS was excluded from the lipid matrix and formed regions of localized high concentration below the transition temperature, T_c . Cadenhead and co-workers¹³ used 2-(9-anthroyl)palmitic acid (2-AP) (14), 12-AS, and 16-(9-anthroyl)palmitic acid (16-AP) (15) to determine the main phase transition temperature of dipalmitoylphosphatidylcholine (DPPC) bilayers. Using 2-AP, T_c was found to be 39°C; 12-AS gave a value of 40°C while 16-AP gave a value of 41.5°C. These values were lower than the value of 41.5-42.5°C determined by differential scanning calorimetry. In similar studies by Thulborn and Sawyer,⁵⁹ however, 2-AP, 6-(9-anthroyl)stearic acid (6-AS) (16), 9-(9-anthroyl)stearic acid (9-AS) (17), and 12-AS all gave a transition temperature of 41.6°C for DPPC bilayers.

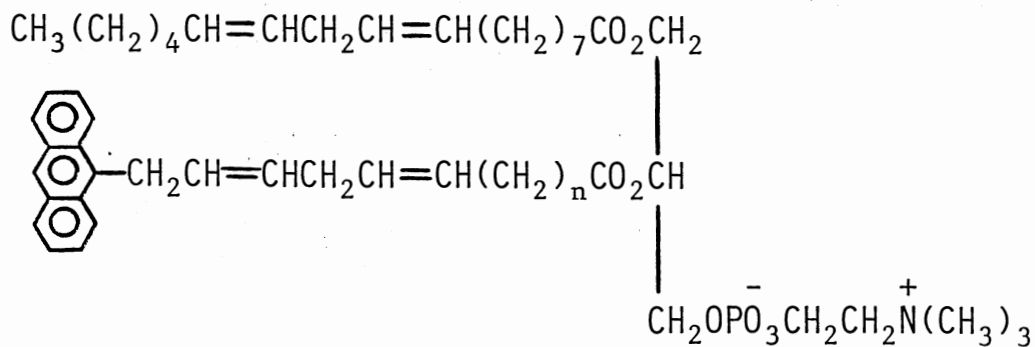
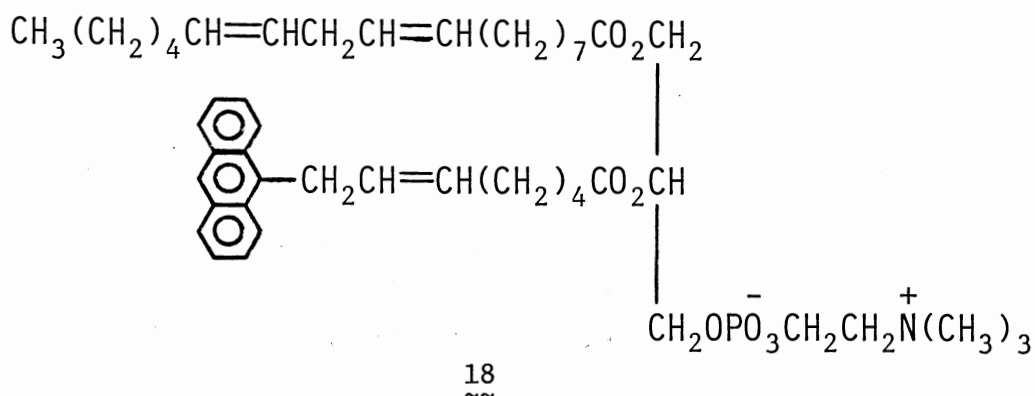


13	m= 5,	n=10
14	m=13,	n= 0
16	m=11,	n= 4
17	m= 8,	n= 7



15

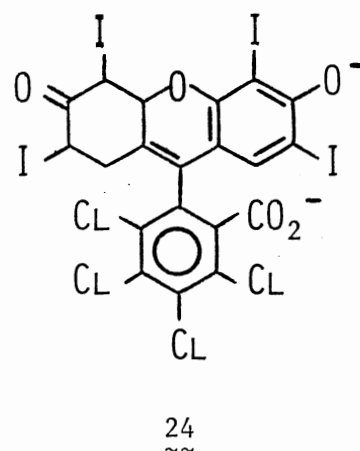
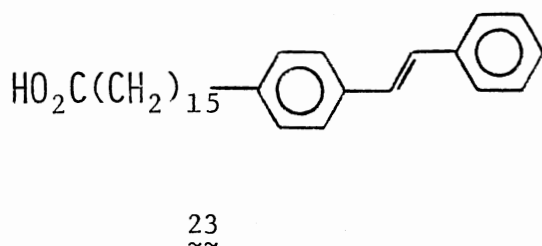
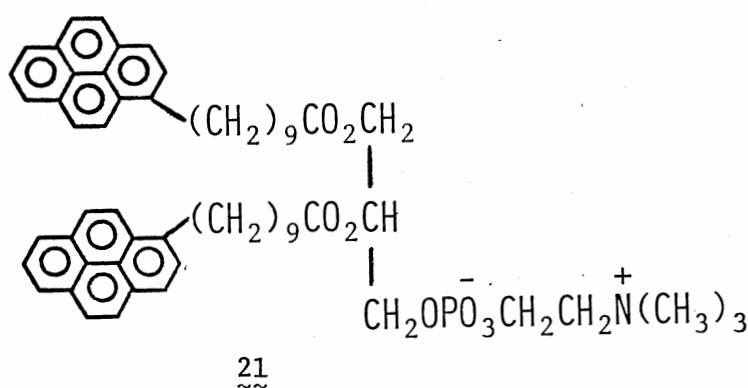
Fluorescent probes have also been used to study interactions of various membrane components. For example, Radda and co-workers¹¹ have calculated the average distance between incorporated ANS probes and the tryptophan moieties of proteins present in erythrocyte ghosts and submitochondrial particles to be 20-25 Å. These distances were determined using fluorescence donor-acceptor measurements. Stoffel and Michaelis^{54,55} have synthesized and examined a variety of phosphatidylcholines in which the second position contains a (9-anthryl)-substituted fatty acid moiety. These probes 18, 19, and 20 were used to study lipid-lipid and lipid-protein interactions in liposomes (DPPC) and phospholipid extracts of an E. coli mutant.



19 n=4

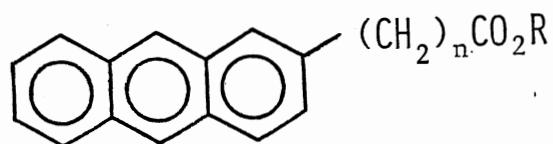
20 n=8

Recently, the synthesis and fluorescence studies of 1,2-bis[ω -(1-pyreno)decanoyl]-sn-glycero-3-phosphorylcholine (DPPL) (21),⁵⁸ ethyl ω -(1-pyreno)decanoate (EP) (22),⁵⁸ and a trans-stilbene-substituted fatty acid (23)⁴⁹ have been reported. In addition, rose bengal (24) has been used to study the extent of exposure of the hydrocarbon chains in aqueous micelles.⁴⁹ Another recent investigation involved saturation studies of the fluorescent probes, 2-AP, 2-AS, 12-AS, and 16-AP.⁴³ Najjar found that these probes reached a critical concentration in lipid vesicles. Above this concentration the probe was found in two different environments, presumably the nonpolar environment of the bilayer and the more polar environment of the buffer solution surrounding the probe.



Although many fluorescent probes are available either commercially or through synthetic pathways reported in the literature, many of these probes do not meet all of the criteria set forth previously. For example, the location of probes such as 1,6-diphenylhexatriene (2) and 9-methylanthracene (11) within the lipid bilayer is uncertain.⁵⁴ In order for the results of fluorescence experiments to be interpreted validly, the location of the probes used must be known. Other probes such as 14, 16, 18, and 21, which contain a pyrene, 9-anthryl, or 9-anthroyl moiety, are believed to perturb the environments being studied to some extent.¹³ The 9-anthroyl moiety of 12-AS (13) has been reported to undergo cleavage from the probe during attempts to incorporate it into a biological system.⁵⁵

The synthesis of a new class of fluorescent probes, the ω -(2-anthryl)substituted fatty esters (25), has been recorded recently.³ It is believed that these probes will offer several advantages over those currently available, namely that (1) the probes will occupy a known location within the bilayer depending upon the length of the fatty acid or ester, (2) the probe will be stable under biological conditions, and (3) the probe should cause less perturbation to the lipid bilayer than those containing a 9-anthryl or 9-anthroyl moiety. Ideally, however, the length of the fatty acid to which the 2-anthryl group is attached should mimic those found in natural membranes. Thus, the ideal fluorescent probe for biological membranes may well be those such as 25 in which $n = 11 - 17$.



25a	n= 2,	R=C ₂ H ₅
25b	n= 4.	R=CH ₃
25c	n= 6,	R=CH ₃
25d	n=11,	R=CH ₃
25e	n=13,	R=CH ₃
25f	n=16,	R=CH ₃

Carbon-13 Spin Lattice Relaxation Times

Although structural and stereochemical assignments for solid organic compounds are readily made using single crystal X-ray diffraction studies, similar determinations for these same compounds in solution or for liquid organic compounds are not as easily accomplished. The most common tools employed in the latter cases include ^1H and ^{13}C NMR chemical shifts and spin-spin coupling constants for these and other NMR active nuclei. The most recent and perhaps most useful method for these determinations, however, involves the use of ^{13}C spin-lattice relaxation times. Unlike the NMR chemical shift and spin-spin coupling data, the relaxation times obtained from these experiments can be used to determine not only molecular structure but also molecular motion and local and overall molecular geometry.³⁷

This section will provide a non-mathematical discussion of the spin-lattice relaxation phenomenon and its use in the determination of molecular structure and motion.

A typical ^{13}C NMR experiment, including both excitation and relaxation processes, can be described most easily using the "rotating frame of reference" (Figure 4).⁴⁶ In this model, the entire coordinate system rotates at the resonance frequency, ω_0 . The external magnetic field, H_0 , is applied along the z axis while the rf field is applied along the x axis. When ^{13}C nuclei are placed in a magnetic field, the spin of each nucleus becomes aligned with or against the applied field. At equilibrium, the distribution of the spins is such that the lower energy level is slightly more populated than the upper energy level resulting in a net equilibrium magnetization, M_0 (Figure 4a). When the sample is excited with rf radiation, the equilibrium distribution of the nuclear spins is perturbed. In terms of the rotating frame of reference, the magnetic component of the rf field rotates M out of alignment with the applied field and toward the y axis. The extent of this rotation is dependent upon the pulse width of the rf radiation. Two pulse widths, which may be determined experimentally, are commonly used - one which results in a tipping of M by 90° (90° pulse) and one in which M is completely inverted (180° pulse).

Immediately after each excitation pulse, the process of spin-lattice relaxation begins. This process, which involves the transfer of the energy absorbed by each nucleus to its surroundings or lattice, corresponds to relaxation along the z axis of the rotating frame of reference (Figure 1b to 1e). In order for this energy transfer to be most efficient, some mechanism that couples the nuclear spins and the lattice is required. In general, four relaxation mechanisms, all of which involve interaction of the magnetic vector of the nucleus with

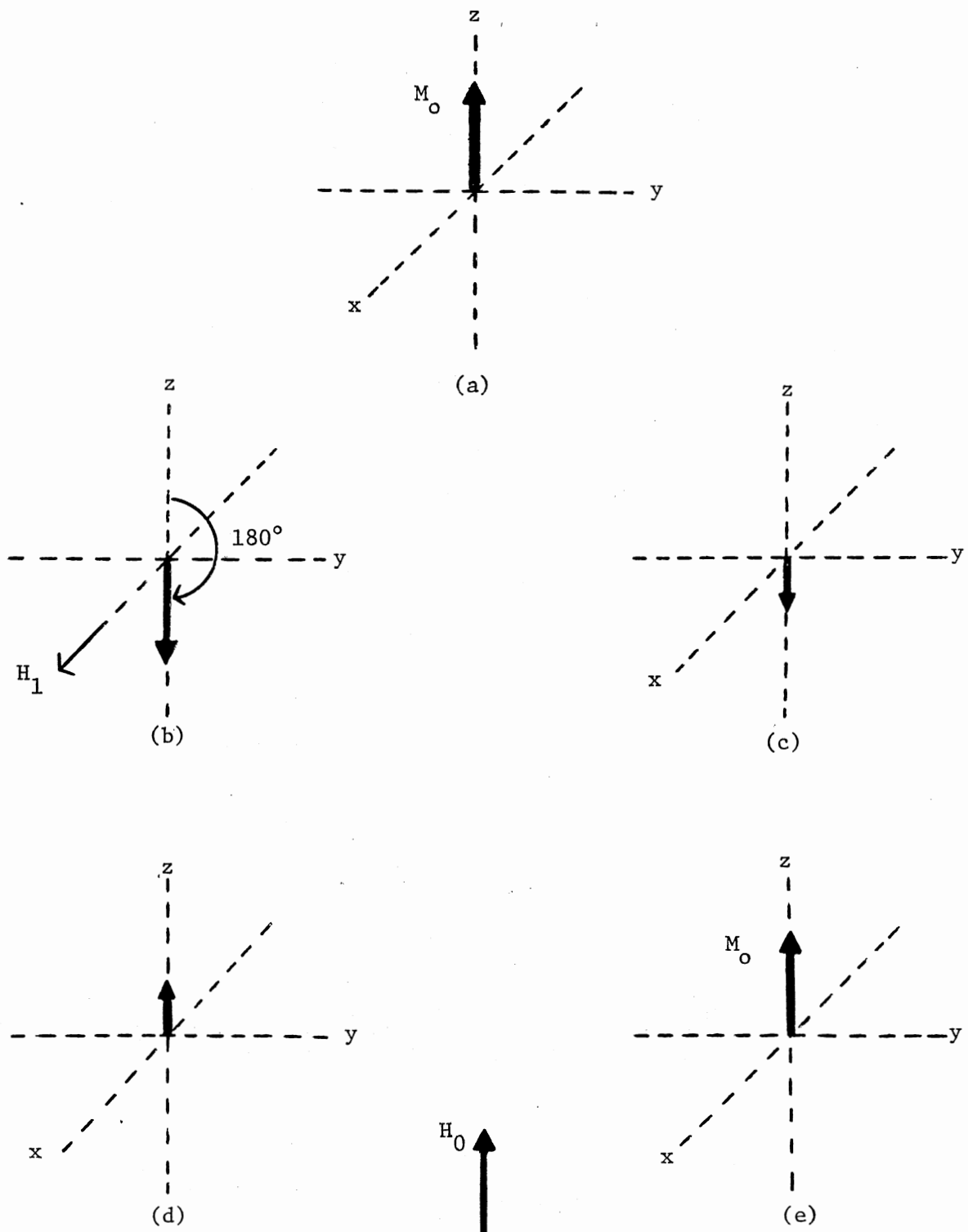


Figure 4. The Rotating Frame of Reference.

fluctuating local fields, are commonly considered.^{1,10,40} These mechanisms, which include dipole-dipole relaxation, spin-rotation relaxation, chemical shift anisotropy relaxation, and scalar coupling relaxation, may contribute in varying amounts to the relaxation of a given ^{13}C nucleus. The first two mechanisms, however, are the most common ones observed in ^{13}C systems.

Dipole-dipole (DD) relaxation, the most common relaxation mechanism for ^{13}C systems, is the result of interactions between a ^{13}C nucleus and neighboring magnetic nuclei or unpaired electrons. If two magnetic nuclei such as ^{13}C and ^1H are bound to each other, then each nucleus feels not only the external applied field but also the local field generated by the nucleus to which it is attached. Since rotations of $^{13}\text{C}-^1\text{H}$ bonds are very fast in solution, the orientation of the two magnetic nuclei relative to the applied field will change continually. This continual reorientation of the two nuclear spins generates fluctuating local fields at each nucleus which contributes to the relaxation of the ^{13}C nucleus. The rate of dipole-dipole, spin-lattice relaxation for a ^{13}C nucleus in a rigid, isotropically tumbling molecule is given by:

$$R_{1\text{DD}} = \frac{1}{T_{1\text{DD}}} = N \hbar^2 \gamma_{\text{C}}^2 \gamma_{\text{H}}^2 r_{\text{C-H}}^{-6} \tau_{\text{C}} \quad (2)$$

where $R_{1\text{DD}}$ is the DD, spin-lattice relaxation rate, $T_{1\text{DD}}$ is the DD, spin-lattice relaxation time, N is the number of directly bound hydrogens, γ_{C} and γ_{H} are magnetogyric ratios for ^{13}C and ^1H , respectively, $r_{\text{C-H}}$ is the C-H internuclear distance, and τ_{C} is the molecular correlation time.⁴⁰

A second relaxation mechanism that is relatively common in ^{13}C

systems is spin rotation (SR) relaxation. In SR, small molecules or freely rotating molecular segments can be relaxed effectively by the fluctuation of local fields generated by the rotation of the magnetic vectors of the bonding electrons involved. In these cases, SR relaxation often competes with DD relaxation for protonated carbons and dominates the relaxation of nonprotonated carbons. For example, C(1) of toluene is relaxed primarily by spin rotation.³⁸ The rate of spin rotation, spin-lattice relaxation for a ^{13}C nucleus in a spherical molecule is given by:

$$R_{1\text{SR}} = \frac{1}{T_{1\text{SR}}} = \frac{2 \pi k T}{\hbar^2} I_m C^2 \tau_{\text{SR}} \quad (3)$$

where $R_{1\text{SR}}$ is the SR, spin-lattice relaxation rate, $T_{1\text{SR}}$ is the SR, spin-lattice relaxation time, k is Boltzmann's constant, T is the temperature in $^{\circ}\text{K}$, I_m is the moment of inertia, C is the isotropic SR interaction constant, and $\tau_{1\text{SR}}$ is the SR correlation time.⁴⁰

A third, less common relaxation mechanism is chemical shift anisotropy (CSA) relaxation. In this mechanism a nucleus in a molecule tumbling in solution may be relaxed by fluctuating magnetic fields arising from anisotropy or directionality in the shielding of that nucleus. The rate of CSA, spin-lattice relaxation for a nucleus in a molecule of cylindrical symmetry is given by:

$$R_{1\text{CSA}} = \frac{1}{T_{1\text{CSA}}} = \frac{2}{15} \gamma_C^2 H_o^2 (\sigma_{\parallel} - \sigma_{\perp})^2 \tau_C \quad (4)$$

where $R_{1\text{CSA}}$ is the CAS, spin-lattice relaxation rate, $T_{1\text{CSA}}$ is the CSA, spin-lattice relaxation time, H_o is the applied magnetic field, and σ_{\parallel} and σ_{\perp} are the values of the shielding tensor parallel and perpen-

dicular to the symmetry axis, respectively.⁴⁰ In general, the CSA relaxation mechanism is significant for ^{13}C nuclei only at very high magnetic field strengths and in systems containing π bonds.

The final relaxation mechanism found in ^{13}C systems is scalar coupling (SC) relaxation. Two nuclei, ^{13}C and X, that are bonded to each other may undergo spin-spin coupling if the lifetime of their respective nuclear magnetic energy levels is sufficiently large. If, however, one nucleus, X, relaxes much faster than the other, no splitting is observed. The fast relaxation of X may, however, generate fluctuating local magnetic fields at the ^{13}C nucleus resulting in relaxation of the ^{13}C nucleus. The rate of SC, spin-lattice relaxation is given by:

$$R_{1\text{SC}} = \frac{1}{T_{1\text{SC}}} = \frac{8 \pi^2 J^2}{3} S(S+1) \frac{\tau_{\text{SC}}}{1 + (\omega_X - \omega_C)^2 \tau_{\text{SC}}^2} \quad (5)$$

where $R_{1\text{SC}}$ is the rate of SC, spin-lattice relaxation, $T_{1\text{SC}}$ is the SC, spin-lattice relaxation time, J is the scalar coupling constant, S is the spin quantum number of X, ω_X and ω_C are the Larmor frequencies of X and ^{13}C , and τ_{SC} is the scalar coupling relaxation correlation time.⁴⁰ In general, the SC, spin-lattice relaxation mechanism is quite uncommon in ^{13}C systems and is important primarily in systems where ^{13}C is bonded to one or more ^{79}Br atoms.³⁶

Since a variety of relaxation mechanisms may contribute to the relaxation of a particular ^{13}C nucleus, the overall relaxation rate may be considered to be the sum of the individual rates for each mechanism, that is,

$$R_{\text{obsv}} = R_{1\text{DD}} + R_{1\text{SR}} + R_{1\text{CSA}} + R_{1\text{SC}} + R_{\text{lother}} \quad (6)$$

or

$$T_{1\text{obsv}} = \frac{1}{R_{1\text{DD}}} + \frac{1}{T_{1\text{SR}}} + \frac{1}{T_{1\text{CSA}}} + \frac{1}{T_{1\text{SC}}} + \frac{1}{T_{1\text{other}}} \quad (7)$$

In some instances the contribution of each mechanism to the relaxation of the nucleus may be determined. Dipole-dipole relaxation may be detected through its temperature dependence. As the temperature of a solution is increased, the overall T_1 for a particular nucleus relaxing primarily by the DD mechanism also increases. The amount of DD relaxation for a ^{13}C nucleus may be calculated from its nuclear Overhauser enhancement (NOE):

$$\% \text{ DD Relaxation} = \frac{\eta}{1.988} \times 100 \quad (8)$$

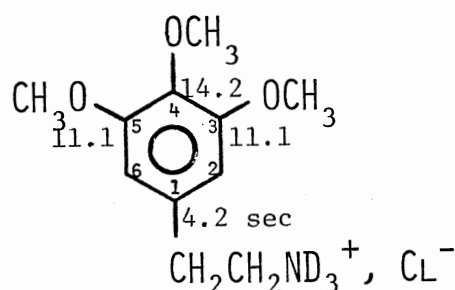
where η is the NOE for a given ^{13}C nucleus and the value of 1.988 is the maximum theoretical value for the ^{13}C NOE.³⁷

Relaxation primarily by spin rotation, chemical shift anisotropy, or scalar coupling may also be detected although the exact contribution of each mechanism is much more difficult to determine. In the case of a nucleus relaxing primarily by the SR mechanism, the observed T_1 decreases with increasing temperature. In contrast to this, predominance of the CSA mechanism may be detected by its dependence on H_0^2 . Scalar coupling relaxation may also show a field dependence but not in such a simple manner.¹⁰

Although a variety of mechanisms may contribute to the overall relaxation of a nucleus, in many ^{13}C systems dipole-dipole relaxation is either the major or exclusive mechanism operating. Since the efficiency of DD interactions depends upon the rate of molecular

reorientation, T_{1DD} may be used to evaluate the overall and local molecular motion in many ^{13}C systems. A variety of equations that describe specific molecular motions are available. In many cases, however, complex mathematical manipulations are not required in order to obtain significant information concerning molecular dynamics from T_1 values.^{2,19} Thus, the relationships between ^{13}C T_1 values and molecular motion form the basis for many applications in organic chemistry.

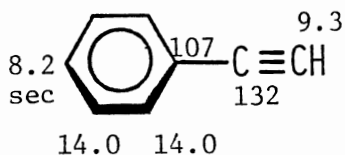
One common application of ^{13}C T_1 values involves the determination of structures of organic molecules. T_1 values may be used to distinguish between protonated and nonprotonated carbons.³⁷ In some cases, ^{13}C T_1 values can also distinguish between the various nonprotonated carbons based on the number of protons attached to adjacent carbons ($\frac{1}{T_{1DD}} \propto r_{\text{C-H}}^{-6}$). For example, C(1), C(3,5), and C(4) of mescaline- \underline{d}_3 (26) may be assigned unequivocally.³⁷ As expected, C(1) with



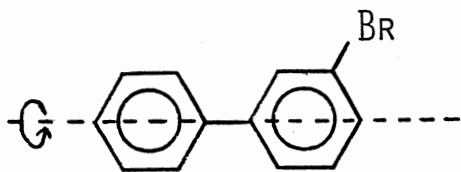
26
~~

two ortho protons shows the smallest T_1 while C(3) and C(5), each with one ortho proton, shows a longer T_1 and C(4) with no ortho protons shows the longest T_1 of the three different nonprotonated carbons.

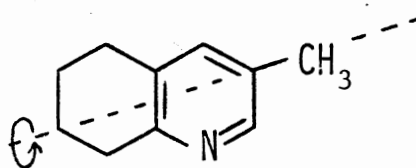
A second application of ^{13}C T_1 values involves the determination of preferred or anisotropic tumbling of a molecule.^{10,37} As a result of many different electrical, chemical, and physical effects, many small, compact molecules tumble anisotropically in solution. For example, rotation about the C_2 molecular symmetry axis is highly favored in monosubstituted benzenes (Figure 5). This leads to modulation of the dipole-dipole interactions of the ortho and meta carbons and their respective protons but not the para carbon and its proton. Thus, for monosubstituted benzenes, such as 27,³⁸ that tumble anisotropically about the C_2 axis, the T_1 value for the para carbon should be shorter than those for the ortho and meta carbons. This behavior may be used to assign similar resonances from more complex molecules such as 3-bromobiphenyl (28)³⁷ and 3-methyl-5,6,7,8-tetrahydroquinoline (29).¹



27



28



29

A third application of ^{13}C T_1 values involves the study of molecular flexibility or segmental motion.^{10,37} In general, the carbons toward each end of a long chain hydrocarbon are more mobile

than those in the middle of the chain. This difference in the mobility of various chain segments in the molecule results in minimum values for T_1 for carbons at the center of the chain and maximum values at the ends. One example of this behavior is decane (30).⁷ The larger T_1 values at the end of the chain and the smaller ones in the middle indicate the presence of more segmental motion at the ends of the long chain.

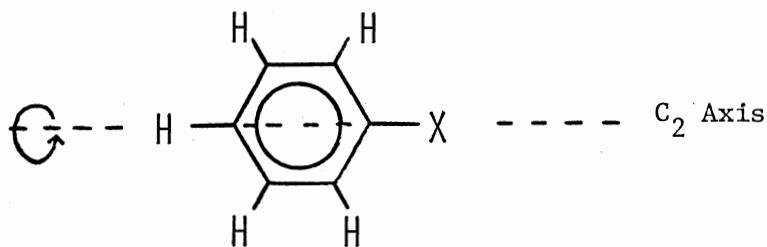
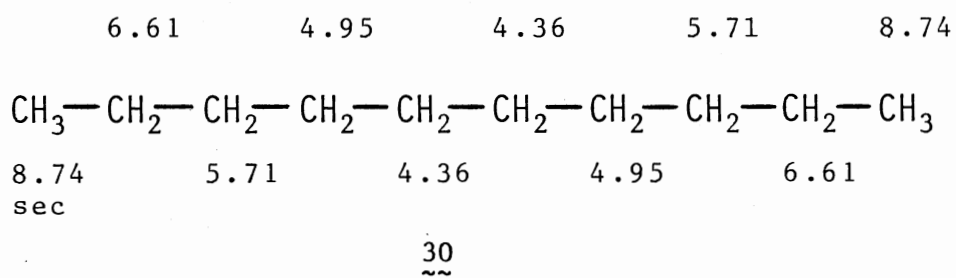
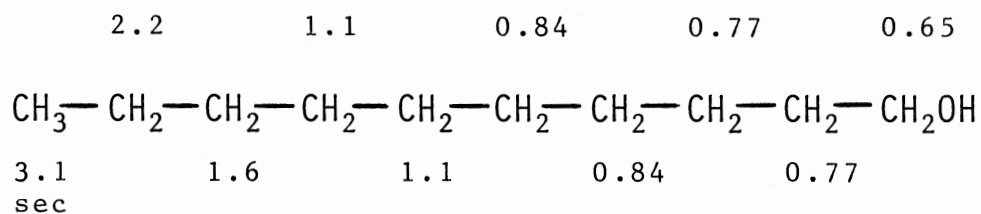


Figure 5. Symmetry Axis in Monosubstituted Benzenes.

Related to this change in segmental motion in various portions of the molecule is the change in molecular flexibility as a result of hydrophobic or hydrophilic interactions and hydrogen bonding. In 1-decanol (31), for example, the ^{13}C T_1 values increase as the distance

from the hydroxyl group increases.¹⁸ Thus, the hydrocarbon end of the chain has more motional freedom than does the hydroxyl end. This behavior can be attributed to intermolecular hydrogen bonding between the hydroxyl groups. This restricts the mobility of the hydroxyl end of the molecule while leaving the hydrocarbon end free to move. In addition to 1-decanol, other alcohols such as the amino alcohols³⁹ show similar effects.

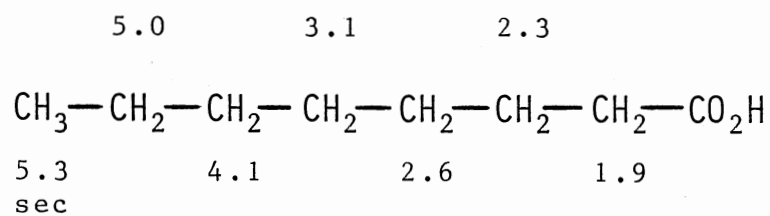


31

The presence of hydrophobic or hydrophilic interactions can also be detected by monitoring ¹³C T₁ values. Many compounds, such as fatty acids, form inverted micelles when dissolved in a nonpolar solvent such as CHCl₃. The formation of an inverted micelle may be detected through the larger T₁ values for carbons at the nonpolar end of the molecule. In octanoic acid (32),²⁹ for example, T₁ values increase steadily from the polar to nonpolar end of the molecule. This indicates greater mobility at the nonpolar end of the molecule and highly restricted motion at the polar end, both of which are indicative of the formation of an inverted micelle.

Finally, some of the most recent applications of ¹³C T₁ values involve the study of biological membranes. Johns and co-workers are currently involved in a series of studies concerning the nature of

chloroplast membranes using ^{13}C T_1 values.^{29,30} Berlin and co-workers as well as several other researchers are currently using ^{13}C T_1 measurements to examine the properties of a series of fluorescent probes for biological membranes.^{3,31}



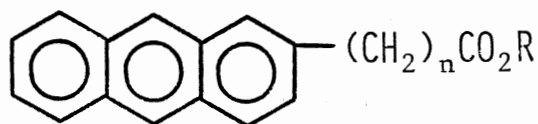
32
~

In conclusion, the development of more sophisticated Fourier transform NMR instrumentation in the past ten years has led to increased interest in the use of ^{13}C spin lattice relaxation measurements. Although many theoretical questions remain to be answered at this time, these measurements offer a unique opportunity to obtain information concerning the molecular dynamics of organic molecules in solution.

CHAPTER II

RESULTS AND DISCUSSION

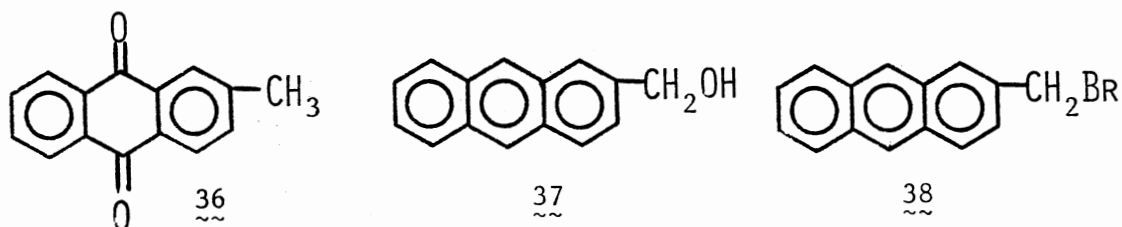
In order for a fluorescent probe to be useful in studies of biological membranes, it must meet several important criteria, namely that (1) the absorption spectrum of the probe should lie to the red (lower energy) of the absorption spectrum of tryptophan ($\lambda_{\text{max}} = 220^{24}$ nm), (2) the location of the probe within the membrane should be known, (3) perturbation resulting from the incorporation of the probe should be minimal, and (4) the probe should be stable under biological conditions. One of the newest classes of fluorescent probes that should meet these criteria is the ω -(2-anthryl)substituted fatty ester 25. The syntheses of three members (25a-25c) of this class of probes have been published recently.³ Reported herein are the syntheses and NMR spectral analyses of three new fluorescent probes of this same class in which $n = 11, 13, \text{ and } 16$ (25d, 25e, and 25f).



<u>25a</u>	$n=2,$	$R=C_2H_5$	<u>25d</u>	$n=11,$	$R=CH_3$
<u>25b</u>	$n=4,$	$R=CH_3$	<u>25e</u>	$n=13,$	$R=CH_3$
<u>25c</u>	$n=6,$	$R=CH_3$	<u>25f</u>	$n=16,$	$R=CH_3$

The synthetic approach designed to prepare the probes 25d-25f (Figure 6) involved a Wittig reaction using phosphonium salt 33 and an appropriate oxo-ester 34a-34c to give the unsaturated esters 35a, 35b, and 35c in good to excellent yields (77%, 90%, and 81%, respectively). Hydrogenation of 35a-35c in ethyl acetate at atmospheric pressure using 10% Pd/C as a catalyst gave the desired saturated esters 25d, 25e, and 25f in good yields (75%, 80%, and 80%, respectively). Each of these esters was purified rigorously by two recrystallizations from 95% ethanol followed by two molecular distillations using a sublimation apparatus. The slightly impure esters were pale yellow solids, whereas, the highly purified compounds were white powders.

The synthesis of the phosphonium salt 33 from the commercially available 2-methylantraquinone (36) was achieved in several steps. Using published procedures,^{6,14,22,25,53} 2-methylantraquinone was converted to 2-hydroxymethylantracene (37) in an overall yield of 45%. Treatment of 37 with triphenylphosphine dibromide in DMF at room temperature gave the corresponding bromide 38 in an 84% yield. As



indicated by melting points, 2-bromomethylantracene prepared by this method was of greater purity than that obtained by bromination of 2-methylantracene using N-bromosuccinimide.³⁴ The desired phosphonium salt 33 was obtained through the treatment of 2-bromomethylantracene with triphenylphosphine in boiling benzene. The phosphonium salt 33

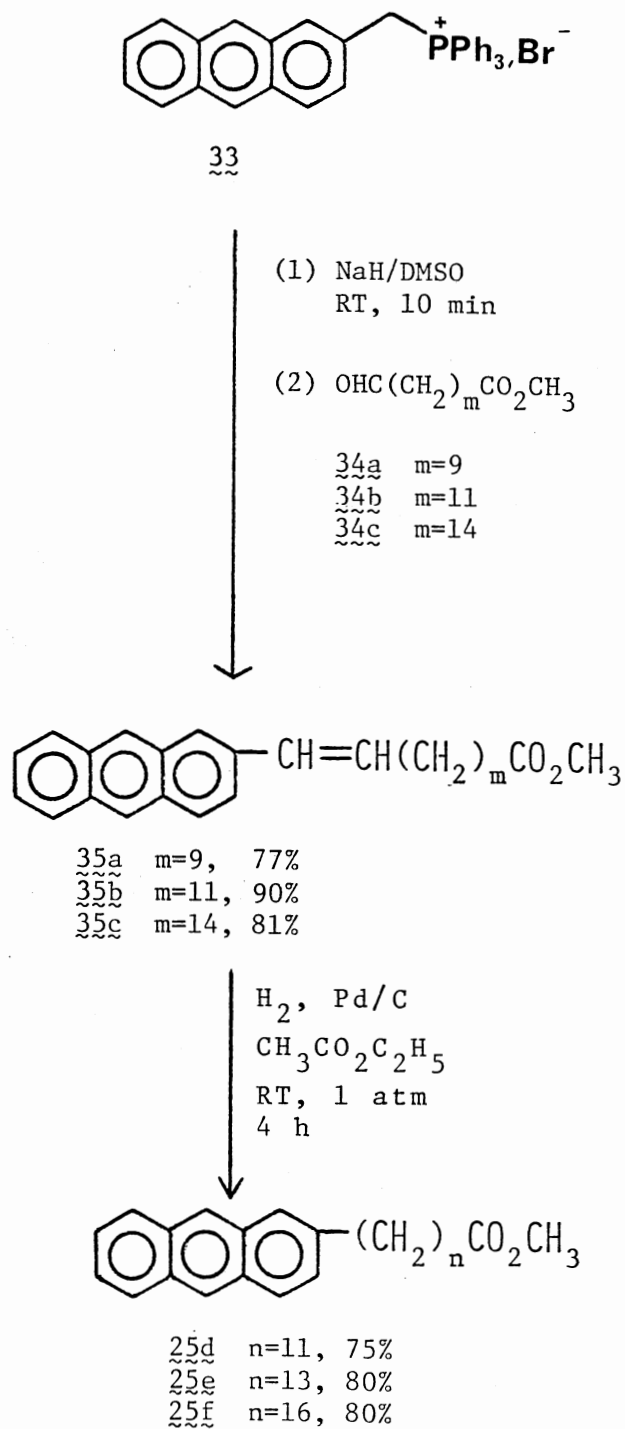


Figure 6. Synthesis of 25d-25f

was somewhat hygroscopic and had to be dried under vacuum over boiling ethanol prior to use.

The ω -oxoesters 34a-34c required for the synthesis of 25d-25f are not available commercially. The methods designed to prepare these compounds are shown in Figure 7. The oxoester 34a was prepared from 11-bromoundecanoic acid (39). Esterification of the acid 39 followed by treatment with pyridine-N-oxide and NaHCO_3 in boiling toluene gave the desired oxoester in a modest overall yield (30%-50%). The oxoester 34b was obtained via alkylation of 2,4,4-trimethyloxazoline using the lithium salt of 11-bromoundecanol at -78°C . Methanolysis of the resulting alkylated oxazoline 41 gave the ω -hydroxyester 42 in a modest overall yield (47%). Oxidation using CrO_3 /pyridine gave the desired ω -oxoester 34b (crude yield of 96%). This oxoester was sufficiently pure to be used in the Wittig reaction without further purification. The final oxoester 34c was prepared by methanolysis of dihydroambrettolide (43) to give the corresponding ω -hydroxyester 44 (85%) which was oxidized to 34c (84%) using CrO_3 /pyridine.

The synthetic approach used to prepare 25d-25f is similar to that used to obtain the shorter chain homologs 25a-25c in which $n = 2, 4,$ and 6 (Figure 8).³ Both methods involved the use of a Wittig reaction to attach the appropriate side chain to the anthracene moiety. Whereas the synthesis of 25d-25f included Wittig reactions using an anthracene-containing phosphonium salt and an appropriate oxoester, the syntheses of the shorter homologs 25a-25c employed reactions of phosphoranes 45a-45c with 2-anthraldehyde (46). Hydrogenation of the resulting unsaturated esters in ethanol at atmospheric pressure using 10% Pd/C as a catalyst reduced not only the double bonds present in

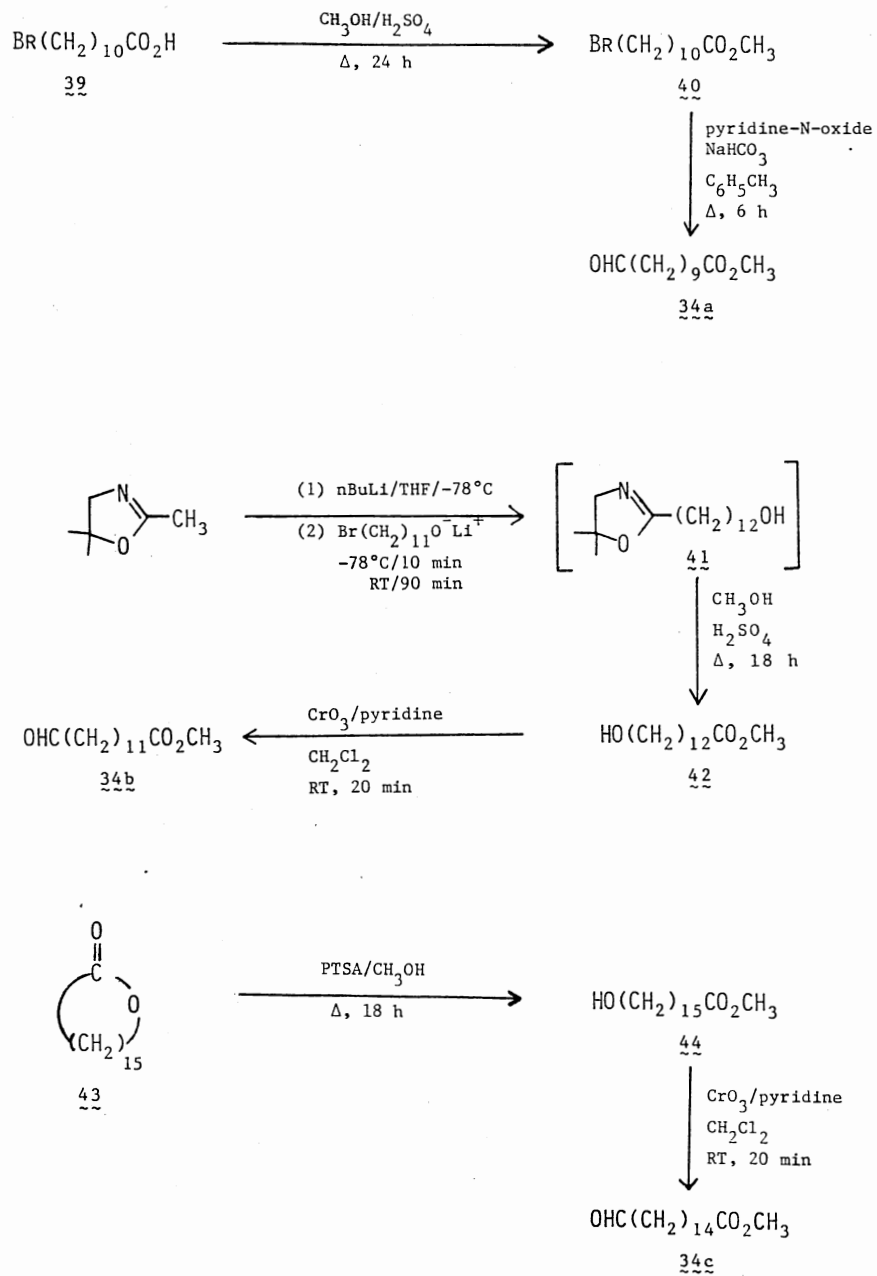
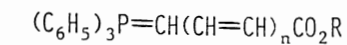
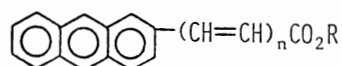
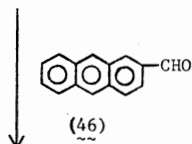


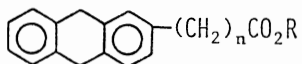
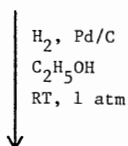
Figure 7. Synthesis of Oxoesters 34a-34c.



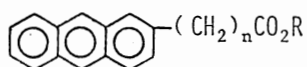
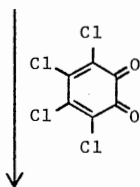
- $\sim\sim\sim$ 45a $n=0$, $\text{R}=\text{C}_2\text{H}_5$
 $\sim\sim\sim$ 45b $n=1$, $\text{R}=\text{CH}_3$
 $\sim\sim\sim$ 45c $n=2$, $\text{R}=\text{CH}_3$



- $\sim\sim\sim$ 47a $n=1$, $\text{R}=\text{C}_2\text{H}_5$, 69%
 $\sim\sim\sim$ 47b $n=2$, $\text{R}=\text{CH}_3$, 36%
 $\sim\sim\sim$ 47c $n=3$, $\text{R}=\text{CH}_3$, 20%



- $n=2$, $\text{R}=\text{C}_2\text{H}_5$
 $n=4$, $\text{R}=\text{CH}_3$
 $n=6$, $\text{R}=\text{CH}_3$



- $\sim\sim\sim$ 25a $n=2$, $\text{R}=\text{C}_2\text{H}_5$
 $\sim\sim\sim$ 25b $n=4$, $\text{R}=\text{CH}_3$
 $\sim\sim\sim$ 25c $n=6$, $\text{R}=\text{CH}_3$

Figure 8. Synthesis of $\sim\sim\sim$ 25a-25c.

the side chain but also the 9,10-positions of the anthracene ring. Subsequent aromatization using o-chloranil gave the desired 2-anthryl-substituted fatty esters 25a, 25b, and 25c.

The method used to prepare the shorter chain homologs 25a-25c³ has several disadvantages in comparison to that used to obtain 25d-25f. First, 2-anthraldehyde (46) is a highly insoluble, light sensitive, and relatively unstable compound. Second, the phosphonium salts used to obtain the phosphoranes 45b and 45c are difficult to obtain in pure form. Third, the Wittig reactions used to obtain the unsaturated esters 47b and 47c in which $n = 2$ and 3 proceed in modest to poor yields (36% and 19.7%, respectively). Fourth, a side reaction, reduction of the 9,10-positions of the anthracene ring, occurred under the conditions used. Finally, the Wittig reactions involving phosphoranes, such as 45b and 45c, cannot be applied readily to the preparation of longer chain homologs because the corresponding starting materials are not readily available either commercially or through published procedures.

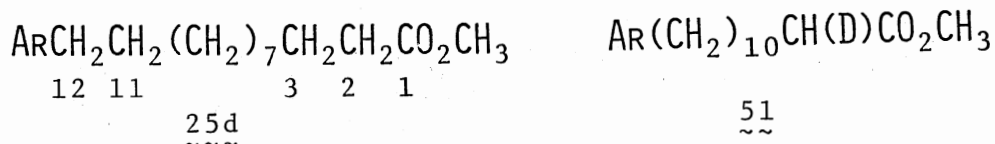
In contrast to this, the route developed for the synthesis of 25d-25f has several advantages. First, the phosphonium salt 33 is quite stable (although hygroscopic) and can be stored for relatively long periods of time. Second, the Wittig reactions used to obtain the unsaturated esters 35a-35c proceed in good to excellent yields. Third, the hydrogenation of the unsaturated esters 35a-35c under the conditions used reduces only the carbon-carbon double bond present in the side chain and not the 9,10-positions of the anthracene ring. Finally, the Wittig reaction using the phosphonium salt 33 can be utilized to prepare the unsaturated esters with any chain length (assuming that the appropriate oxoester can be obtained).

Initially, reduction of the 9,10-positions of the anthracene ring was expected in the conversion of the unsaturated esters 35a-35c to the corresponding saturated esters 25d-25f due to previous work.³ Under the conditions employed, however, only the carbon-carbon double bonds present in the side chain were reduced. Two factors may account for the reduction of the 9,10-positions in 47a-47c but not in 35a-35c. First, esters 47a-47c contain a highly conjugated side chain which may increase the reactivity of the 9,10-positions of the anthracene ring. Second, the hydrogenation of the esters 47a-47c was performed using the protic solvent ethanol, whereas, reduction of 35a-35c was performed using the aprotic solvent, ethyl acetate.

The ¹H NMR spectral assignments (100 MHz) for 25d-25f are shown in the Experimental Section. In all three esters, the methoxy protons appeared as a singlet at δ 3.64, 3.63, and 3.65, respectively. The protons alpha to the carbonyl, H(2), appeared as triplets centered at δ 2.28, 2.27, and 2.29, respectively. The protons alpha to the anthracene ring [H(12), H(14), and H(17), respectively] appeared as triplets centered at δ 2.78, 2.78, and 2.79. The remaining methylene protons of 25d-25f gave multiplets between δ 1.2-1.9, 1.2-1.7, and 1.2-1.85. An ¹H NMR spectrum performed using a Varian XL-300 NMR distinguished H(3) and H(11) of 25d. In this spectrum, H(3) appeared as a multiplet at δ 1.48-1.62 while H(11) appeared as a multiplet at δ 1.62-1.74.

Since later experiments required unequivocal assignment of H(2), H(3), H(11), and H(12) of 25d, isotope incorporation and selective homonuclear decoupling experiments were performed. The assignments for H(2) and H(12) were distinguished by the incorporation of deuterium

into 25d. The ester 25d was treated with NaOCH₃ in CH₃OD at reflux for one hour. Quenching with D₂O, filtration, and recrystallization from C₂H₅OD gave the ester 51 in which the protons on C(2) had been partially replaced by deuterium. The ¹H NMR spectrum for ester 51 showed a decreased intensity for the triplet at δ 2.28. A comparison of the integration for the signals at δ 2.78 and 2.28 indicated a ratio of 2:1.5 for the labeled ester, whereas in 26d the ratio was 2:2. Since the deuterium could only have been incorporated at C(2), this experiment permitted the assignment of the triplet at δ 2.28 to H(2). The triplet at δ 2.78 was, therefore, assigned to H(12). The assignments for H(3) and H(11) of 25d were made using homonuclear decoupling techniques. Irradiation of the triplet at δ 2.28 resulted in the collapse of the multiplet at δ 1.48-1.62 to a triplet. Therefore, the protons, H(3), must correspond to the multiplet at δ 1.48-1.62. Irradiation of the triplet at δ 2.78 resulted in the collapse of the multiplet at δ 1.62-1.74 to a triplet. Therefore, this multiplet at δ 1.62-1.74 must correspond to H(11).



Ar = 2-Anthryl

The assignments for the aromatic protons in 25d-25f cannot be made unequivocally except possibly through very complex labeling and selective decoupling experiments. Tentative assignments for ¹H signals for the aromatic protons are shown in the Experimental Section. The

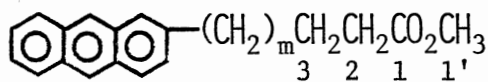
manner in which these assignments were made will be discussed later in connection with the ^{13}C assignments for the aromatic carbons.

The ^{13}C NMR assignments and spin-lattice relaxation times (T_1 values) for the carbons in the side chain of 25d-25f are shown in Table I. The assignments for carbons 1', 1, 2, 3, and those α and β to the anthracene ring in 25d were made initially using model compounds (Table II).^{50,57} The assignments for these carbons, with the exception of C(11) (β to the ring), agree quite closely with those for the appropriate models.

Since the ^{13}C NMR spectral assignments for the shorter chain homologs 25d and 25c had been published previously, a comparison of those assignments with the ones made initially for 25d using model compounds was made (Table III). Although one would expect slight shift differences (especially for the esters such as 25a with very short side chains), in general, analogous carbons within these compounds should have similar chemical shifts. The assignments for carbons 1', 1, and 3 in 25b, 25c, and 25d agreed quite closely. The assignments for carbons 2, α , and β differed drastically. Since these esters are very similar, it was expected that the signals at 36.2 (25d), 36.0 (25c), and 35.8 ppm (25b) should be assigned to analogous carbons. Similarly, the group of signals at 34.1 (25d), 33.9 (25c), and 33.8 ppm (25b) and the group at 30.9 (25d), 30.6 (25c), and 30.2 ppm (25d) should each be assigned to analogous carbons.

Because of the discrepancy in the assignments for carbons 2, α , and β in 25b, 25c, and 25d, two selective heteronuclear decoupling experiments were performed using 25d in order to assign the signals

TABLE I
 ^{13}C NMR CHEMICAL SHIFTS (T_1 VALUES (SEC)) FOR THE CARBONS IN
 THE SIDE CHAIN OF 25d-25f



25d m= 9
25e m=11
25f m=13

Carbon Number	Chemical Shift ^a (T_1 Value (sec))		
	<u>25d</u>	<u>25e</u>	<u>25f</u>
1	174.0 (44.5)	173.9 (45.3)	174.0 (44.1)
2	34.1 (1.96)	34.0 (1.92)	34.0 (2.07)
3	24.9 (1.61)	24.9 (1.56)	24.9 (1.83)
4	29.1 (1.27)	29.1 (1.31)	29.1 (1.42)
5	29.2 (1.18)	29.2 (1.14)	29.2 (1.25)
6	29.4 (1.12)	29.4 (0.98)	29.4 (1.09)
7	29.5 (0.96)	29.5 (0.90)	29.6 (0.96)
8	29.5 (0.96)	29.5 (0.90)	29.6 (0.96)
9	29.5 (0.96)	29.5 (0.90)	29.6 (0.96)
10	29.3 (0.93)	29.5 (0.90)	29.6 (0.96)
11	30.9 (0.85)	29.5 (0.90)	29.6 (0.96)
12	36.2 (0.78)	29.3 (0.79)	29.6 (0.96)
13		30.9 (0.78)	29.6 (0.96)
14		36.2 (0.69)	29.6 (0.96)
15			29.36 (0.92)
16			31.0 (0.89)
17			36.2 (0.80)
1'	51.3 (6.3)	51.2 (5.9)	51.3 (6.3)

^a Measured in ppm downfield from TMS.

TABLE II

 ^{13}C NMR CHEMICAL SHIFTS FOR 25d AND SELECTED MODEL COMPOUNDS

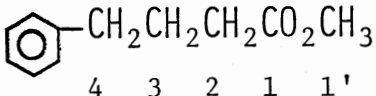
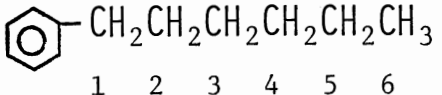
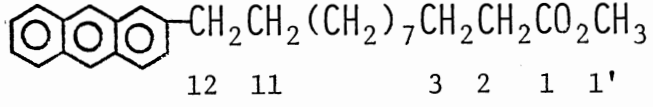
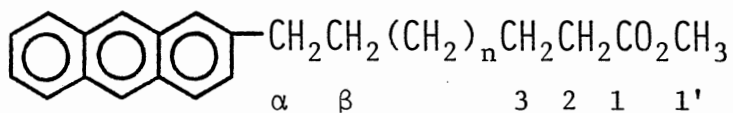
Model Compound	Carbon Number	Chemical Shift (ppm)
$\text{CH}_3(\text{CH}_2)_{10}\text{CH}_2\text{CH}_2\text{CO}_2\text{CH}_3$ 3 2 1 1'	1	174.0
	2	34.1
	3	25.0
	1'	51.2
 4 3 2 1 1'	1	173.6
	2	33.3
	3	26.5
	4	35.1
	1'	51.3
 1 2 3 4 5 6	1	36.4
	2	32.3
 12 11 3 2 1 1'	1	174.0
	2	34.1
	3	24.9
	11	30.9
	12	36.2
	1'	51.3

TABLE III

COMPARISON OF ^{13}C NMR CHEMICAL SHIFTS REPORTED FOR 25b AND 25c
 WITH ASSIGNMENTS MADE FOR 25d USING MODEL COMPOUNDS



25b $n=0$

25c $n=2$

25d $n=7$

Carbon Number	Chemical Shift (ppm)		
	<u>25b</u>	<u>25c</u>	<u>25d</u>
1'	51.3	51.2	51.3
1	173.6	173.8	174.0
2	35.8	36.0	34.1
3	24.6	24.8	24.9
α	33.8	33.9	30.9
β	30.2	30.6	36.2

for these carbons unequivocally. In the first experiment, the decoupler on the NMR was set at a frequency such that only H(2) of 25d were irradiated. In the resulting ^{13}C spectrum, all of the signals in the aliphatic region, with the exception of the one at 34.1 ppm, were shortened and broadened due to coupling with the attached protons. The signal at 34.1 ppm appeared as a single, sharp peak. Since this experiment was performed by selectively decoupling only H(2), the signal at 34.1 ppm was assigned unequivocally to C(2) of 25d. This agrees with the assignment made initially for C(2) of 25d using model compounds (Table II).

In the second selective heteronuclear decoupling experiment, the decoupler was set at a frequency such that only H(12) (α to the anthracene ring) were irradiated. In the resulting ^{13}C spectrum, all of the signals in the aliphatic region, with the exception of the one at 36.2 ppm, were shortened and broadened due to coupling with the attached protons. The signal at 36.2 ppm appeared as a single, relatively sharp peak. Since this experiment was performed by selectively decoupling only the protons of 25d, the signal at 36.2 ppm was assigned to C(11) in 25d. The results of both selective heteronuclear decoupling experiments indicate that the assignments made initially for 25d using model compounds are correct.

Further evidence that the correct assignments were made initially for C(2), C(11), and C(12) in 25d using model compounds was obtained from an heteronuclear correlated 2-dimensional (HETCOR 2-D) NMR experiment (Figure 9). This experiment was performed in the ^{13}C region between approximately 20 ppm and 37 ppm and in the ^1H region between approximately δ 1 and δ 3. At the lower right hand corner

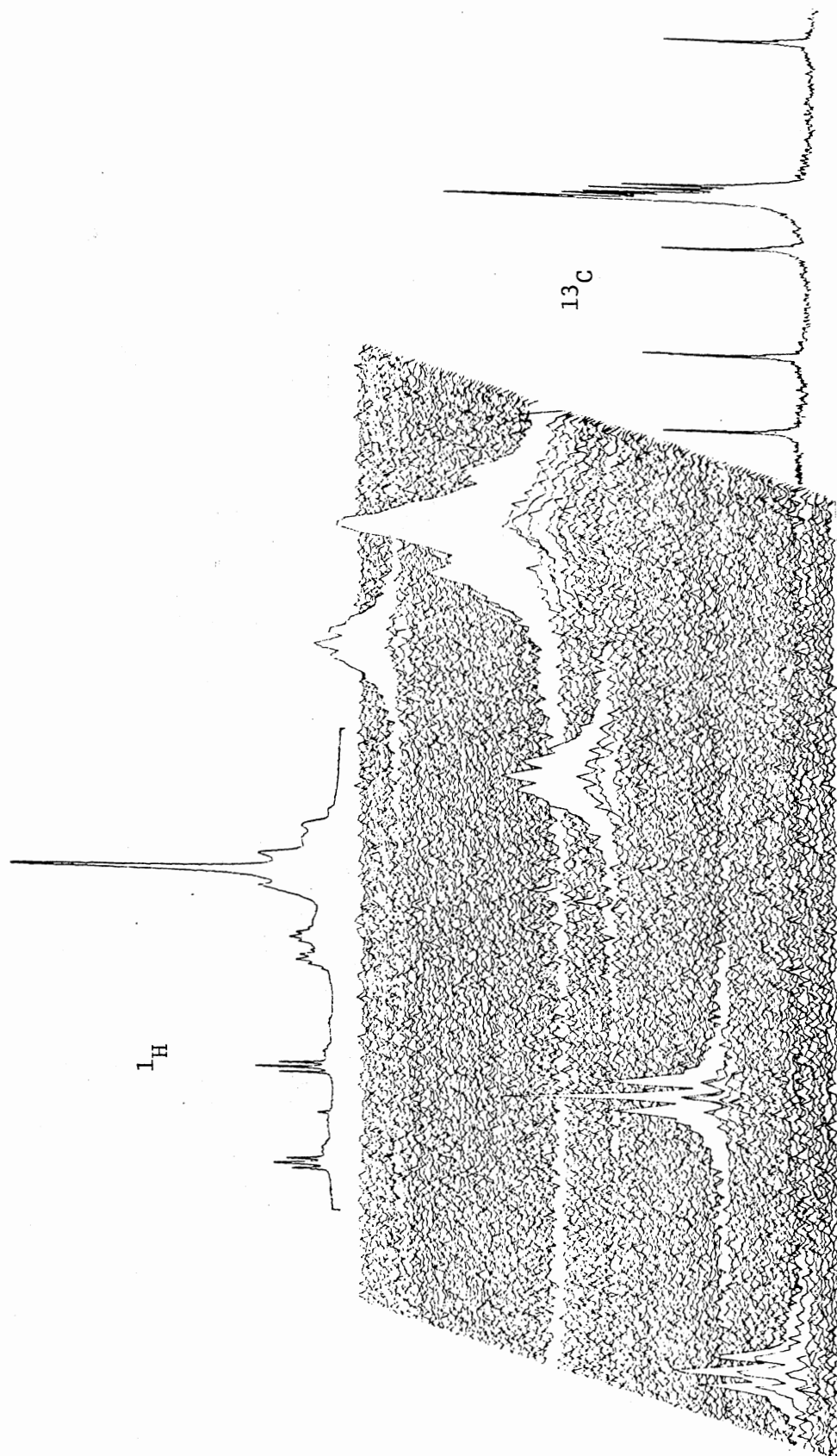


Figure 9. HETCOR 2-D Spectrum of 25d in the Aliphatic Region

of Figure 9 the proton decoupled ^{13}C spectrum for 25d in this region is shown, while in the upper portion of Figure 9 the proton spectrum in this region is shown. If all of the peaks in the HETCOR 2-D spectrum are compressed into one horizontal plane, the spectrum obtained is identical to the ^1H spectrum shown. If the 2-D spectrum is observed from the right-hand side, and all of the peaks are compressed into one vertical plane, the spectrum obtained is identical to the ^{13}C spectrum shown.

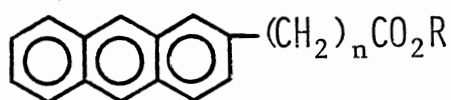
An HETCOR 2-D experiment can be used to correlate the ^1H signal for a particular set of protons with the ^{13}C signal for the carbon to which those protons are attached.²³ In order to utilize the information contained in the 2-D spectrum, either the ^1H or ^{13}C NMR spectrum must be assigned unequivocally. In this case, the ^1H NMR spectrum of 25d was assigned using labelling and homonuclear decoupling experiments as discussed earlier. From these techniques, the triplet at δ 2.78 in the ^1H spectrum was assigned to H(12). Using the HETCOR 2-D spectrum it was found that these protons were attached to the carbon giving a signal at 36.2 ppm in the ^{13}C spectrum. The signal at 36.2 ppm was, therefore, assigned unequivocally to C(12). Similarly, the protons, H(2), that gave a triplet at δ 2.28 in the ^1H spectrum were attached to the carbon that gave a signal at 34.1 ppm in the ^{13}C spectrum. The protons, H(11), that gave a multiplet at δ 1.62-1.74 in the ^1H spectrum were attached to the carbon that gave a signal at 30.9 ppm in the ^{13}C spectrum. The protons, H(3), that gave a multiplet at δ 1.48-1.62 in the ^1H spectrum were attached to the carbon that gave a signal at 24.9 ppm in the ^{13}C spectrum. The remaining protons, H(4)-H(10), that

gave a multiplet at δ 1.1-1.4 in the ^1H spectrum were attached to the carbons that gave signals between 29.1 and 29.5 ppm in the ^{13}C spectrum. The assignments made using the HETCOR 2-D experiment were identical to those made using the model compounds and selective heteronuclear decoupling experiments. The assignments shown in Table I for C(1'), C(1), C(2), C(3), C(α), and C(β), where C(α) and C(β) refer to C(14) and C(13) in 25e and C(17) and C(16) in 25f, were made by comparison to the analogous carbons of 25d.

There is no reasonable explanation why the analogous carbons of 25b and 25c should have drastically different chemical shifts from those determined for 25d. The results of the selective heteronuclear decoupling and HETCOR 2-D experiments using 25d indicate that the assignments reported for C(2), C(α), and C(β) in 25b and 25c were incorrect.³ The corrected assignments along with the T_1 values reported³ for these compounds are shown (Table IV). Although 25a contains a very short side chain and comparison to the longer homologs might be less valid, the assignments for C(2) and C(3) are almost certainly reversed. Again, the corrected assignments for 25a are given (Table IV).

The ^{13}C NMR assignments for the carbons at the center of the side chains of 25d-25f were made using the corresponding ^{13}C spin-lattice relaxation times (T_1 values). In 25d-25f, an anthracene ring is attached to the terminal position of a fatty ester. The anthracene ring is very bulky and should, therefore, act as an anchor for the entire molecule. As a result of this anchoring effect, the mobility of the carbons attached most closely to the anthracene ring should be

TABLE IV
CORRECTED ^{13}C NMR ASSIGNMENTS AND T_1 VALUES FOR 25a-25c



25a n=2, R=C₂H₅

25b n=4, R=CH₃

25c n=6, R=CH₃

Carbon Number	Chemical Shift ^a (T_1 Value ^b)		
	<u>25a</u>	<u>25b</u>	<u>25c</u>
1	172.6	173.6 (37.2)	173.8 (38.5)
2	31.3	33.8 (1.7)	33.9 (1.9)
3	35.5	24.6 (1.4)	24.8 (1.4)
4		30.2 (1.1)	28.8 (1.1)
5		35.8 (1.1)	28.8 (1.1)
6			30.6 (1.0)
7			36.0 (1.0)
1'	60.3	51.3 (6.1)	51.2 (6.2)
2'	14.2		

^a Measured in ppm downfield from TMS.

^b Measured in seconds.

greatly reduced. For carbons progressively further along the chain away from the anthracene ring, the freedom of motion should increase. In other words, the relative mobility of the methylene carbons in the side chain of 25d-25f should be smallest for the carbon attached to the anthracene ring and should increase progressively to C(2).

This change in mobility along the side chain is reflected in the T_1 values for each distinguishable carbon. Since a large T_1 value indicates an increased mobility at a given carbon (assuming the same relaxation mechanism is operative for all carbons being compared), the T_1 values for the methylene carbons in the side chains of the esters should be smallest for C(12), C(14), and C(17) of 25d, 25e, and 25f, respectively, and should increase progressively to higher T_1 values for C(2) of these compounds. Using this trend, the assignments for C(4)-C(10) of 25d, C(4)-C(12) of 25e, and C(4)-C(15) of 25f were made as shown in Table I. These assignments have not been verified by isotope labelling experiments since the appropriately labelled compounds would be extremely difficult to prepare. Supportive evidence for the rather unusual trend in T_1 values proposed here is shown in Table IV. When the assignments for the carbons in the side chains of 25b and 25c are corrected to reflect the results of the selective heteronuclear decoupling and HETCOR 2-D experiments using 25d, the T_1 values of the methylene carbons of 25b and 25c exhibit the same trend. That is, the T_1 values for the methylene carbons are smallest for the carbon attached to the anthracene ring and increase progressively to C(2).

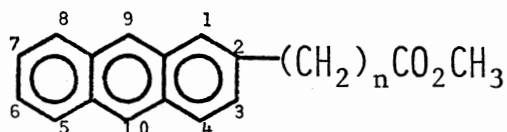
Unequivocal assignments for the signals in the aromatic region of the ^{13}C spectra of 25d-25f are very difficult to make. Although other workers^{3,41} have made assignments for the aromatic carbons in various

2-alkylanthracenes, these assignments have not been absolutely confirmed. To assign the aromatic carbons in 25d-25f based upon the assignments reported for the substituted anthracenes would not be defensible at this time.

Tentative assignments for the aromatic carbons of 25d-25f are shown in Table V. The assignments shown for the protonated aromatic carbons of 25d were made using an HETCOR 2-D experiment (Figure 10). This experiment was performed between δ 6.9 and 8.7 in the ^1H domain and between 114 and 134 ppm in the ^{13}C domain.

In order to use the information in this 2-D spectrum to assign the ^{13}C signals for the protonated aromatic carbons of 25d, the corresponding ^1H spectrum must be assigned. The assignments for these ^1H signals were made using the expected splitting patterns for each aromatic proton as shown in Table VI. It must be recognized, however, that some of these assignments are tentative and may be interchanged as noted. Using these ^1H assignments and the HETCOR 2-D experiment, the ^{13}C assignments were made as shown in Table V. Again, it must be recognized that some of the assignments may be interchanged as noted. It was possible to identify the ^{13}C signals for C(3), C(4), C(6), and C(7) unequivocally. Since H(3) and H(4) were readily distinguished in the ^1H spectrum by their splitting patterns, the ^{13}C assignments for the corresponding carbons were established using the HETCOR 2-D spectrum. The ^1H signals for H(6) and H(7) overlapped and could not be distinguished. The HETCOR 2-D experiment indicated that C(6) and C(7) gave signals at 124.6 and 124.9 ppm in the ^{13}C spectrum. The assignments for these carbons were made unequivocally using spin-lattice relaxation time measurements (Table V). As noted earlier, a protonated

TABLE V
 ^{13}C NMR ASSIGNMENTS (T_1 VALUES) OF AROMATIC CARBONS OF 25d-25f



25d n=11

25e n=13

25f n=16

Carbon Number	Chemical Shift ^a (T_1 Values (sec))		
	<u>25d</u>	<u>25e</u>	<u>25f</u>
1 ^b	125.5 (1.30)	125.5 (1.43)	125.5 (1.48)
2	139.6 (14.3)	139.5 (14.0)	139.6 (13.9)
3	127.3 (1.05)	127.3 (1.16)	127.3 (1.21)
4	127.8 (1.28)	127.8 (1.46)	127.8 (1.43)
5 ^c	127.9 (1.30)	127.9 (1.48)	128.0 (1.40)
6	124.6 (0.71)	124.6 (0.58)	124.7 (0.71)
7	124.9 (1.11)	124.9 (1.33)	125.0 (1.25)
8 ^c	127.8 (1.28)	127.8 (1.46)	127.8 (1.43)
9 ^b	125.1 (1.34)	125.1 (1.38)	125.1 (1.44)
10 ^b	125.7 (1.46)	125.6 (1.43)	125.7 (1.38)
4a ^d	131.6 (25.1)	131.6 (25.4)	131.6 (23.7)
8a ^d	130.4 (24.3)	130.3 (22.7)	130.4 (23.9)
9a ^d	131.0 (23.8)	131.0 (26.4)	131.0 (23.9)
10a ^d	131.8 (23.5)	131.7 (26.8)	131.8 (22.8)

^a Measured in ppm downfield from TMS.

^b May be interchanged.

^c May be interchanged.

^d May be interchanged.

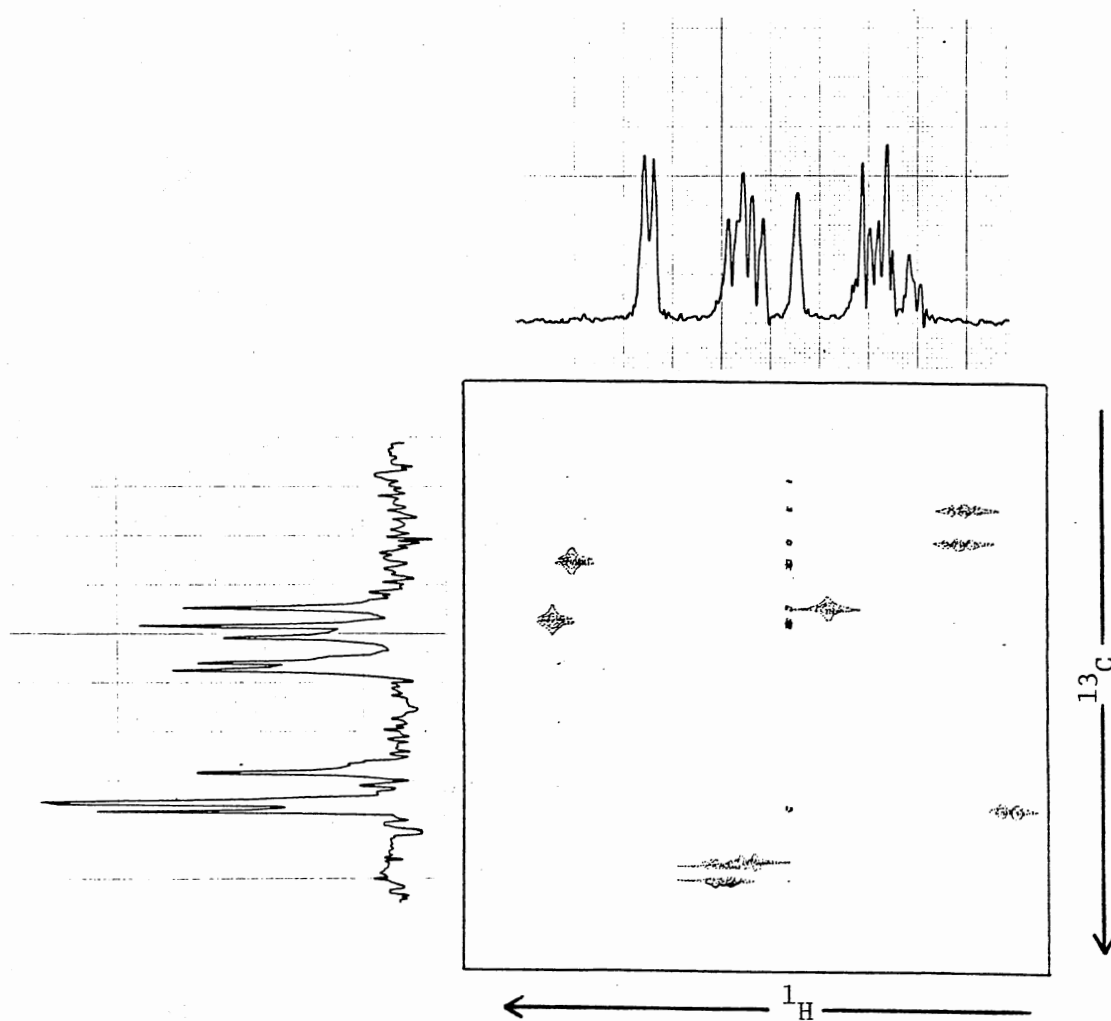
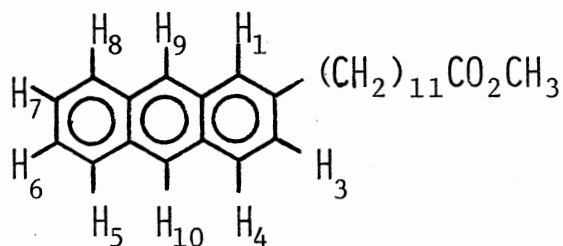


Figure 10. HETCOR 2-D Spectrum in the Aromatic Region for 25d

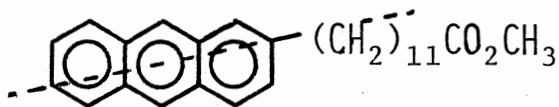
TABLE VI

¹H NMR ASSIGNMENTS FOR THE AROMATIC PROTONS OF 25d

Proton Number	Expected Splitting Pattern ^c	Observed	
		Chemical Shift (ppm)	Splitting Pattern ^c
1 ^a	d	7.68	br s
3	dd	7.27	dd
4	d	7.87	d
5 ^b	dd	7.89-7.96	m
6	ddd or pseudotriplet	7.35-7.42	pseudo t
7	ddd or pseudotriplet	7.35-7.42	pseudo t
8 ^b	dd	7.89-7.96	m
9 ^a	s	8.27	s
10 ^a	s	8.31	s

^aAssignments may be interchanged.^bAssignments may be interchanged.^cs=singlet, d=doublet, dd=doublet of doublets, t=triplet, m=multiplet.

carbon along an axis of symmetry in an aromatic molecule can be identified by its short T_1 . In 25d an axis of symmetry can be drawn through C(2) and C(6). The assignment for C(6) was made by comparison

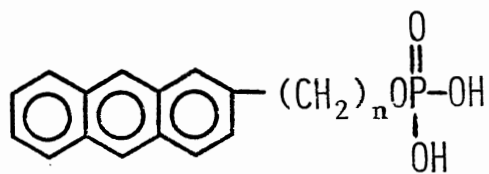


25d

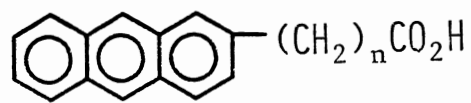
of the measured T_1 values. The carbon giving a signal at 124.6 ppm had a T_1 value of 0.71 seconds; whereas, all of the remaining aromatic carbons had T_1 values of greater than 1 second. The signal at 124.6 ppm was therefore assigned to C(6) leaving the signal at 124.9 ppm to be assigned to C(7). The assignments for the aromatic carbons of 25e and 25f were made by comparison to 25d (Table V). Again, some of these assignments may be interchanged as noted.

Suggestions for Future Work

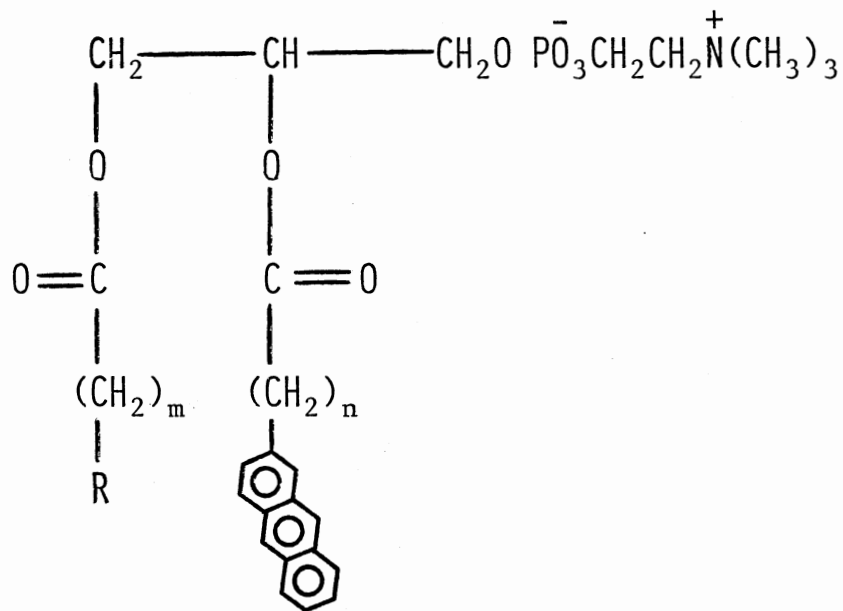
The synthesis of 25d-25f opens the door for the development of many related fluorescent probes which are potentially even more useful in studies of biological membranes. The probes 48-50 are the most obvious choices for expanding this new class of probes. The syntheses of 48 and 49 should be straightforward while synthesis of 50 will be more challenging. Finally, fluorescence experiments using 25d-25f as probes of biological membranes should be performed to determine whether these compounds are, in fact, suitable for this purpose.



48



49



50

CHAPTER III

EXPERIMENTAL SECTION

General Information

Reactions were carried out under a nitrogen atmosphere where necessary. All reactions were stirred using a magnetic stirrer unless otherwise specified. During work-up, solvents were removed using a rotatory evaporator unless otherwise stated. NMR spectral data was obtained using either a Varian XL-100(15) NMR equipped with a Nicolet TT-100 PFT accessory or a Varian XL-300 NMR. All NMR data was reported in ppm downfield from TMS using either TMS or CDCl_3 as an internal reference. IR spectral data was obtained using a Perkin Elmer 681 IR spectrophotometer. Melting points were determined using a Thomas Hoover melting point apparatus and were uncorrected.

Starting Materials

The following starting materials and special reagents were purchased from the source listed and were used without further purification: 2-methylanthraquinone (Aldrich, mp $170-173^\circ\text{C}$), 11-bromoundecanoic acid (Aldrich, mp $48-51^\circ\text{C}$), 11-bromoundecanol (Aldrich, mp $46-49^\circ\text{C}$), dihydroambrettolide (Columbia), pyridine-N-oxide (Aldrich, mp $60-64^\circ\text{C}$), and *n*-BuLi/hexane (1.6 M, Aldrich). Dry solvents were obtained as discussed below. Benzene, toluene, and diethyl ether were distilled from sodium prior to use. THF was freshly distilled from LiAlH_4 . DMF was dried

over P_2O_5 , decanted, and distilled under vacuum. DMSO was distilled under vacuum from CaH.

2-(Hydroxymethyl)anthracene (37)

2-(Hydroxymethyl)anthracene was prepared from 2-methylanthraquinone (36) using published procedures^{6,14,22,25,53} in a yield of 45%.

2-(Bromomethyl)anthracene (38)

Bromine (1.5 mL) was added dropwise under N_2 to a stirred solution of triphenylphosphine (7.0 g, 26.72 mmol) in dry DMF (40 mL) in a 100-mL round bottom flask. The alcohol 37 (5.0 g, 24.04 mmol) was added as a solid to the resulting orange suspension. After 5 min, a pale yellow solid precipitated. After stirring for an additional 75 min, the yellow solid was filtered (vacuum). A second crop of the solid was obtained by cooling the filtrate to $0^\circ C$ for 4 h. The combined solids were recrystallized ($CHCl_3$) to give 5.48 g (84.1%) of 38 as a pale yellow powder: mp $198.5-199^\circ C$ (lit.³⁴ $160^\circ C$); 1H NMR ($CDCl_3$) δ 4.79 (s, 2 H, CH_2Br), 7.24-8.37 (m, 9 H, Ar-H); Anal. Calcd for $C_{15}H_{11}Br$: C, 66.45; H, 4.06; Br, 29.49. Found: C, 66.1; H, 4.16; Br, 29.52.

(2-Anthrylmethyl)triphenylphosphonium

Bromide (33)³⁴

A solution of 38 (1.7 g, 6.27 mmol) and triphenylphosphine (1.7 g, 6.49 mmol) in dry benzene (75 mL) was heated at reflux under N_2 for 24 h in a 200-mL round bottom flask equipped with a condenser. The mixture was cooled and filtered. The resulting solid was reprecipitated from

CHCl_3 using anhydrous ether, washed with dry ether (50 mL), and dried under vacuum to give 3.0 g (89.8%) of 33 as an off-white powder: mp $> 220^\circ\text{C}$; ^1H NMR (CDCl_3) δ 5.54–5.68 (d, 2 H, CH_2P^+), 7.0–8.2 (m, 24 H, Ar-H); ^{31}P NMR (CDCl_3) 22.9 ppm (85% H_3PO_4 reference).

Methyl 11-Bromoundecanoate (40)

A solution of 11-bromoundecanoic acid (39, 20.0 g, 0.103 mol) and conc. H_2SO_4 (2 mL) in methanol (200 mL) was heated at reflux under N_2 through 3 Å molecular sieve for 48 h in a 500-mL round bottom flask equipped with a Soxhlet and a condenser. The solution was concentrated to a volume of 50 mL, diluted with ether (50 mL), and washed successively with 10% aqueous NaHCO_3 (2 x 50 mL), H_2O (25 mL), and saturated aqueous NaCl (25 mL). The solution was dried (Na_2SO_4), and the solvent was removed. Vacuum distillation gave 15.8 g (75%) of 40 as a clear, colorless liquid: bp $93\text{--}96^\circ\text{C}/0.025$ mm (lit.¹² $126\text{--}128^\circ\text{C}/0.65$ mm); IR (neat) 1740 cm^{-1} (C=O); ^1H NMR (CDCl_3) δ 1.28–1.9 [m, 16 H, $(\text{CH}_2)_8$], 2.29 [t, 2 H, $\text{CH}_2\text{CO}_2\text{Me}$], 3.39 [t, 2 H, CH_2Br], 3.64 [s, 3 H, OCH_3]; ^{13}C NMR (CDCl_3) ppm 173.9 [C(1)], 51.3 [C(1')], 34.0, 33.8, 32.8, 29.3, 29.1, 29.1, 28.7, 28.1, 24.9 [C(2)].

Methyl 11-Oxoundecanoate (34a)⁵⁶

A mixture of 40 (7.0 g, 25.1 mmol), pyridine-N-oxide (4.8 g, 50.5 mmol), and NaHCO_3 (4.2 g, 50.0 mmol) in dry toluene (32 mL) in a 100-mL, round bottom flask equipped with a condenser was heated at reflux under N_2 with vigorous stirring for 6 h. The resulting dark brown mixture was cooled, washed with H_2O (2 x 25 mL), and dried (Na_2SO_4). Removal of the solvent (vacuum) gave a dark brown oil which

was distilled (vacuum) to give 3.7 g (69%) of 34a as a colorless liquid: bp 95-98°C/0.05 mm; IR (neat) 1720-1740 cm⁻¹ (C=O); ¹H NMR (CDCl₃) δ 1.3-1.7 [m, 14 H, (CH₂)₇], 3.23-3.5 [m, 4 H, H(2), H(10)], 3.66 [s, 3 H, OCH₃], 9.74 [t, 1 H, CHO].

Methyl 12-(2-Anthryl)-11-dodecenoate (35a)

A solution of 33 (2.5 g, 4.69 mmol) in anhydrous DMSO (65 mL) was added dropwise with stirring under N₂ at room temperature (RT) to a 50% mineral oil dispersion of NaH (0.25 g, 5.208 mmol) in a 250-mL round bottom flask. The resulting blood-red solution was stirred at RT for 10 min. A solution of the aldehyde 34a (1.9 g, 8.879 mmol) in dry DMSO (5 mL) was then added in one portion. The mixture was stirred for an additional 48 h at RT, diluted with H₂O (150 mL), and acidified (litmus) with conc. HCl. The resulting yellow solid was filtered (vacuum) and air-dried in the dark. The solid was digested twice with 95% ethanol (50 mL) and dried in the dark to give 1.4 g (76.9%) of 35a as a light yellow powder: mp 121->250°C; ¹H NMR (CDCl₃) δ 1.2-1.7 [m, 14 H, (CH₂)₇], 2.18-2.62 [m, 4 H, CH=CHCH₂ and CH₂CO₂Me], 3.63 [s, 3 H, OCH₃], 6.34-6.56 [m, 1 H, ArCH=CH, trans], 7.22-8.35 [m, 10 H, Ar-H and ArCH=CH, trans]. A small amount (~23%) of the cis isomer was present as indicated by ¹H NMR signals at δ 5.6-5.94 [m, ArCH=CH, cis] and 6.6-6.7 [d, ArCH=CH, cis]. The wide mp is probably due to the cis-trans mixture.

Methyl 12-(2-Anthryl)dodecanoate (25d)

A solution of 35a (0.4 g, 1.031 mmol) in ethyl acetate (75 mL) was hydrogenated at RT and atmospheric pressure in the presence of 10% Pd/C (0.1 g) for 4 h. Addition of diatomaceous earth followed by vacuum

filtration and evaporation of the solvent gave an off-white solid. The solid was recrystallized (95% ethanol) twice and then subjected twice to molecular distillation ($110^{\circ}\text{C}/5 \times 10^{-4}$ mm) to give 0.3 g (74.6%) of 25d as a white powder: mp 104.5°C - 105°C ; ^1H NMR (CDCl_3) δ 1.29-1.9 [m, 18 H, $(\text{CH}_2)_9$], 2.28 [t, 2 H, $\text{CH}_2\text{CO}_2\text{Me}$], 2.78 [t, 2 H, ArCH_2], 3.64 [s, 3 H, OCH_3], 7.21-8.34 [m, 9 H, Ar-H]; Anal. Calcd for $\text{C}_{27}\text{H}_{34}\text{O}_2$: C, 83.08; H, 8.72. Found: C, 83.02; H, 8.99; Mass spectral data for $\text{C}_{27}\text{H}_{34}\text{O}_2$: m/e (M^+) 390.2559; Found: 390.2550.

Methyl 13-Hydroxytridecanoate (42)

A solution of n-butyllithium in hexane (1.6 M, 44.3 mL, 70.88 mmol) was added dropwise under N_2 to a stirred solution of 2,4,4-trimethyloxazoline (8.0 g, 70.796 mmol) in dry THF (80 mL) at -78°C in a 500-ml round bottom flask. The solution was stirred at -78°C for an additional 10 min at which time a solution of lithium 11-bromoundecoxide in THF [generated by treatment of 11-bromoundecanol (17.8 g, 70.94 mmol) in 45 mL of dry THF with n-butyllithium in hexane (1.6 M, 44.4 mL, 71.04 mmol)] was added dropwise. The mixture was stirred at -78°C for 10 min and at RT for an additional 2 h. The mixture was poured into ice water (250 mL), acidified (litmus) with conc. HCl, and extracted with ether (100 mL). The aqueous layer was neutralized with cooling (ice bath) using 40% aqueous NaOH and extracted with ether (3 x 100 mL). The organic layer was washed with saturated aqueous NaCl (2 x 100 mL) and dried (MgSO_4). The solvent was evaporated to leave 41 as a tan oil which solidified upon cooling (15.95 g, 79.1%). A solution of the crude oxazoline 41 in CH_3OH (300 mL), H_2O (10 mL), and conc. H_2SO_4 (12 mL) was heated at reflux in a 500-mL round bottom flask

for 18 h. The solution was concentrated to 75 mL, poured into cold H₂O (150 mL), and extracted with ether (2 x 100 mL). The organic layer was washed successively with 5% aqueous NaHCO₃ (2 x 100 mL) and saturated aqueous NaCl (2 x 100 mL) and dried (MgSO₄). Removal of the solvent left a tan oil which solidified upon cooling. Recrystallization (petroleum ether), with cooling to 0°C, gave 8.2 g (47.5%) of 42 as a white solid: mp 38.5-39.5°C (lit.³³ 40.5-41.5°C); IR (melt) 2900-3600 (OH), 1740 cm⁻¹ (C=O); ¹H NMR (CDCl₃) δ 1.28-1.7 [m, 20 H, (CH₂)₁₀], 1.8-1.9 [br s, 1 H, OH], 2.42 [t, 2 H, CH₂CO₂Me], 3.58-3.70 [m, 5 H, OCH₃ and CH₂OH]; ¹³C NMR (CDCl₃) ppm 174.1 [C(1)], 62.9 [C(13)], 51.3 [C(α)], 34.1 [C(2)], 32.8, 29.6, 29.5, 29.4, 29.3, 29.2, 29.1, 25.7, 24.9 [C(3)].

Methyl 13-Oxotridecanoate (34b)⁴¹

Chromium trioxide (6.2 g, 62.00 mmol) was added under N₂ to a stirred solution of pyridine (9.7 g, 122.8 mmol) in CH₂Cl₂ (150 mL) in a 300-mL round bottom flask. After 20 min, a solution of the alcohol 42 (2.5 g, 10.25 mmol) in CH₂Cl₂ (20 mL) was added in one portion. After stirring for an additional 20 min, the solution was decanted, and the tarry residue was washed with ether (2 x 75 mL). The combined organic solutions were washed with 5% aqueous NaOH (4 x 100 mL), 5% aqueous HCl (2 x 100 mL), saturated aqueous NaHCO₃ (2 x 100 mL), and saturated aqueous NaCl (150 mL). After drying (MgSO₄), the solvent was removed to give 2.38 g (96%) of crude 34b as a light yellow oil. The aldehyde 34b was used in subsequent reactions without further purification. IR (neat) 1720-1740 cm⁻¹ (C=O); ¹H NMR (CDCl₃) δ 1.2-1.7 [m, 18 H, (CH₂)₉], 2.2-2.5 (m, 4 H, CH₂CO₂Me and CH₂CHO), 3.66 (s, 3 H,

OCH₃), 9.74 (t, 1 H, CHO); ¹³C NMR (CDCl₃) ppm 202.6 [C(13)], 174.0 [C(1)], 51.3 [C(α)], 43.8 [C(12)], 34.0 [C(2)], 29.4, 29.35, 29.3, 29.3, 29.1, 24.9 [C(3)], 22.1 [C(11)].

Methyl 14-(2-Anthryl)-13-tetradecenoate (35b)

A solution of the phosphonium salt 33 (2.0 g, 3.753 mmol) in dry DMSO (75 mL) was added rapidly under N₂ to a stirred 50% mineral oil dispersion of NaH (0.2 g, 4.167 mmol) in a 100-mL round bottom flask. The resulting blood-red solution was stirred for 10 min, and a solution of the aldehyde 34b (1.4 g, 5.785 mmol) in dry ether (5 mL) was then added in one portion. The resulting mixture was stirred for 24 h at RT, diluted with H₂O (75 mL), and acidified (litmus) with conc. HCl. Vacuum filtration gave a bright yellow solid which was digested in 95% ethanol (50 mL) and air-dried in the dark (1.4 g, 89.7%): mp 108→250°C; ¹H NMR (CDCl₃) δ 1.04-1.76 [m, 18 H, (CH₂)₉], 2.12-2.58 [m, 4 H, CH=CHCH₂, CH₂CO₂CH₃], 3.63 [s, 3 H, OCH₃], 6.32-6.54 [m, 1 H, ArCH=CH, trans], 7.24-8.36 [m, 10 H, Ar-H, ArCH=CH, trans]. A small amount of the cis isomer was present as indicated by ¹H NMR signals at δ 5.58-5.9 [m, ArCH=CH, cis] and 6.56-6.69 [m, ArCH=CH, cis]. The wide mp is probably due to the cis-trans mixture.

Methyl 14-(2-Anthryl)tetradecanoate (25e)

A solution of 35b (0.5 g, 1.202 mmol) in warm ethyl acetate (150 mL) was hydrogenated at atmospheric pressure in the presence of 10% Pd/C (0.1 g) for 4 h in a 300-mL hydrogenation flask. Diatomaceous earth was added, and the mixture was filtered. Evaporation of the solvent left a pale yellow solid. Recrystallization (95% ethanol) (twice) and molecular distillation (110°C, 5 x 10⁻⁴ mm) (twice) gave

0.4 g (79.6%) of 25e as a white powder: mp 103–103.5°C; ^1H NMR (CDCl_3) δ 1.2–1.7 [m, 22 H, $(\text{CH}_2)_{11}$], 2.27 [t, 2 H, $\text{CH}_2\text{CO}_2\text{Me}$], 2.78 [t, 2 H, ArCH_2], 3.63 [s, 3 H, OCH_3], 7.2–8.34 [m, 9 H, Ar-H]; Mass spectral data for $\text{C}_{29}\text{H}_{38}\text{O}_2$: m/e (M^+) 418.2872; Found: 418.2862.

Methyl 16-Hydroxyhexadecanoate (44)

A solution of dihydroambrettolide (43, 5.0 g, 19.685 mmol) and *p*-toluenesulfonic acid (PTSA, 1.0 g) in methanol (250 mL) was heated at reflux under N_2 for 18 h in a 500-mL round bottom flask equipped with a condenser. The solution was concentrated to 75 mL, poured into cold H_2O (100 mL), and extracted with ether (3 x 75 mL). The organic layer was washed with 10% aqueous NaHCO_3 (2 x 75 mL) and dried (MgSO_4). Removal of the solvent left a waxy white solid. Recrystallization (petroleum ether, bp 37.7–56.9°C) gave 4.8 g (85.3%) of 44 as a flakey white solid: mp 56–57°C; IR (melt) 2900–3600 (OH), 1740 cm^{-1} (C=O); ^{13}C NMR (CDCl_3) ppm 174.1 [C(1)], 62.8 [C(16)], 51.3 [C(α)], 34.1 [C(2)], 32.8, 29.6, 29.4, 29.2, 29.1, 25.8, 24.9 [C(3)].

Methyl 16-Oxohexadecanoate (34c)

Chromium trioxide (6.3 g, 63.0 mmol) was added under N_2 to a stirred solution of pyridine (9.9 g, 125.3 mmol) in CH_2Cl_2 (150 mL) in a 300-mL round bottom flask. After 20 min, a solution of the alcohol 44 (3.0 g, 10.489 mmol) in CH_2Cl_2 (20 mL) was added in one portion. After an additional 20 min, the solution was decanted, and the tarry residue was washed with ether (2 x 75 mL). The combined organic solutions were washed successively with 5% aqueous NaOH (4 x 100 mL), 5% aqueous HCl (2 x 100 mL), saturated aqueous NaHCO_3 (2 x

100 mL), and saturated aqueous NaCl (150 mL). After drying (MgSO_4), the solvent was evaporated to give 2.5 g (83.9%) of crude 34c as a white solid. This solid was used in subsequent reactions without further purification: mp 67–69°C; IR (melt) 1720–1740 cm^{-1} (C=O); ^{13}C NMR (CDCl_3) ppm 202.4 [C(16)], 173.9 [C(1)], 51.2 [C(α)], 43.7 [C(15)], 34.0 [C(2)], 29.5, 29.4, 29.3, 29.2, 29.1, 29.0, 24.8 [C(3)], 22.0 [C(14)].

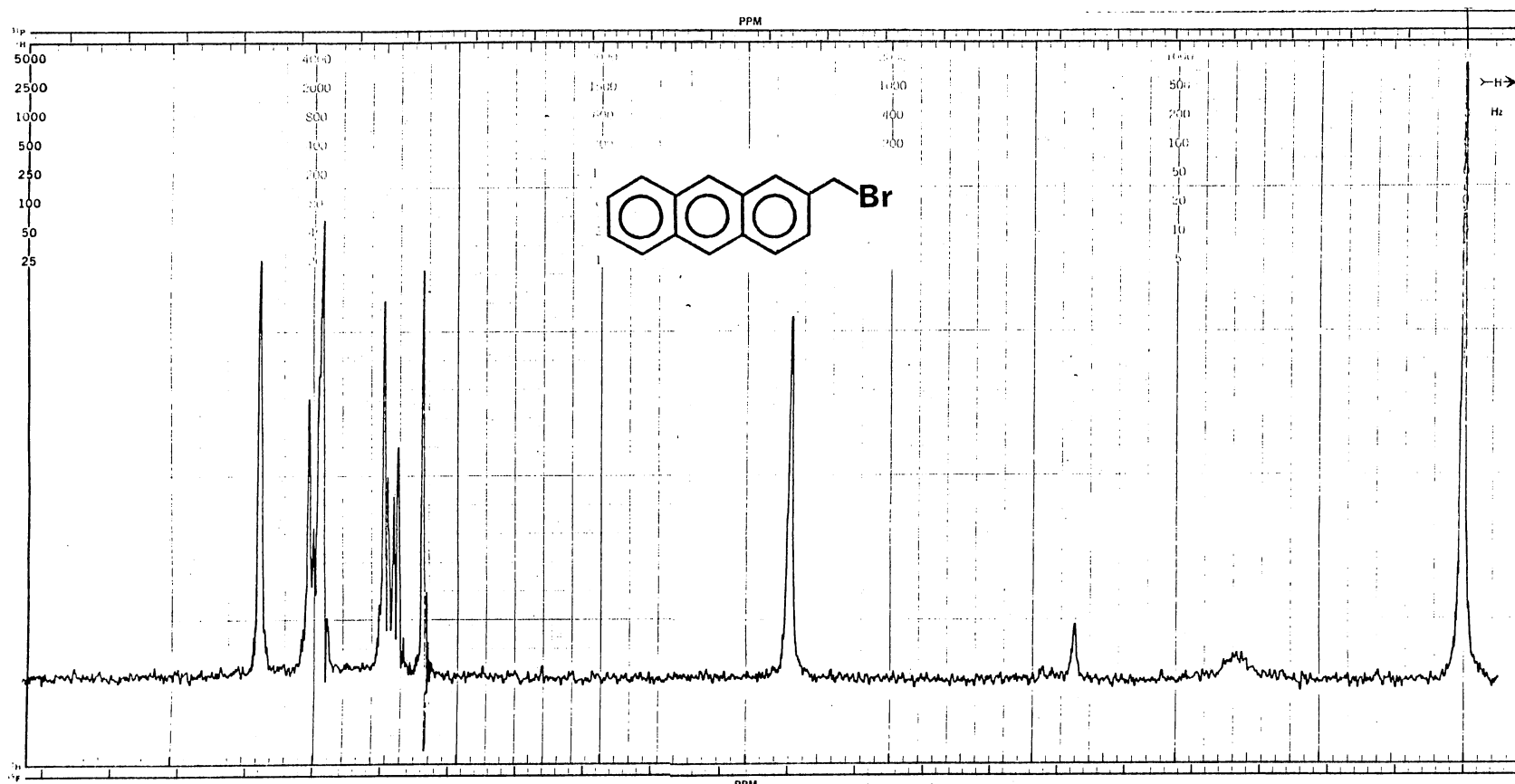
Methyl 17-(2-Anthryl)-16-heptadecenoate (35c)

A solution of the phosphonium salt 33 (2.0 g, 3.753 mmol) in dry DMSO (75 mL) was added rapidly under N_2 to a stirred mineral oil dispersion of NaH (50%, 0.2 g, 4.167 mmol) in a 300-mL round bottom flask. After 10 min, a solution of the crude aldehyde 34c (1.9 g, 6.69 mmol) in dry ether (50 mL) was added to the blood-red solution. After stirring for 30 h at RT, the mixture was diluted with H_2O (100 mL) and acidified (litmus) with conc. HCl. The mixture was filtered (vacuum) to give a yellow powder. The filtrate was extracted with CHCl_3 (3 x 50 mL). The organic layers were combined and dried (Na_2SO_4). Removal of the solvent left a yellow semisolid. The combined solids were digested in 95% ethanol (40 mL) and air-dried in the dark to give 1.4 g (81.4%) of 35c as a yellow powder: mp 110–>250°C; ^1H NMR (CDCl_3) δ 1.1–1.75 [m, 24 H, $(\text{CH}_2)_{12}$], 2.17–2.6 [m, 4 H, $\text{CH}=\text{CHCH}_2$, $\text{CH}_2\text{CO}_2\text{CH}_3$], 3.65 [s, 3 H, OCH_3], 6.55–6.8 [m, 1 H, $\text{ArCH}=\text{CH}$, trans], 7.45–8.6 [m, 10 H, Ar-H , $\text{ArCH}=\text{CH}$, trans]. A small amount of the cis isomer was present as indicated by the ^1H NMR signals at δ 5.85–6.2 [m, $\text{ArCH}=\text{CH}$, cis] and 6.8–6.9 [m, $\text{ArCH}=\text{CH}$, cis]. The wide mp is probably due to the cis-trans mixture.

Methyl 17-(2-Anthryl)heptadecanoate (25f)

A warm solution of 35c (0.5 g, 1.092 mmol) in ethyl acetate (175 mL) was hydrogenated at atmospheric pressure in the presence of 10% Pd/C (0.1 g) for 4 h in a 300-mL hydrogenation flask. Addition of diatomaceous earth, vacuum filtration, and evaporation of the solvent gave an off-white powder. The solid was recrystallized twice (95% ethanol) and subjected twice to molecular distillation (140°C/5 x 10⁻⁴ mm) to give 0.4 g (80%) of 25f as a white powder: mp 104.5-105.5°C; ¹H NMR (CDCl₃) δ 1.2-1.85 [m, 28 H, (CH₂)₁₄], 2.29 [t, 2 H, CH₂CO₂Me], 2.79 [t, 2 H, ArCH₂], 3.65 [s, 3 H, OCH₃], 7.2-8.34 [m, 9 H, Ar-H]; Mass spectral data for C₃₂H₄₄O₂: m/e (M⁺) 460.3341; Found: 460.3349.

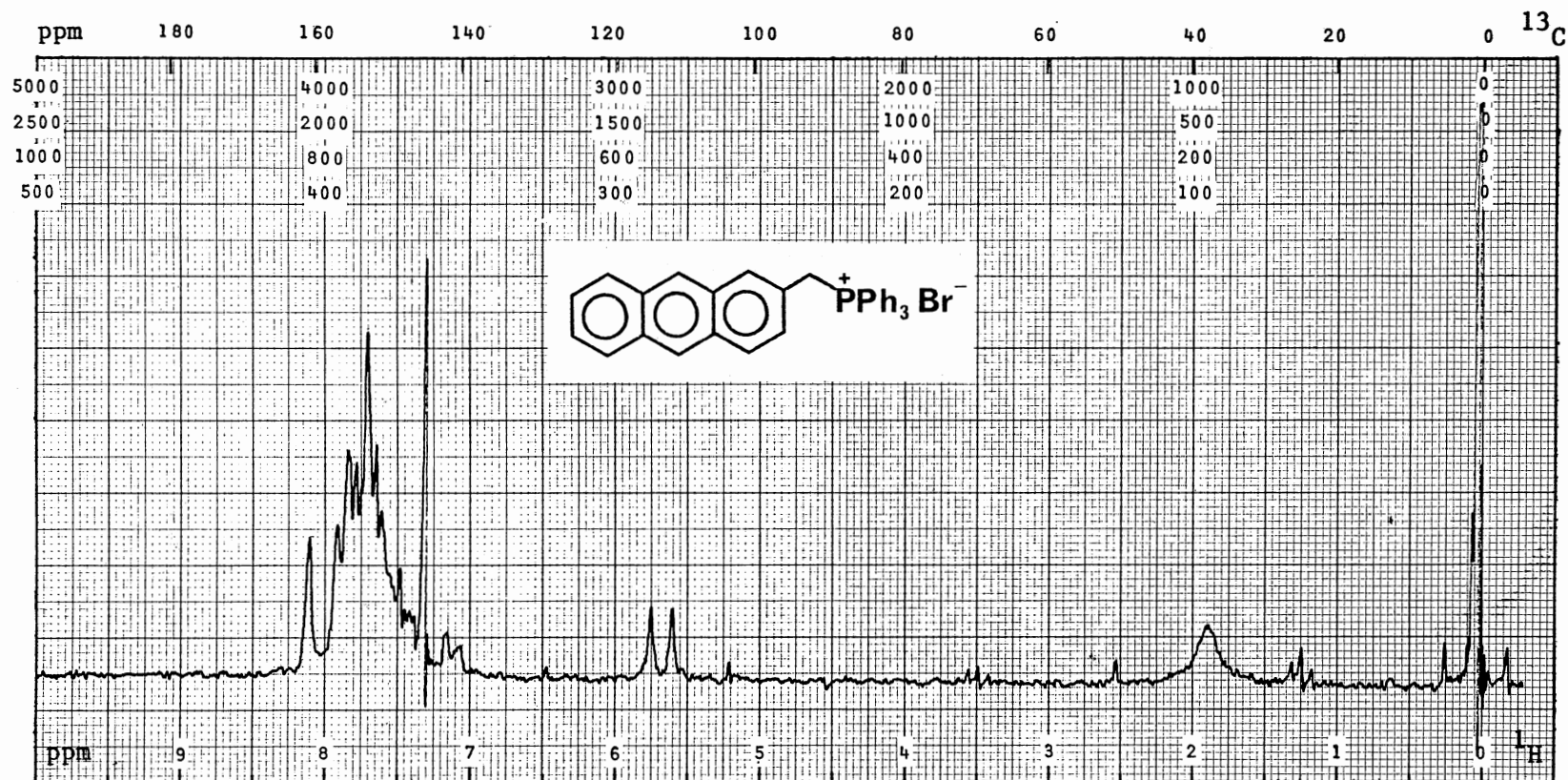
PLATE I



¹H NMR Spectrum of 38

PFT _ CW X ; Solvent. . . CDCl₃ ; SO. . 85771 Hz ; PW. . 1000 Hz ; T. . 30 °C ; Acq/SA. .
 Size. . K ; P2/RF. . 65 μs/dB ; SF. . 100.1 Hz ; FB. . 2 Hz ; Lock. . ²H ; D5/ST. . 250 s
 DC. . ; Gated Off. . ; Offset. . Hz ; RF. . W/dB ; NBW. . Hz

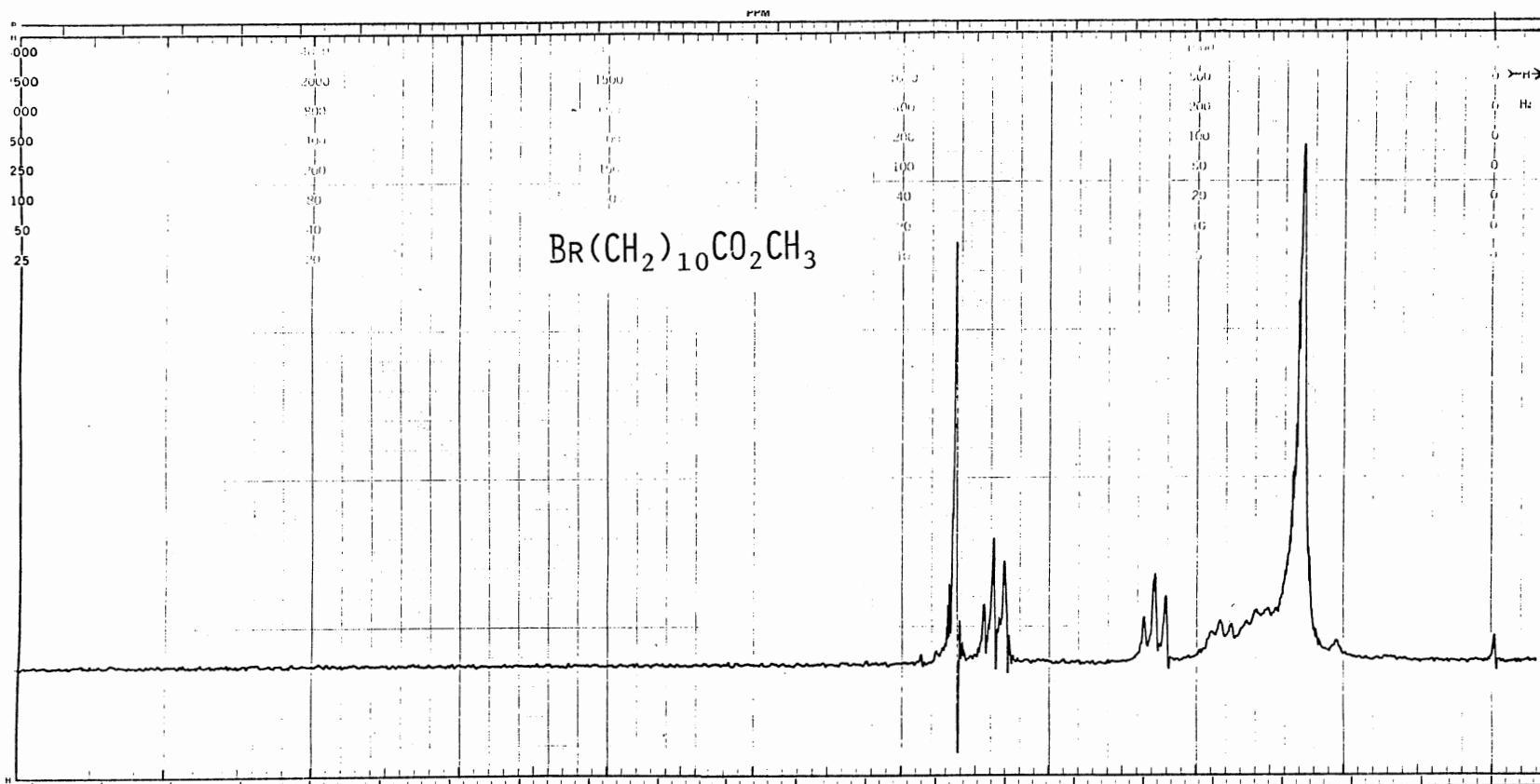
PLATE II



^1H NMR Spectrum of 33

PFT_CW_X; Solvent. . CDCl_3 ; SO. . 85771 Hz; PW. . 1000 Hz; T. . 30 °C; Acq/SA. .
 Size. . K; P2/RF. . 57 $\mu\text{s}/\text{dB}$; SF. . 100.1 Hz; FB. . 2 Hz; Lock. . ^2H ; D5/ST. . 250 s
 DC. . ; Gated Off. . ; Offset. . Hz; RF. . W/dB; NBW. . Hz

PLATE III



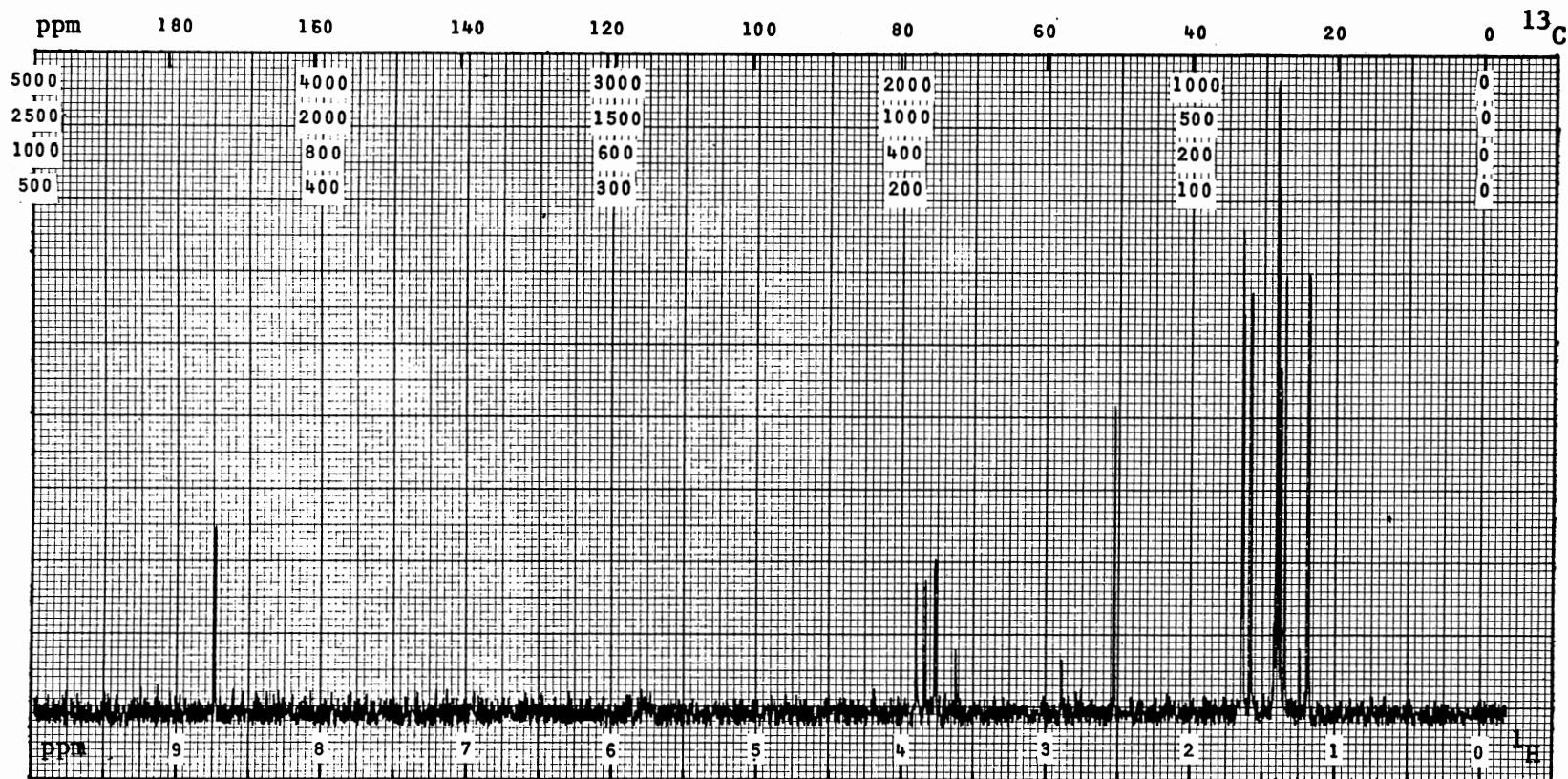
¹H NMR Spectrum of 40

PFT _ CW X ; Solvent . . CDCl₃ ; SO . . 85771 Hz ; PW . . 1000 Hz ; T . . 30 °C ; Acq/SA . .

Size . . K ; P2/RF . . 60 μs/dB ; SF . . 100.1 Hz ; FB . . 2 Hz ; Lock . . ²H ; D5/ST . . 250 s

DC . . ; Gated Off . . ; Offset . . Hz ; RF . . W/dB ; NBW . . Hz

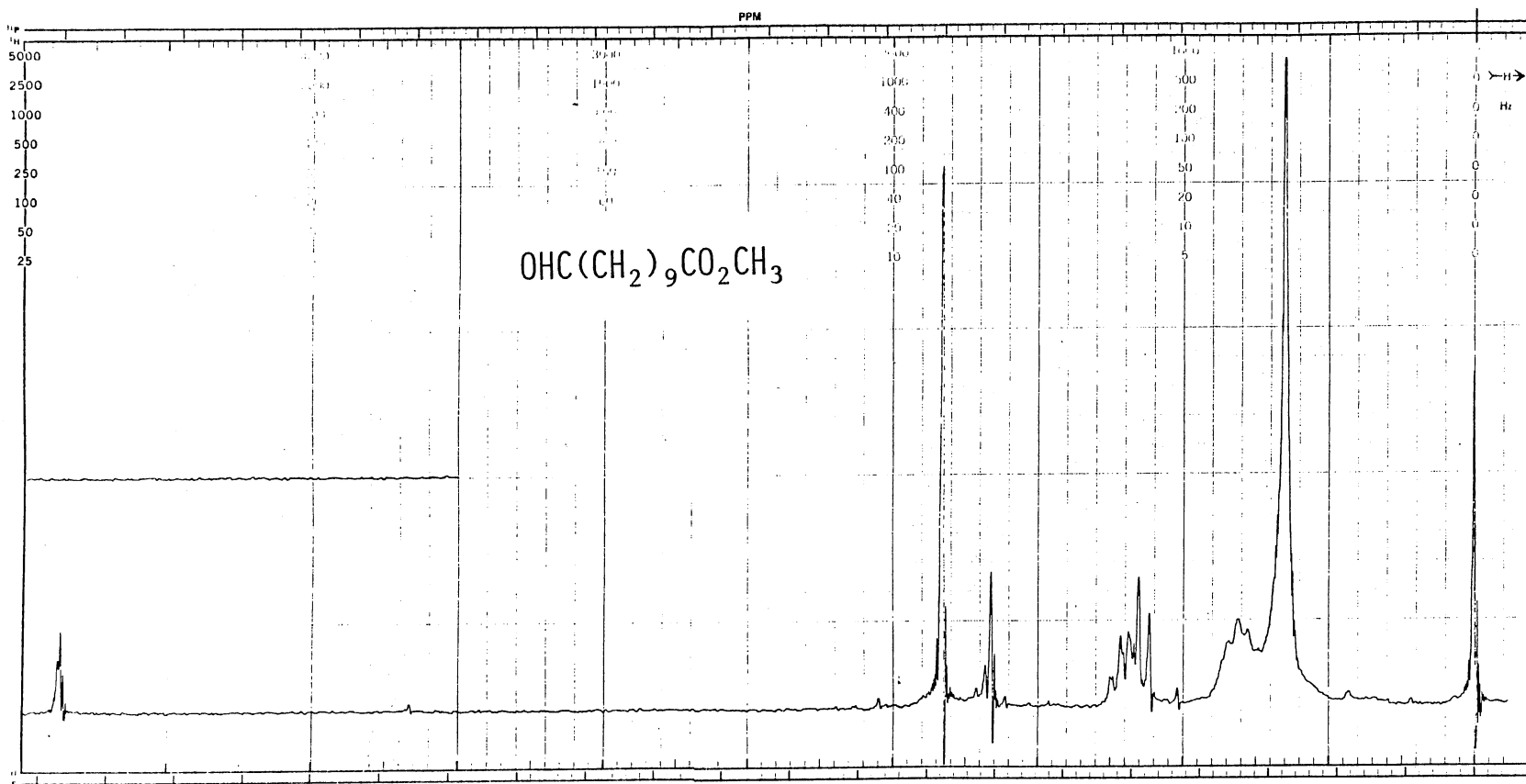
PLATE IV



^{13}C NMR Spectrum of 40

PFT X CW ; Solvent. . CDCl_3 ; SO. . 35101 Hz; PW. . 5000 Hz; T. . 30 °C; Acq/SA. . 500
 Size. . 8 K; P2/RF. . 10 $\mu\text{s}/\text{dB}$; SF. . 25.2 Hz; FB. . Hz; Lock. . ^2H ; D5/ST. . 5 s
 DC. . ^1H ; Gated Off. . ; Offset. . 45051 Hz; RF. . 9 W/dB; NBW. . Hz

PLATE V



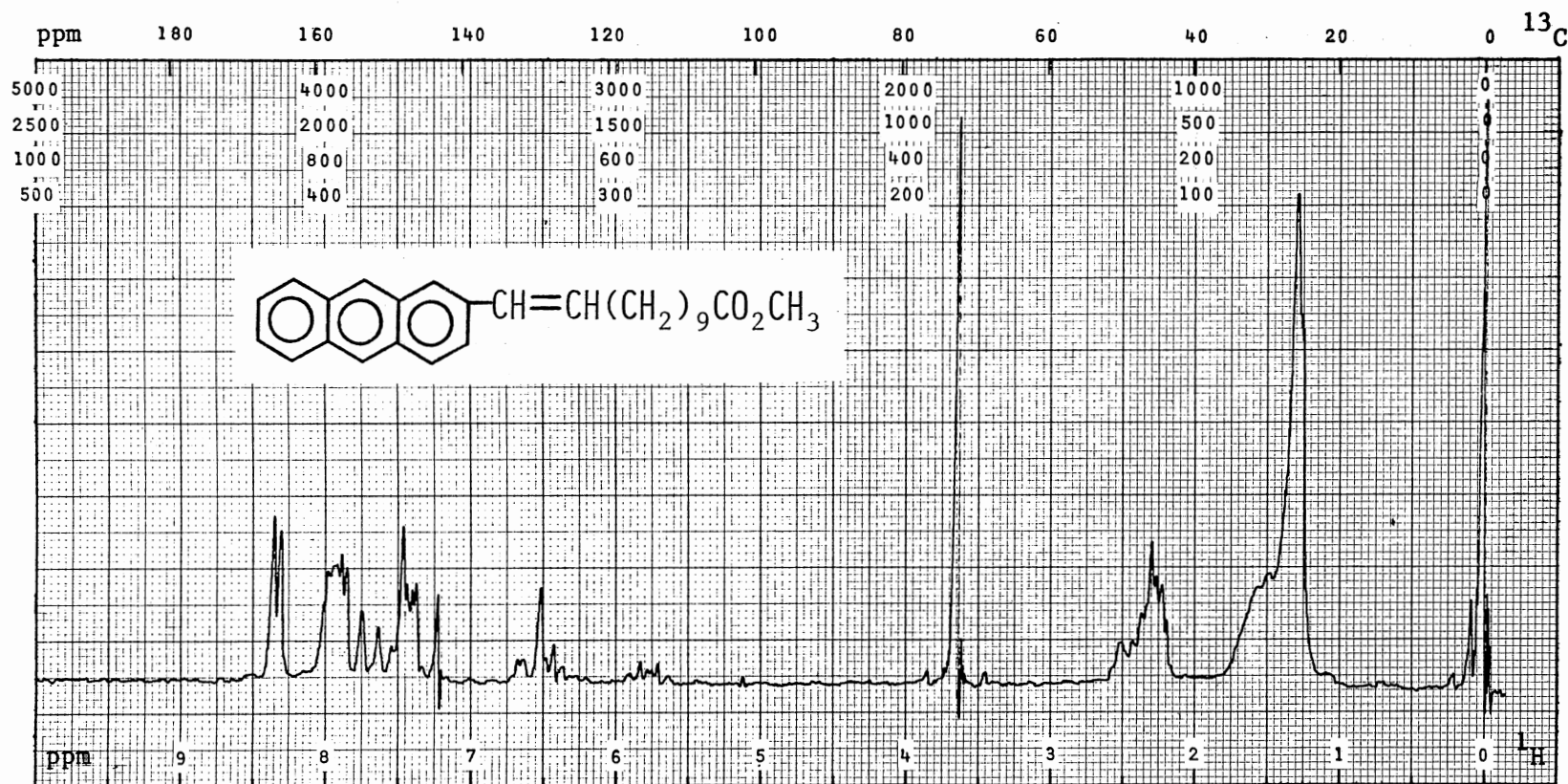
¹H NMR Spectrum of 34a

PFT _ CW X ; Solvent . . CDCl₃ ; SO . . 85771 Hz; PW . . 1000 Hz; T . . 30 °C; Acq/SA . .

Size . . K; P2/RF . . 58 μs/dB; SF . . 100.1 Hz; FB . . 2 Hz; Lock . . ²H ; D5/ST . . 250 s

DC . . ; Gated Off . . ; Offset . . Hz; RF . . W/dB; NBW . . Hz

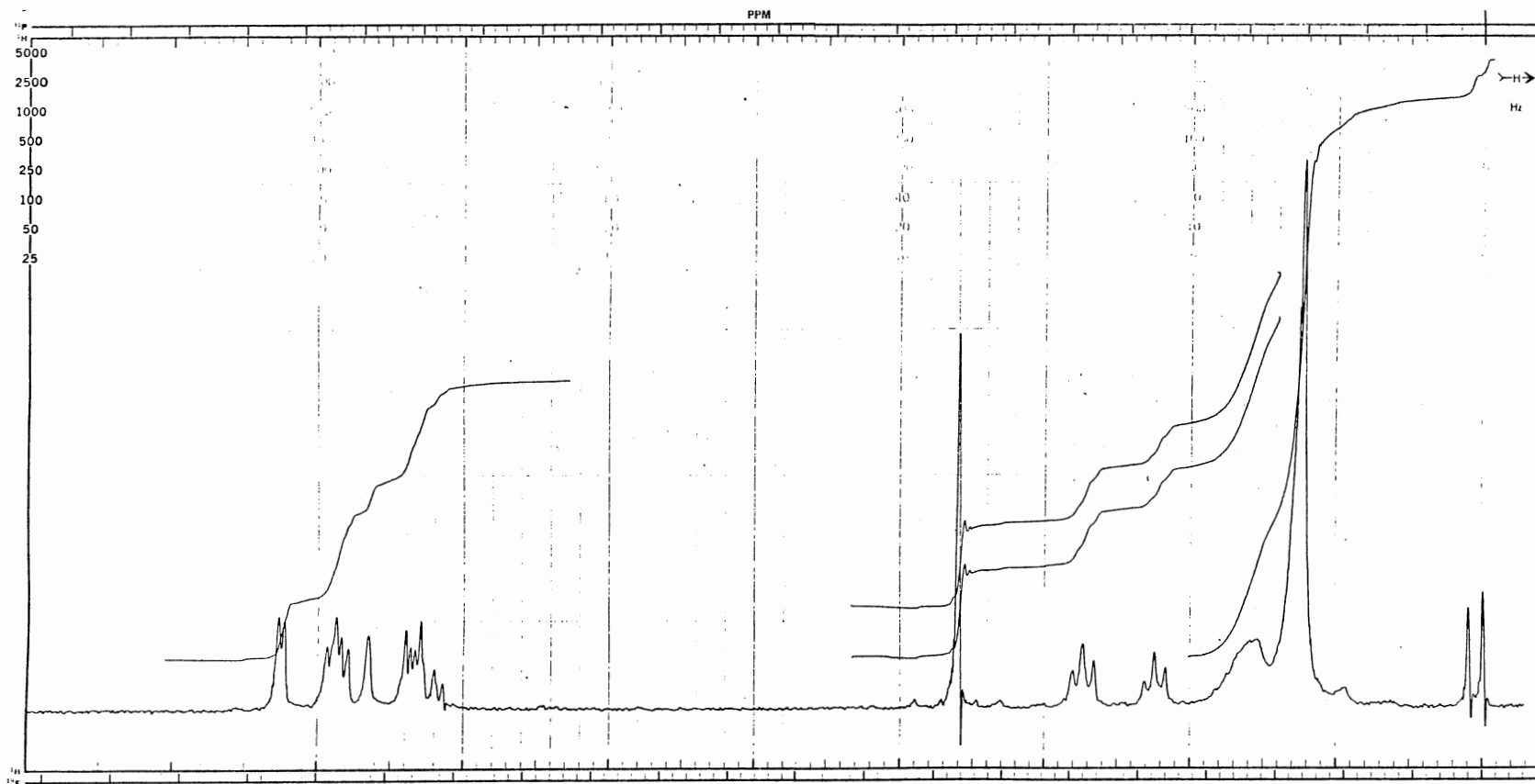
PLATE VI



^1H NMR Spectrum of 35a

PFT _ CW _ X; Solvent. . CDCl_3 ; SO. . 85771 Hz; PW. . 1000 Hz; T. . 30 °C; Acq/SA. .
 Size. . K; P2/RF. . 60 $\mu\text{s}/\text{dB}$; SF. . 100.1 Hz; FB. . 2 Hz; Lock. . ^2H ; D5/ST. . 250 s
 DC. . ; Gated Off. . ; Offset. . Hz; RF. . W/dB; NBW. . Hz

PLATE VII



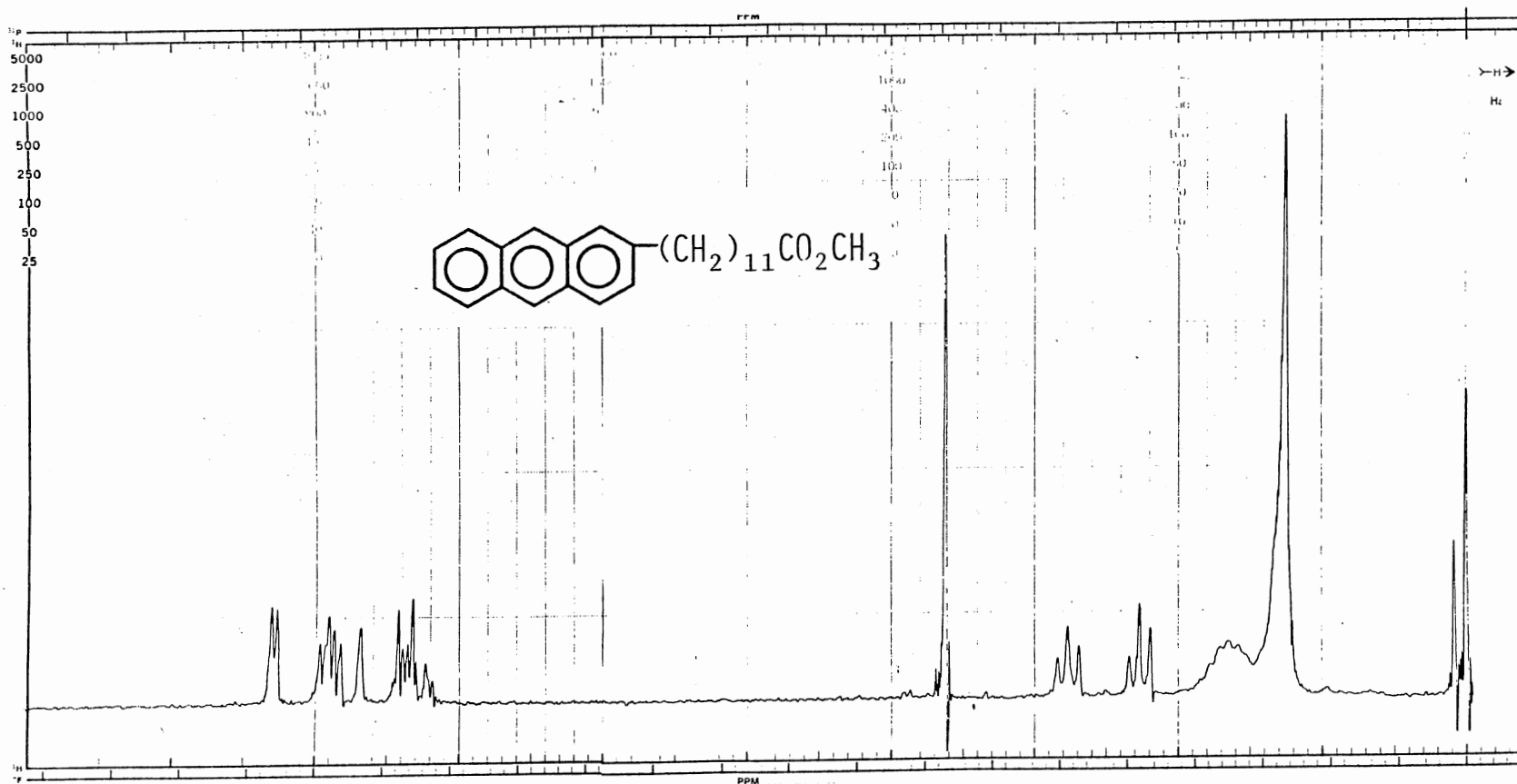
^1H NMR Spectrum of 51

PFT _ CW X ; Solvent. . CDCl_3 ; SO. .85771 Hz; PW. . 1000 Hz; T. . 30 °C; Acq/SA. .

Size. . K; P2/RF. . 59 $\mu\text{s}/\text{dB}$; SF. .100.1 Hz; FB. . 2 Hz; Lock. . ^2H ; D5/ST. . 250 s

DC. . ; Gated Off. . ; Offset. . Hz; RF. . W/dB; NBW. . Hz

PLATE VIII



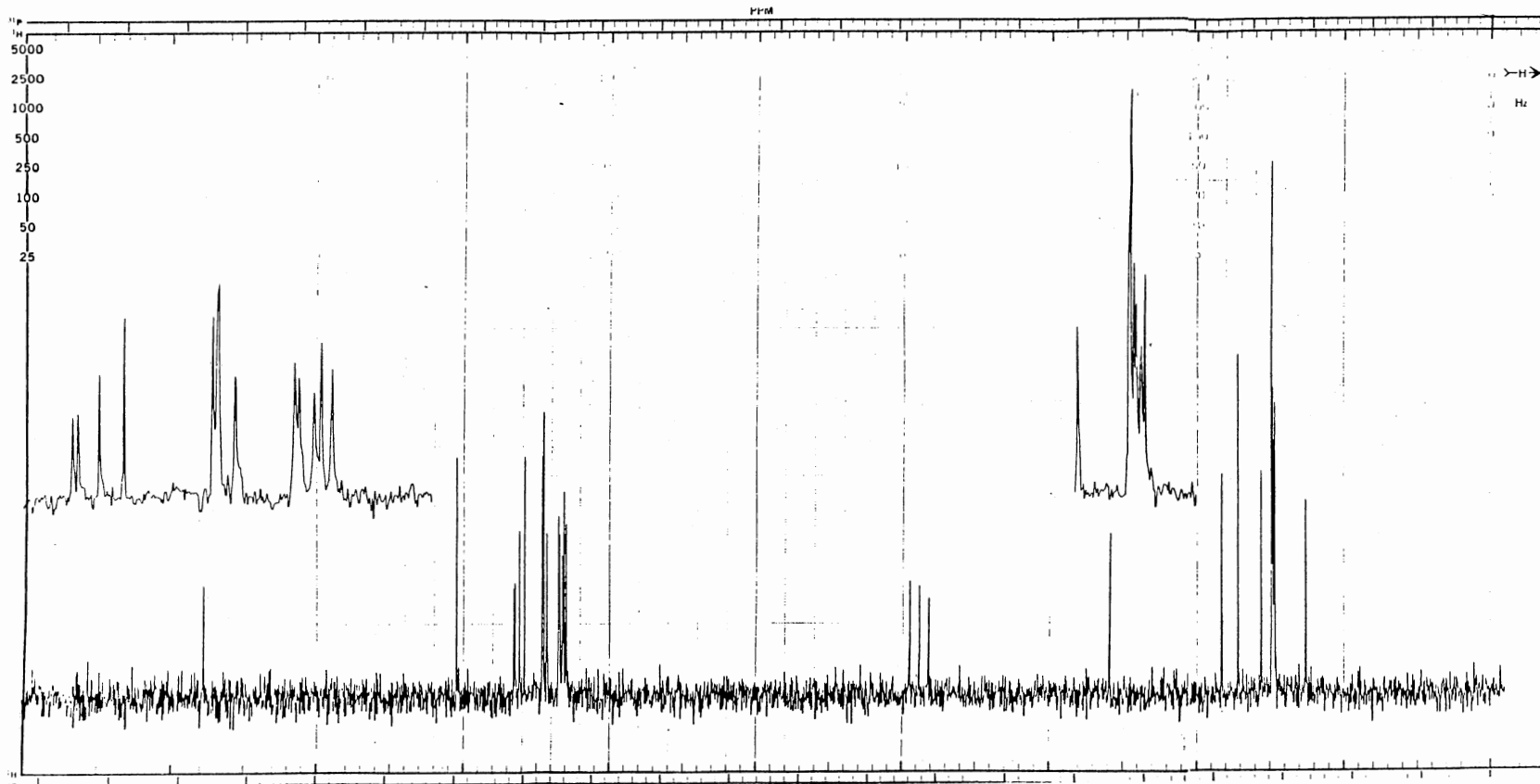
¹H NMR Spectrum of 25d

PFT _ CW _ X; Solvent. . CDCl₃ ; SO. . 85771 Hz; PW. . 1000 Hz; T. . 30 °C; Acq/SA. .

Size. . K; P2/RF. . 58 μs/dB; SF. . 100.1 Hz; FB. . 2 Hz; Lock. . ²H ; D5/ST. . 250 s

DC. . ; Gated Off. . ; Offset. . Hz; RF. . W/dB; NBW. . Hz

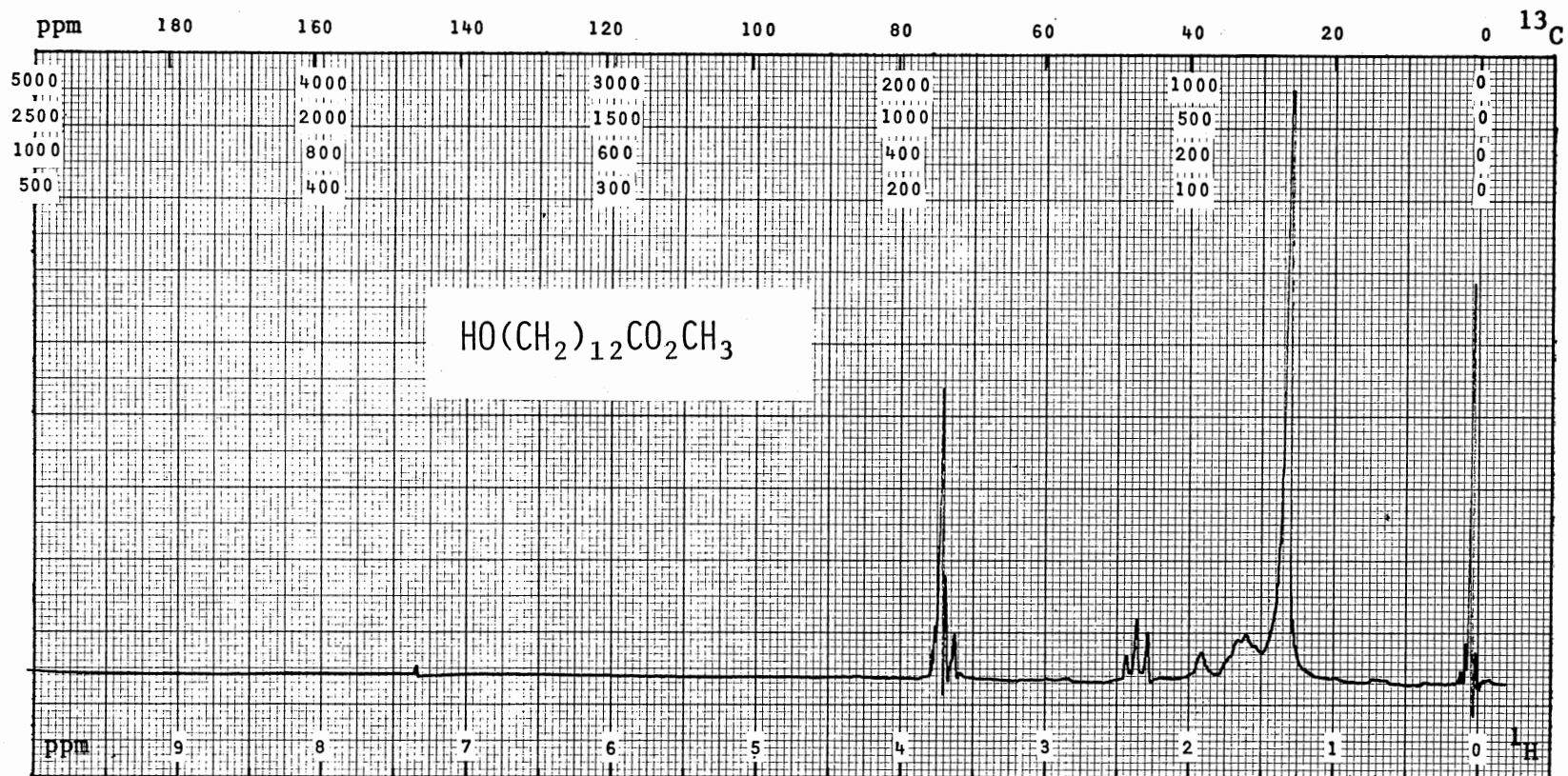
PLATE IX



^{13}C NMR Spectrum of 25d

PFT X CW _ ; Solvent. . CDCl_3 ; SO. . 35101 Hz; PW. . 5000 Hz; T. . 30 °C; Acq/SA. . 500
 Size. . 8 K; P2/RF. . 10 $\mu\text{s}/\text{dB}$; SF. . 25.2 Hz; FB. . Hz; Lock. . ^2H ; D5/ST. . 5 s
 DC. . ^1H ; Gated Off. . ; Offset. . 45051 Hz; RF. . 9 W/dB; NBW. . Hz

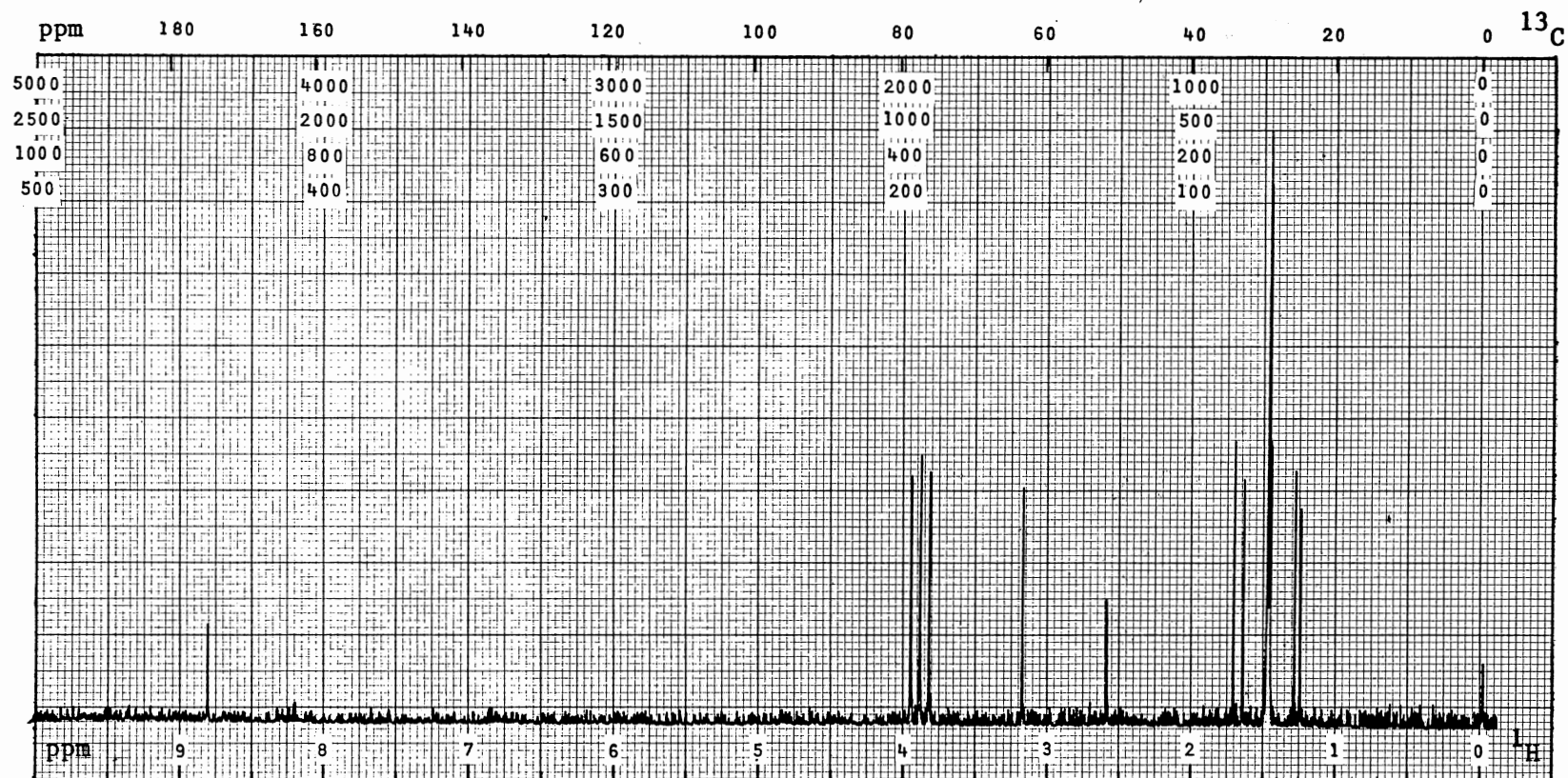
PLATE X



^1H NMR Spectrum of 42

PFT _ CW X; Solvent. . CDCl_3 ; SO. . 85771 Hz; PW. . 1000 Hz; T. . 30 °C; Acq/SA. .
 Size. . K; P2/RF. . 61 $\mu\text{s}/\text{dB}$; SF. . 100.1 Hz; FB. . 2 Hz; Lock. . ^2H ; D5/ST. . 250 s
 DC. . ; Gated Off. . ; Offset. . Hz; RF. . W/dB; NBW. . Hz

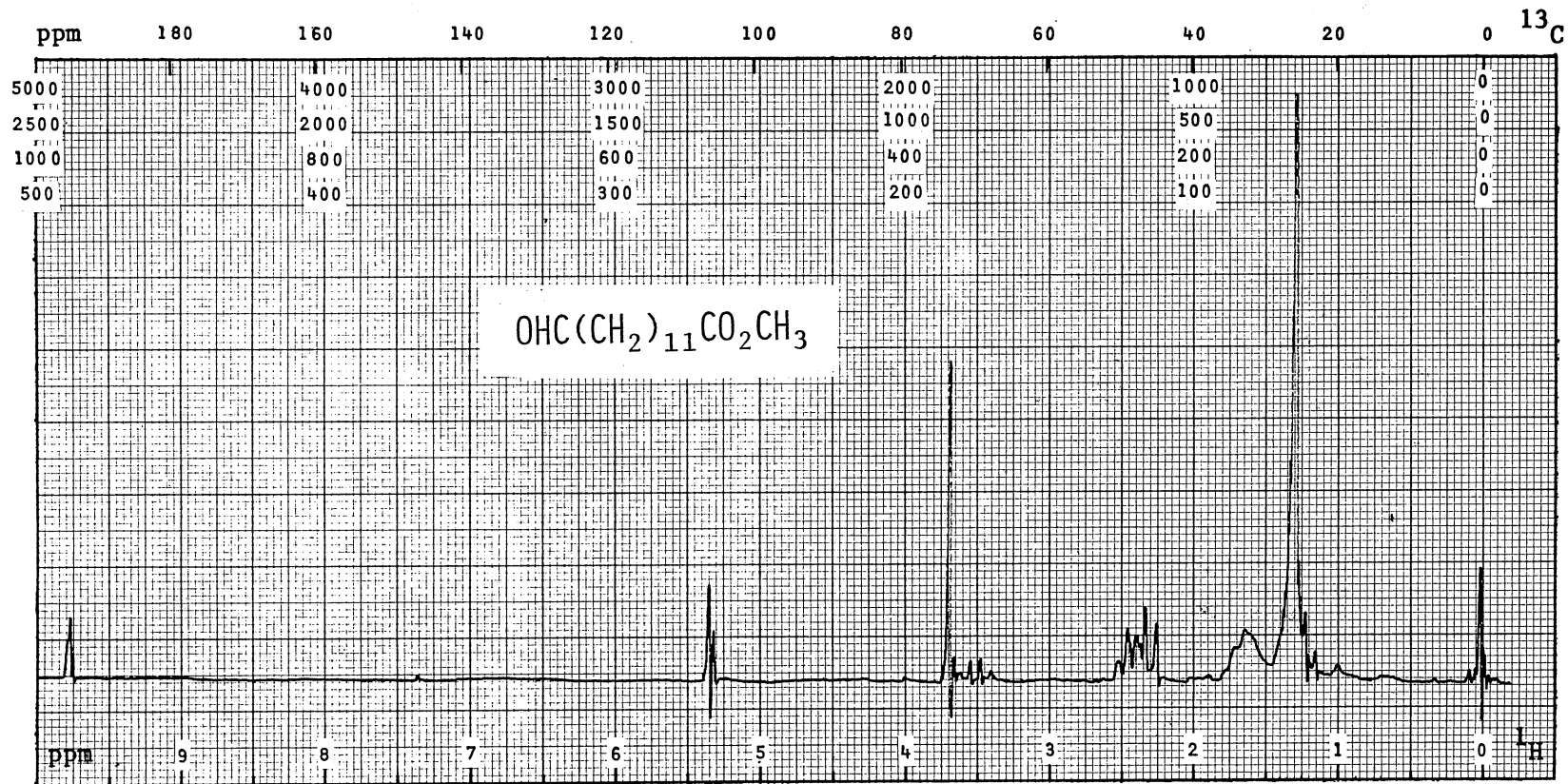
PLATE XI



^{13}C NMR Spectrum of 42

PFT X CW ; Solvent. . CDCl_3 ; SO. . 35101 Hz; PW. . 5000 Hz; T. . 30 °C; Acq/SA. . 400
 Size. . 8 K; P2/RF. . 10 $\mu\text{s}/\text{dB}$; SF. . 25.2 Hz; FB. . Hz; Lock. . ^2H ; D5/ST. . 5 s
 DC. . ^1H ; Gated Off. . ; Offset. . Hz; RF. . W/dB; NBW. . Hz

PLATE XII



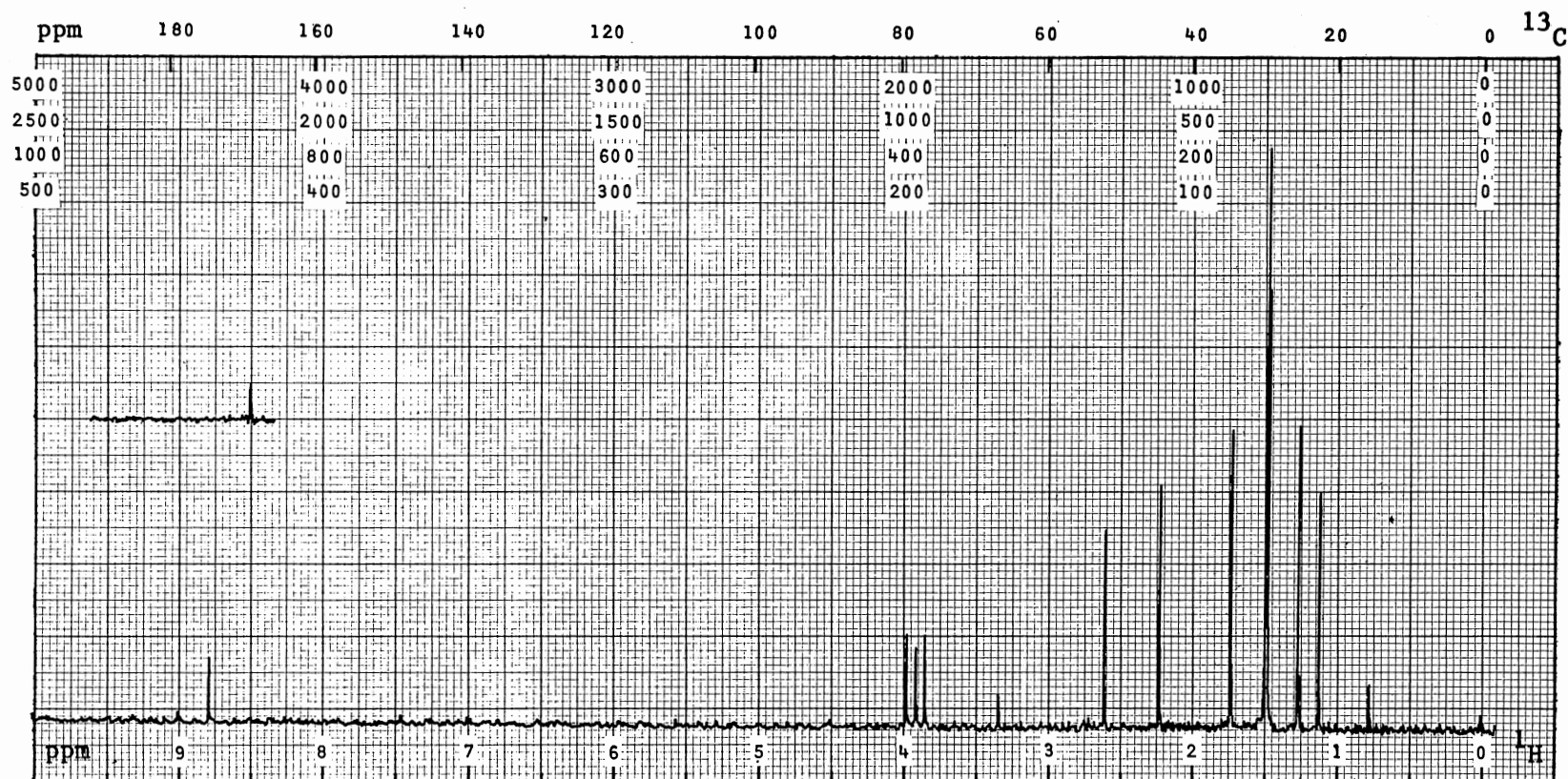
^1H NMR Spectrum of 34b

PFT _ CW X ; Solvent. . CDCl_3 ; SO. . 85771 Hz; PW. . 1000 Hz; T. . 30 °C; Acq/SA. .

Size. . K; P2/RF. . 59 $\mu\text{s}/\text{dB}$; SF. . 100.1 Hz; FB. . 2 Hz; Lock. . ^2H ; D5/ST. . 250 s

DC. . ; Gated Off. . ; Offset. . Hz; RF. . W/dB; NBW. . Hz

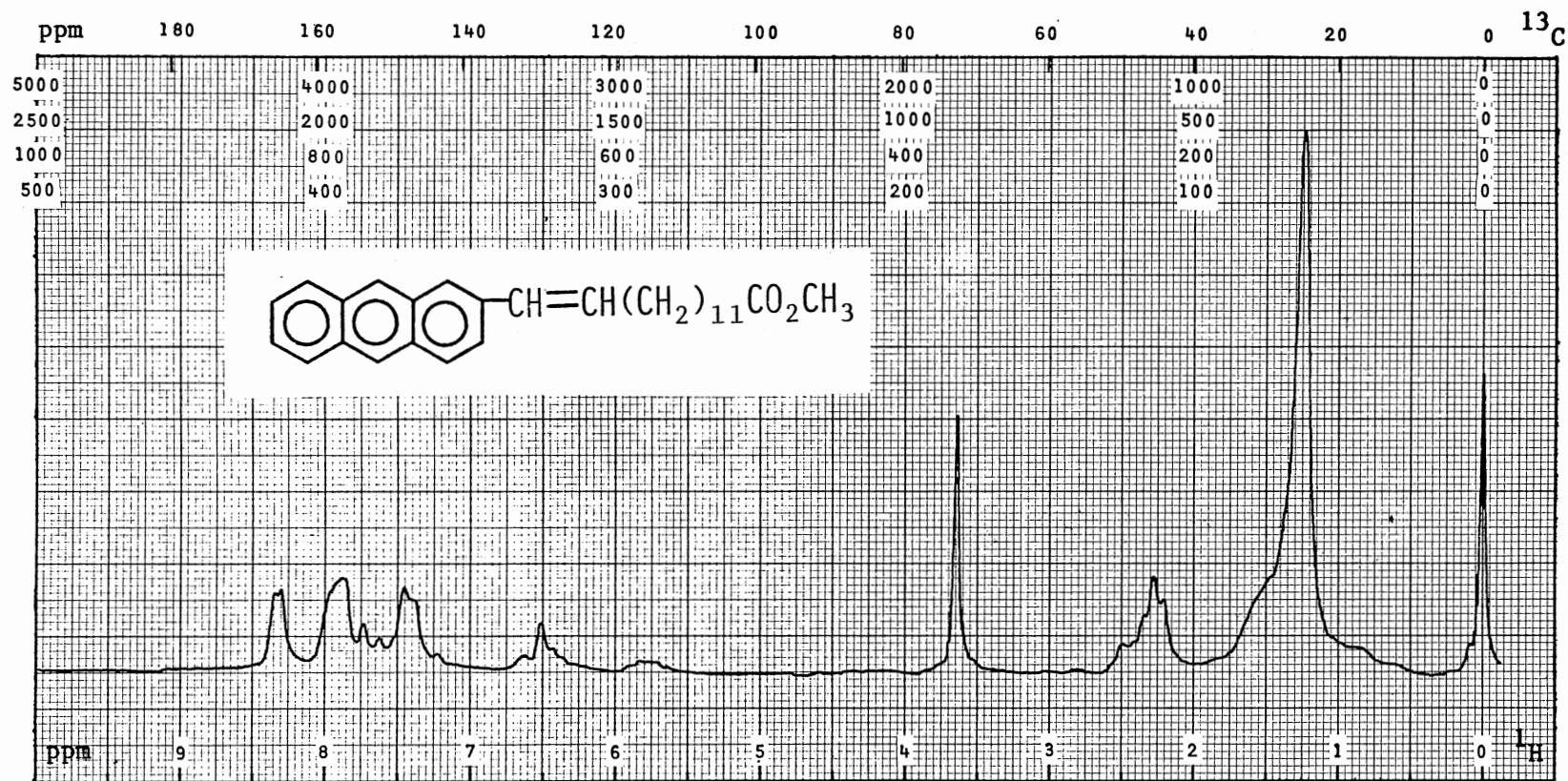
PLATE XIII



^{13}C NMR Spectrum of 34b

PFT X CW ; Solvent. .CDCl₃ ; SO. .35101 Hz; PW. . 5000 Hz; T. . 30 °C; Acq/SA. . 600
 Size. . 8 K; P2/RF. . 10 μs/dB; SF. . 25.2 Hz; FB. . Hz; Lock. . ^2H ; D5/ST. . 5 s
 DC. . ^1H ; Gated Off. . ; Offset. . 45051 Hz; RF. . 9 W/dB; NBW. . Hz

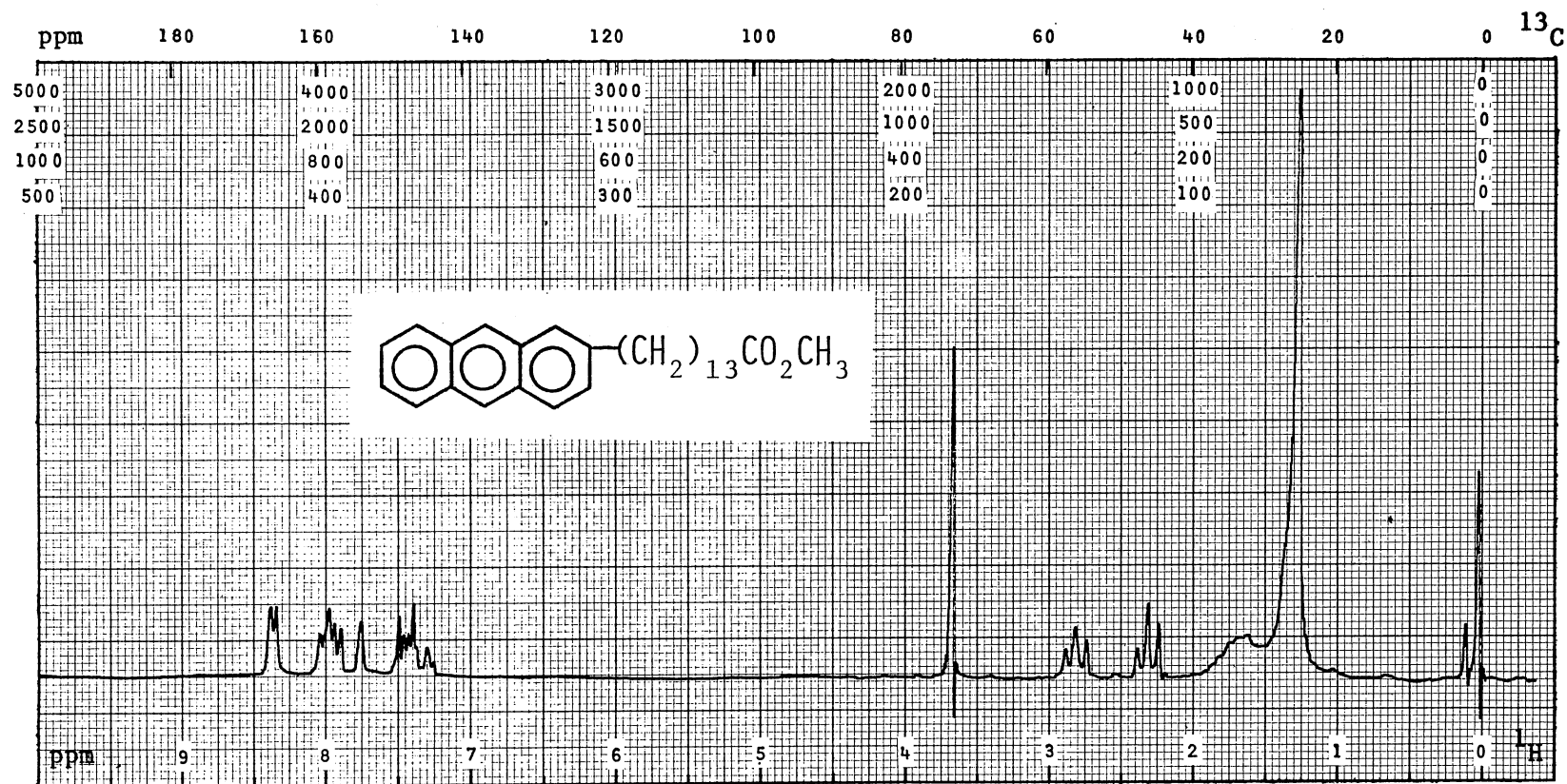
PLATE XIV



^1H NMR Spectrum of 35b

PFT _ CW X ; Solvent. . CDCl_3 ; SO. . 85771 Hz; PW. . 1000 Hz; T. . 30 °C; Acq/SA. .
 Size. . K; P2/RF. . 59 $\mu\text{s}/\text{dB}$; SF. . 100.1 Hz; FB. . 2 Hz; Lock. . ^2H ; D5/ST. . 250 s
 DC. . ; Gated Off. . ; Offset. . Hz; RF. . W/dB; NBW. . Hz

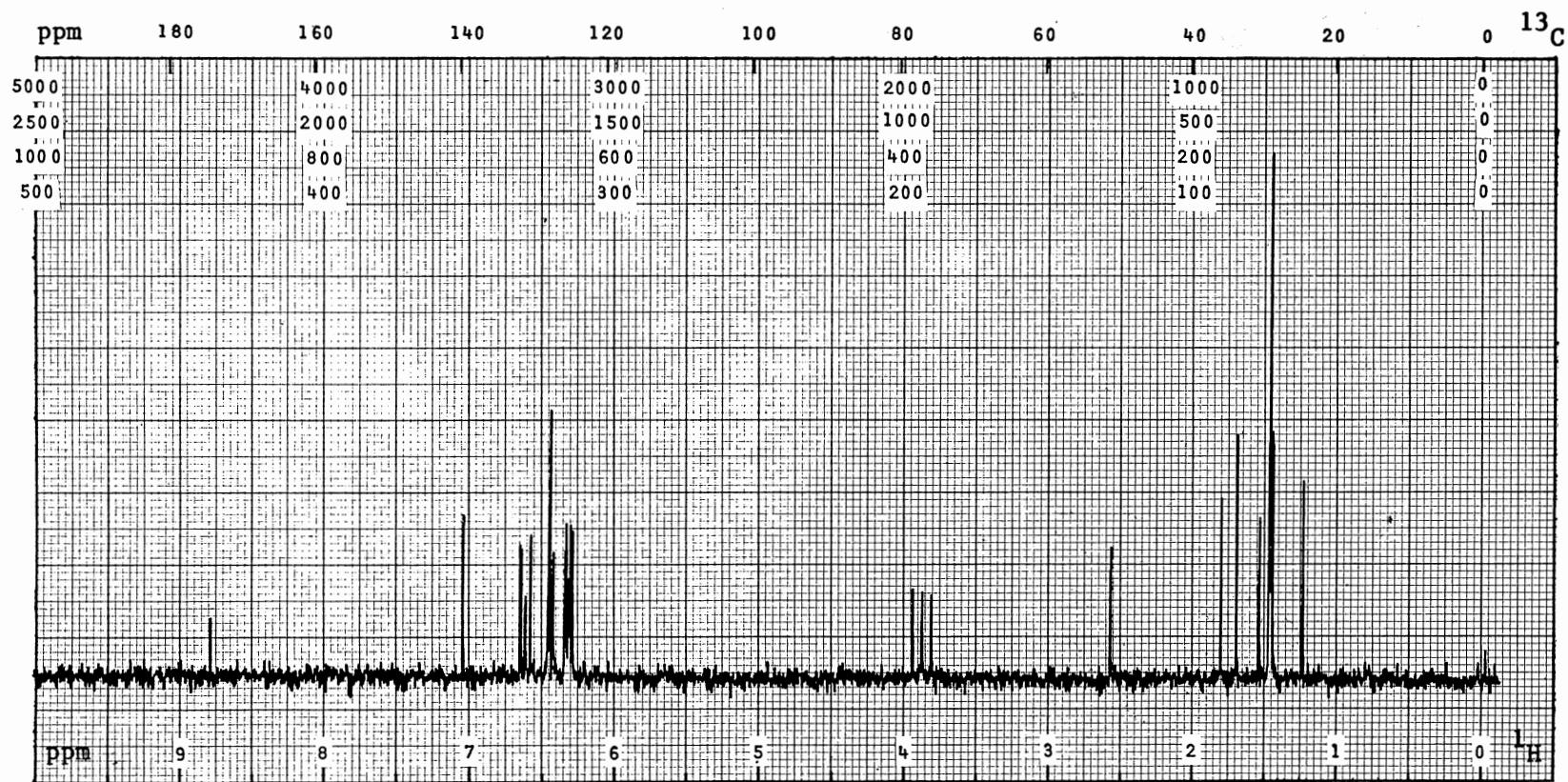
PLATE XV



^{13}C NMR Spectrum of 25e

PFT _ CW X; Solvent. . CDCl_3 ; SO. . 85771 Hz; PW. . 1000 Hz; T. . 30 °C; Acq/SA. .
 Size. . K; P2/RF. . 60 $\mu\text{s}/\text{dB}$; SF. . 100.1 Hz; FB. . 2 Hz; Lock. . ^2H ; D5/ST. . 250 s
 DC. . ; Gated Off. . ; Offset. . Hz; RF. . W/dB; NBW. . Hz

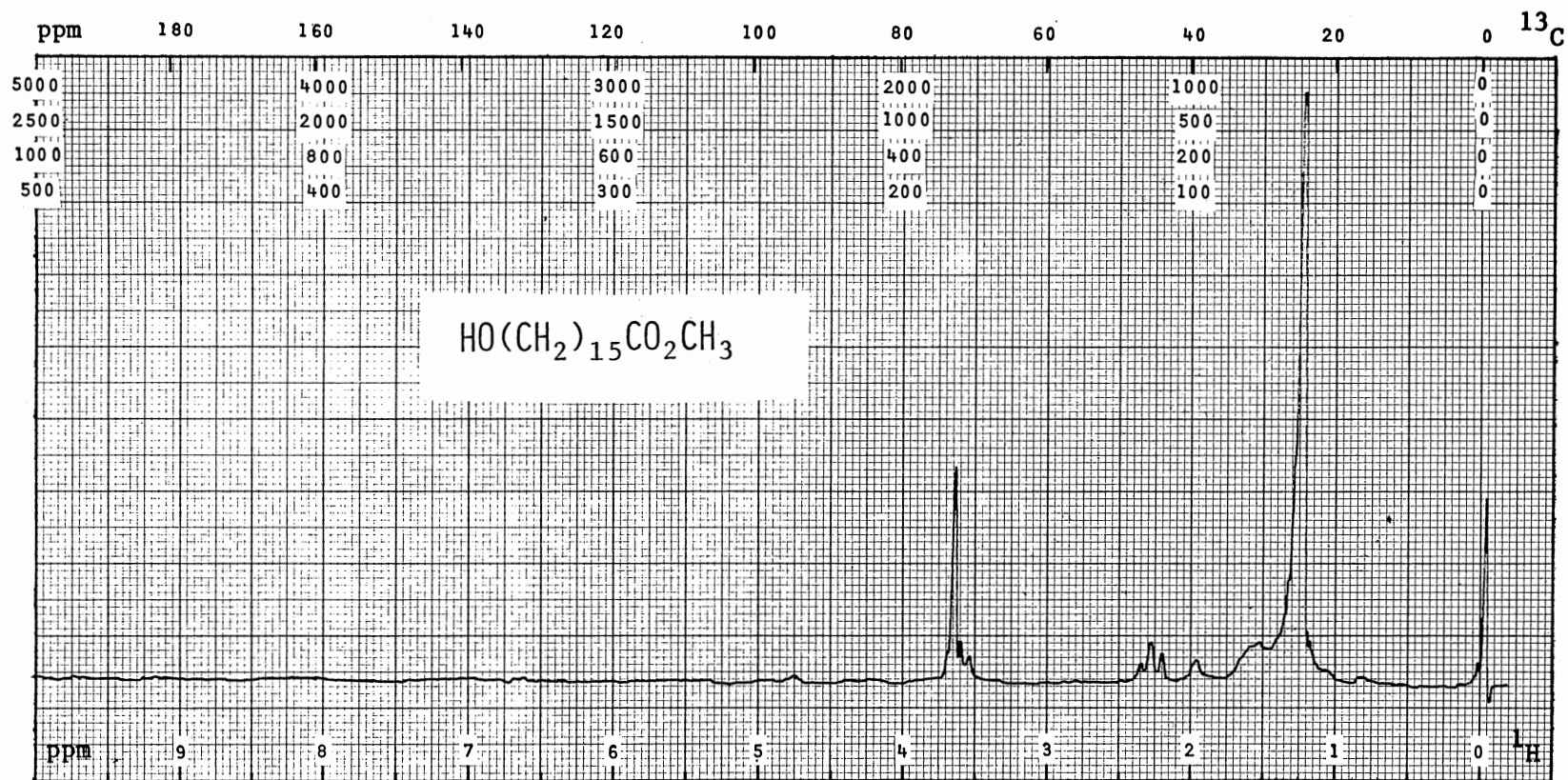
PLATE XVI



^{13}C NMR Spectrum of 25e

PFT X CW _ ; Solvent. . CDCl_3 ; SO. .35101 Hz; PW. .5000 Hz; T. . 30 °C; Acq/SA. .420
 Size. . 8 K; P2/RF. . 10 $\mu\text{s}/\text{dB}$; SF. . 25.2 Hz; FB. . Hz; Lock. . ^2H ; D5/ST. . 5 s
 DC. . ^1H ; Gated Off. . ; Offset. .45051 Hz; RF. . 9 W/dB; NBW. . Hz

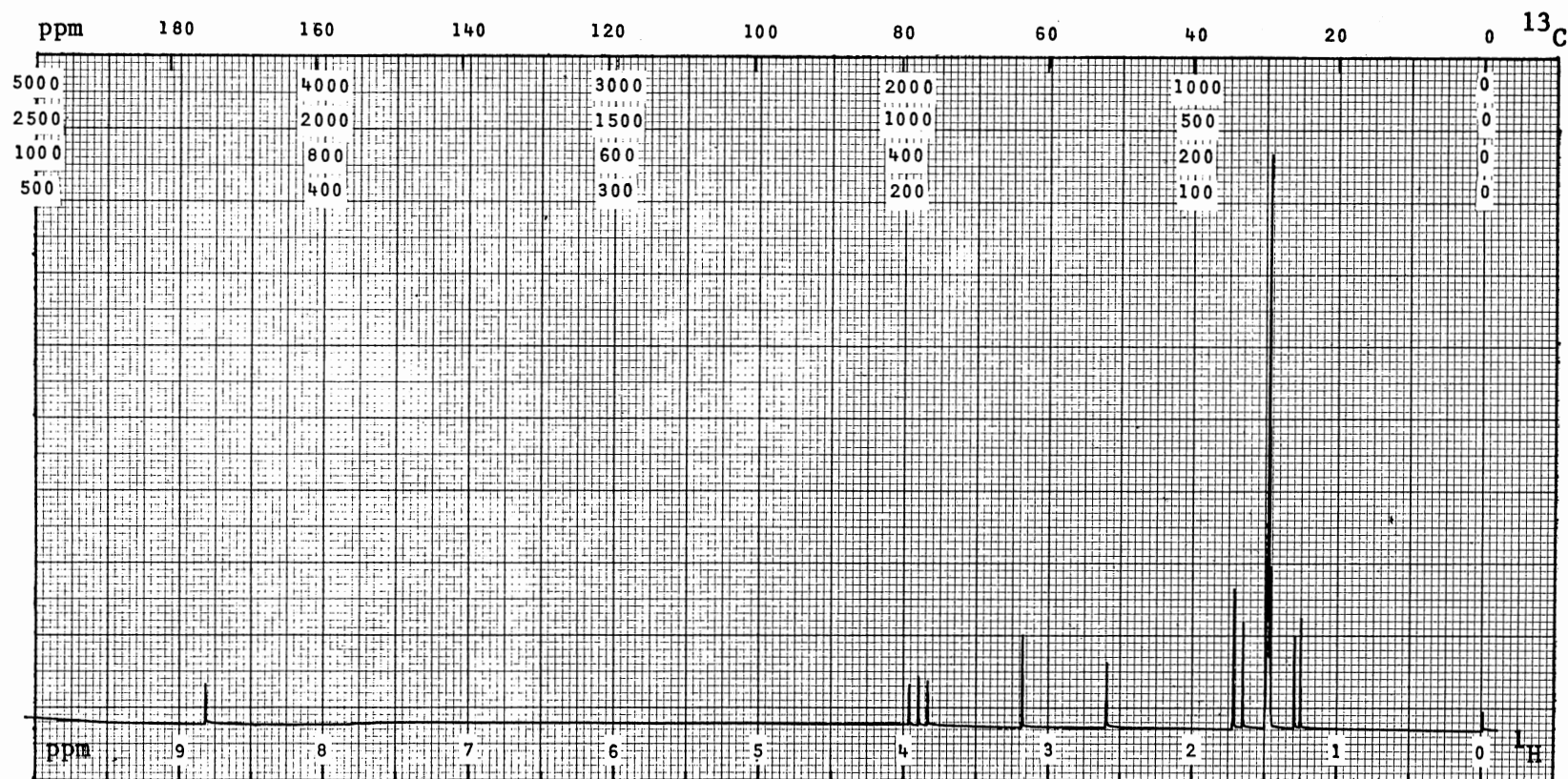
PLATE XVII



^1H NMR Spectrum of 44

PFT CW X ; Solvent. . CDCl_3 ; SO. . 85771 Hz; PW. . 1000 Hz; T. . 30 °C; Acq/SA. .
 Size. . K; P2/RF. . 59 $\mu\text{s}/\text{dB}$; SF. . 100.1 Hz; FB. . 2 Hz; Lock. . ^2H ; D5/ST. . 250 s
 DC. . ; Gated Off. . ; Offset. . Hz; RF. . W/dB; NBW. . Hz

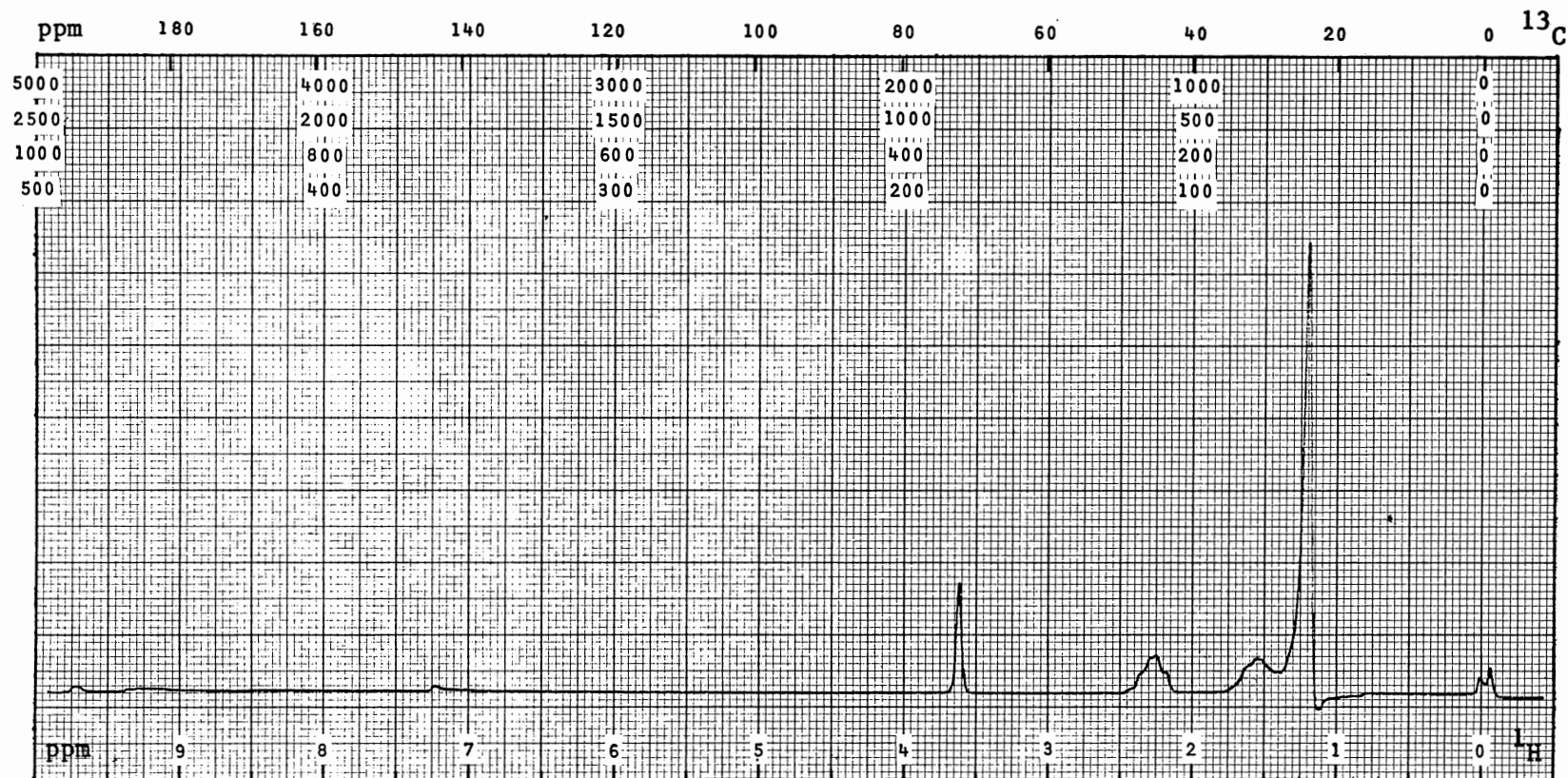
PLATE XVIII



^{13}C NMR Spectrum of 44

PFT X CW ; Solvent. . CDCl_3 ; SO. . Hz; PW. . 20000Hz; T. . 22 °C; Acq/SA. .100
 Size. . K; P2/RF. . 12 $\mu\text{s}/\text{dB}$; SF. . 75.4 Hz; FB. . Hz; Lock. . ^2H ; D5/ST. . 5 s
 DC. . ^1H ; Gated Off. . ; Offset. . Hz; RF. . W/dB; NBW. . Hz

PLATE XIX



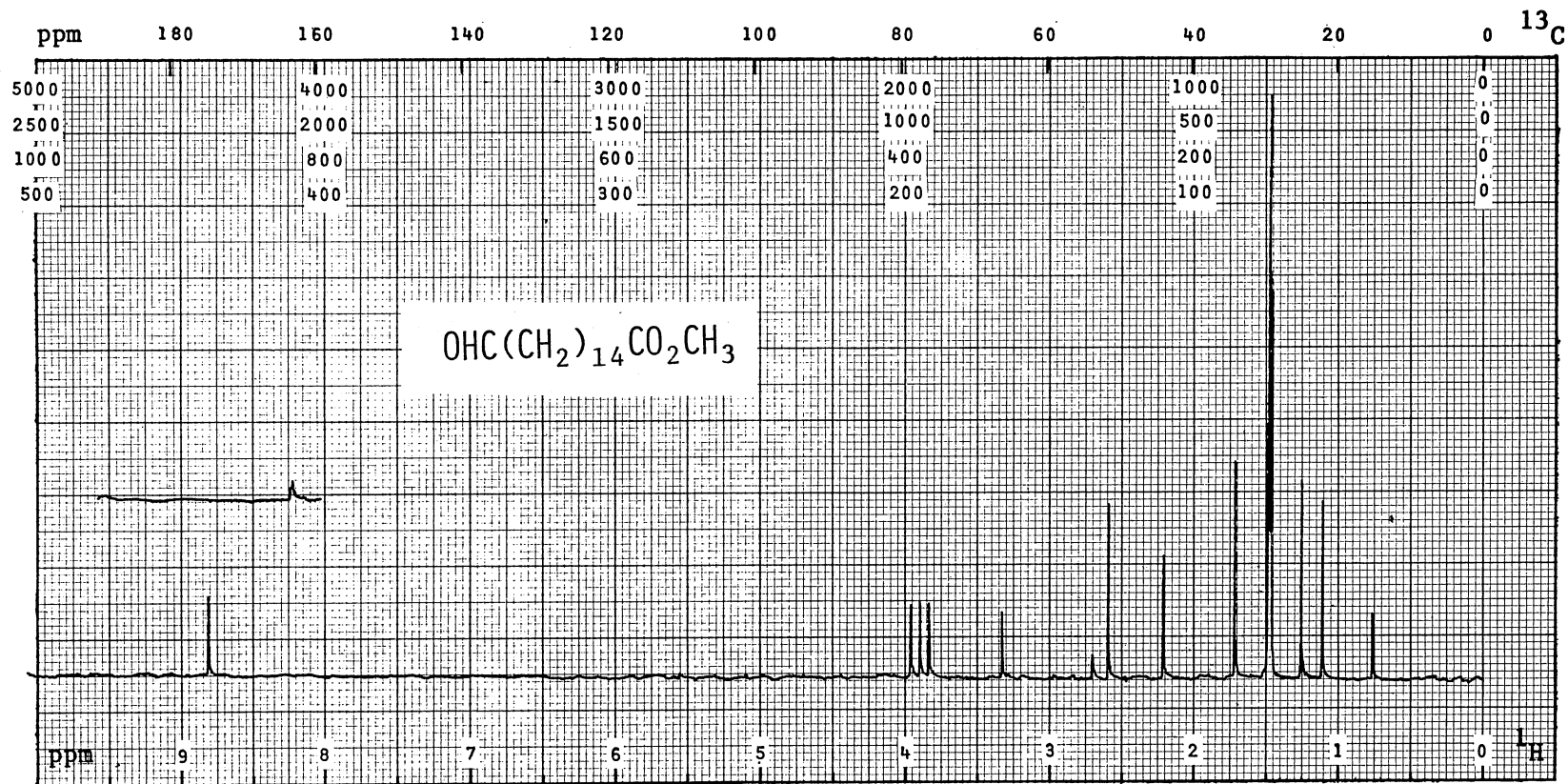
^1H NMR Spectrum of 34c

PFT _ CW X ; Solvent. . CDCl_3 ; SO. . 85771 Hz; PW. . 1000 Hz; T. . 30 °C; Acq/SA. .

Size. . K; P2/RF. . 59 $\mu\text{s/dB}$; SF. . 100.1 Hz; FB. . 2 Hz; Lock. . ^1H ; D5/ST. . 250 s

DC. . ; Gated Off. . ; Offset. . Hz; RF. . W/dB; NBW. . Hz

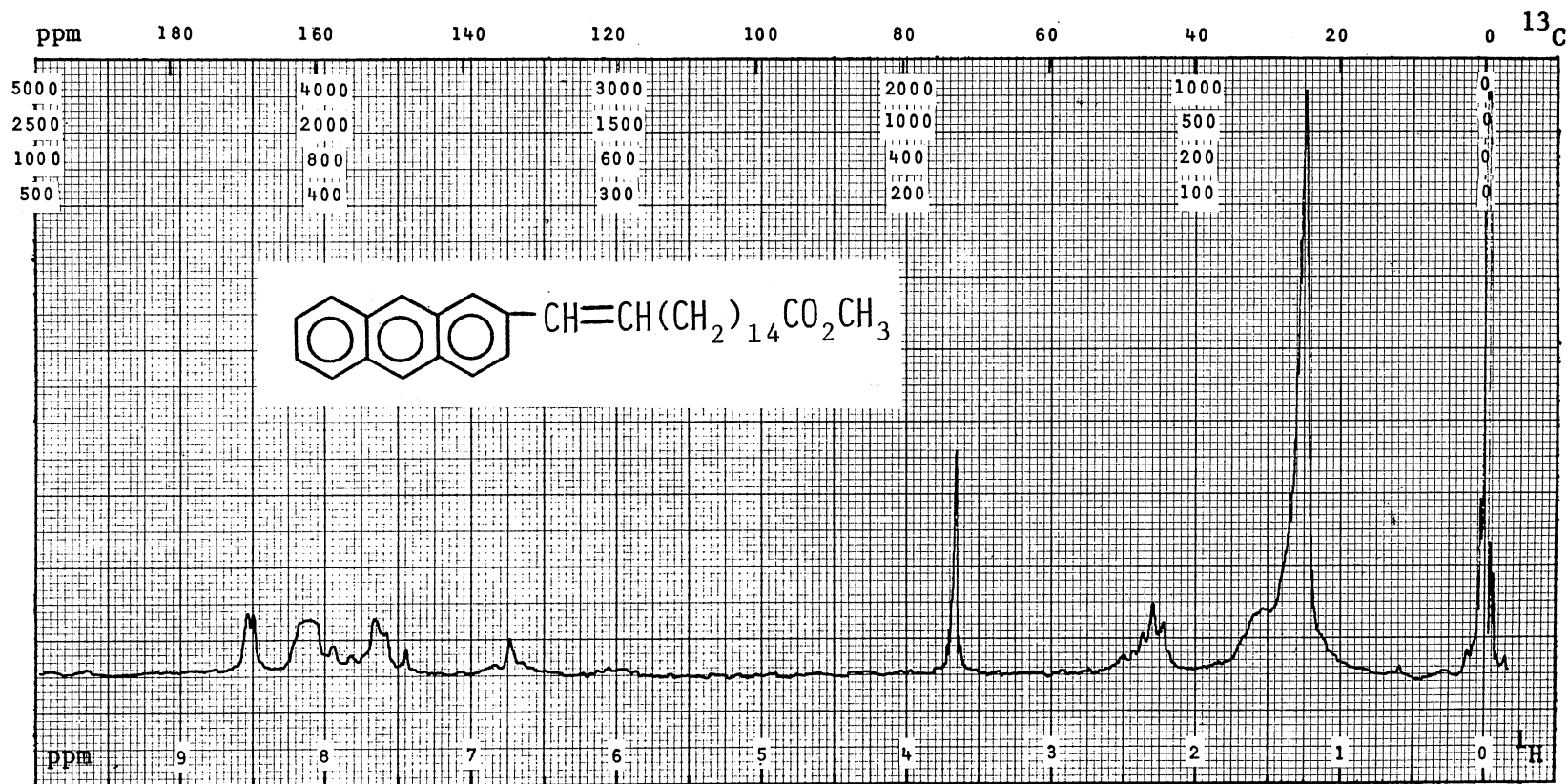
PLATE XX



^{13}C NMR Spectrum of 34c

PFT X CW _ ; Solvent. . CDCl_3 ; SO. . 35101 Hz; PW. . 5000 Hz; T. . 30 °C; Acq/SA. . 600
 Size. . 8 K; P2/RF. . 10 $\mu\text{s}/\text{dB}$; SF. . 25.2 Hz; FB. . Hz; Lock. . ^2H ; D5/ST. . 5 s
 DC. . ^1H ; Gated Off. . ; Offset. . 45051 Hz; RF. . 9 W/dB; NBW. . Hz

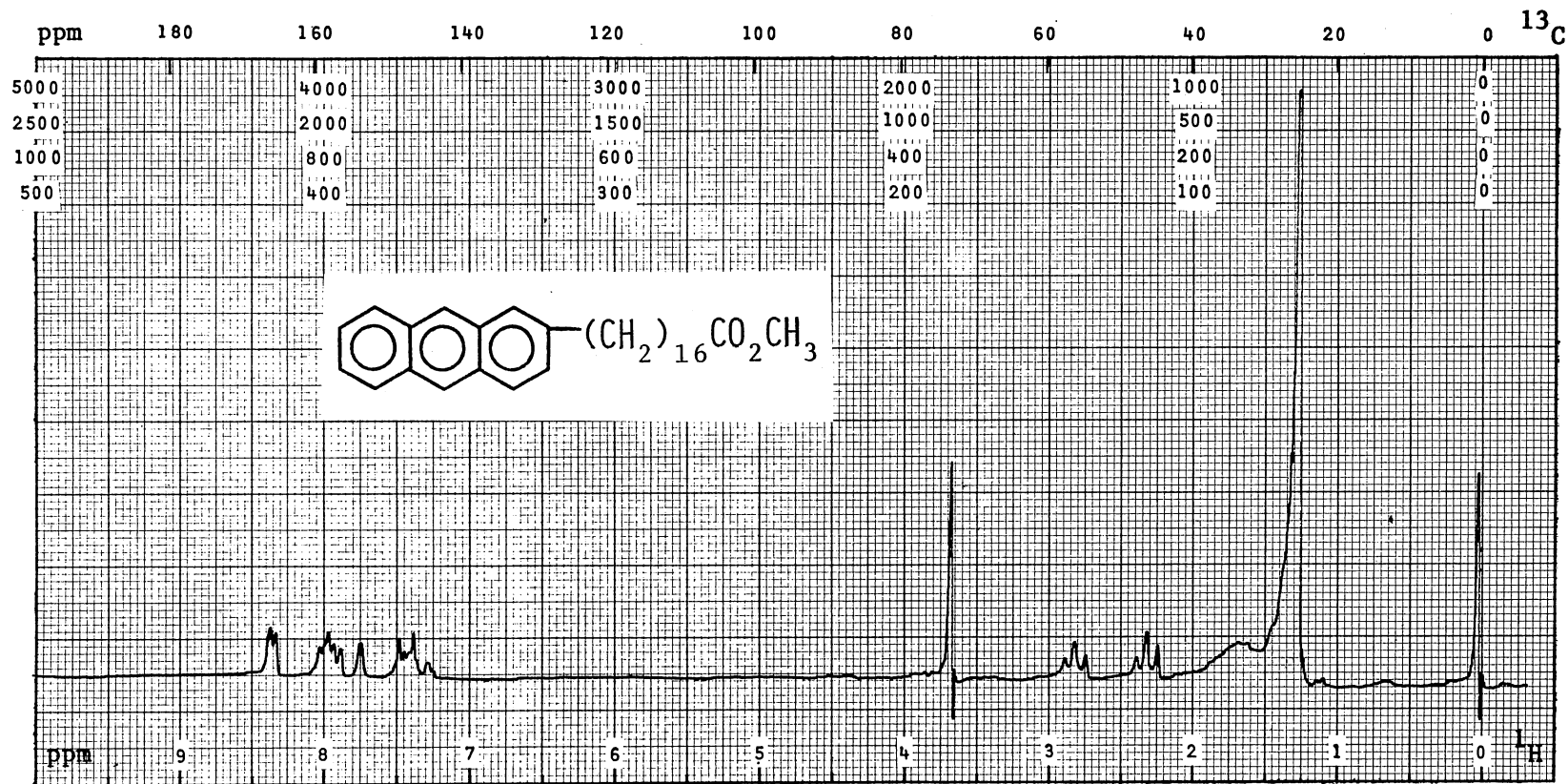
PLATE XXI



^1H NMR Spectrum of 35c

PFT _ CW _ X; Solvent. . CDCl_3 ; SO. . 85771 Hz; PW. .1000 Hz; T. . 30 °C; Acq/SA. .
 Size. . K; P2/RF. . 58 $\mu\text{s}/\text{dB}$; SF. . 100.1 Hz; FB. . 2 Hz; Lock. . ^2H ; D5/ST. . 250 s
 DC. . ; Gated Off. . ; Offset. . Hz; RF. . W/dB; NBW. . Hz

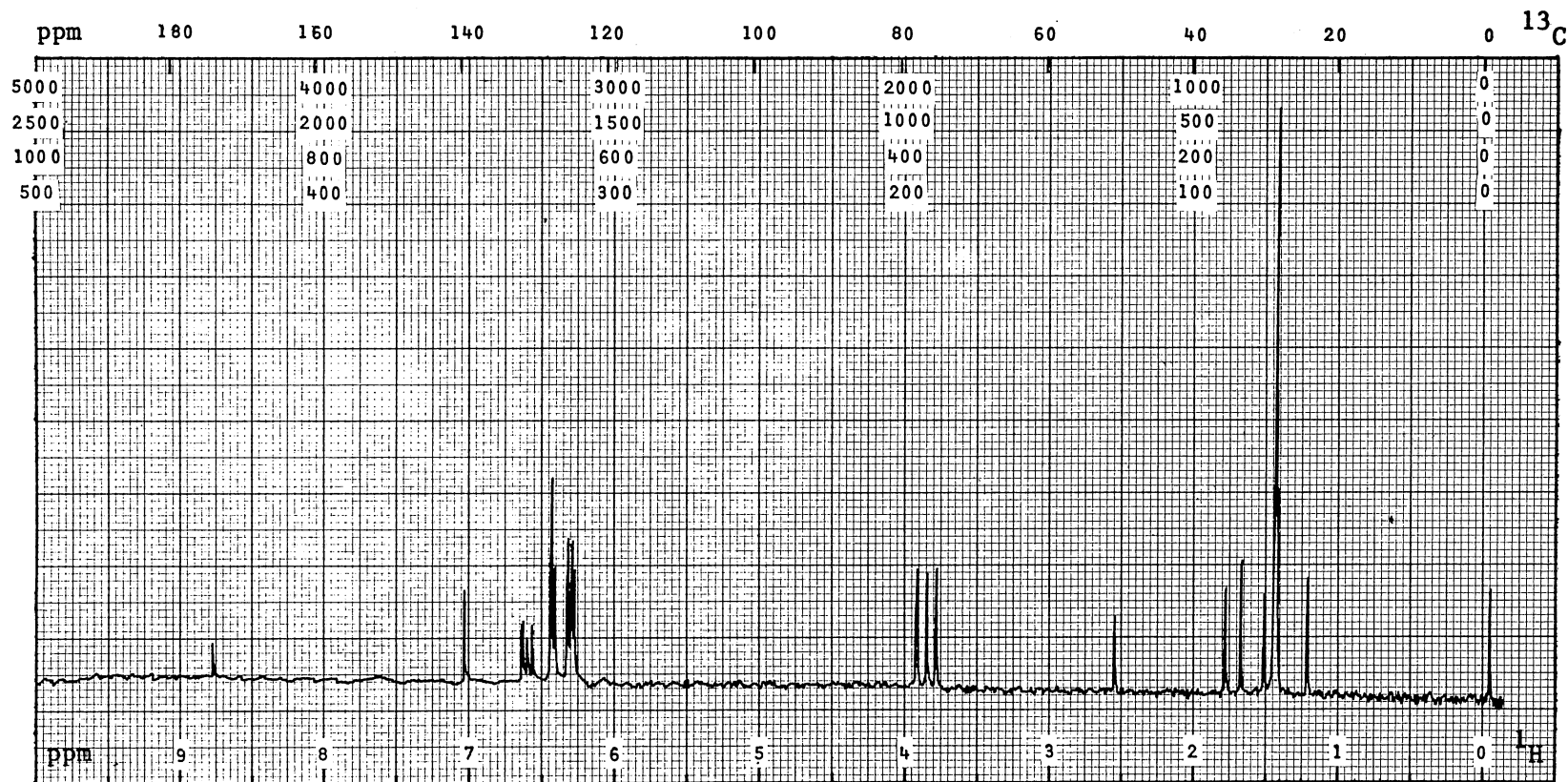
PLATE XXII



¹H NMR Spectrum of 25f

PFT _ CW X ; Solvent. . CDCl₃ ; SO. . 85771 Hz; PW. . 1000 Hz; T. . 30 °C; Acq/SA. .
 Size. . K; P2/RF. . 59 μs/dB; SF. . 100.1 Hz; FB. . 2 Hz; Lock. . ²H ; D5/ST. . 250 s
 DC. . ; Gated Off. . ; Offset. . Hz; RF. . W/dB; NBW. . Hz

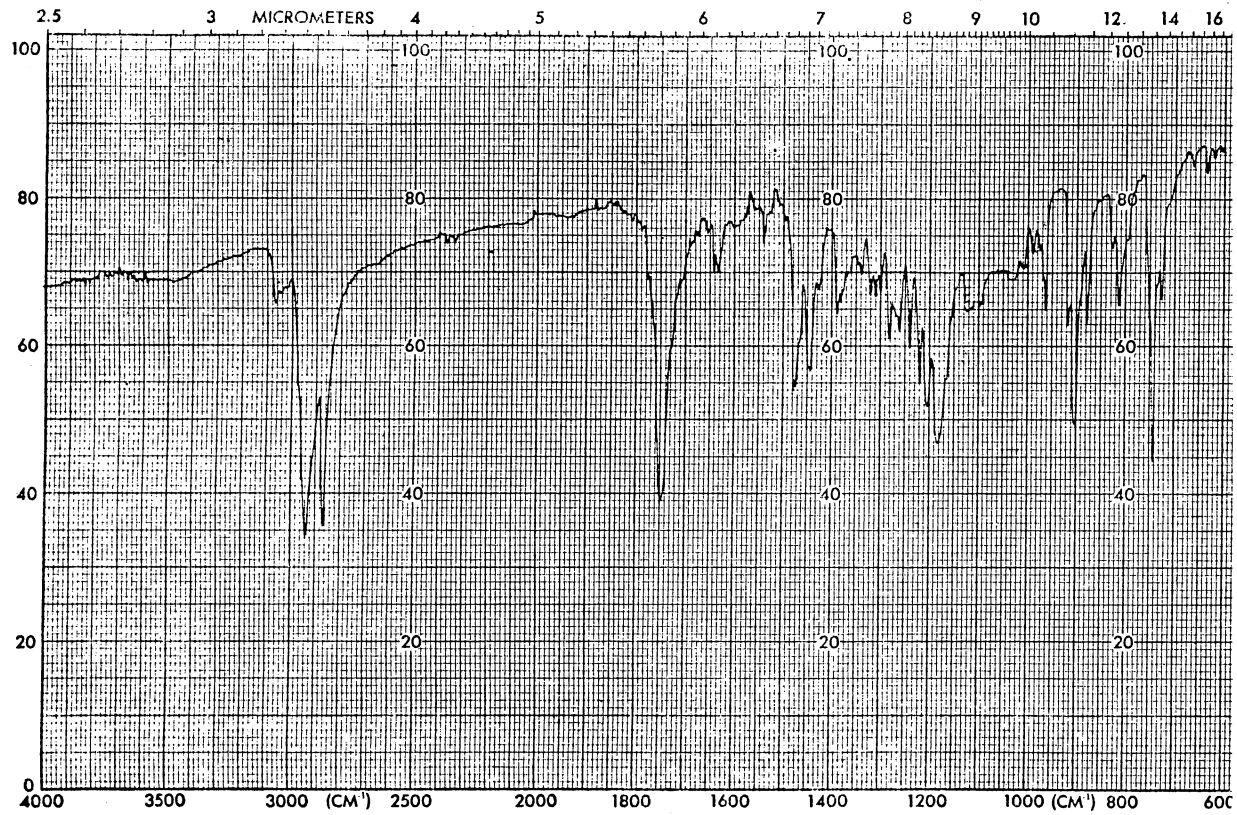
PLATE XXIII



^{13}C NMR Spectrum of 25c

PFT X CW ; Solvent. . CDCl_3 ; SO. . 35101 Hz; PW. . 5000 Hz; T. . 30 °C; Acq/SA. . 500
 Size. . 8 K; P2/RF. . 10 $\mu\text{s}/\text{dB}$; SF. . 25.2 Hz; FB. . Hz; Lock. . ^2H ; D5/ST. . 5 s
 DC. . ^1H ; Gated Off. . ; Offset. . 45051 Hz; RF. . 9 W/dB; NBW. . Hz

PLATE XXIV



IR Spectrum of 25f

BIBLIOGRAPHY

1. Abraham, R.; Loftus, P. "Proton and ¹³C NMR Spectroscopy", Heyden and Son, Philadelphia, 1978.
2. Allerhand, A.; Doddrell, D.; Komoroske, R. J. Chem. Phys., 1971, 55, 189.
3. Arjunan, P.; Shymasundar, N.; Berlin, K. D.; Najjar, D.; Rockley, M. G. J. Org. Chem. 1981, 46, 626-629.
4. Augustin, J.; Hasselbach, W. Eur. J. Biochem., 1973, 35, 114-121.
5. Beddard, G. S.; West, M. A. "Fluorescent Probes", Academic Press, New York, 1981.
6. Bernstein, E. Ber., 1883, 16, 2609.
7. Birdsall, N.; Lee, A.; Levine, Y.; Metcalfe, J.; Partington, P.; Roberts, G. J. Chem. Soc. Chem. Commun., 1973, 757.
8. Bradley, R. A. in "Modern Fluorescence Spectroscopy", Vol. II Wehry, E. L. (ed.); Plenum Press, New York, 1976, Chapter 3.
9. Branton, D. Proc. Natl. Acad. Sci., 1966, 55, 1048-1056.
10. Breitmaier, E.; Spohn, K.; Berger, S. Angew. Chem. Internat. Edit., 1975, 14, 144.
11. Brocklehurst, J. R.; Freedman, R. B.; Hancock, D. J.; Radda, G. K. Biochem. J., 1970, 116, 621.
12. Brown, H. C.; Lane, C. F. J. Am. Chem. Soc., 1970, 92, 6660.
13. Cadenhead, D. A.; Kellner, B. M. J.; Jacobson, K.; Papahadjopoulos, D. Biochemistry, 1977, 16, 5386-5392.
14. Carlack, E. A.; Mossetig, E. J. Am. Chem. Soc., 1945, 67, 2255.
15. Caspar, M. L.; Stothers, J. B.; Wilson, N. K. Can. J. Chem., 1975, 53, 1958.
16. Caswell, A. H.; Hutchison, J. D. Biochem. Biophys. Res. Commun., 1971, 42, 43-49.
17. Caswell, A. H.; Warren, S. Biochem. Biophys. Res. Commun., 1972, 46, 1757-1763.

18. Doddrell, D.; Allerhand, A. J. Am. Chem. Soc., 1971, 93, 1558.
19. Doddrell, D.; Glushko, V.; Allerhand, A. J. Chem. Phys., 1972, 3683.
20. Faucon, J.; Lussan, C. Biochim. Biophys. Acta, 1973, 307, 454-466.
21. Fox, C. F. Scientific American, 1972, 226, 30-38.
22. Golden, R.; Stock, L. M. J. Am. Chem. Soc., 1972, 94, 3081.
23. Gray, G. R. Varian Instrument Applications, 1982, 16, 11-12.
24. Harrison, R.; Lunt, G. G. "Biological Membranes — Their Structure and Function", John Wiley and Sons, New York, 1975.
25. Iljinsky, M. A.; Gindin, L. G.; Kasakova, V. A. C. R. Acad. Sci. URSS, 1938, 20, 555.
26. Jacobs, R. E.; Oldfield, E. Progress in NMR Spectroscopy, 1981, 14, 113.
27. Janiak, M. J.; Small, D. M.; Shipley, G. G. Biochemistry, 1976, 15, 4575.
28. Jasaitis, A. A.; Kuliene, V. V.; Skulachev, V. P. Biochim. Biophys. Acta, 1971, 234, 177-181.
29. Johns, S.; Leslie, D.; Willing, R.; Bishop, D. Aust. J. Chem., 1977, 30, 813.
30. Johns, S.; Leslie, D.; Willing, R.; Bishop, D. Aust. J. Chem., 1977, 30, 827.
31. Johns, S.; Willing, R. Chem. Phys. Lipids, 1979, 24, 11.
32. Jost, P.; Waggoner, A. S.; Griffith, O. H. in "Structure and Function of Biological Membranes", Rothfield, L. I. (ed.); Academic Press, New York, 1971, Chapter 3.
33. Kimura, K.; Takahashi, M.; Tanaka, A. Chem. Pharm. Bull. (Tokyo), 1960, 8, 1059.
34. Laarhoven, W. H.; Cuppen, Th. J. H. M.; Nivard, R. J. F. Tetrahedron, 1970, 26, 4865.
35. Levine, Y. K.; Birdsall, N. J. M.; Lee, A. G.; Metcalfe, J. C. Biochemistry, 1972, 11, 1416.
36. Levy, G. C. J. Chem. Soc. Chem. Commun., 1972, 352.
37. Levy, G. C. Acc. Chem. Res., 1973, 6, 161.

38. Levy, G. C.; Cargroli, J.; Anet, F. J. Am. Chem. Soc., 1973, 95, 1527.
39. Levy, G. C.; Komoroski, R.; Halstead, J. J. Am. Chem. Soc., 1974, 96, 5456.
40. Levy, G. C.; Lichter, R.; Nelson, G. "¹³C Nuclear Magnetic Resonance Spectroscopy", 2nd ed., Wiley and Sons, New York, 1980.
41. Marcinkiewicz, J.; Zeierzykowski, W.; Murawski, R. Chem. Stosow., 1972, 16, 297. Chem. Abstr., 1973, 78, 57688v.
42. McGrath, A. E.; Morgan, C. G.; Radda, G. K. Biochim. Biophys. Acta, 1976, 426, 173-185.
43. Najjar, D. Ph.D. Dissertation, Oklahoma State University, 1981.
44. Overath, P.; Trauble, H. Biochemistry, 1973, 12, 2625-2634.
45. Podo, F.; Blasie, J. K. Proc. Natl. Acad. Sci., 1977, 74, 1032-1036.
46. Rabi, I.; Ramsey, N.; Schwinger, J. Rev. Mod. Phys., 1954, 26 167.
47. Reed, W.; Politi, M. J.; Fendler, J. H. J. Am. Chem. Soc., 1981, 103, 4591-4593.
48. Robinson, J. D.; Birdsall, N. J. M.; Lee, A. G.; Metcalfe, J. C. Biochemistry, 1972, 11, 2903-2909.
49. Russell, J. C.; Costa, S. B.; Seiders, R. P.; Whitten, D. G. J. Am. Chem. Soc., 1980, 102, 5679-5680.
50. "Sadtler Standard C-13 Nuclear Magnetic Resonance Spectra", Sadtler Research Labs, Philadelphia.
51. Schuldiner, S.; Rottenberg, H.; Avron, M. Eur. J. Biochem., 1972, 25, 64-70.
52. Singer, S. J.; Nicholson, G. L. Science, 1972, 175, 720-731.
53. Stewart, F. H. C. Aust. J. Chem., 1960, 13, 478.
54. Stoffel, W.; Michaelis, G. Hoppe-Seyler's Z. Physiol. Chem., 1976, 357, 7-19.
55. Stoffel, W.; Michaelis, G. Hoppe-Seyler's Z. Physiol. Chem., 1976, 357, 21-33.
56. Stiller, K.; Waiss, A. C.; Haddon, W. F. Chem. Ind. (London), 1975, 652.

57. Stothers, J. B. "Carbon-13 NMR Spectroscopy", Academic Press, New York, 1972, p. 98.
58. Sunamoto, J.; Kondo, H.; Nomura, T.; Okamoto, H. J. Am. Chem. Soc., 1980, 102, 1146-1152.
59. Thulborn, K. R.; Sawyer, W. H. Biochim. Biophys. Acta, 1978, 511, 125-140.
60. Verkleij, A. J.; Ververgaert, P. Ann. Rev. Phys. Chem., 1975, 26, 101.
61. Wallach, D. F. H.; Ferber, E.; Selin, D.; Weidekamm, E.; Fischer, H. Biochim. Biophys. Acta, 1970, 203, 67-76.
62. Willard, H. H.; Merritt, L. L.; Dean, J. A. "Instrumental Methods of Analysis", D. Van Nostrand Co.; New York, 1974.

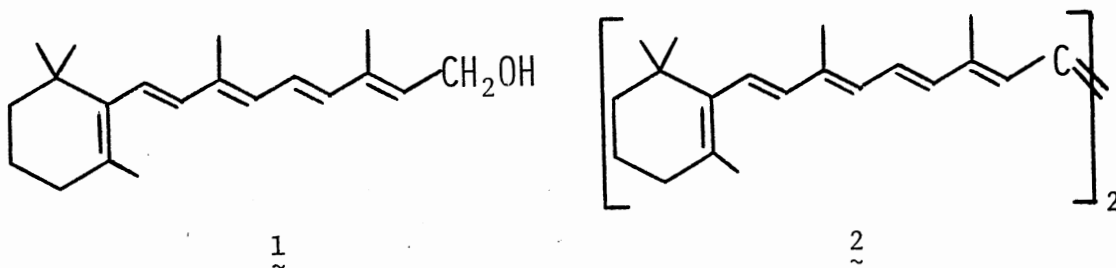
PART II

SYNTHESES AND CHARACTERIZATIONS OF
SELECTED HETEROAROTINIDS

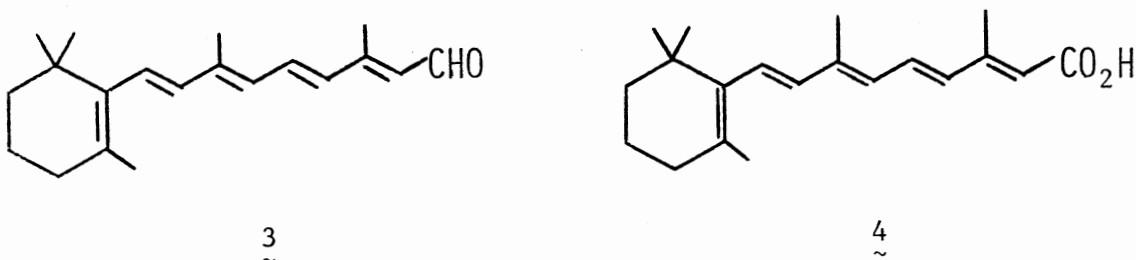
CHAPTER I

HISTORICAL

The discovery of the identity and biological importance of vitamin A or retinol (1) was the result of many research efforts during the early part of this century. In 1909-1911, a fat-soluble extract from egg yolk, fat-soluble A or vitamin A as it was later named, was found to be essential for life.^{48,49} Between 1928 and 1930, the relationship between vitamin A and the carotenoid pigments, such as β -carotene (2), was discovered.^{10,20,33} In 1930-1931, Karrer and co-workers isolated



purified, and determined the structural formula for vitamin A.^{11,24,25} Since that time, two other natural retinoids, retinal (3)^{36,37,51,52} and trans-retinoic acid (4),¹ have been isolated or prepared.



Although the structures of vitamin A and its derivatives were not determined until the early 1930's to mid 1940's, the biological importance of these substances has long been recognized. Egyptian documents dating back to about 1500 B.C. describe the use of liver, which has a high vitamin A content, as a treatment for night blindness.⁴⁰ Early sailors suffering from night blindness also found that eating fish liver restored their normal vision.³⁴ As early as 1925, the importance of retinol in the maintenance and differentiation of epithelial tissue was known.¹⁶ In 1935, Wald demonstrated that retinal was vital to the vision cycle.^{9,10} In 1946, Arens and co-workers found that retinoic acid was important in the promotion of growth.¹ Figure 1 shows the biological importance and interconversions of the natural retinoids, retinol, retinal, and trans-retinoic acid.⁴⁰

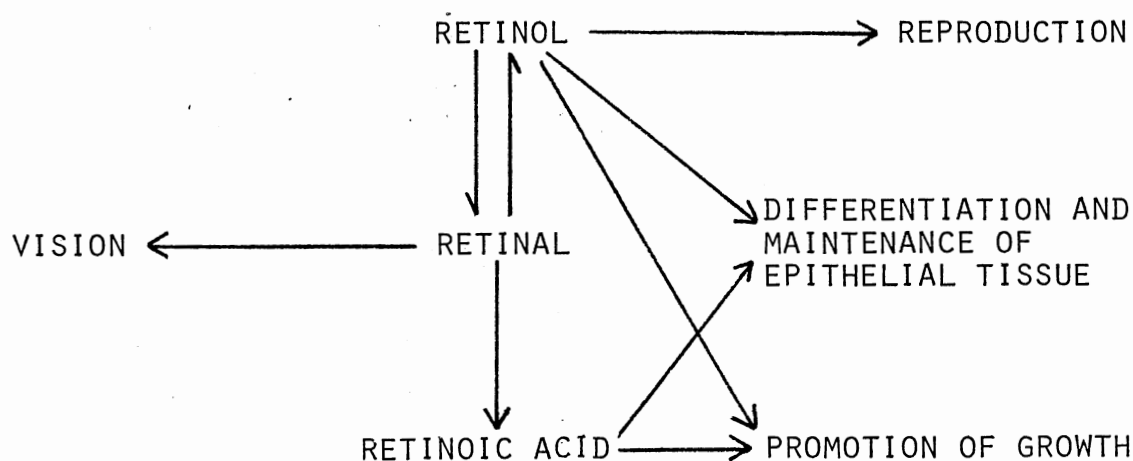


Figure 1. Biological Importance and Interconversions of Natural Retinoids

Vitamin A deficiency causes a multitude of health problems^{2,34}

including night blindness and xerophthalmia. In xerophthalmia, one of the first histological changes observed is the keratinization of the cornea and conjunctiva of the eye.⁵⁵ Untreated, this condition leads ultimately to blindness. Another result of vitamin A deficiency is the abnormal keratinization of the epithelia of the lungs, trachea, skin, gastrointestinal tract, and urinary tract.^{2,34} For example, in rats, normal tracheal epithelium³⁴ consists of a regular, columnar arrangement of cells, all of which have cilia pointing into the lumen. After three weeks of vitamin A deficiency, crowding and disarrangement of the epithelial cells is observed, and the cilia are missing in many places.³⁴ After four weeks, an area of metaplasia consisting of superimposed, stratified cells is seen.³⁴ After five weeks of vitamin A deficiency, squamous metaplasia is observed.³⁴ Flattened, stratified cells have replaced the original columnar arrangement of epithelial cells, and sheets of keratin can be seen peeling off into the lumen.

Although vitamin A deficiency causes many health problems, an excess of retinol or the other natural retinoids is also harmful. Hypervitaminosis A, the condition resulting from excessive intake of vitamin A or its derivatives, produces a variety of symptoms depending upon the amount of retinoid ingested and the length of time it is used in excess. Acute toxic effects resulting from a single large dose of a retinoid include drowsiness, irritability, headache, increased intracranial pressure, and vomiting.² Chronic toxic effects resulting from the ingestion of large doses of a retinoid for long periods of time include faulty formation of keratin in epithelial tissue, thickening of the skin, softening and fractures of the bones, and hemorrhaging.^{2,34} During pregnancy, large doses of vitamin A and other retinoids cause

birth defects such as cleft palate, exencephaly, and skeletal anomalies.

Many dermatological diseases, including acne, psoriasis, and ichthyoses, are the results of changes in epithelial keratinization. The abnormal keratinization found in these skin disorders and in certain precancerous conditions is similar to that found in vitamin A deficiency. Since vitamin A and its derivatives are important in the normal maintenance and differentiation of epithelial tissue, natural and synthetic retinoids have been investigated for use in the prevention and treatment of skin disorders and cancer.

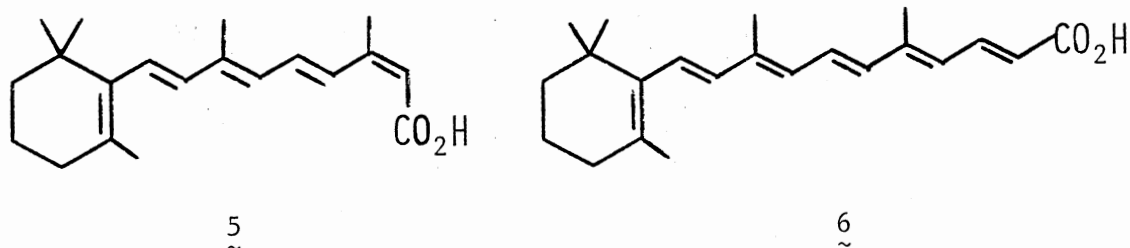
Retinoids in the Treatment of Skin Disorders

Two recent books present an overview of some of the most recent advances in the treatment of dermatological diseases using retinoids,^{39,45} In 1941, Peck and co-workers reported the use of vitamin A in the treatment of Darier's disease.⁴¹ In 1951, Porter described the effects of retinol on pityriasis rubra pilaris.⁴³ trans-Retinoic acid in a mixture of ethanol and ethylene glycol effectively clears acne vulgaris after 4-6 weeks for mild cases and after 2-3 months for severe ones.²⁶ The retinoid is applied for long periods of time at a concentration (0.05-0.25 weight %) such that noticeable irritation of the skin occurs.

Topical application of retinal is also reported to be effective in the treatment of acne.⁵⁰ At concentrations between 0.05 and 1 weight % in 95% ethanol or propylene glycol, this retinoid is at least 50% effective. Retinal has the advantage over trans-retinoic acid in that it does not produce irritation or inflammation of the skin. Retinal is also effective in the treatment of actinic and nonactinic keratosis.⁵⁷

Several synthetic retinoids have been studied for use in the

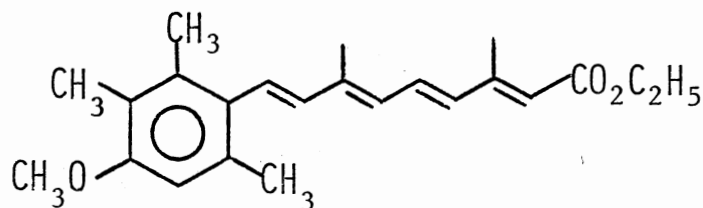
treatment of dermatological diseases. For example, 13-cis-retinoic acid (5) is useful in the treatment of severe or "therapy resistant" acne.^{23,42} This retinoid is given orally in doses ranging from 0.05 to 2.0 mg/kg body weight. Within 12 weeks, almost all lesions disappear, and few lesions recur after 80 weeks. The C₂₂ analog of retinoic acid, namely 6 and its Na⁺ and K⁺ salts, has proven useful



in the treatment of seborrheic and ichthyosiform dermatoses.²⁹ Two desmethyl analogs of retinoic acid 7 and 8 have proven more valuable



than either retinol or retinoic acid for the healing of wounds.²⁸ The retinoid 7 has also been effective in the treatment of psoriasis and acne. The aromatic retinoid 9 was of value in the treatment of various types of psoriasis.^{15,22}



9

Retinoids in the Prevention and Treatment of Cancer

In 1926, the relationship between vitamin A deficiency and cancer was reported by Fujimaki.¹³ In the study, rats that were fed a vitamin A deficient diet developed carcinomas of the stomach. Since that time other researchers have reported similarities between vitamin A deficient epithelial tissue and certain precancerous lesions. For example, the addition of retinoids can reverse the anaplastic epithelial lesions induced in prostate glands by chemical carcinogens.^{7,27} In another study, the administration of retinyl palmitate prevented the formation of tracheal tumors in hamsters that were treated with the carcinogen, benzo[a]pyrene, and iron oxide.⁴⁴ More recently, Bollag demonstrated that skin papillomas induced by 7,12-dimethylbenzo[a]anthracene and croton oil regressed when treated with trans-retinoic acid.^{3,4}

Although many of these early studies indicated that natural retinoids were potentially useful in the prevention and treatment of certain forms of cancer, they also demonstrated that the natural retinoids had two distinct disadvantages.⁴⁰ First of all, with the exception of trans-retinoic acid which is not stored in the body, natural retinoids are stored in the liver. Even after a massive dose

of these compounds, the retinoid level in the blood does not increase proportionately. Thus, in vivo it is difficult to obtain an adequate distribution of natural retinoids within the body and, more importantly, at specific target sites within the body. The second disadvantage of the natural retinoids is the toxicity related to high doses. This toxicity, hypervitaminosis A, distinctly limits the clinical use of natural retinoids.

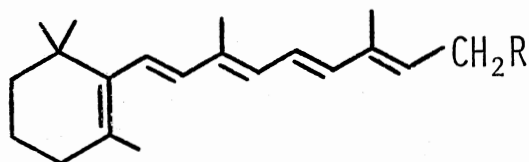
In an effort to overcome the disadvantages of the natural retinoids, a variety of synthetic retinoids have been prepared and tested for use in the prevention and treatment of cancer. Two methods are commonly employed to examine the activity of these new retinoids. In the first, papillomas of the skin are induced in mice using 7,12-dimethylbenzanthracene as the initiator and croton oil as the promoter.³⁰ After multiple papillomas (with an average diameter of 3 mm) have developed, the experimental retinoid is applied intraperitoneally at days 1 and 8 as a suspension or solution in arachis oil. On day 14, the average sum of the papilloma diameters is measured and compared to the corresponding initial value. In conjunction with the antipapilloma activity studies, the retinoids are tested for toxicity. The experimental substance in arachis oil is injected intraperitoneally into mice for a 14 day period. The results of these two tests are expressed as a therapeutic ratio. This ratio is the quotient of the effective dose resulting in 50% regression of papillomas in two weeks and the minimum daily dose that causes hypervitaminosis A during the same length of time.

The second method used to determine the pharmacological activity of synthetic retinoids was developed by Sporn and co-workers for use at

the National Cancer Institute.³⁸ This procedure determines the in vitro ability of an agent to reverse keratinization in tracheal organ cultures from vitamin A deficient hamsters. The tracheas are cultured in a serum-free medium and are gassed with 50% O₂, 45% N₂, and 5% CO₂. After 3 days in the retinoid-free medium, some of the tracheas are harvested and examined. In general, most of the specimens examined have significant squamous metaplasia. The remaining cultures are divided into two groups. The first one is treated with the experimental retinoid in spectrograde DMSO. The second set of cultures is treated with an equivalent amount of DMSO. The culture medium is changed 3 times a week for the next 10 days. At that time, all of the tracheas are harvested, fixed in 10% buffered formalin, and embedded in paraffin. Cross-sections of the tracheas are then examined under a microscope for the presence of keratin and keratohyaline granules. In 90% of the control cultures, both keratin and keratohyaline granules are seen. A synthetic retinoid is judged to be active if neither keratin nor keratohyaline granules are seen or if only keratohyaline granules are not present. If both are seen, the retinoid is considered to be inactive.

All of the synthetic retinoids reported result from modifications of the hydrocarbon ring, hydrocarbon side chain, or polar terminal group of vitamin A (Figure 2). One of the earliest modifications of retinol was the preparation of the corresponding methyl ether 10.^{17,19,56} This retinoid was found to be as active as retinol in supporting growth in rats and less toxic than retinol when given in large doses. Other synthetic retinoids in which the terminal polar group of retinol has been modified are 11-14. Retinoid 11 is reported to be active in the hamster tracheal organ culture and relatively nontoxic to tracheal

cartilage.⁴⁷ Retinoids 12-14 have been assayed using the same method. At 10^{-8} M, 12-14 are 20%, 33.3%, and 80% active, respectively. This compares to the 72.7% activity of retinol at the same concentration.⁵³



- 10 R=OCH₃
11 R=NHCOCH₃
12 R=SC₆H₅
13 R=SCOCH₃
14 R=SeC₆H₅

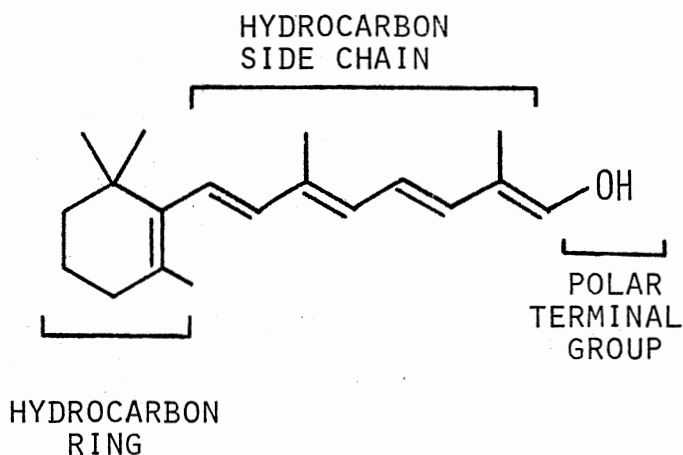
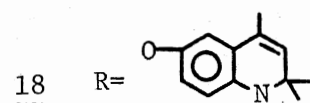
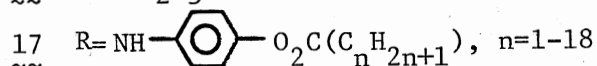
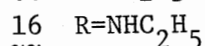
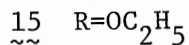
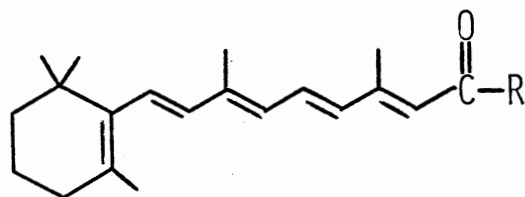


Figure 2. Regions of the Vitamin A Molecule.

Several retinoids (15-18) in which the carboxyl group of retinoic acid has been modified have been reported. The effective dose at which



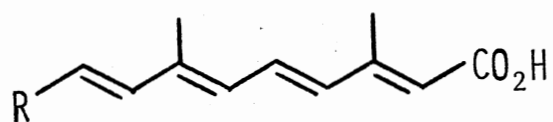
50% reversal of keratinization occurs in the hamster tracheal organ culture (ED₅₀) is 5×10^{-10} M for 15 and 2×10^{-9} M for 16.⁴⁶ The retinoids 17 are reported to show low systemic toxicity and adequate specificity for epithelial cancer sites.¹⁴ The retinoid 18 is 100% active in the tracheal organ culture at 10^{-9} M while trans-retinoic acid is 88.4% active at the same concentration.⁵⁴

Another large group of retinoids that have been synthesized and assayed³⁸ are those in which the hydrocarbon ring of trans-retinoic acid has been modified. The structures and ED₅₀'s for some of these compounds are shown in Table I.

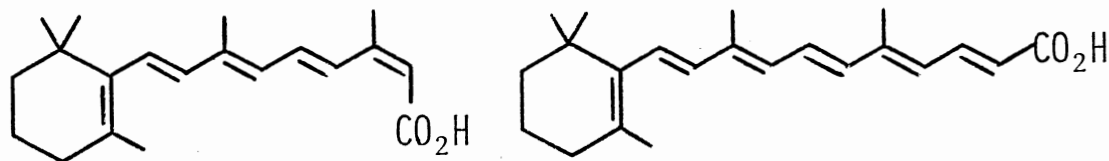
Retinoids in which the hydrocarbon side chain of retinol or retinoic acid has been modified are not as common. Assays using the tracheal organ culture have been reported for 19 and 20.³⁸ The C₂₂ analog 6 has an ED₅₀ of 3×10^{-9} M while 13-cis-retinoic acid (19) has an ED₅₀ of 3×10^{-11} M.

A number of retinoids involving several modifications of retinol have also been synthesized and assayed. Some of these are shown in

TABLE I
STRUCTURE AND ACTIVITY OF RING-MODIFIED RETINOIDS³⁸



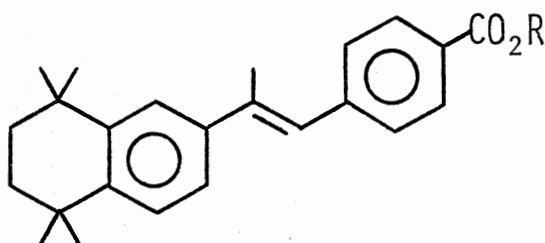
R	Hamster Tracheal Organ Culture ED ₅₀ (M)
	7×10^{-10}
	7×10^{-10}
	2×10^{-8}
	inactive
	$>1 \times 10^{-8}$
	3×10^{-7}
	2×10^{-9}



19

6

Tables II and III. The arotinoid 20 and its corresponding acid 21 have also been assayed using the hamster tracheal organ culture.³⁸ The ED_{50} values for both compounds were 1×10^{-11} M.



20 R=C₂H₅
21 R=H

Although a large variety of synthetic retinoids have been prepared and tested for use in the prevention and treatment of epithelial cancer, only a few of these compounds (19, 20, and 21) have been shown activity comparable to that of trans-retinoic acid ($ED_{50} = 3 \times 10^{-11}$ M). 13-cis-Retinoic acid is currently used clinically in the treatment of acne, but it has not been approved for the prevention or treatment of cancer. The two aromatic retinoids, or "arotinoids" 20 and 21, have shown promising activity in both common assays. These two compounds, however, are hundreds of times more toxic than retinoic acid. Further research in

TABLE II
 STRUCTURE AND ACTIVITY OF RETINOIDS WITH MULTIPLE MODIFICATIONS³⁰

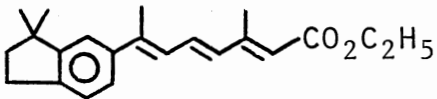
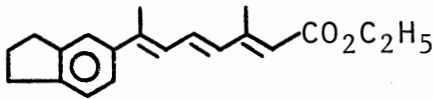
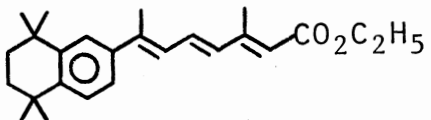
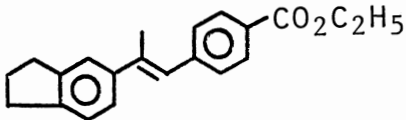
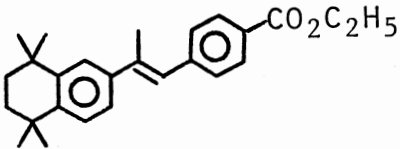
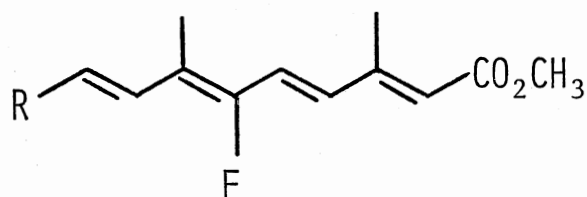
Structure	Hypervitaminosis A	Papilloma Effect	
	Dose (mg/kg)	Dose (mg/kg)	% Change
	12.5	12.5	-48
	3	3	-52
	0.75	0.75	-44
	200	200	-34
	0.2	0.05	-48

TABLE III

STRUCTURE AND ACTIVITY OF RETINOIDS WITH MULTIPLE MODIFICATIONS³¹

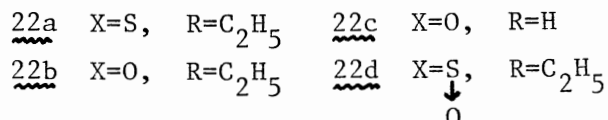
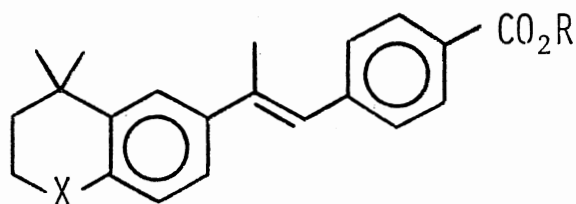
R	Hypervitaminosis A	Papilloma Effect	
	Dose (mg/kg)	Dose (mg/kg)	% Change
	50	40	-79
		20	-60
	200	40	-41
	50	20	-56
	200	80	-64
	>200	80	-58

the modification of natural retinoids is needed before synthetic retinoids will be clinically useful in the prevention and treatment of epithelial cancer.

CHAPTER II

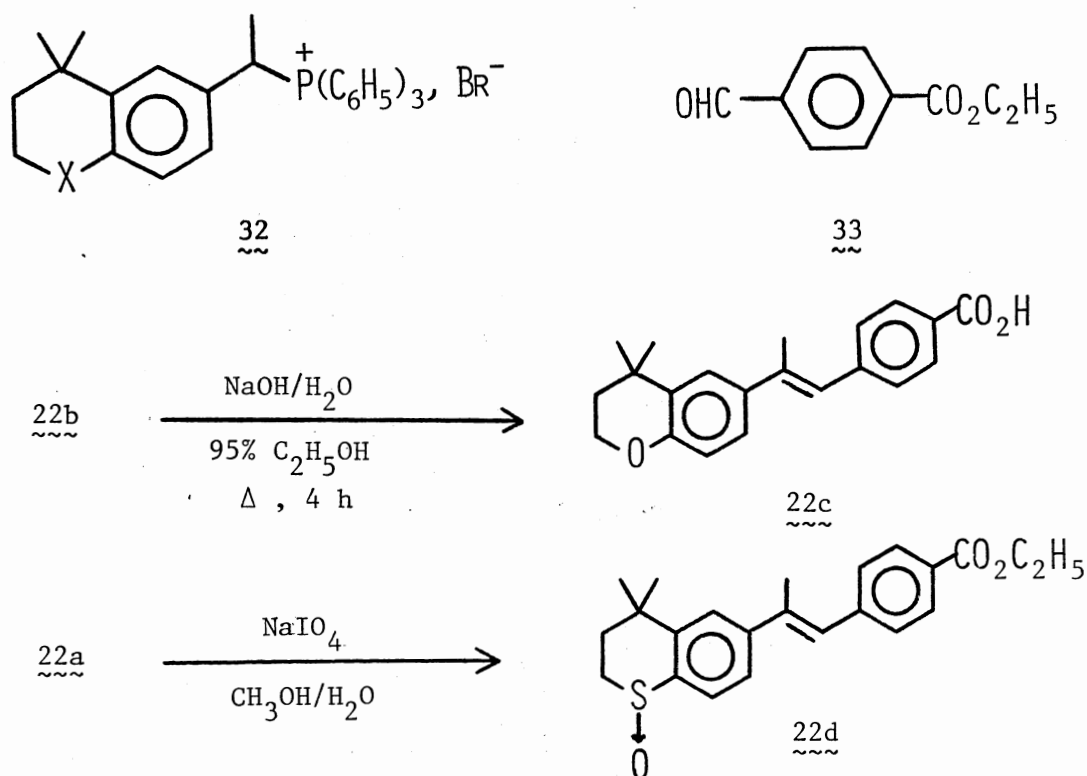
RESULTS AND DISCUSSION

Although a vast number of modified retinoids have been synthesized and assayed for use in the prevention and treatment of cancer, few of these vitamin A derivatives are clinically useful due to the toxic effects associated with hypervitaminosis A. Ideally a modified retinoid suitable for clinical use should be at least as active and less toxic than trans-retinoic acid. Two aromatic retinoids ("arotinoids") 20 and 21 which have approximately the same activity as trans-retinoic acid in the hamster tracheal organ culture assay are hundreds of times more toxic than trans-retinoic acid.³⁸ In order for these "arotinoids" to be clinically useful, structural modifications must be made such that the activity is maintained and the toxicity is reduced. Reported herein are the syntheses and pharmacological activity of four "hetero-arotinoids" 22a-22d in which a heteroatom has been incorporated into the arotinoid molecule.

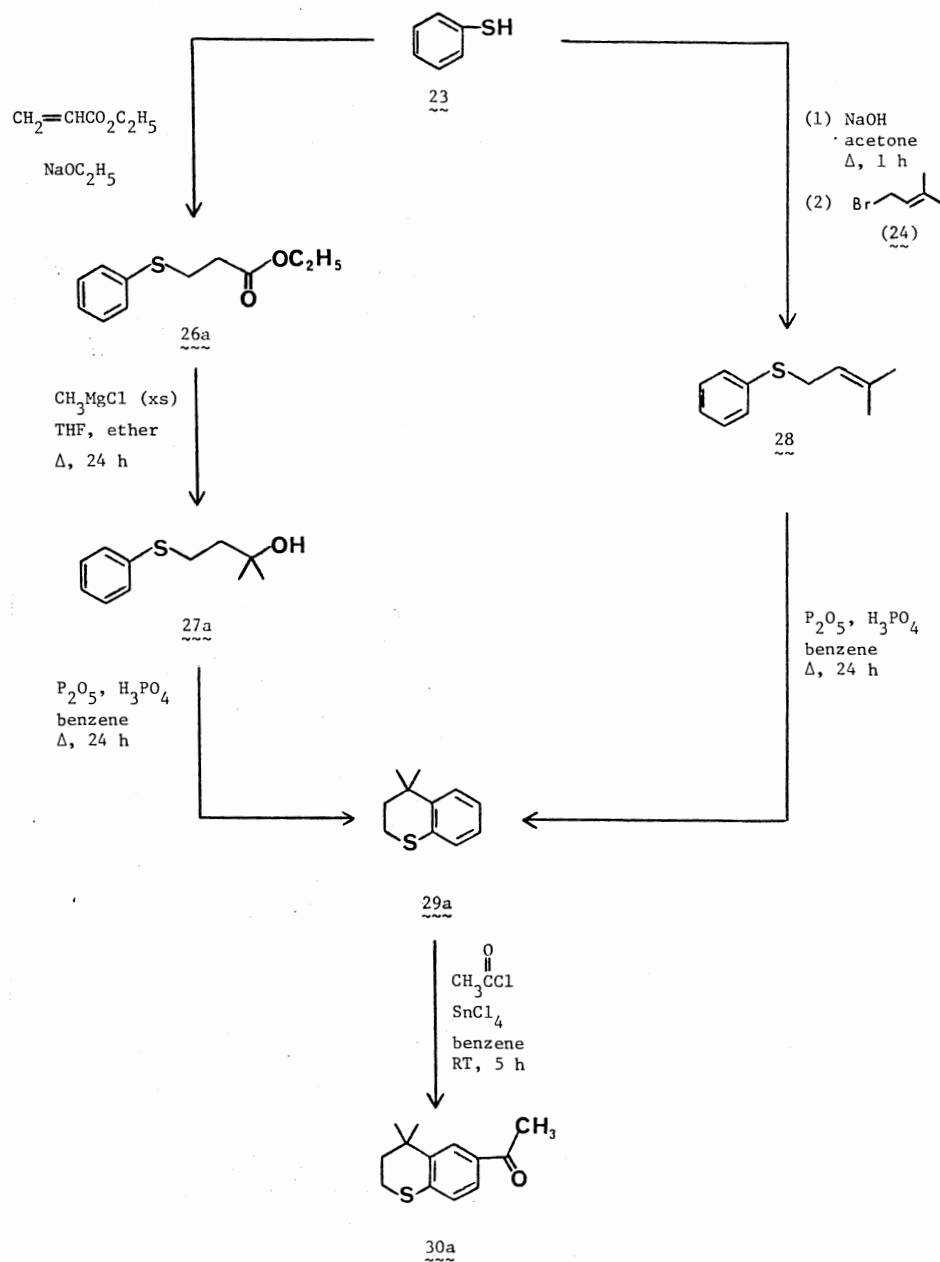


Synthesis of Heteroarotinoids

The synthetic routes used to prepare 22a and 22b from 23-32 are shown in Figures 3-5. The final step used to form the C-C double bond of the heteroarotinoid molecule involved a Wittig reaction using an appropriate phosphonium salt 32 and ethyl 4-formylbenzoate (33). The acid 22c was prepared (73.4%) by saponification of the corresponding ester 22b. The sulfoxide 22d was obtained (44.7%) by treatment of the sulfide 22a with NaIO_4 in methanol and water.



The sulfide 22a was prepared by a Wittig reaction between the phosphonium salt 32a and ethyl 4-formylbenzoate (33). The phosphonium salt 32a was obtained in several steps beginning with thiophenol. Two synthetic routes were developed to obtain the thiochroman ring system.

Figure 3. Synthesis of Ketone **30a**.

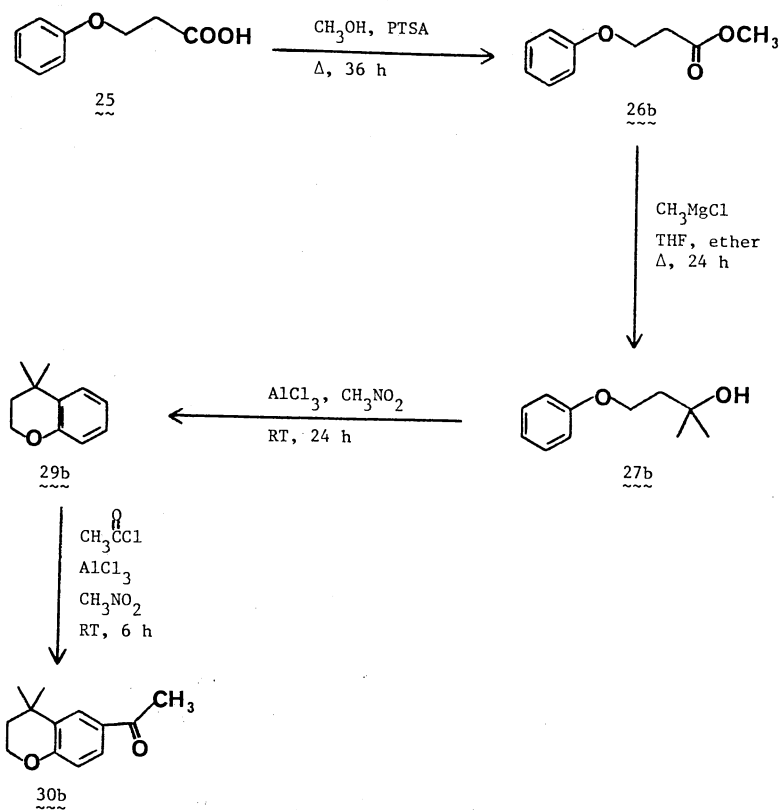


Figure 4. Synthesis of Ketone 30b.

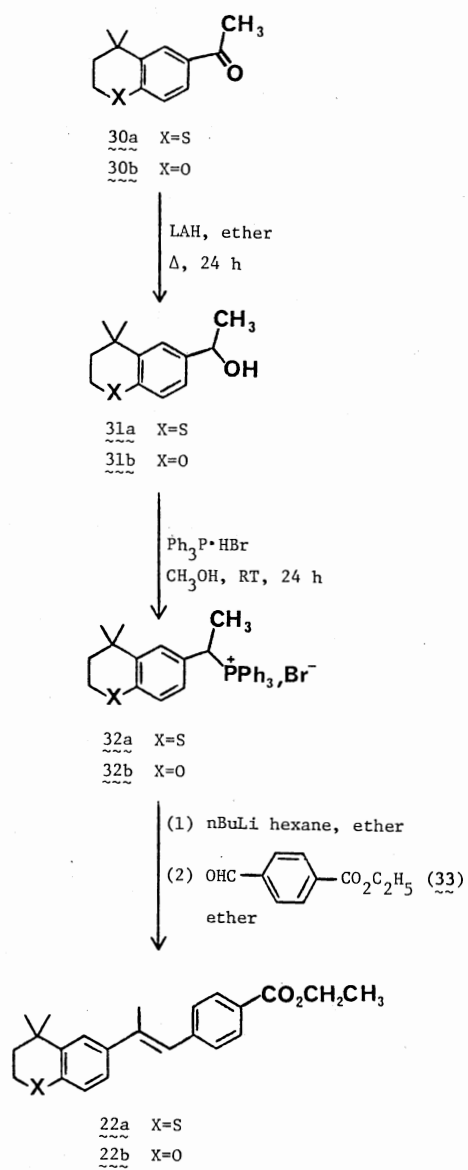
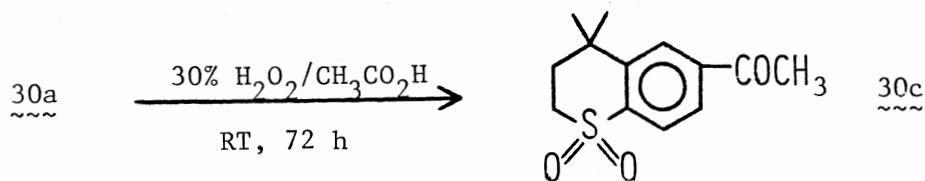


Figure 5. Synthesis of Heteroarotinoids 22a and 22b

In the best procedure, sodium thiophenoxide and 1-bromo-3-methyl-2-butene (24) were heated in acetone for 24 h to give 3-methyl-1-(phenylthio)-2-butene (28) in a yield of 83.4%. Cyclization of 28 using P_2O_5 and 85% H_3PO_4 in refluxing benzene gave 4,4-dimethylthiochroman (29a) (75.8%). In the second method, ethyl 3-(phenylthio)propionate (26a) was prepared (82.5%) by treatment of thiophenol (23) with ethyl acrylate in the presence of a catalytic amount of sodium ethoxide. A Grignard reaction using methylmagnesium chloride with 26a gave 2-methyl-4-(phenylthio)-2-butanol (27a, 80.1%). Cyclization of 27a using P_2O_5 and 85% H_3PO_4 in refluxing benzene gave 4,4-dimethylthiochroman (29a, 81.5%).

4,4-Dimethylthiochroman (29a) was acetylated using acetyl chloride and stannic chloride in benzene at room temperature for 5 h. The only product isolated from this reaction was 4,4-dimethylthiochroman-6-yl methyl ketone (30a). The absolute structure of 30a was determined by a single crystal X-ray diffraction analysis of the corresponding sulfone 30c. The sulfone 30c was prepared by treatment of the sulfide 30a with 30% H_2O_2 in glacial acetic acid at room temperature for 72 h.

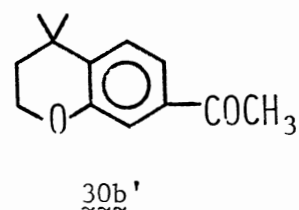
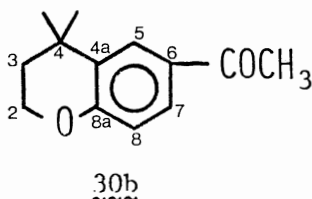


The ketone 30a was reduced to the corresponding alcohol 31a (94%, crude) by treatment with $LiAlH_4$ in ether. The desired phosphonium salt 32a was prepared by treating 31a with triphenylphosphine hydrobromide in methanol at room temperature for 26 hours. A Wittig

reaction involving 32a and ethyl 4-formylbenzoate gave the desired hetero-arotinoid 22a in which the C-C double bond had the E configuration. The manner in which the configuration about the double bond was determined will be discussed later.

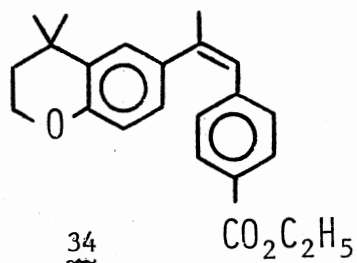
The ether 22b was prepared by a Wittig reaction involving the phosphonium salt 32b and ethyl 4-formylbenzoate (33). Several methods for the synthesis of the chroman ring system are available.^{6,8} An alternate route was designed and used to prepare 4,4-dimethylchroman (29b). 3-Phenoxypropionic acid (25) was esterified using conventional techniques to give the corresponding methyl ester 26b. Treatment with methylmagnesium chloride gave 2-methyl-4-phenoxy-2-butanol (27b, 76.4%). Cyclization of 27b using anhydrous aluminum chloride in nitromethane at room temperature gave 29b (62%).

4,4-Dimethylchroman (29b) was acetylated by treatment with acetyl chloride and aluminum chloride in nitromethane. Only one of the four possible regioisomers was isolated. Using the splitting patterns of the aromatic protons in the ¹H NMR spectrum, the regioisomer isolated must be either the 6- or 7-acetyl isomer (30b or 30b'). Of these two, the 6-acetyl isomer 30b was expected since the directing influence of oxygen is normally greater than that of carbon. Based upon this expectation and the fact that acetylation of 4,4-dimethylthiochroman (29a) gave the 6-acetyl isomer, the regioisomer isolated in the acetylation of 29b should be 30b.



The ketone 30b was reduced to the corresponding alcohol (59.4%) using LiAlH_4 . The phosphonium salt 32b was prepared (80.3%) by treatment of 31b with triphenylphosphine hydrobromide in methanol at room temperature for 24 hours. The reaction time used in the preparation of 32b was very important. When a reaction time of 48 hours was used, a mixture of products was obtained. ^1H NMR spectral data indicated that ring opening may have occurred during the longer reaction time.

A Wittig reaction involving the phosphonium salt 32b and ethyl 4-formylbenzoate (33) gave the desired heteroarotinoid 22b. Purification of 22b was achieved with difficulty. The yellow oil obtained initially was chromatographed on neutral alumina using 5% ether/hexane. ^1H NMR spectral data of the resulting oil indicated the presence of not only the desired heteroarotinoid 22b but also a small amount ($\approx 18\%$) of the corresponding Z isomer, 34. The E isomer 22b was obtained in pure form by recrystallization from 95% $\text{C}_2\text{H}_5\text{OH}$ with cooling to 0°C and scratching to induce crystallization. The Z isomer 34 was not isolated.



Ethyl 4-formyl benzoate (33), which was used in the Wittig reactions, was obtained in three steps (Figure 6) from *p*-toluic acid (35). The acid (35) was esterified using conventional techniques to give the corresponding ethyl ester 36 (75%). Oxidation of 36 at $0-5^\circ\text{C}$

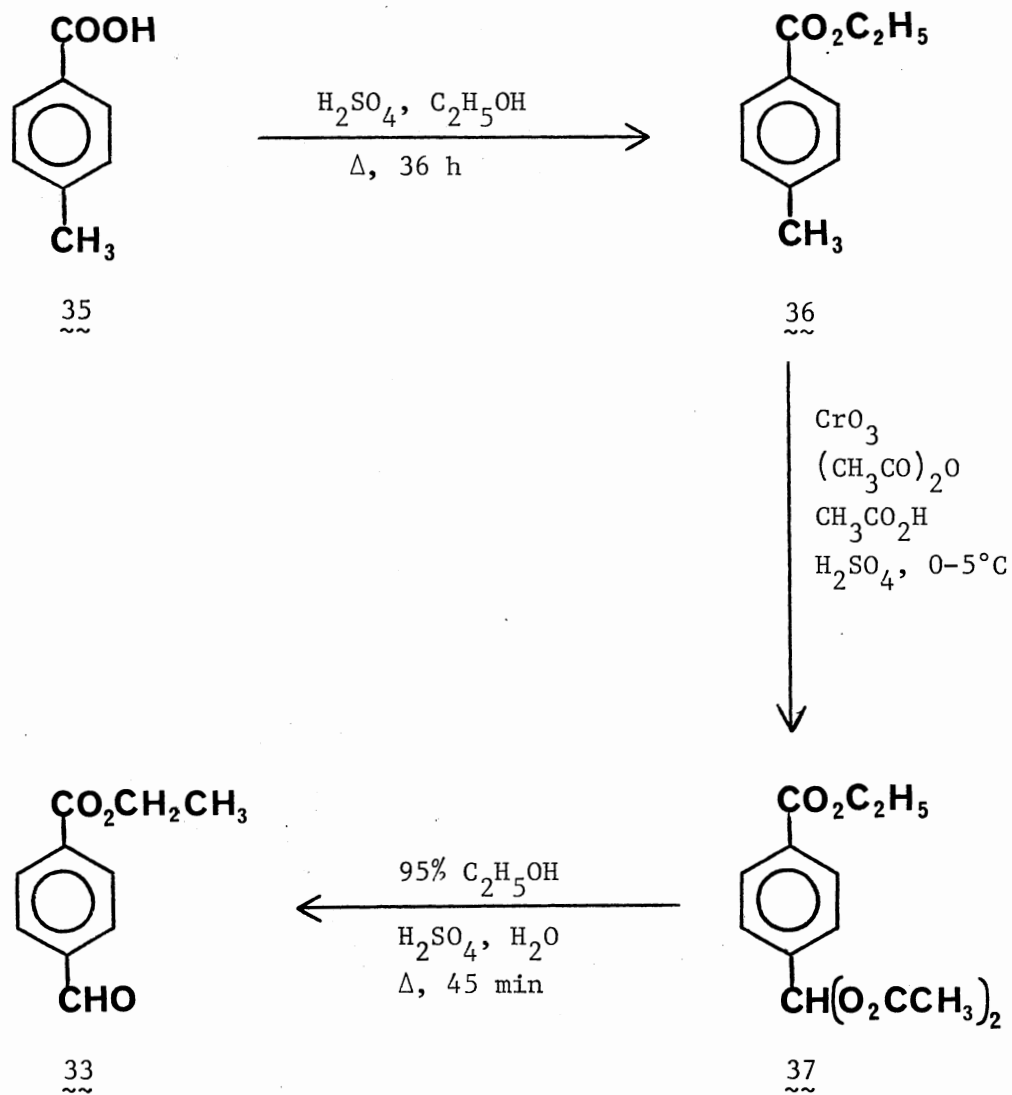
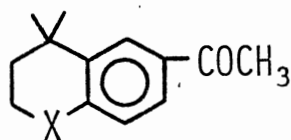


Figure 6. Preparation of Ethyl 4-Formylbenzoate.

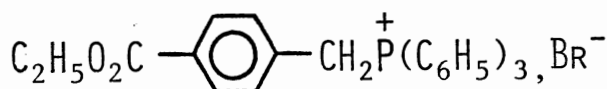
using CrO_3 in the presence of H_2SO_4 , acetic anhydride, and acetic acid gave the diacetate 37 (55.6%). Hydrolysis of 37 using H_2SO_4 , ethanol, and water gave the corresponding aldehyde 33 (50.9%).

Initially, a shorter synthetic route to the heteroarotinoids 22a and 22b was considered. In this route, the C-C double bonds of 22a and 22b were to be formed with Wittig reactions involving the ketones 30a and 30b and the phosphonium salt 38. Ketones 30a and 30b were prepared using the methods discussed earlier. The phosphonium salt 38 was synthesized in two steps from α -bromo-p-toluic acid (39). Acid 39 was treated with H_2SO_4 in refluxing ethanol for 70 minutes to give a mixture of products. The major product ($\sim 90\%$) obtained was the desired bromoester 40. The minor product ($\sim 10\%$) obtained was the ester 41. These compounds were not separated. Treatment of the crude mixture containing 40 and 41 with triphenylphosphine in refluxing benzene for 18 hours gave the desired phosphonium salt 38 (84.3%).

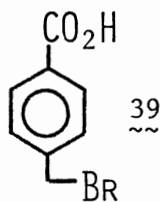


30a X=S

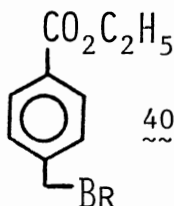
30b X=O



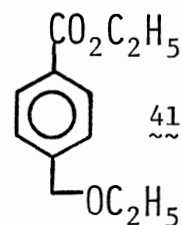
38



39



40

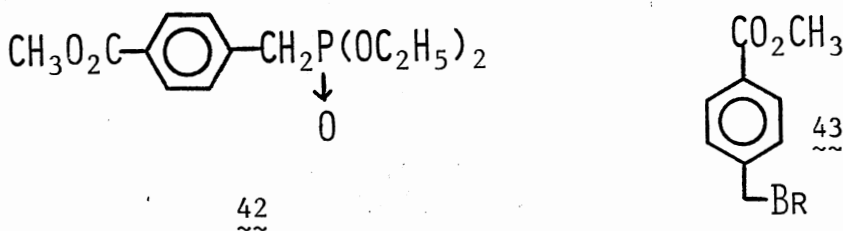


41

A Wittig reaction involving phosphonium salt 38 and ketone

30a was attempted. Treatment of a solution of 38 in DMSO with NaH at room temperature gave the corresponding ylid as indicated by the bright orange color. A solution of the ketone 30a in DMSO was added, and the resulting mixture was stirred at room temperature for 12 hours. Work-up gave an orange-brown oil. IR spectral data indicated the presence of unreacted 30a. The reaction was repeated using benzene instead of DMSO. After the ketone 30a was added to the red-brown solution containing the ylid, the mixture was heated at reflux for 72 hours. Work-up gave an orange-brown oil. IR spectral data again indicated the presence of a large amount of unreacted 30a.

A modified Wittig reaction using the phosphonate 42 and the ketone 30a was attempted. The phosphonate 42 was prepared from α -bromo-*p*-toluic acid (39). Esterification of 39 using H_2SO_4 in



refluxing methanol for 75 minutes gave the corresponding methyl ester 43 (75%). The ester 43 was treated with triethyl phosphite at reflux for 1 hour. A mixture of the resulting crude phosphonate 42 and the ketone 30a was treated with NaOCH₃ in refluxing methanol for 18 hours. Work-up gave a yellow oil which contained a large amount of unreacted ketone 30a as indicated by IR spectral data. Since the ketone 30a appeared to be unreactive in a Wittig reaction, it was converted to the phosphonium salt 32a. The phosphonium salt 32a was then used successfully in a Wittig reaction with ethyl 4-formylbenzoate as

described earlier

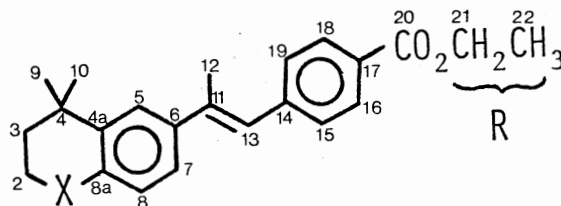
NMR Analysis of the Heteroarotinoids

The ^1H NMR spectral data for the heteroarotinoids 22a-22d are shown in the Experimental Section. The ^{13}C NMR spectral data for 22a-22d are shown in Table IV. In general, the assignments for the aliphatic carbons and protons were made by comparison to the appropriate precursors. The assignments for the aromatic protons in the chroman and thiochroman rings were based upon the observed splitting patterns. The assignments for the protonated aromatic and vinylic carbons were made using heteronuclear correlated 2-dimensional (HETCOR 2-D) NMR.

Although the assignments for the aliphatic protons of the heteroarotinoids 22a-22d were straightforward in most cases, the assignments for H(2) and H(3) of the sulfoxide 22d were not as obvious. These assignments were made using a heteronuclear correlated 2-dimensional (HETCOR 2-D) NMR experiment. A contour plot of the resulting 2-D spectrum is shown in Figure 7.

A HETCOR 2-D NMR experiment can be used to correlate the ^1H NMR chemical shift of a particular set of protons with the ^{13}C NMR chemical shift of the corresponding carbon.¹⁶ In order to utilize the information contained in a 2-D or contour plot, either the ^1H or ^{13}C NMR spectrum must be assigned unequivocally. For 22d, the ^{13}C NMR spectrum in the aliphatic region was assigned easily using INEPT experiments.³⁵ A comparison of the contour plot of the HETCOR 2-D NMR experiment, the ^{13}C NMR spectrum in the region between approximately 12 and 45 ppm, and the ^1H NMR spectrum between approximately δ 1.0 and 3.6 allowed the

TABLE IV
 ^{13}C NMR DATA FOR THE HETEROAROTINOIDS



22a X=S; 22b X=O; 22c X=O, R=H; 22d X=SO

Carbon Number	Chemical Shifts			
	<u>22a</u>	<u>22b</u>	<u>22c</u>	<u>22d</u>
2	23.0	63.1	63.1	42.9
3	37.6	37.6	37.6	29.4
4	33.1	30.7	30.7	34.4
9	30.2	31.1	31.1	31.3
10	30.2	31.1	31.1	31.1
12	17.6	17.7	17.8	17.7
21	60.8	60.8	-	60.9
22	14.3	14.4	-	14.3
5	124.0 ✓	124.5	124.6	125.5
7	123.7 ✓	124.9	124.9	124.8
8	126.4	116.8	116.8	130.5
13	125.7 ✓	125.1	125.0 ^a	128.4
15(19)	128.9 ^a ✓	129.0 ^a	129.1 ^a	129.0 ^a
16(18)	129.4 ^a ✓	129.4 ^a	130.1 ^a	129.5 ^a
20	166.5 ✓	166.1	172.1	166.3
Nonprotonated	143.0	153.4	153.5	147.1
Aromatic and	141.7	143.3	144.3	144.6
Vinylic Carbons	139.3	139.4	139.9	142.2
	139.2	135.7	135.6	138.6
	131.4	131.3	131.3	136.9
	128.0		126.8	128.7

^aMay be interchanged.

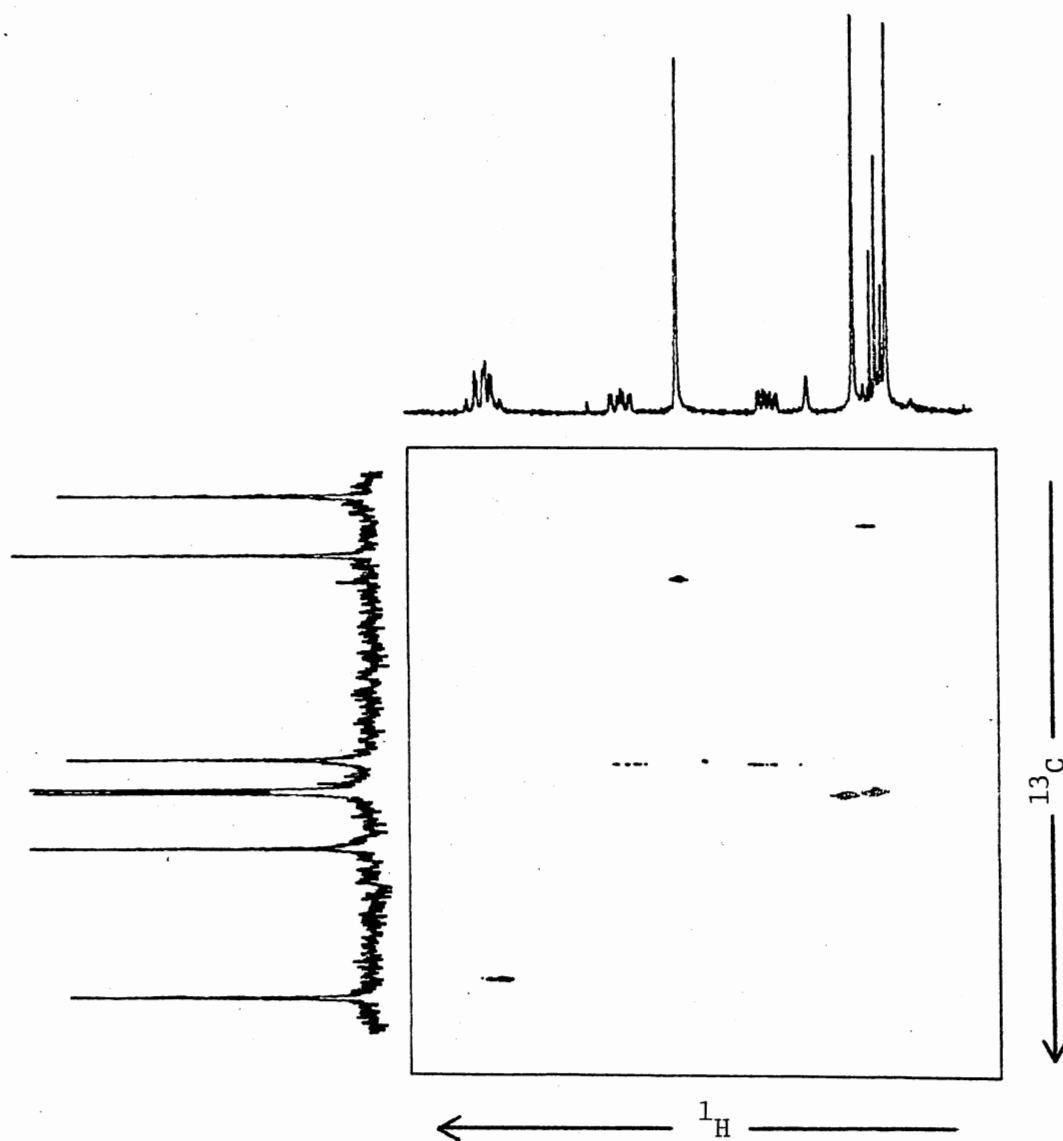


Figure 7. Contour Plot of HETCOR 2-D Spectrum of 22d in the Aliphatic Region

assignments for H(2) and H(3) to be made easily. Further information concerning the use of HETCOR 2-D NMR experiments can be found in Part I, Chapter II. In 22d, the multiplet at δ 1.84-1.94 (1 H) was assigned to H(3)_a while the multiplet at δ 2.48-2.62 (1 H) was assigned to H(3)_e. The multiplet at δ 3.06-3.25 (2 H) was assigned to H(2)_a and H(2)_e.

The assignments for the aromatic protons, H(5), H(7), and H(8), of the chroman and thiochroman rings in 22a-22d were made using the observed splitting patterns. In the heteroarotinooids, H(5) was expected to give a doublet with $J = 2-3$ Hz. In 22a, H(5) actually gave a broad singlet while in 22b-22d H(5) gave a doublet with $J = 3$ Hz. H(7) was expected to give a doublet of doublets with $J = 2-3, 7-10$ Hz. In 22a, H(7) actually gave a multiplet while in 22b-22d H(7) gave the expected doublet of doublets with $J = 3, 9$ Hz. H(8) was expected to give a doublet with $J = 7-10$ Hz. In 22a-22d, H(8) gave the expected doublet with $J = 9$ Hz.

The ¹³C NMR assignments for the protonated aromatic and olefinic carbons of 22a, 22b, and 22d (Table IV) were made using HETCOR 2-D NMR experiments in the aromatic region. The results of these experiments are shown in Figures 8-10. Similar assignments for 22c were made by comparison to 22b.

The ¹H NMR chemical shifts of the vinylic protons and vinylic methyl groups in 22a-22d were used to tentatively assign the configurations of the C-C double bonds in these modified retinoids. In 22a-22d, the vinylic proton gave a singlet at δ 6.82, 6.77, 6.80, and 6.86, respectively. In the E-arotinooids 20, 21, 44, and 45, the vinylic proton gave a singlet at δ 6.85, 6.88, 6.72, and 6.82, respectively, while the Z-arotinooid 46 gave a singlet at δ 6.46. In the heteroarotinooids 22a-22d, the vinylic methyl group gave a singlet at δ 2.28,

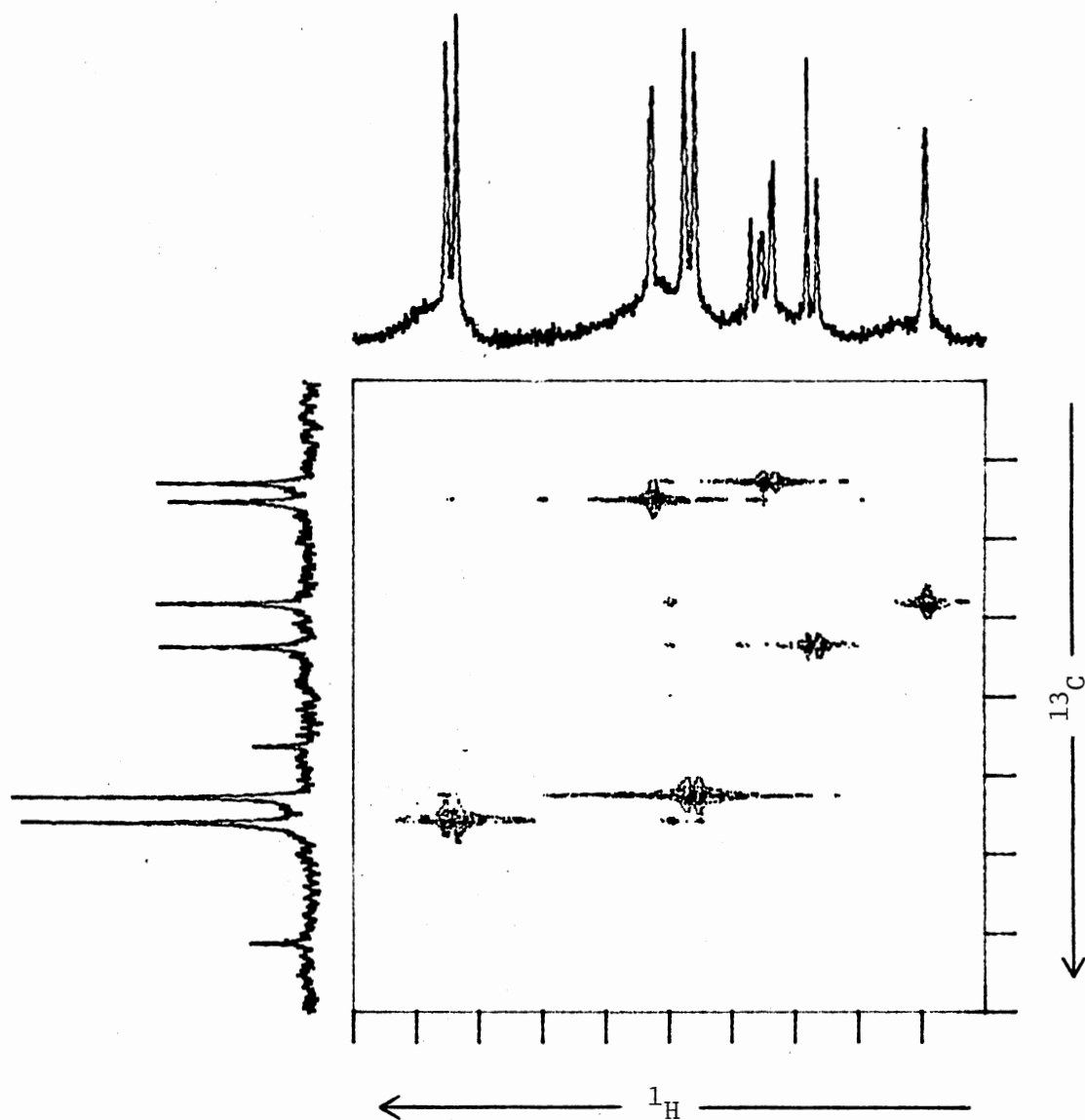


Figure 8. Contour Plot of HETCOR 2-D Spectrum of 22a in the Aromatic Region

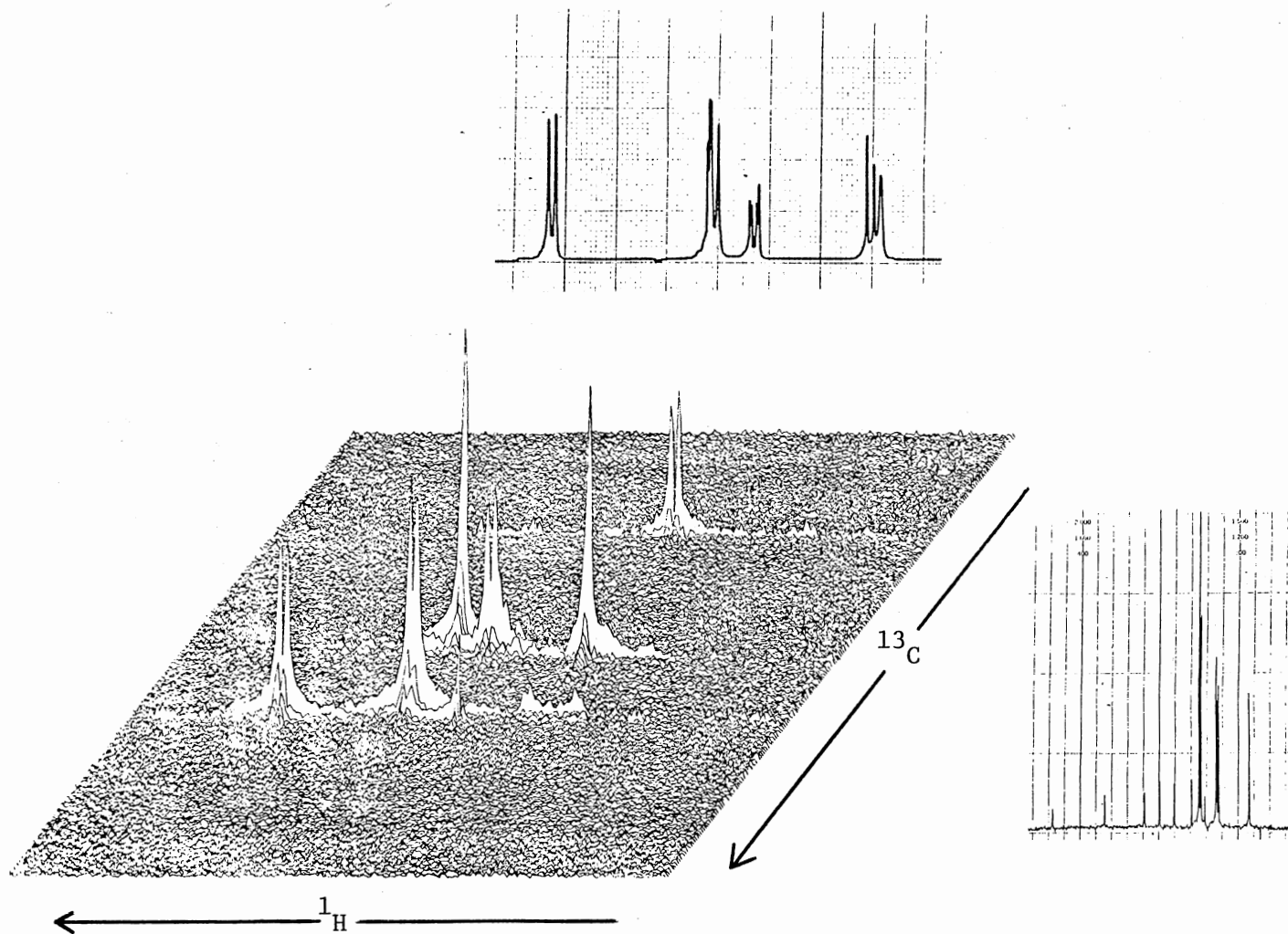


Figure 9. HETCOR 2-D Spectrum of 22b in the Aromatic Region

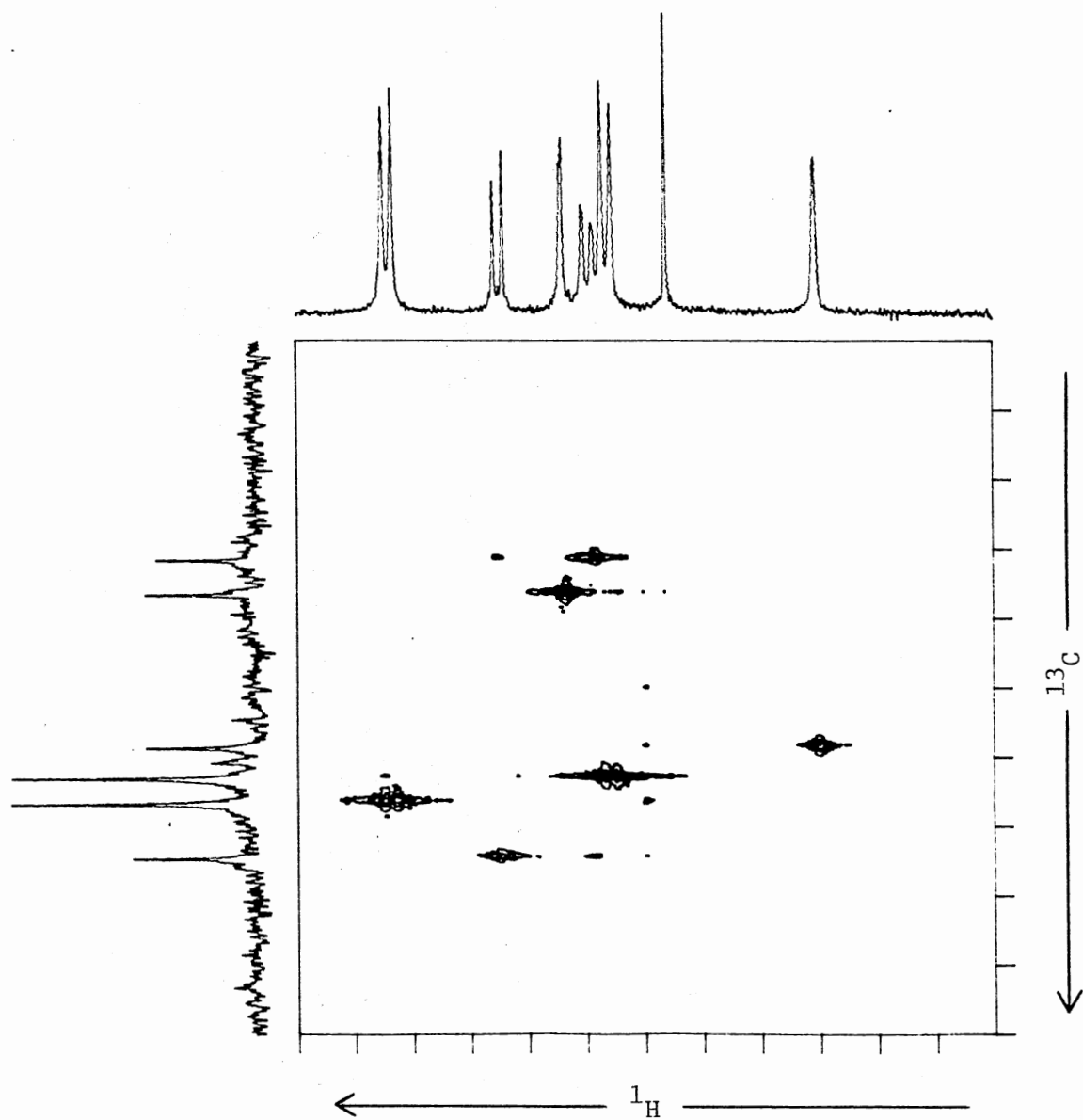
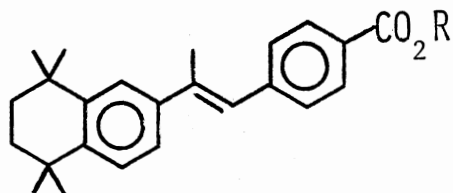
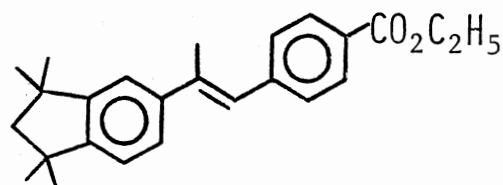


Figure 10. Contour Plot of HETCOR 2-D Spectrum of 22d in the Aromatic Region

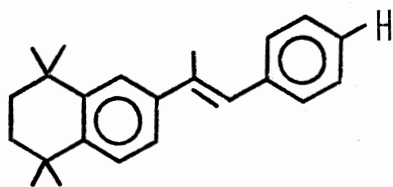
2.27, 2.31, and 2.30, respectively. In the E-arotinoids 20, 21, 44, and 45, the corresponding signals were observed at δ 2.30, 2.37, 2.27, and 2.28, respectively, while in the Z-arotinoid 46, a signal at δ 2.23 was observed. A comparison of these data indicated that the heteroarotinoids 22a-22d should have the E-configuration.



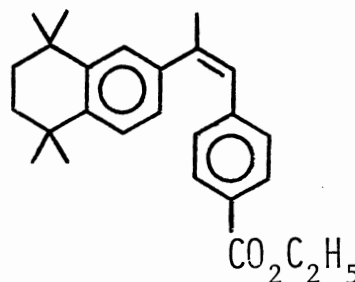
20 R=C₂H₅
21 R=H



44



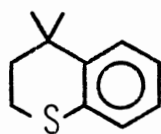
45



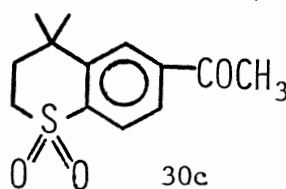
46

X-Ray Diffraction Analysis of 30c

A single crystal X-ray diffraction analysis of the sulfone 30c was performed by Dr. E. M. Holt to verify the identity of the regioisomer obtained in the acetylation of 4,4-dimethylthiochroman (29a). As shown



29a



30c

in Figure 11, the results of the analysis indicated that 29a was acetylated in the 6-position. The important bond angles and bond distances are shown in Table V.

X-Ray Diffraction Analysis of Heteroarotinoid 22a

The preliminary results of a single crystal X-ray diffraction analysis of the heteroarotinoid 22a are shown in Figure 12. Two modifications of 22a were found in the crystal examined. In both of these, the C-C double bond had the E-configuration as predicted using ^1H NMR spectral data. Further data is needed before a comparison of the conformation of this heteroarotinoid to that of other retinoids can be made. Examination of the degree of planarity between the two aromatic rings and comparison to other retinoid systems would be very interesting.

Pharmacological Activity of the Heteroarotinoids

The pharmacological activity of the heterotinoids 22a-22d was assessed at the Illinois Institute of Technology Research Institute using the method developed by Sporn and co-workers³⁸ as discussed in Chapter I. In this assay, the in vitro ability of 22a-22d to reverse keratinization in vitamin A deficient hamster tracheal organ cultures was determined. A retinoid was considered to be active if neither keratin nor keratohyaline granules were seen or if only keratohyalin granules were not present. If both were seen, the retinoid was considered to be inactive.

The preliminary assays of 22a, 22b, and 22d have been completed. The results for these heteroarotinoids are summarized in Table VI. The assay of the acid 22c is currently in progress. A comparison of the

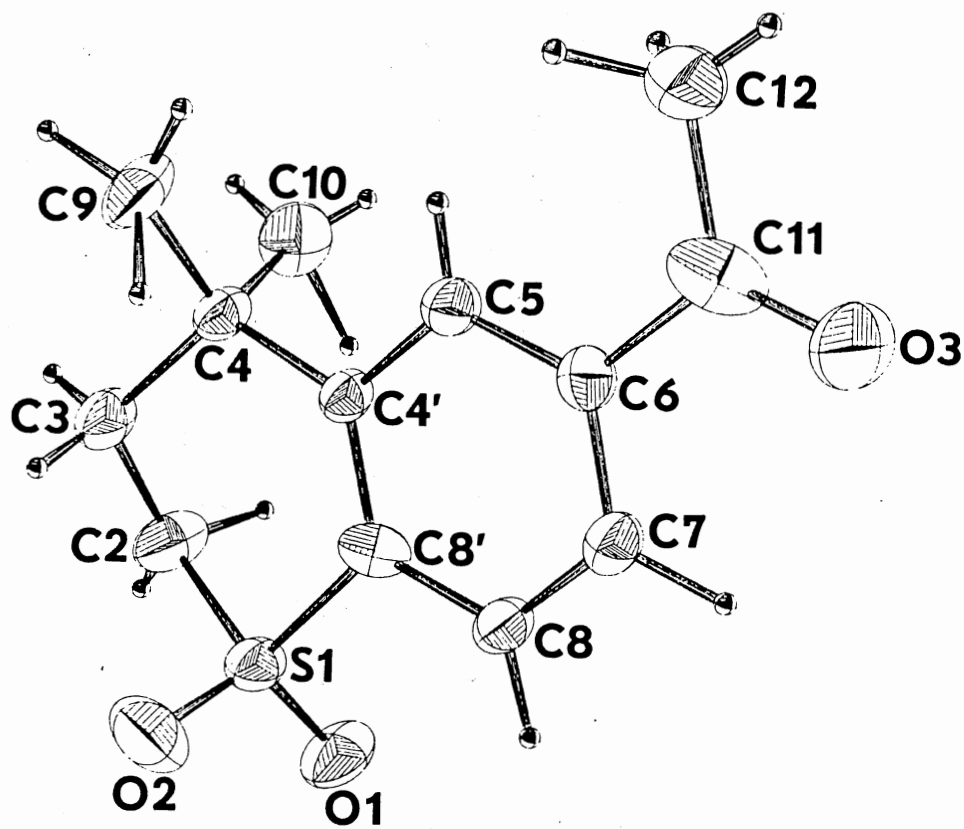


Figure 11. Structure of Ketone 30c

TABLE V
 BOND ANGLES AND DISTANCES OF 30c

Angle	Angle (°)	Bond	Bond Distance (Å)
O1-S1-O2	117.4(2)	S1-O1	1.443(3)
O1-S1-C2	109.3(2)	S1-O2	1.447(4)
O1-S1-C8'	109.3(2)	S1-C2	1.761(4)
O2-S1-C2	110.1(2)	S1-C8'	1.767(3)
O2-S1-C8'	107.3(2)	C2-C3	1.539(5)
C2-S1-C8'	102.2(2)	C3-C4	1.535(5)
S1-C2-C3	107.7(2)	C4-C9	1.548(5)
C2-C3-C4	113.5(4)	C4-C10	1.546(6)
C3-C4-C9	106.3(3)	C4-C4'	1.537(4)
C3-C4-C10	110.3(3)	C4'-C5	1.397(4)
C3-C4-C4'	112.3(3)	C5-C6	1.394(5)
C9-C4-C4'	110.4(2)	C6-C11	1.501(4)
C10-C4-C4'	107.4(3)	C6-C7	1.399(5)
C4-C4'-C5	118.9(3)	C7-C8	1.374(4)
C4-C4'-C8'	124.4(2)	C8-C8'	1.409(5)
C5-C4'-C8'	116.7(3)	C11-C12	1.505(6)
C6-C5-C4'	121.8(3)	C11-O3	1.227(5)
C5-C6-C7	120.1(3)		
C5-C6-C11	121.7(3)		
C6-C6-C11	118.2(3)		
C6-C7-C8	119.6(3)		
C7-C8-C8'	119.6(3)		
S1-C8'-C8	114.9(2)		
S1-C8'-C4'	122.8(2)		
C8-C8'-C4'	122.2(2)		
O3-C11-C12	121.5(3)		
O3-C11-C6	119.5(3)		
C6-C11-C12	119.0(4)		

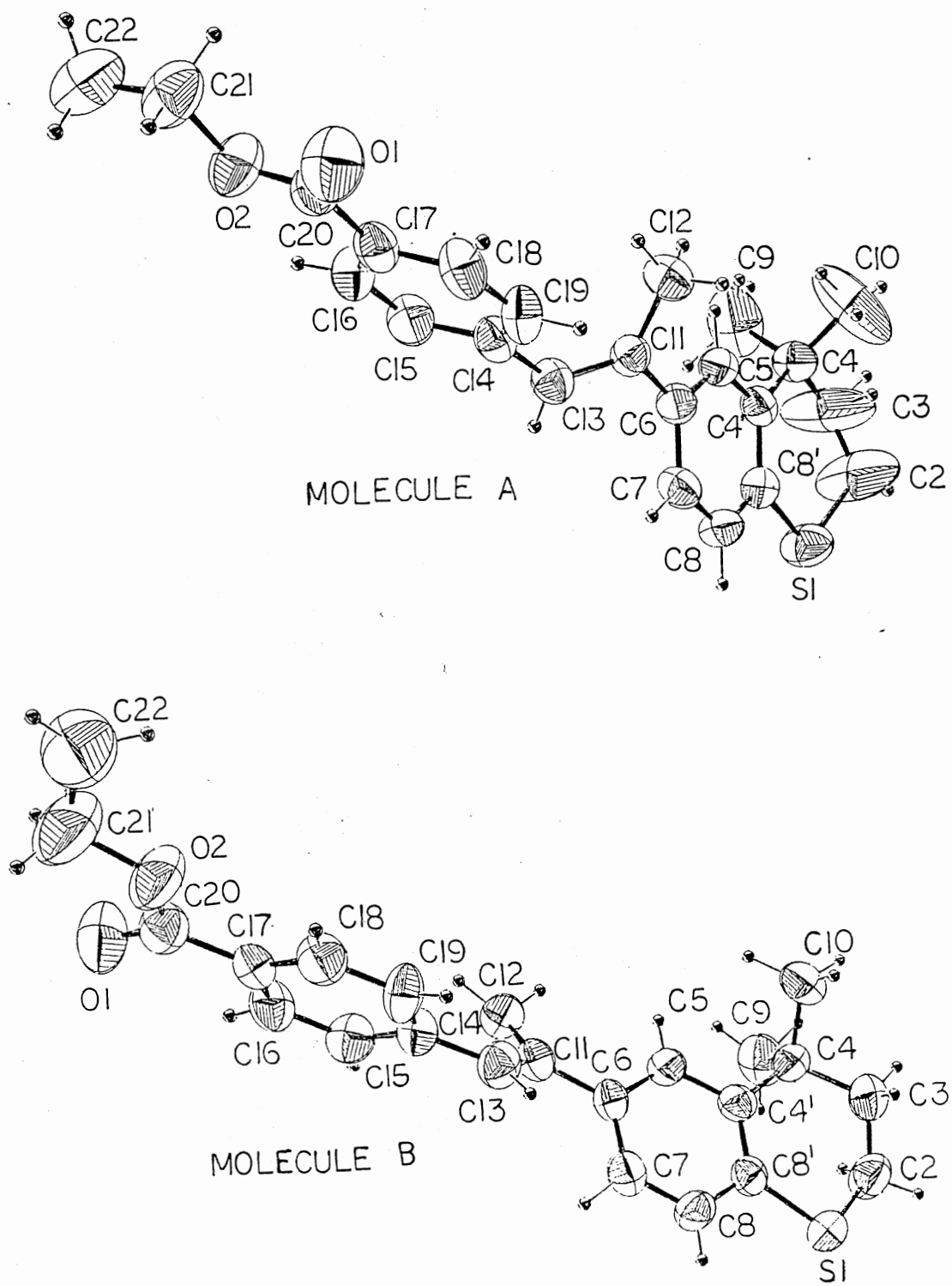


Figure 12. Structure of Heteroarotinoid 22a.

TABLE VI

ACTIVITY OF THE HETEROAROTINOLIDS IN THE HAMSTER TRACHEAL ORGAN CULTURE

Retinoid	Concentration (M)	% Active	ED ₅₀ (M)
<u>trans-retinoic acid</u> ^a	10 ⁻¹⁰	76.9	2 x 10 ⁻¹¹
	10 ⁻¹¹	41.7	
	10 ⁻¹²	23.1	
<u>22a</u>	10 ⁻⁸	100	6 x 10 ⁻¹¹
	10 ⁻⁹	100	
	10 ⁻¹⁰	53.8	
	10 ⁻¹¹	28.6	
	10 ⁻¹²	33.7	
<u>trans-retinoic acid</u> ^a	-	-	8 x 10 ⁻¹²
<u>22b</u>	10 ⁻⁸	100	~ 8 x 10 ⁻¹¹
	10 ⁻⁹	100	
	10 ⁻¹⁰	55.6	
<u>22d</u>	10 ⁻⁸	71.4	~ 3 x 10 ⁻¹⁰
	10 ⁻⁹	71.4	
	10 ⁻¹⁰	28.6	

^aThe activity of trans-retinoic acid was determined for each set of experiments.

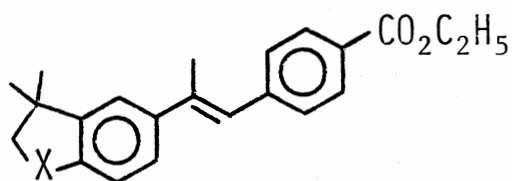
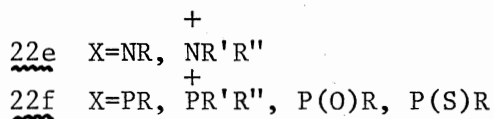
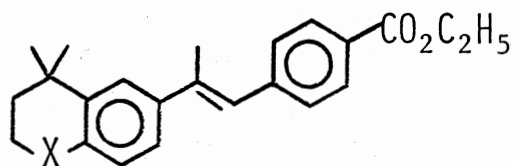
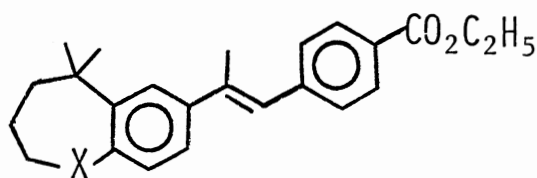
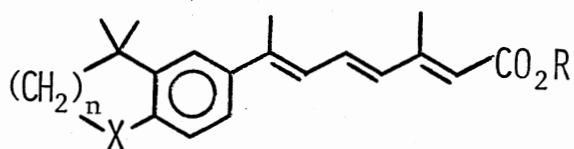
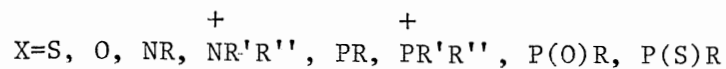
ED₅₀ values for 22a, 22b, and 22d with the ED₅₀ value for the standard, trans-retinoic acid, indicates that all three of the heteroarotinoids are active. The activities of the sulfide 22a and the ether 22b are very high although slightly less than those of the standard, trans-retinoic acid, and the arotinoids 20 and 21 (ED₅₀ = 1 x 10⁻¹¹ M).³⁷ The activity of the sulfoxide 22d is approximately one order of magnitude lower than that of the sulfide 22a.

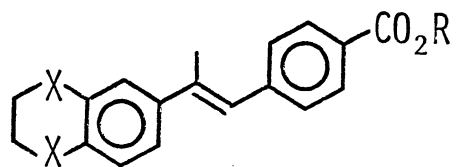
The initial purpose of this work was to modify the basic arotinoid structure in such a way as to maintain the high degree of activity of the arotinoids while simultaneously reducing the associated toxicity. The incorporation of the heteroatoms, S and O, into the basic arotinoid structure appears to meet the first objective. The heteroarotinoids 22a and 22b show a high degree of activity. At this time, toxicity studies of 22a-22d have not been performed. It is, therefore, not possible to determine whether the incorporation of a heteroatom such as S or O effectively reduces the toxicity associated with the arotinoid molecules.

Suggestions for Future Work

Toxicity studies of the heteroarotinoids 22a-22d must be performed to determine what effect, if any, the heteroatom has on the overall toxicity of the retinoids. If the toxicity studies are promising, a variety of modifications can be made on the heteroarotinoid structure to improve the activity and reduce the toxicity. Modifications which could prove useful include: (1) the incorporation of other heteratoms such as N or P (22e, 22f), (2) expansion or contraction of the heteroatom-containing ring (47, 48), (3) changes in the side chain to give

the heteroretinoids such as 49, (4) changes in the terminal polar group to include the corresponding acids, alcohols, amides, aldehydes, and ethers, and (5) the incorporation of two heteroatoms into the arotinoid structure (50-53).

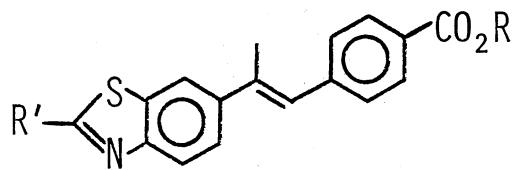
474849a n=149b n=249c n=3



50 X=O

51 X=S +

52 X=NR, NR'R''



53

CHAPTER III

EXPERIMENTAL SECTION

General Information

Reactions were carried out under a nitrogen atmosphere when necessary. All reactions were stirred using a magnetic stirrer unless otherwise specified. During work-up, solvents were removed using a rotary evaporator unless otherwise stated. NMR spectral data were obtained using either a Varian XL-100 (15) NMR spectrometer equipped with a Nicolet TT-100 PFT accessory or a Varian XL-300 NMR spectrometer. All NMR data were reported in ppm or δ values downfield from TMS using either TMS or CDCl_3 as an internal reference. IR spectral data were obtained using a Perkin-Elmer 681 IR spectrophotometer. Melting points were determined using a Thomas Hoover melting point apparatus and were uncorrected. ^{13}C NMR spectral data for some compounds have been included in Chapter II.

Starting Materials

The following starting materials and special reagents were purchased from the source listed and were used without further purification: thiophenol (Aldrich, bp 169°C), ethyl acrylate (Aldrich, bp 99°C), 1-bromo-3-methyl-2-butene (Columbia, bp $50\text{--}52^\circ\text{C}/50\text{ mm}$), acetyl chloride (Fisher, bp $49\text{--}50^\circ\text{C}$), methylmagnesium chloride/THF (2.9 M, Aldrich), *p*-toluic acid (Aldrich, mp $180\text{--}182^\circ\text{C}$), α -bromo-*p*-toluic acid (Aldrich,

mp 223-227^oC), stannic chloride (Baker), aluminum chloride (Fisher), and 3-phenoxypropionic acid (Columbia, mp 97-98^oC). Anhydrous solvents were obtained as discussed below. Ether and thiophene-free benzene were distilled from sodium prior to use. All other solvents were used without purification.

Ethyl 3-(Phenylthio)propionate (26a)

Freshly distilled ethyl acrylate (75 mL) was added dropwise under N₂ to a stirred, ice-cold mixture of thiophenol (23, 31.5 g, 0.286 mol) and sodium ethoxide (1.0 g) in a 250-mL round bottom flask. The ice bath was removed, and the mixture was stirred at RT for 24 h. The mixture was diluted with ether (30 mL) and filtered. The ether and excess ethyl acrylate were removed (vacuum). Vacuum distillation gave 49.6 g (82.5%) of 26a as a colorless liquid: bp 115-118/0.2 mm (lit.²¹ 117^oC/2.5 mm); IR (neat) 1730-1750 cm⁻¹ (C=O); ¹H NMR (CDCl₃) δ 1.22 (t, 3 H, OCH₂CH₃), 2.58 (t, 2 H, CH₂CO₂C₂H₅), 3.14 (t, 2 H, SCH₂), 4.1 (q, 2 H, OCH₂CH₃), 7.07-7.37 (m, 5 H, Ar-H); ¹³C NMR (CDCl₃) ppm 171.3 [C(1)], 135.2, 129.8, 128.8, 126.3, 60.5 [C(α)], 34.4 [C(2)], 29.0 [C(3)], 14.2 [C(β)].

2-Methyl-4-(phenylthio)-2-butanol (27a)

A solution of ethyl 3-(phenylthio)propionate (26a, 20.0 g, 0.0952 mol) in dry ether (5 mL) was added under N₂ to a stirred solution of methylmagnesium chloride in THF (2.9 M, 105 mL, 0.3045 mol) in a 300-mL round bottom flask equipped with a condenser at a rate such that the solution boiled. The solution was then heated at reflux for an additional 36 h. The mixture was cooled to RT and quenched with saturated

aqueous NH_4Cl . The supernatant liquid was decanted, and the residue was washed with dry ether (3 x 50 mL). The combined organics were dried (Na_2SO_4), and the ether was removed (vacuum). Vacuum distillation of the crude oil gave 14.95 g (80.1%) of 27a as a colorless liquid: bp $93\text{--}98^\circ\text{C}/0.01\text{ mm}$ (lit.³² $110\text{--}113^\circ\text{C}/0.7\text{ mm}$); IR (neat) $3200\text{--}3600\text{ cm}^{-1}$ (OH); $^1\text{H NMR}$ (CDCl_3) δ 1.17 [s, 6 H, $(\text{CH}_3)_2$], 1.66–1.84 [m, 2 H, $\text{ArSCH}_2\text{CH}_2$], 2.38–2.47 [br s, 1 H, OH], 2.88–3.05 [m, 2 H, ArSCH_2], 7.04–7.34 [m, 5 H, Ar-H]; $^{13}\text{C NMR}$ (CDCl_3) ppm 28.2 [C(4)], 28.9 [C(1)], 42.4 [C(3)], 70.2 [C(2)], 125.3 [C(4')], 128.2, 128.4 [C(2'), C(3')], 136.1 [C(1')].

3-Methyl-1-(phenylthio)-2-butene (28)^{9,12}

A mixture of thiophenol (23, 16.3 g, 0.148 mol) and NaOH (6.0 g, 0.150 mol) in acetone (100 mL) was heated at reflux under N_2 with vigorous stirring for 1 h in a 250-mL round bottom flask equipped with a condenser. A solution of 1-bromo-3-methyl-2-butene (24, 22.3 g, 0.1498 mol) in acetone (20 mL) was then added dropwise. The resulting mixture was maintained at reflux for 24 h. The mixture was concentrated to 30 mL, diluted with H_2O (75 mL), and extracted with ether (2 x 50 mL). The organic layers were combined and washed with 5% aqueous NaOH (3 x 30 mL), H_2O (50 mL), and brine (50 mL). After drying (Na_2SO_4) the solution, the solvent was removed to leave a pale yellow liquid. Vacuum distillation gave 22.0 g (83.4%) of 28 as a pale yellow liquid: bp $76\text{--}78^\circ\text{C}/0.15\text{ mm}$; $^1\text{H NMR}$ (CDCl_3) δ 1.55 [s, 3 H, CH_3], 1.68 [s, 3 H, CH_3], 3.52 [d, 2 H, PhSCH_2], 5.24–5.34 [m, 1 H, $(\text{CH}_3)_2\text{C}=\text{CH}$], 7.1–7.36 [m, 5 H, Ar-H]; $^{13}\text{C NMR}$ (CDCl_3) ppm 136.7, 136.0, 129.4, 128.4, 125.7, 119.2, 32.1, 25.6, 17.6.

4,4-Dimethylthiochroman or 3,4-Dihydro-4,4-dimethyl-2H-1-benzothiopyran (29a)⁵

Method I. A mixture of 2-methyl-4-(phenylthio)-2-butanol (27a, 10.0 g, 0.0510 mol), H_3PO_4 (85%, 5 mL) and P_2O_5 (3 x 6.0 g, 0.1268 mol) in benzene (50 mL) was heated at reflux under N_2 with vigorous stirring for 24 h in a 100-mL round bottom flask equipped with a condenser. The P_2O_5 was added in three equal portions at 6 to 8 h intervals. After cooling, the solution was decanted from the reddish-purple residue, and the residue was washed with ether (2 x 25 mL). The combined organics were washed with 5% aqueous NaHCO_3 (2 x 50 mL) and saturated aqueous NaCl (3 x 50 mL). After drying (Na_2SO_4) the solution, the solvent was removed, and the residual oil was vacuum distilled to give 7.4 g (81.5%) of 29a as a colorless liquid: bp 80–85°C/0.01 mm; ^1H NMR (CDCl_3) δ 1.29 [s, 6 H, (CH_3)₂], 1.84–1.97 [m, 2H, H(3)], 2.91–3.03 [m, 2 H, H(2)], 6.9–7.35 [m, 4 H, Ar-H]; ^{13}C NMR (CDCl_3) ppm 23.1 [C(2)], 30.2 [C(4')], 32.9 [C(4)], 37.7 [C(3)], 123.8, 125.8, 126.26, 126.3 [C(5), C(6), C(7), C(8)], 131.5 [C(4a)], 141.7 [C(8a)].

Method II. A mixture of 3-methyl-1-(phenylthio)-2-butene (28, 21.5 g, 0.1208 mol), H_3PO_4 (85%, 15 mL), and P_2O_5 (17.2 g, 0.1211 mol) in benzene (200 mL) was heated at reflux under N_2 with vigorous stirring for 20 h in a 500-mL round bottom flask equipped with a condenser. After cooling, the supernatant liquid was decanted from the phosphorus-containing residue, and the residue was washed with ether (3 x 50 mL). The organics were combined and washed with 5% NaHCO_3 (2 x 75 mL), H_2O (75 mL), and brine (2 x 75 mL). After drying (Na_2SO_4) the solution, the solvent was evaporated leaving a yellow oil. Vacuum distillation

gave 16.3 g (75.8%) of 29a as a pale yellow liquid: bp 80-85°C/0.01 mm. The spectral data obtained (^1H and ^{13}C NMR) were identical to those obtained for 29a prepared by Method I.

4,4-Dimethylthiochroman-6-yl Methyl Ketone or
1-(3,4-Dihydro-4,4-dimethyl-2H-1-benzothio-
pyran-6-yl)ethanone (30a)

Stannic chloride (4.7 mL, 0.0501 mol) was added dropwise under N_2 to a stirred solution of 4,4-dimethylthiochroman (29a, 6.6 g, 0.0371 mol) and acetyl chloride (3.1 g, 0.0395 mol) in dry, thiophene-free benzene (30 mL) in a 100-mL, round bottom flask. The resulting dark green solution was stirred at RT for 5 h and then diluted with water (30 mL) and conc. HCl (15 mL). The resulting mixture was heated to just below the boiling point for 15 min. The mixture was allowed to cool to RT, and the two layers were separated. The aqueous layer was extracted with benzene (5 x 20 mL), and the combined organic layers were washed with H_2O (2 x 50 mL), 5% aqueous Na_2CO_3 (2 x 40 mL), H_2O (50 mL), and brine (60 mL). After drying (Na_2SO_4) the solution, the solvent was removed (vacuum) leaving a viscous brown oil. Vacuum distillation gave 4.92 g (60.3%) of 30a as a pale yellow oil: bp 126-130°C/0.02 mm; IR (neat) 1675-1685 cm^{-1} (C=O); ^1H NMR (CDCl_3) δ 1.32 [s, 6 H, $(\text{CH}_3)_2$], 1.84-1.97 [m, 2 H, H(3)], 2.51 [s, 3 H, $\text{CH}_3\text{C=O}$], 2.95-3.07 [m, 2 H, H(2)], 7.07 [d, 1 H, $J = 8$ Hz, H(8)], 7.53 [dd, 1 H, $J = 2$ Hz, H(7)], 7.95 [d, 1 H, $J = 2$ Hz, H(5)]; ^{13}C NMR (CDCl_3) ppm 23.1 [C(2)], 26.2 [C(10)], 29.7 [C(4')], 32.9 [C(4)], 36.8 [C(3)], 125.7, 126.1, 132.8, 139.3, 141.6, 196.7 [C(9)]; Mass spectral data for $\text{C}_{13}\text{H}_{16}\text{OS}$: m/e (M^+) 220.0922; Found: 220.0922.

4,4-Dimethylthiochroman-6-yl MethylKetone 1,1-Dioxide (30c)

A solution of 30% H₂O₂ (13 mL) was added dropwise under N₂ to a stirred solution of the sulfide 30a (0.5 g, 2.294 mmol) in glacial acetic acid (10 mL) in a 50-mL round bottom flask. The mixture was stirred at RT for 72 h during which time a white solid precipitated. The mixture was poured into ice water (25 mL). The resulting white solid was filtered, washed with water (10 mL), and air dried. Recrystallization (95% ethanol) gave 0.3 g (52.3%) of 30c as white crystals: mp 197–197.5^oC; IR (KBr) 1680–1690 (C=O), 1280–1295 (SO₂), 1130–1150 cm⁻¹ (SO₂); ¹H NMR (CDCl₃) δ 1.46 [s, 6 H, (CH₃)₂], 2.36–2.48 [m, 2 H, H(3)], 2.63 [s, 3 H, CH₃C=O], 3.37–3.50 [m, 2 H, H(2)], 7.91–8.04 [m, 3 H, Ar-H]; ¹³C NMR (CDCl₃) ppm 26.8 [C(10)], 30.6 [C(4')], 34.5 [C(4)], 35.4 [C(3)], 47.0 [C(2)], 124.2, 126.9, 127.2, 139.8, 140.9, 145.1 [Ar-C], 196.6 [C(9)]; Mass spectral data for C₁₃H₁₆O₃S: m/e (M⁺) 252.0820; Found: 252.0817.

α,4,4-Trimethylthiochroman-6-methanol or 3,4-Dihydro-α,4,4-trimethyl-2H-1-benzothio-pyran-6-methanol (31a)

A solution of 4,4-dimethylthiochroman-6-yl methyl ketone (30a, 4.0 g, 0.0182 mol) in dry ether (20 mL) was added dropwise under N₂ to a stirred suspension of LiAlH₄ (1.0 g, 0.0264 mol) in ether (75 mL) in a 250-mL round bottom flask equipped with a condenser. The resulting mixture was heated at reflux for 24 h. Ethyl acetate was then added dropwise to destroy the excess LiAlH₄. A solution of 5% HCl (50 mL) was added, and the mixture was stirred for 10 min. The layers were

separated, and the aqueous layer was extracted with ether (2 x 30 mL). The combined organic layers were washed with 5% aqueous Na_2CO_3 (2 x 50 mL) and brine (2 x 50 mL). After drying (Na_2SO_4) the solution, the solvent was removed leaving 3.8 g (94% of 31a) as a colorless oil. Recrystallization (hexane) with cooling to 0°C gave a white granular powder: IR (melt) $3120\text{--}3640\text{ cm}^{-1}$ (OH); ^1H NMR (CDCl_3) δ 1.3 [s, 6 H, $(\text{CH}_3)_2$], 1.39 [d, 3 H, CH_3CHOH], 1.84–2.0 [m, 2 H, SCH_2CH_2], 2.74–2.86 [br s, 1 H, OH], 2.9–3.06 [m, 2 H, SCH_3], 4.71 [q, 1 H, CH_3CHOH], 6.94–7.02 [m, 2 H, Ar-H], 7.3–7.36 [m, 1 H, Ar-H]; ^{13}C NMR (CDCl_3) ppm 142.0, 141.6, 130.7, 126.6, 123.6, 123.2, 70.2 [C(9)], 37.7 [C(3)], 33.1 [C(4)], 30.2 [C(4')], 25.0 [C(10)], 23.0 [C(2)].

[1-(4,4-Dimethylthiochroman-6-yl)ethyl]tri-
phenylphosphonium Bromide or [1-(3,4-di-
hydro-4,4-dimethyl-2H-1-benzythiopyran-
6-yl)ethyl]triphenylphosphonium
Bromide (32a)

A solution of the alcohol 31a (0.5 g, 2.252 mmol) and triphenylphosphine hydrobromide (0.78 g, 2.275 mmol) in CH_3OH (20 mL) was stirred at RT under N_2 for 26 h in a 100-mL round bottom flask. Removal of the solvent left a yellow oil which solidified after repeated trituration with dry ether. The resulting powder was stirred in dry ether (30 mL) for 8 h, filtered, and dried ($110^\circ\text{C}/2\text{ mm}$) to give 0.9 g (73.1%) of 32a as a tan powder: mp $139\text{--}145^\circ\text{C}$ (dec); ^1H NMR (CDCl_3) δ 1.07 [s, 3 H, CH_3], 1.15 [s, 3 H, CH_3], 1.75 [d, 3 H, CHCH_3], 1.80–1.88 [m, 2 H, H(3)], 2.96–3.02 [m, 2 H, H(2)], 6.40–6.55 [m, 1 H, CHP^+Ph_3],

6.58 [d, 1 H, H(7)], 6.86 [d, 1 H, H(8)], 7.45 [br s, 1 H, H(5)],
7.62-7.90 [m, 15 H, P⁺(C₆H₅)₃].

Ethyl (E)-p-[2-(4,4-Dimethylthiochroman-6-yl)-
propenyl]benzoate or Ethyl (E)-4-[2-(2,3-Di-
methyl-2H-1-benzothiopyran-6-yl)-1-pro-
penyl]benzoate (22a)

A solution of n-butyllithium in hexane (1.55 M, 1.3 mL, 2.015 mmol) was added dropwise under N₂ to a stirred suspension of the phosphonium salt 32a (1.1 g, 2.011 mmol) in dry ether (30 mL) in a 100-mL, round bottom flask. The resulting dark red mixture was stirred for 5 min. A solution of the freshly distilled aldehyde 33 (0.4 g, 2.247 mmol) in dry ether (15 mL) was then added all at once. The mixture became creamy yellow and then cream-colored, and a large amount of off-white solid precipitated. After stirring at RT for 36 h, the mixture was filtered. The solid was washed with ether (50 mL). The combined filtrates were concentrated to give a yellow oil which was dissolved in warm 95% ethanol (50 mL). The resulting solution was filtered and then concentrated to 10 mL. After cooling slowly to RT, the resulting solid was filtered and washed with cold 95% ethanol. After drying in the air, 0.30 g (40.7%) of 22a was obtained as a white solid: mp 92-93°C; IR (KBR) 1710-1725 cm⁻¹ (C=O); ¹H NMR (CDCl₃) δ 1.38 [s, 6 H, (CH₃)₂], 1.41 [t, 3 H, OCH₂CH₃], 1.96-2.02 [m, 2 H, SCH₂CH₂], 2.28 [s, 3 H, CH=C-CH₃], 3.04-3.09 [m, 2 H, SCH₂], 4.4 [q, 2 H, OCH₂], 6.82 [s, 1 H, C=CH], 7.11 [d, 1 H, H(8)], 7.21-7.28 [m, 1 H, H(7)], 7.44 [d, 2 H, Ar-H], 7.54 [s, 1 H, H(5)], 8.07 [d, 2 H, Ar-H]; Mass spectral data for C₂₃H₂₆O₂S: m/e (M⁺) 366.1653; Found

366.1650. An experiment using NaH/DMSO gave 33a (33.6%).

Ethyl (E)-p-[2-(4,4-Dimethylthiochroman-1-oxo-6-yl)propenyl]benzoate or Ethyl (E)-4-[2-(3,4-Dihydro-4,4-dimethyl-2H-1-benzothiopyran-1-oxo-6-yl)-1-propenyl]benzoate (22d)

A solution of NaIO_4 (0.14 g, 0.654 mmol) in H_2O (1 mL) was added in one portion under N_2 to a stirred suspension of 22a (0.118 g, 0.322 mmol) in methanol (10 mL) in a 100-mL round bottom flask. The mixture was stirred at RT for an additional 36 h. A large amount of white solid precipitated during this time. The mixture was concentrated. The residue was dissolved in CHCl_3 (20 mL) and then filtered and concentrated. The resulting oil was triturated with cold hexane to induce crystallization. Recrystallization (hexane) gave 55 mg (44.7%) of 22d as a white powder: mp 91-93°C; IR (KBr) 1700-1715 (C=O), 1030-1040 cm^{-1} (S→O); ^1H NMR (CDCl_3) δ 1.37 [s, 3 H, CH_3], 1.41 [t, 3 H, OCH_2CH_3], 1.51 [s, 3 H, CH_3], 1.84-1.94 [m, 1 H, H(3)], 2.30 [s, 3 H, $\text{CH}=\text{C}(\text{CH}_3)$], 2.48-2.60 [m, 1 H, H(3)], 3.08-3.23 [m, 2 H, H(2)], 4.41 [q, 2 H, OCH_2CH_3], 6.86 [s, 1 H, $\text{CH}=\text{C}(\text{CH}_3)$], 7.46 [d, 2 H, Ar-H], 7.51 [dd, J = 9 Hz, J = 3 Hz, 1 H, H(7)], 7.58 [d, J = 3 Hz, 1 H, H(5)], 7.77 [d, J = 9 Hz, 1 H, H(8)], 8.09 [d, 2 H, Ar-H]; Mass spectral data for $\text{C}_{23}\text{H}_{26}\text{O}_3\text{S}$: m/e (M^+) 382.1603; Found 382.1595.

Methyl 3-Phenoxypropionate (26b)

A solution of 3-phenoxypropionic acid (25, 10.0 g, 0.0602 mol) and PTSA (0.6 g) in methanol (250 mL) was heated at reflux through 3 Å molecular sieve for 36 h under N_2 in a 500-mL round bottom flask equipped

with a Soxhlet extractor and a condenser. The solution was allowed to cool to RT. The solution was then concentrated to a volume of 50 mL, diluted with water (50 mL), and extracted with ether (2 x 75 mL). The combined organic layers were washed with 5% aqueous NaHCO₃ (75 mL), H₂O (75 mL), and brine (75 mL). After drying (Na₂SO₄) the solution, the solvent was removed (vacuum). Vacuum distillation gave 9.45 g (87.1%) of 26b as a colorless liquid: bp 85-87°C/0.1 mm (lit.⁵² 109-112°C/3 mm); IR (neat) 1740-1750 cm⁻¹ (C=O); ¹H NMR (CDCl₃) δ 2.78 (t, 2 H, CH₂CH₂CH₃), 3.70 (s, 3 H, OCH₃), 4.23 (t, ¹³C NMR (CDCl₃) ppm 34.3 [C(2)], 51.7 [C(α)], 63.2 [C(3)], 114.5 [C(2')], 120.8 [C(4')], 129.2 [C(3')], 158.3 [C(1')], 171.1 [C(1)].

2-Methyl-4-phenoxy-2-butanol (27b)

A solution of methyl 3-phenoxypropionate (26b, 7.0 g, 0.0389 mol) in dry ether (20 mL) was added dropwise under N₂ to a stirred solution of CH₃MgCl in THF (2.9 M, 40.2 mL, 0.1166 mol) in a 200-mL round bottom flask equipped with a condenser. The mixture was heated at reflux for 24 h, allowed to cool to RT, and quenched with saturated aqueous NH₄Cl. The supernatant liquid was decanted, and the residue was washed with dry ether (3 x 50 mL). The combined organic solutions were dried (Na₂SO₄), and the solvent was removed. Vacuum distillation gave 5.35 g (76.4%) of 27b as a colorless liquid: bp 81-84°C/0.07 mm; IR (neat) 3140-3620 cm⁻¹ (OH); ¹H NMR (CDCl₃) δ 1.26 s, 6 H, (CH₃)₂, 1.95 (t, 2 H, ArOCH₂CH₂), 2.8-3.0 (br s, 1 H, OH), 4.12 (t, 2 H, ArOCH₂), 6.82-6.96 (m, 3 H, Ar-H), 7.16-7.3 (m, 2 H, Ar-H); ¹³C NMR (CDCl₃) ppm 29.5 [C(1)], 41.6 [C(3)], 64.9 [C(4)], 70.3 [C(2)], 114.3 [C(2')], 120.8 [C(4')], 129.3 [C(3')], 158.3 [C(1')].

4,4-Dimethylchroman or 3,4-Dihydro-4,4-dimethyl-
2H-1-benzopyran (29b)

A solution of 2-methyl-4-phenoxy-2-butanol (27b, 7.8 g, 0.0433 mol) in nitromethane (50 mL) was added dropwise under N₂ to a stirred suspension of anhydrous AlCl₃ (7.8 g, 0.0584 mol) in nitromethane (30 mL) in a 200-mL round bottom flask. After stirring at RT for an additional 24 h, a solution of 6 M HCl (80 mL) was added slowly. The resulting mixture was stirred for 10 min and diluted with ether (50 mL). The layers were separated, and the organic layer was washed with H₂O (50 mL), saturated aqueous NaHCO₃ (4 x 50 mL), H₂O (50 mL), and brine (4 x 50 mL). After drying (Na₂SO₄) the solution, the solvent was removed. Vacuum distillation of the resulting dark brown oil gave 4.35 g (62%) of 29b as a colorless liquid: bp 74-80°C/0.7 mm (lit.⁸ 93°C/10 mm); ¹H NMR (CDCl₃) δ 1.31 [s, 6 H, (CH₃)₂], 1.80-1.84 [m, 2 H, H(3)], 4.16-4.20 [m, 2 H, H(2)], 6.78-7.29 [m, 4 H, Ar-H]; ¹³C NMR (CDCl₃) ppm 30.5 [C(4)], 31.1 [C(4')], 37.7 [C(3)], 63.0 [C(2)], 116.9 [C(8)], 120.4, 126.9, 127.0, 131.6 [C(4a)], 153.5 [C(8a)].

4,4-Dimethylchroman-6-yl Methyl Ketone or 1-
(3,4-Dihydro-4,4-dimethyl-2H-1-benzopyran-
-6-yl)ethanone (30b)

Anhydrous AlCl₃ (3.4 g, 0.0255 mol) was added in small portions to a solution of 4,4-dimethylchroman (29b, 4.0 g, 0.0247 mol) and acetyl chloride (2.0 g, 0.0255 mol) in CH₃NO₂ (35 mL) under N₂ in a 100-mL, round bottom flask. After stirring at RT for 6 h, 6 M HCl (35 mL) was added slowly, and the resulting mixture was stirred for 10 min. The mixture was diluted with ether (40 mL), and the layers were separated

The organic layer was washed with H₂O (40 mL), saturated aqueous NaHCO₃ (4 x 30 mL), H₂O (40 mL), and brine (2 x 40 mL). After drying (Na₂SO₄) the solution, the solvent was removed leaving a dark reddish brown oil. Vacuum distillation gave 3.4 g (67.5%) of 30b as a pale yellow liquid: bp 108–112°C/0.01 mm; IR (neat) 1675–1685 cm⁻¹ (C=O); ¹H NMR (CDCl₃) δ 1.36 [s, 6 H, (CH₃)₂], 1.83–1.87 [m, 2 H, H(3)], 2.55 [s, 3 H, CH₃C=O], 4.24–4.28 [m, 2 H, H(2)], 6.83 [d, J = 9 Hz, 1 H, H(8)], 7.71 [dd, J = 9 Hz, J = 3 Hz, 1 H, H(7)], 7.98 [d, J = 3 Hz, H(5)]; ¹³C NMR (CDCl₃) ppm 26.3 [C(10)], 30.6 [C(4)], 30.7 [C(4')], 37.0 [C(3)], 63.4 [C(2)], 116.9 [C(8)], 127.8, 128.16 [C(5), C(7)], 130.0, 131.6 [C(4a), C(6)], 158.0 [C(8a)]; Mass spectral data for C₁₃H₁₆O₂: m/e (M⁺) 204.1150; Found 204.1153.

α-4,4-Trimethylchroman-6-methanol or 3,4-Dihydro-α,4,4-trimethyl-2H-1-benzopyran-6-methanol (31b)

A solution of the ketone 30b (3.0 g, 0.0147 mol) in anhydrous ether (15 mL) was added dropwise under N₂ to a stirred suspension of LiAlH₄ (0.8 g, 0.0211 mol) in dry ether (50 mL) in a 200-mL round bottom flask equipped with a condenser. The mixture was heated at reflux for 24 h. After cooling to RT, ethyl acetate was added dropwise to destroy the excess LiAlH₄. A solution of 5% HCl (50 mL) was then added, and the resulting mixture was stirred for 5 min. The layers were separated, and the aqueous layer was washed with ether (2 x 50 mL). The combined organic layers were washed with 5% aqueous Na₂CO₃ (2 x 50 mL) and brine (2 x 50 mL). After drying (Na₂SO₄) the solution, the solvent was removed leaving a yellow oil which solidified after

scratching. Recrystallization (hexane) gave 1.8 g (59.4%) of 31b as a white solid: mp 70-71^oC; IR (KBr) 3140-3640 cm⁻¹ (OH); ¹H NMR (CDCl₃) δ 1.31 [s, 6 H, (CH₃)₂], 1.43 [d, 3 H, CH₃CHOH], 1.74-1.83 [m, 2 H, H(3)], 2.4-2.44 [s, 1 H, OH], 4.10-4.18 [m, 2 H, H(2)], 4.76 [q, 1 H, CHOH], 6.76 [d, J = 9 Hz, 1 H, H(8)], 7.07 [dd, J = 9 Hz, J = 3 Hz, 1 H, H(7)], 7.28 [d, J = 3 Hz, 1 H, H(5)], ¹³C NMR (CDCl₃) ppm 25.0 [C(10)], 30.6 [C(4)], 31.0 [C(4')], 37.6 [C(3)], 63.0 [C(2)], 70.2 [C(9)], 116.9 [C(8)], 124.0, 124.3 [C(5), C(7)], 131.4, 137.7 [C(4a), C(6)], 152.9 [C(8a)]; Mass spectral data for C₁₃H₁₈O₂: m/e (M⁺) 206.1307; Found 206.1308.

[1-(4,4-Dimethylchroman-6-yl)ethyl]triphenyl-
phosphonium Bromide or [1-(3,4-Dihydro-4,4-
dimethyl-2H-1-benzopyran-6-yl)ethyl]tri-
phenylphosphonium Bromide (32b)

A solution of the alcohol 31b (0.7 g, 3.4 mmol) and triphenylphosphine hydrobromide (1.2 g, 3.5 mmol) in methanol (30 mL) was stirred under N₂ at RT for 24 h in a 100-mL round bottom flask. The solvent was removed (vacuum), and the resulting oil was triturated repeatedly with dry ether until it solidified. The white solid was stirred in dry ether (30 mL) at RT under N₂ for 4 h, filtered, and dried (110^oC/∞2 mm) to give 1.45 g (80.3%) of 32b as a white powder: mp 149-155^oC (dec); ¹H NMR (CDCl₃) δ 1.08 [s, 3 H, CH₃], 1.14 [s, 3 H, CH₃], 1.72-1.78 [m, 2 H, H(3)], 1.83 [d, 3 H, CHCH₃], 4.12-4.18 [m, 2 H, H(2)], 6.2-6.32 [m, 1 H, CHPh₃⁺, Br⁻], 6.57 [d, 1 H, H(8)], 6.67 [d, 1 H, H(7)], 7.24 [br s, 1 H, H(5)], 7.63-7.84 [m, 15 H, P⁺(C₆H₅)₃].

Ethyl (E)-p-[2-(4,4-Dimethylchroman-6-yl)propenyl]benzoate or Ethyl (E)-4-[2-(3,4-Dihydro-4,4-dimethyl-2H-1-benzopyran-6-yl)-1-propenyl]benzoate (22b)

A solution of n-butyllithium in hexane (1.55 M, 2.13 mL, 3.301 mmol) was added dropwise under N₂ to a stirred suspension of the phosphonium salt 32b (1.75 g, 3.296 mmol) in dry ether (30 mL) in a 100-mL round bottom flask. The resulting dark reddish brown mixture was stirred at RT for 5 min. A solution of the aldehyde 33 (0.6 g, 3.371 mmol) in dry ether (15 mL) was then added. The mixture changed from reddish brown to creamy yellow, and a large amount of off-white solid precipitated. After stirring at RT for 36 h, the mixture was filtered. The resulting solid was washed with ether (75 mL), and the combined filtrates were concentrated to give a yellow oil. The oil was chromatographed through a column (8 x 200 nm) packed with neutral alumina (about 10 g). The product was eluted with 5% ether/hexane (250 mL). Concentration of the eluent gave a viscous oil which was dissolved in a minimum amount of boiling 95% ethanol. Cooling the solution to 0°C and scratching gave 0.30 g (26.0%) of 33b as a white granular solid: mp 72.5–73.5°C; IR (KBr) 1710–1725 cm⁻¹ (C=O); ¹H NMR (CDCl₃) δ 1.37 [s, 6 H, (CH₃)₂], 1.39 [t, 3 H, OCH₂CH₃], 1.81–1.87 [m, 2 H, H(3)], 2.27 [s, 3 H, CH=C(CH₃)], 4.17–4.24 [m, 2 H, H(2)], 4.38 [q, 2 H, OCH₂CH₃], 6.77 [s, 1 H, CH=C(CH₃)], 6.81 [d, J = 9 Hz, 1 H, H(8)], 7.26 [dd, J = 9 Hz, J = 3 Hz, 1 H, H(7)], 7.41 [d, 2 H, Ar=H], 7.44 [d, J = 3 Hz, 1 H, H(5)], 8.06 [d, 2 H, Ar=H]; Mass spectral data for C₂₃H₂₆O₃: m/e (M⁺) 350.1882; Found 350.1884. The presence of the Z isomer in the oil obtained from chromatography was indicated by the following ¹H NMR

signals: δ 2.76-2.81 [m, H(3)], 2.20 [s, \underline{Z} $\underline{CH=C(CH_3)}$], 4.16-4.20 [m, H(2)], 6.44 [br s, \underline{Z} $\underline{CH=C(CH_3)}$].

(E)-p-[2-(4,4-Dimethylchroman-6-yl)propenyl]-benzoic Acid or (E)-4-[2-(3,4-Dihydro-4,4-dimethyl-2H-1-benzopyran-6-yl)-1-propenyl]benzoic Acid (22c)

The heteroarotinoid 22b (0.20 g, 0.571 mmol) was heated at reflux under N_2 for 4 h in a solution of NaOH (0.1 g, 2.50 mmol) in 95% C_2H_5OH (2 mL) and H_2O (5 mL) in a 25-mL round bottom flask equipped with a condenser. After cooling slowly to RT, the solution was acidified (litmus) with conc. HCl. The resulting white solid was filtered, washed with water, and air-dried. Recrystallization (95% ethanol) gave 0.135 g (73.4%) of 22c as a white solid: mp 183-183.5°C; IR (KBr) 2390-3320 (OH, CH), 1670-1695 cm^{-1} (C=O) 1H NMR ($CDCl_3$) δ 1.38 [s, 6 H, $(\underline{CH_3})_2$], 1.84-1.9 [m, 2 H, H(3)], 2.30 [s, 3 H, $\underline{CH=C(CH_3)}$], 4.21-4.26 [m, 2 H, H(2)], 6.80 [s, 1 H, $\underline{CH=C(CH_3)}$], 6.83 [d, J = 9 Hz, 1 H, H(8)], 7.29 [dd, J = 9 Hz, J = 3 Hz, 1 H, H(7)], 7.46 [d, J = 3 Hz, 1 H, H(5)], 7.48 [d, 2 H, Ar- \underline{H}], 8.15 [d, 2 H, Ar- \underline{H}]; Mass spectral data for $C_{21}H_{22}O_3$: m/e (M^+) 322.1569; Found 322.1570.

Ethyl 4-Formylbenzoate (33)

A solution of ethyl p-toluate (36, 6.0 g, 0.0366 mol), glacial acetic acid (57 mL), and acetic anhydride (57 mL) in a 300-mL round bottom flask equipped with a thermometer and a mechanical stirrer was cooled to 0-5°C in an ice-salt bath. Conc. H_2SO_4 (8.5 mL) was added slowly to the stirred solution. Chromium trioxide (10.0 g, 0.10 mol)

was added in small portions over a period of 25 min. The temperature of the mixture was maintained below 5°C at all times. After stirring at 0-5°C for an additional 20 min, the mixture was poured into a 100-mL beaker filled 2/3 full with ice. Cold water was then added to bring the total volume to 600 mL. The resulting dark green-brown mixture was extracted with ether (3 x 250 mL), and the organic layers were combined. The organic layer was washed with water (3 x 200 mL), 5% aqueous Na₂CO₃ (2 x 200 mL), and brine (200 mL). After drying (Na₂SO₄) the solution, the solvent was removed leaving the diacetate 37 as a pale yellow liquid. A mixture of the diacetate 37, conc. H₂SO₄ (2 mL), water (20 mL), and 95% ethanol (20 mL) was heated at reflux under N₂ for 45 min. in a 100-mL round bottom flask equipped with a condenser. The solution was allowed to cool to RT. After diluting the solution with water (40 mL), the resulting mixture was extracted with ether (3 x 40 mL). The combined organic layers were washed with 5% aqueous NaHCO₃ (2 x 50 mL) and water (50 mL). After drying (Na₂SO₄) the solution, the solvent was removed leaving a yellow liquid. Vacuum distillation gave 3.1 g (47.6%) of 33 as a colorless liquid: bp 80-84°C/0.05 mm (lit.⁹ 142-144 C/15 mm); IR (neat) 1705-1735 cm⁻¹ (C=O); ¹H NMR (CDCl₃) δ 1.42 (t, 3 H, OCH₂CH₃), 4.41 (q, 2 H, OCH₂CH₃), 7.87-8.22 (pseudo q, 4 H, Ar-H), 10.08 (br s, 1 H, CHO); ¹³C NMR (CDCl₃) ppm 191.2 (CHO), 165.2 (CO₂C₂H₅), 138.9, 135.2, 129.9, 129.2 (Ar-C), 61.4 (OCH₂CH₃), 14.2 (OCH₂CH₃).

Attempted Preparation of 22a

A solution of the phosphonium salt 38 (1.0 g, 1.981 mmol) in dry DMSO (20 mL) was added rapidly under N₂ to a 50% mineral oil dispersion

of NaH (0.1 g, 2.083 mmol) in a 100-mL round bottom flask. The resulting bright orange mixture was stirred for 5 min. A solution of the ketone 30a (0.44 g, 2.00 mmol) in DMSO (5 mL) was then added. Stirring was continued at RT for 12 h. The mixture was diluted with H₂O (50 mL), acidified (litmus) with conc. HCl, and extracted with CH₂Cl₂ (4 x 20 mL). The organic layer was washed with H₂O (25 mL) and dried (Na₂SO₄). The solution was concentrated to give an orange-brown oil. IR spectral data indicated the presence of approximately equivalent amounts of starting ketone 30a (1680-1690 cm⁻¹) and an ester (1715-1725 cm⁻¹).

Attempted Preparation of 22a

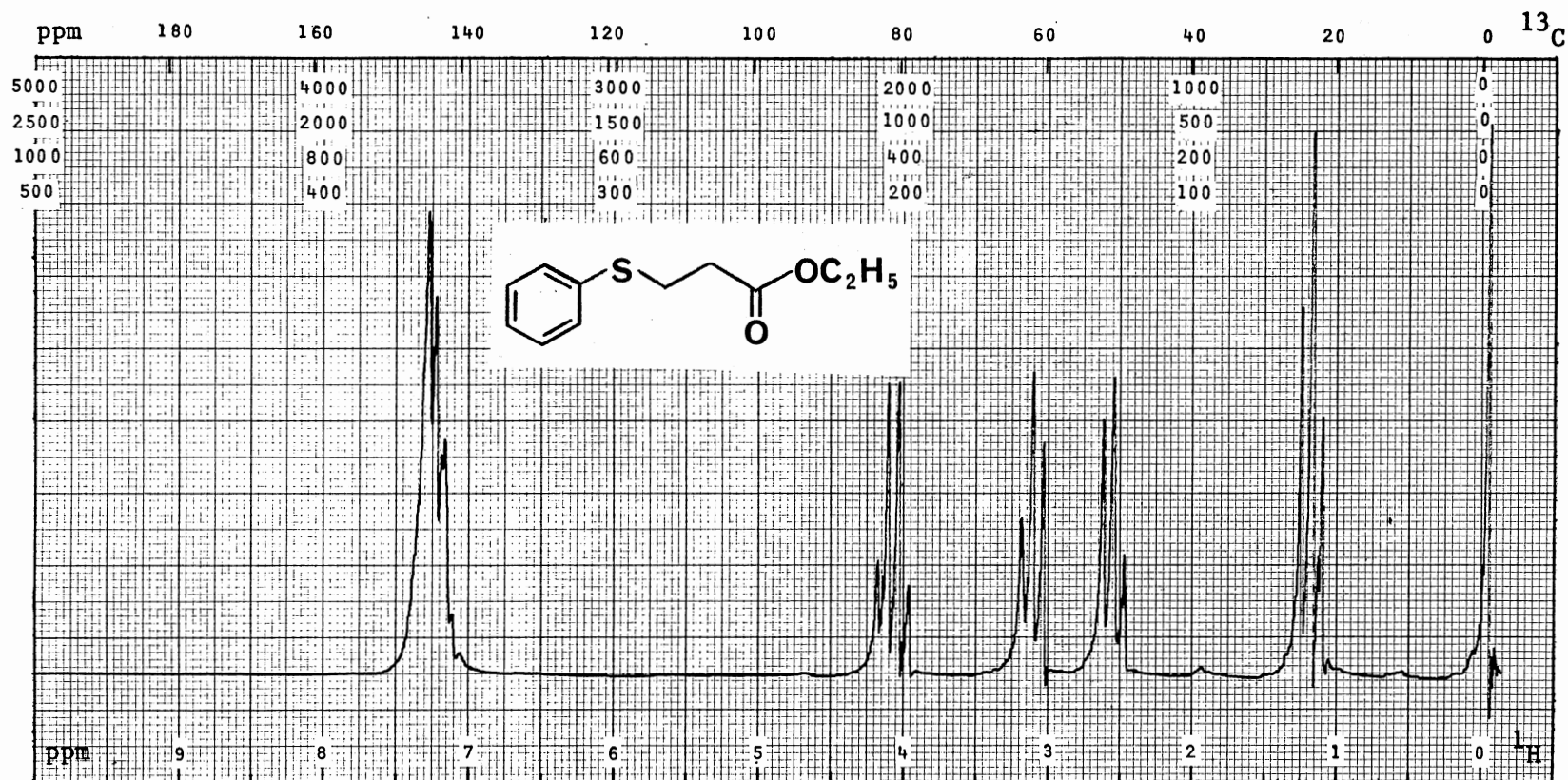
A solution of the phosphonium salt 38 (1.0 g, 1.981 mmol) in dry DMSO (10 mL) was added rapidly under N₂ to a 50% mineral oil dispersion of NaH (0.1 g, 2.083 mmol) in a 100-mL round bottom flask equipped with a condenser. The resulting bright orange mixture was stirred for 5 min. A solution of the ketone 30a (0.44 g, 2.00 mmol) in dry benzene (50 mL) was then added. The resulting mixture was heated at reflux for 72 h. Water (40 mL) and conc. HCl (10 mL) were then added to the cooled solution. The layers were separated, and the organic layer was washed with H₂O (30 mL) and brine (30 mL). After drying (Na₂SO₄) the solution, the solvent was removed leaving an orange-brown oil. IR spectral data indicated the presence of approximately equivalent amounts of starting ketone 30a (1680-1690 cm⁻¹) and an ester (1720-1730 cm⁻¹).

Attempted Preparation of 22a

A mixture of methyl α -bromo-p-toluate (43, 0.8 g, 3.495 mmol) and

triethyl phosphite (0.6 g, 3.614 mmol) was heated at reflux under N_2 for 1 h in a 10-mL round bottom flask equipped with a condenser. After cooling to RT, the solution was diluted with CH_3OH (5 mL) and ketone 30a (0.77 g, 3.90 mmol). The resulting solution was added dropwise under N_2 to a stirred solution of $NaOCH_3$ (0.10 g, 3.518 mmol) in CH_3OH (17 mL). The solution was heated at reflux for 18 h. After cooling to RT, the solution was diluted with H_2O (50 mL), and the pH was checked to ensure that the mixture was strongly basic (litmus). The mixture was extracted with ether (2 x 30 mL). After drying the (Na_2SO_4) the organic layer, the solvent was removed leaving a yellow oil. IR spectral data indicated the presence of a large amount of unreacted ketone 30a ($1680-1690\text{ cm}^{-1}$).

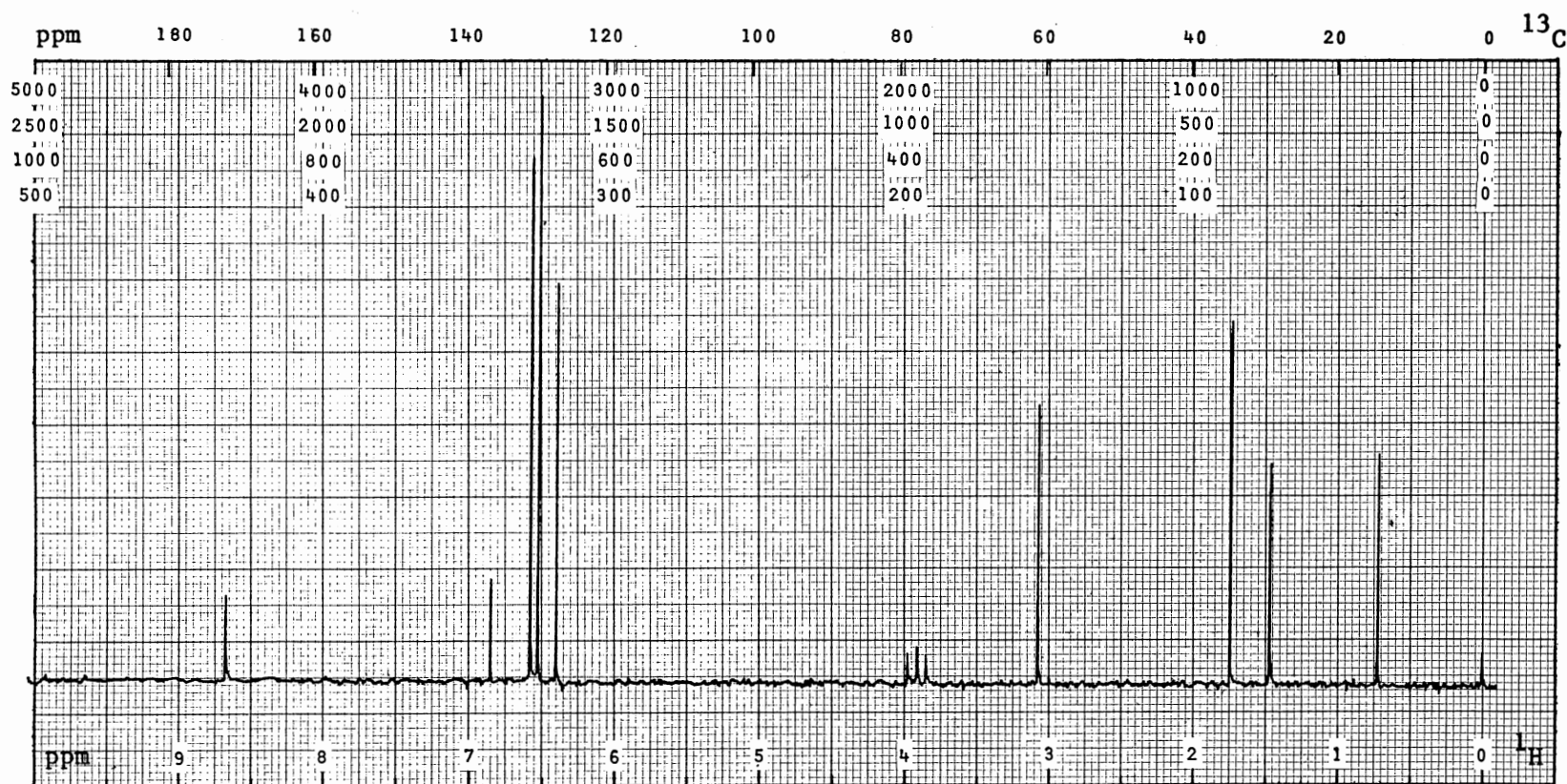
PLATE I



¹H NMR Spectrum of 26a

PFT _ CW X ; Solvent. . CDCl₃ ; SO. . 85771 Hz; PW. .1000 Hz; T. . 30 °C; Acq/SA. .
 Size. . K; P2/RF. . 60 μs/dB; SF. . 100.1 Hz; FB. . 2 Hz; Lock. . ²H ; D5/ST. . 250 s
 DC. . ; Gated Off. . ; Offset. . Hz; RF. . W/dB; NBW. . Hz

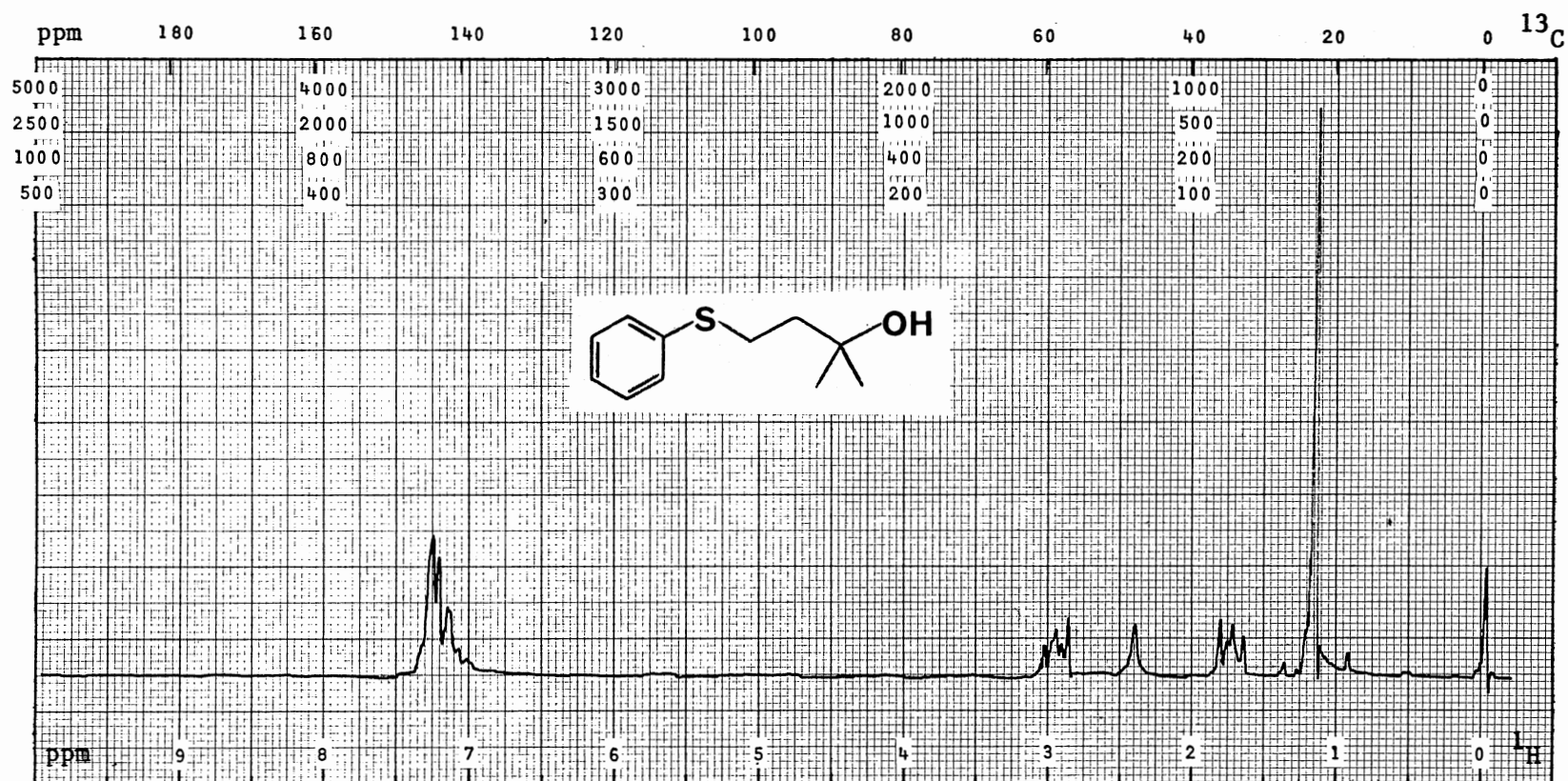
PLATE II



^{13}C NMR Spectrum of 26a

PFT X CW ; Solvent. . CDCl_3 ; SO. . 35101 Hz; PW. . 5000 Hz; T. . 30 °C; Acq/SA. . 400
 Size. . 8 K; P2/RF. . 10 $\mu\text{s}/\text{dB}$; SF. . 25.2 Hz; FB. . Hz; Lock. . ^2H ; D5/ST. . 5 s
 DC. . ^1H ; Gated Off. . ; Offset. . 45051 Hz; RF. . 9W/dB; NBW. . Hz

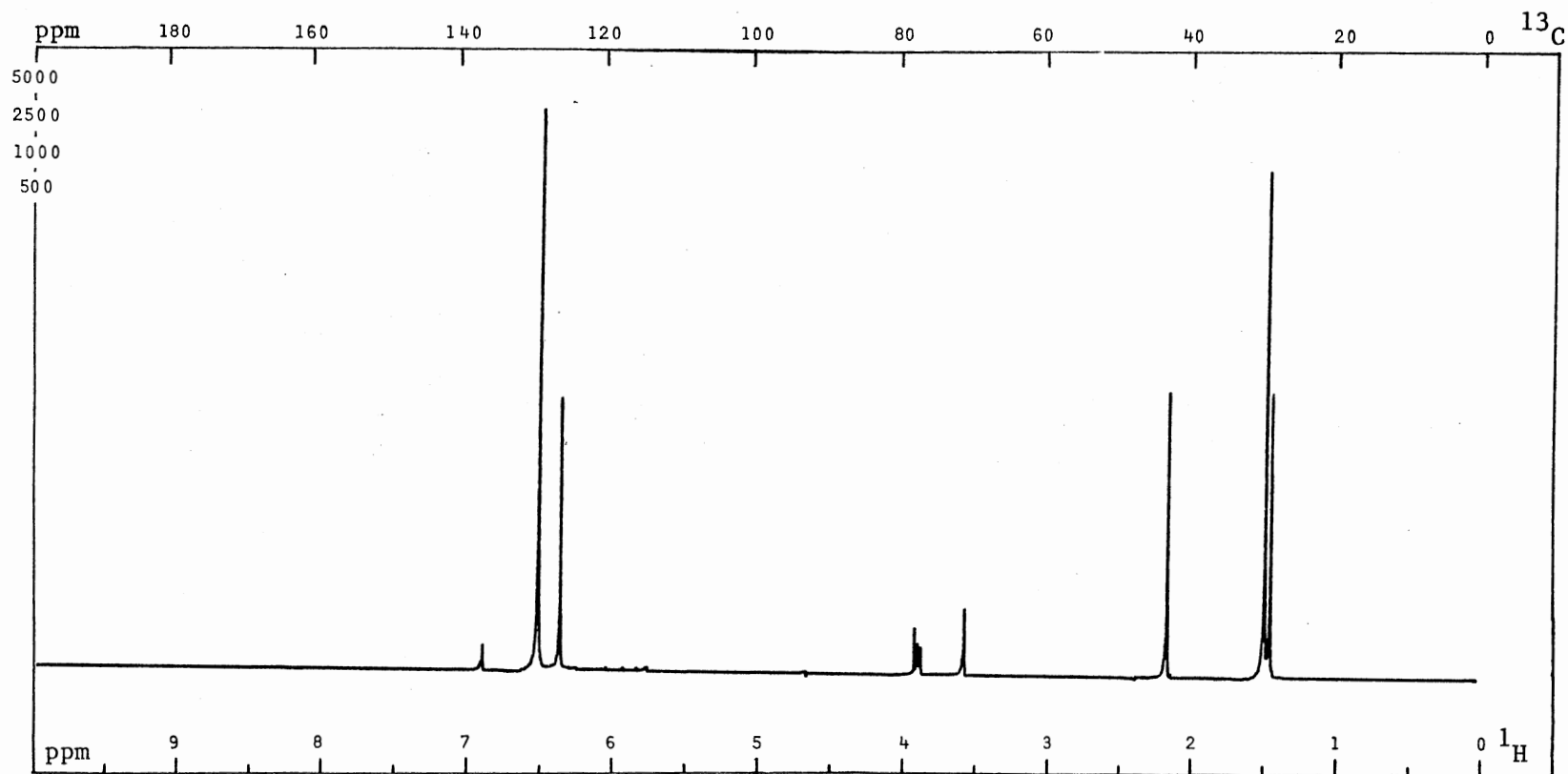
PLATE III



¹H NMR Spectrum of 27a

PFT _ CW X ; Solvent. . CDCl₃ ; SO. . 85771 Hz; PW. . 1000 Hz; T. . 30 °C; Acq/SA. .
 Size. . K; P2/RF. . 58 μs/dB; SF. . 100.1 Hz; FB. . 2 Hz; Lock. . ²H ; D5/ST. . 250 s
 DC. . ; Gated Off. . ; Offset. . Hz; RF. . W/dB; NBW. . Hz

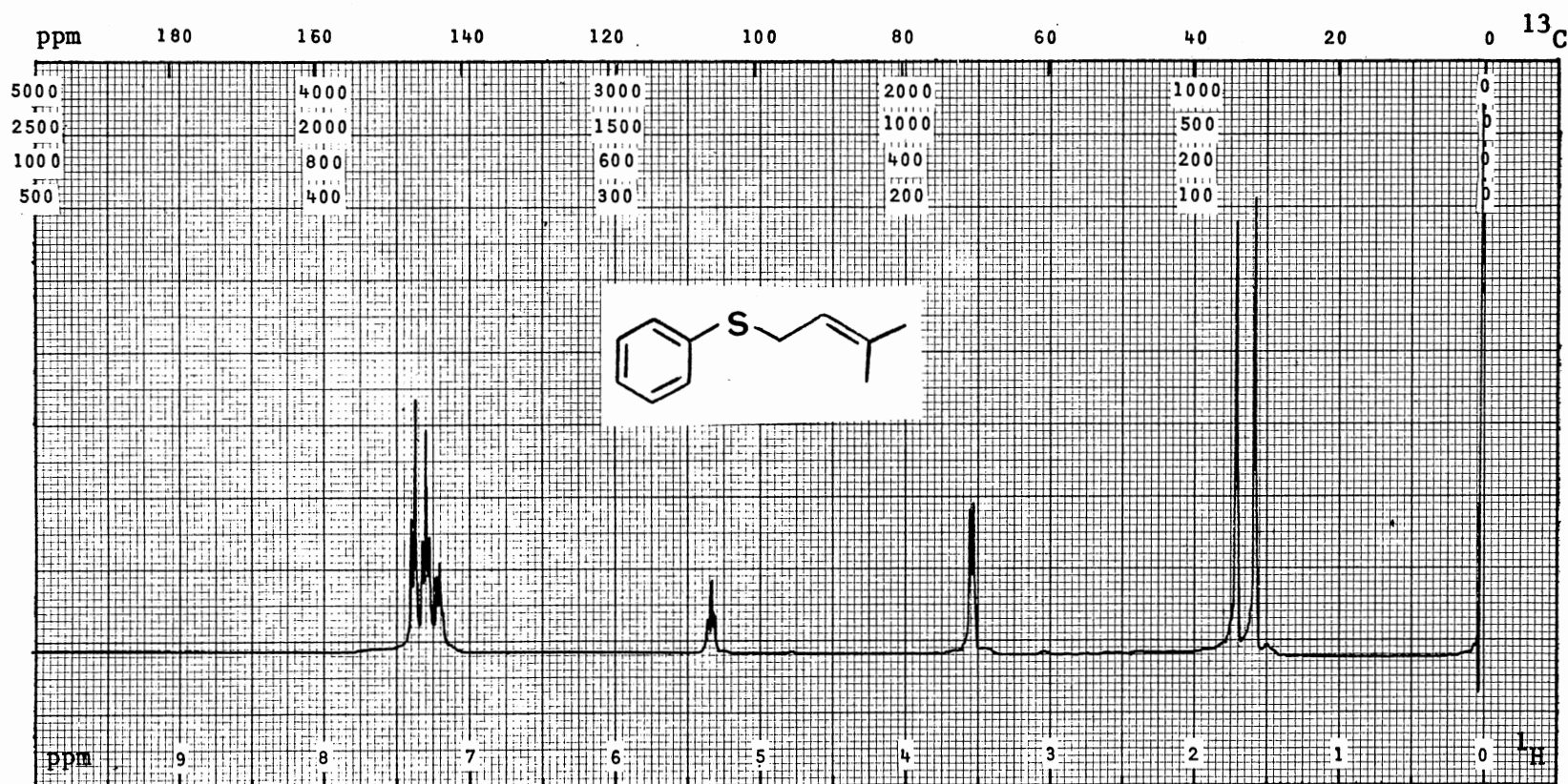
PLATE IV



^{13}C NMR Spectrum of 27a

PFT X CW _ ; Solvent. . CDCl_3 ; SO. . Hz; PW. .20000 Hz; T. . 25 °C; Acq/SA. .100
 Size. . K; P2/RF. . 12 $\mu\text{s}/\text{dB}$; SF. .75.4 Hz; FB. . Hz; Lock. . ^2H ; D5/ST. . 5 s
 DC. . ^1H ; Gated Off. . ; Offset. . Hz; RF. . W/dB; NBW. . Hz

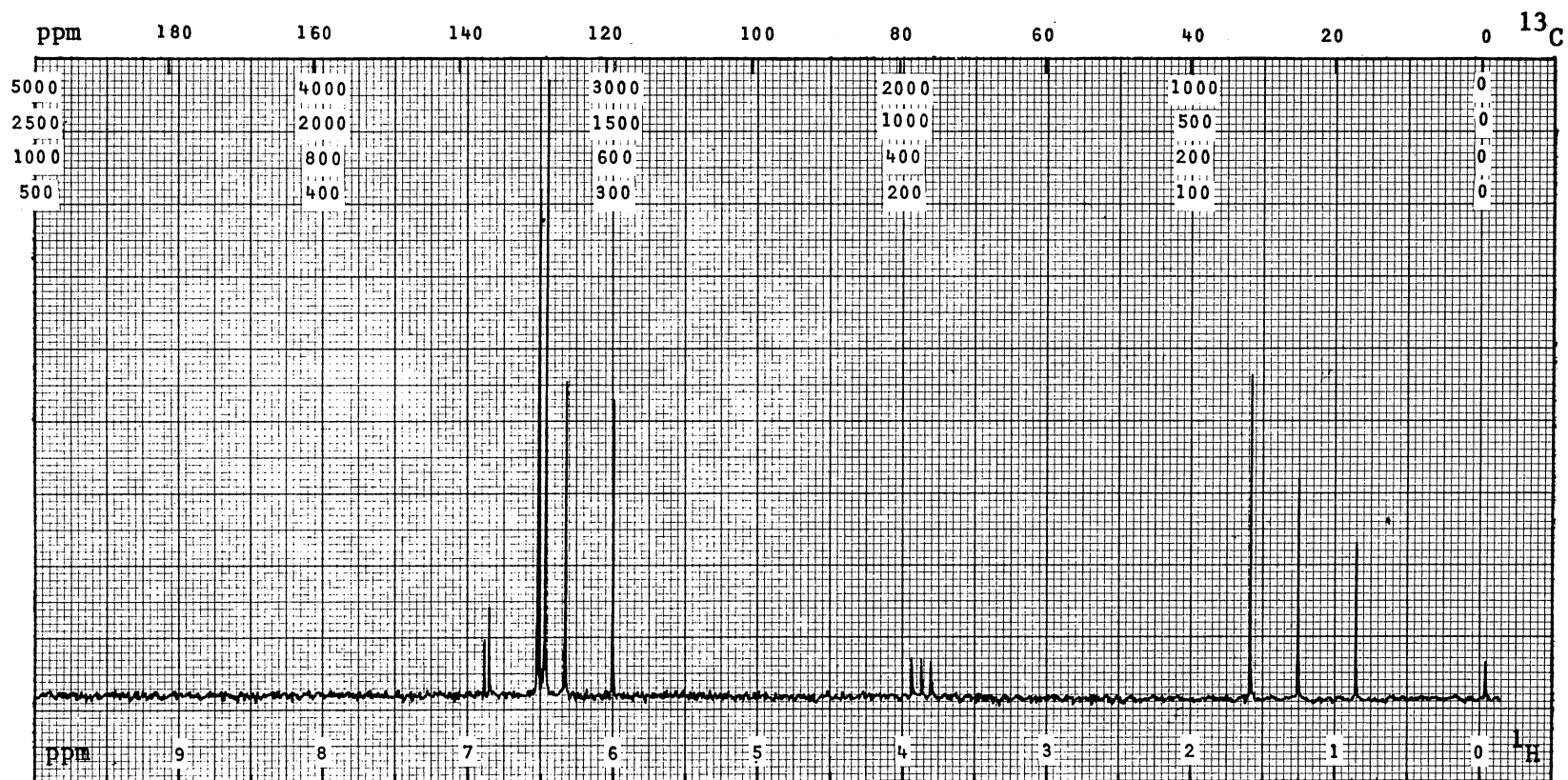
PLATE V



¹H NMR Spectrum of 28

PFT X CW ; Solvent. . CDCl₃ ; SO. . Hz; PW. . 4000 Hz; T. . 25 °C; Acq/SA. . 16
 Size. . K; P2/RF. . 3 μs/dB; SF. . 299.9 Hz; FB. . Hz; Lock. . ²H ; D5/ST. . 1 s
 DC. . ; Gated Off. . ; Offset. . Hz; RF. . W/dB; NBW. . Hz

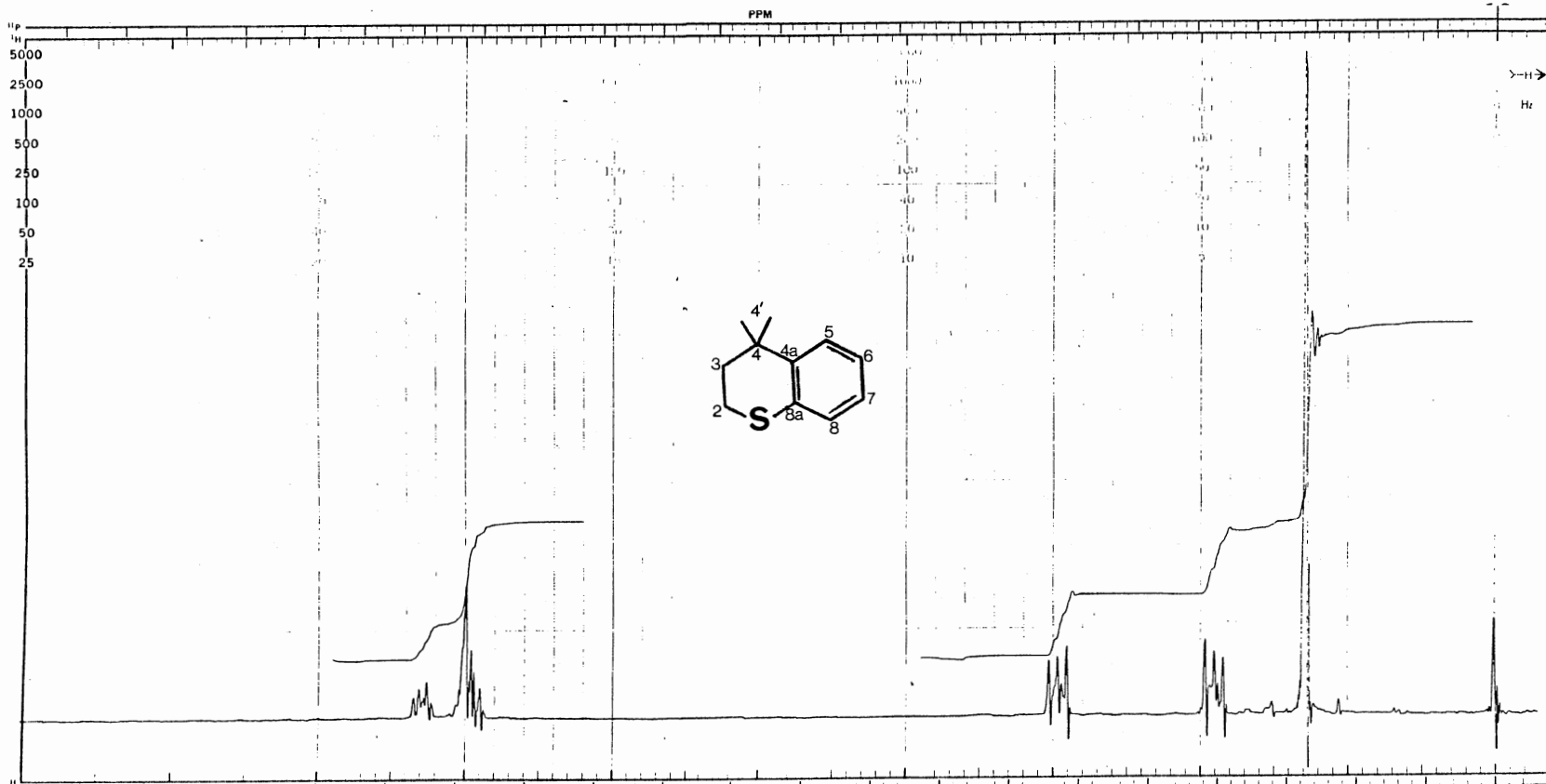
PLATE VI



^{13}C NMR Spectrum of 28

PFT X CW ; Solvent. . CDCl_3 ; SO. . 35101 Hz; PW. . 5000 Hz; T. . 30 °C; Acq/SA. . 400
 Size. . 8 K; P2/RF. . 10 $\mu\text{s}/\text{dB}$; SF. . 25.2 Hz; FB. . Hz; Lock. . ^2H ; D5/ST. . 5 s
 DC. . ^1H ; Gated Off. . ; Offset. . 45051 Hz; RF. . 9 W/dB; NBW. . Hz

PLATE VII



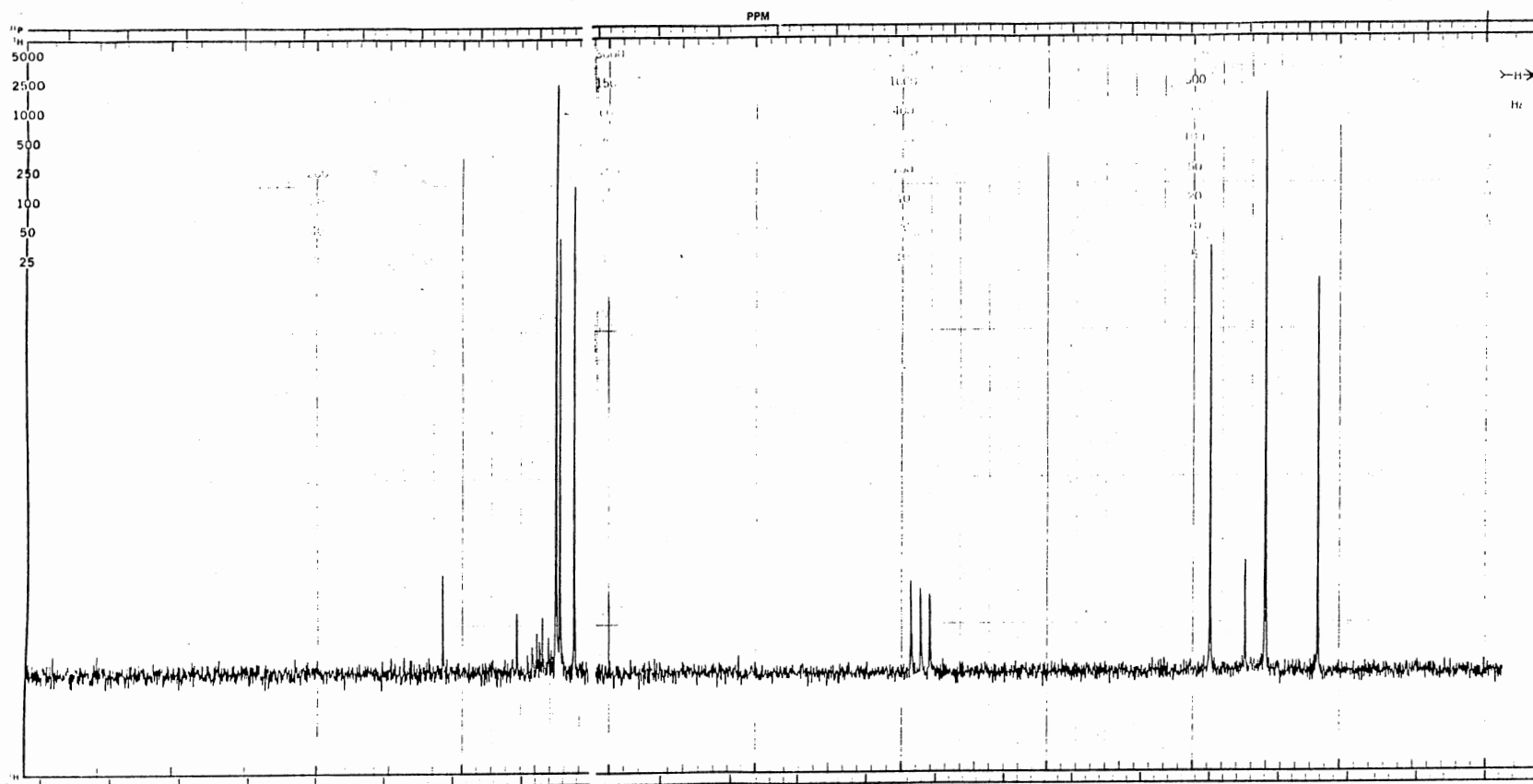
¹H NMR Spectrum of 29a

PFT _ CW X ; Solvent. . CDCl₃ ; SO. . 85771 Hz; PW. .1000 Hz; T. . 30 °C; Acq/SA. .

Size. . K; P2/RF. . 62 μs/dB; SF. . 100.1 Hz; FB. . 2 Hz; Lock. . ²H ; D5/ST. . 250 s

DC. . ; Gated Off. . ; Offset. . Hz; RF. . W/dB; NBW. . Hz

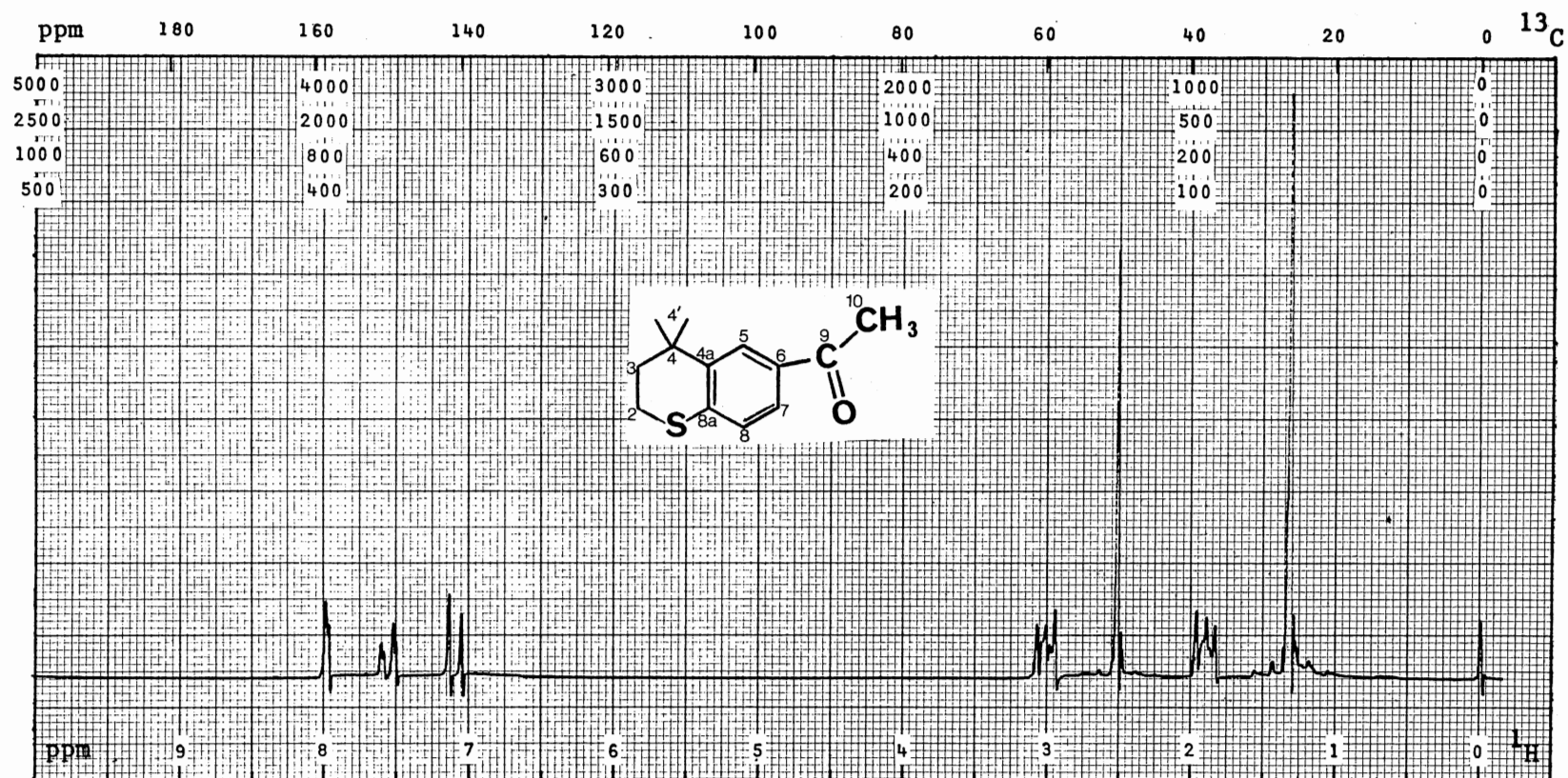
PLATE VIII



^{13}C NMR Spectrum of 29a

PFT X CW __ ; Solvent. . CDCl_3 ; SO. . 35101 Hz; PW. . 5000 Hz; T. . 30 °C; Acq/SA. . 500
 Size. . 8 K; P2/RF. . 10 $\mu\text{s}/\text{dB}$; SF. . 25.2 Hz; FB. . Hz; Lock. . ^2H ; D5/ST. . 5 s
 DC. . ^1H ; Gated Off. . ; Offset. . 45101 Hz; RF. . 9 W/dB; NBW. . Hz

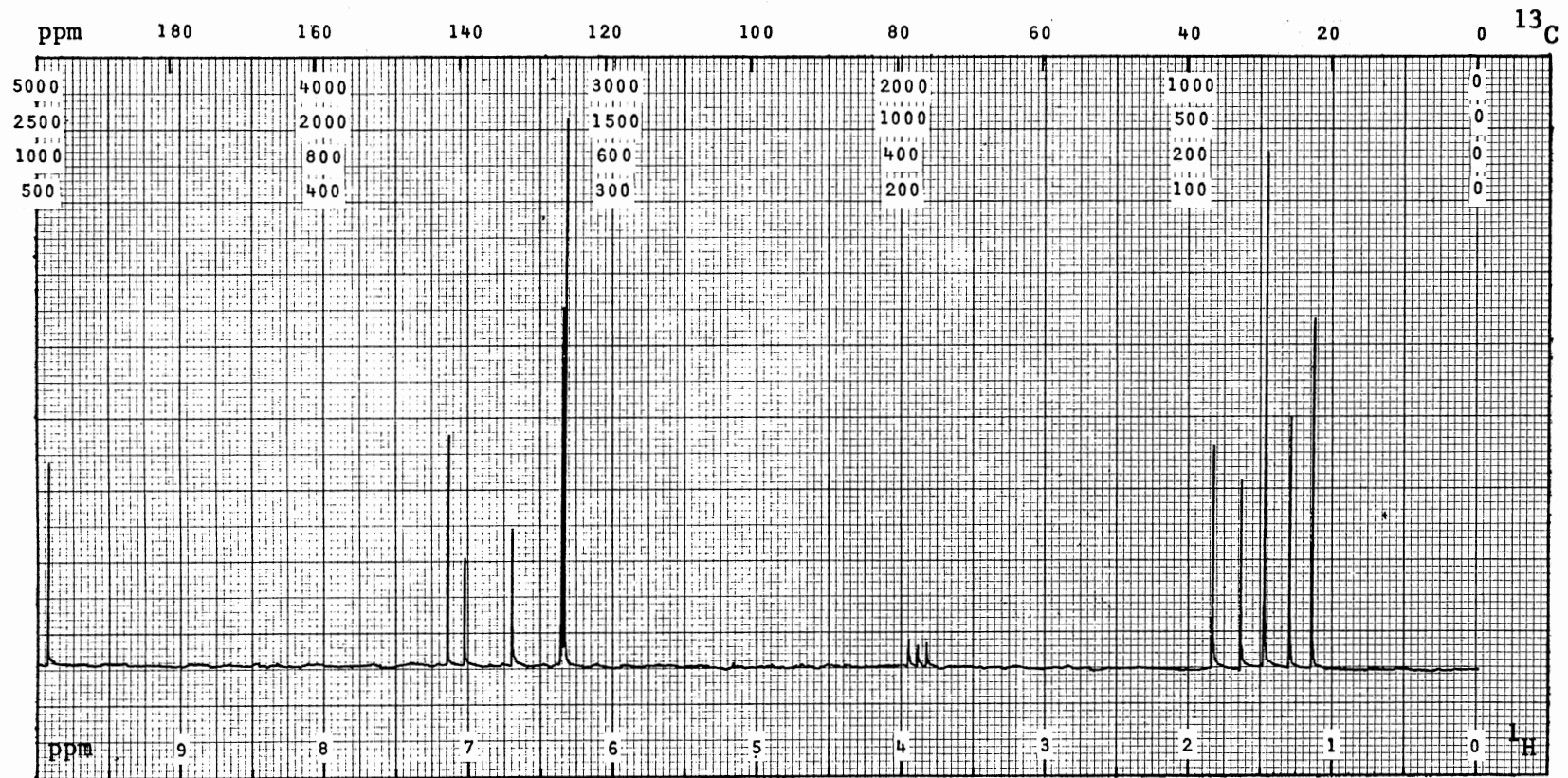
PLATE IX



^1H NMR Spectrum of 30a

PFT _ CW ; Solvent. . CDCl_3 ; SO. . 85771 Hz; PW. .1000 Hz; T. . 30 °C; Acq/SA. .
 Size. . K; P2/RF. . 63 $\mu\text{s}/\text{dB}$; SF. . 100.1 Hz; FB. . 2 Hz; Lock. . ^2H ; D5/ST. . 250 s
 DC. . ; Gated Off. . ; Offset. . Hz; RF. . W/dB; NBW. . Hz

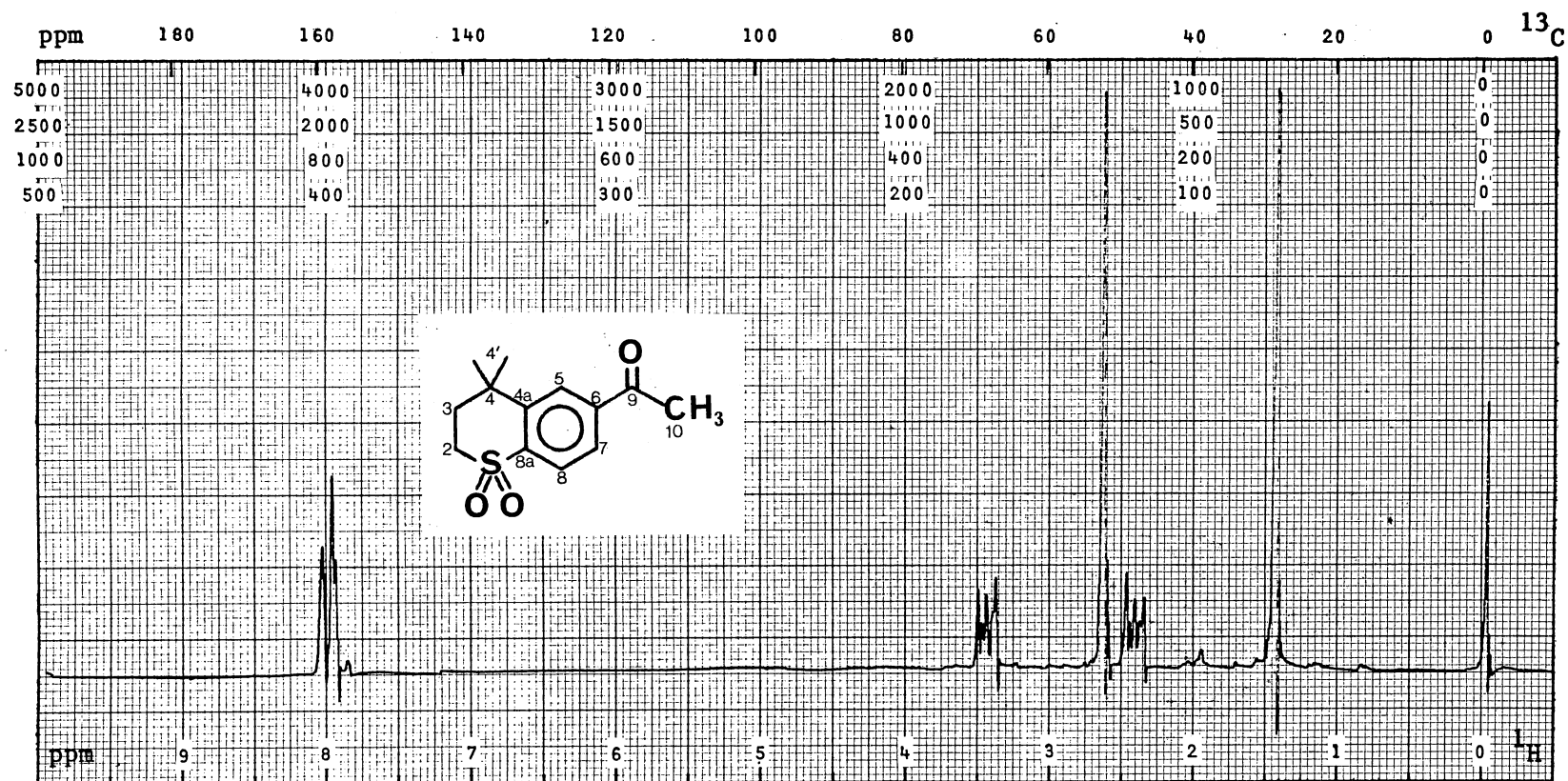
PLATE X



^{13}C NMR Spectrum of 30a

PFT X CW _ ; Solvent. . CDCl_3 ; SO. . 35101 Hz; PW. . 5000 Hz; T. . 30 °C; Acq/SA. . 500
 Size. . 8 K; P2/RF. . 10 $\mu\text{s}/\text{dB}$; SF. . 25.2Hz; FB. . Hz; Lock. . ^2H ; D5/ST. . 5 s
 DC. . ^1H ; Gated Off. . ; Offset. . 45051 Hz; RF. . 9 W/dB; NBW. . Hz

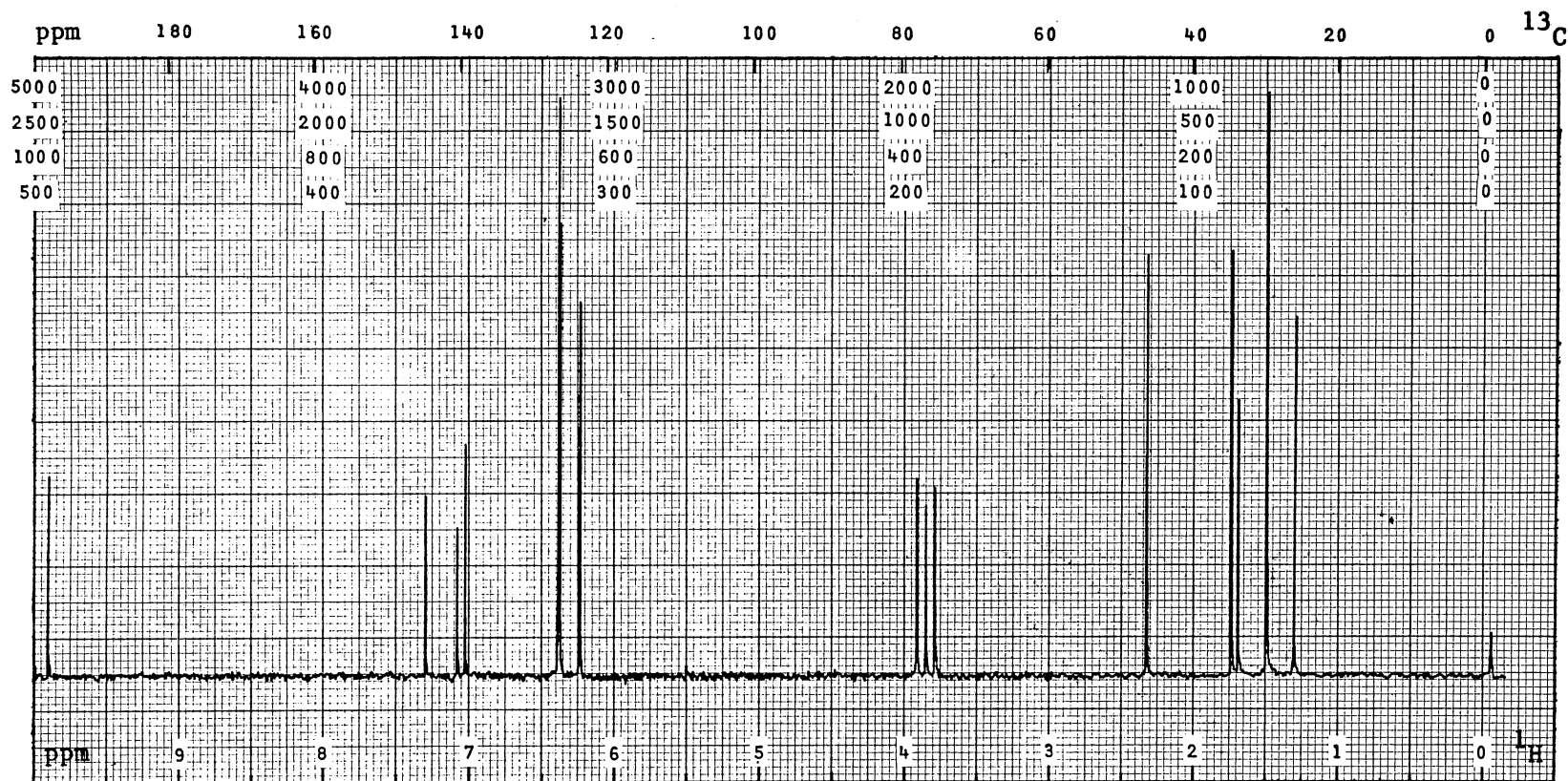
PLATE XI



^1H NMR Spectrum of 30c

PFT CW X ; Solvent. . CDCl_3 ; SO. . 85771 Hz; PW. . 1000 Hz; T. . 30 °C; Acq/SA. .
 Size. . K; P2/RF. . 61 $\mu\text{s}/\text{dB}$; SF. . 100.1 Hz; FB. . 2 Hz; Lock. . ^2H ; D5/ST. . 250 s
 DC. . ; Gated Off. . ; Offset. . Hz; RF. . W/dB; NBW. . Hz

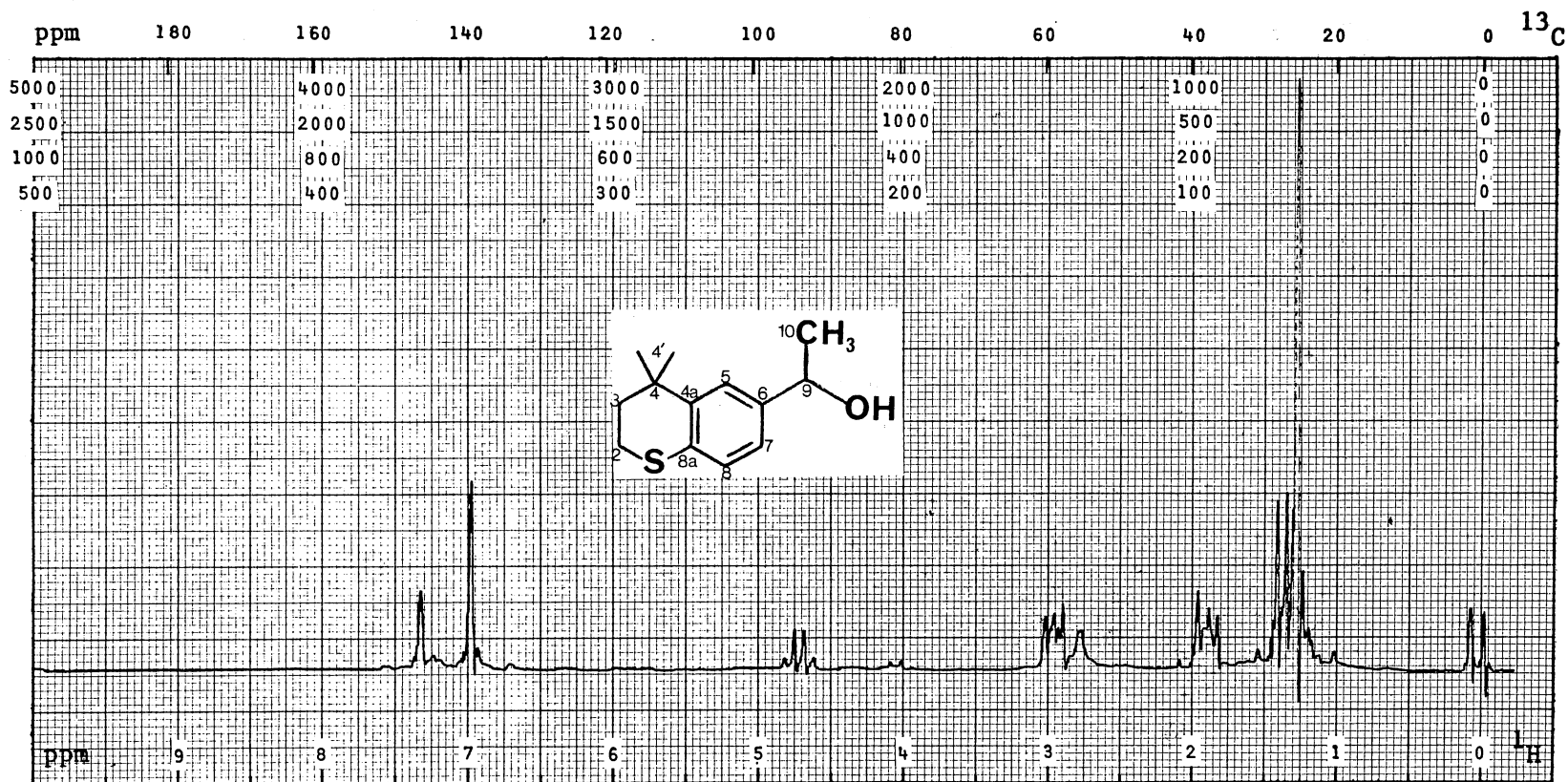
PLATE XII



^{13}C NMR Spectrum of 30c

PFT X CW _ ; Solvent. . CDCl_3 ; SO. . 35101 Hz; PW. . 5000 Hz; T. . 30 °C; Acq/SA. . 400
 Size. . 8 K; P2/RF. . 10 $\mu\text{s}/\text{dB}$; SF. . 25.2 Hz; FB. . Hz; Lock. . ^2H ; D5/ST. . 5 s
 DC. . ^1H ; Gated Off. . ; Offset. . 45051 Hz; RF. . 9 W/dB; NBW. . Hz

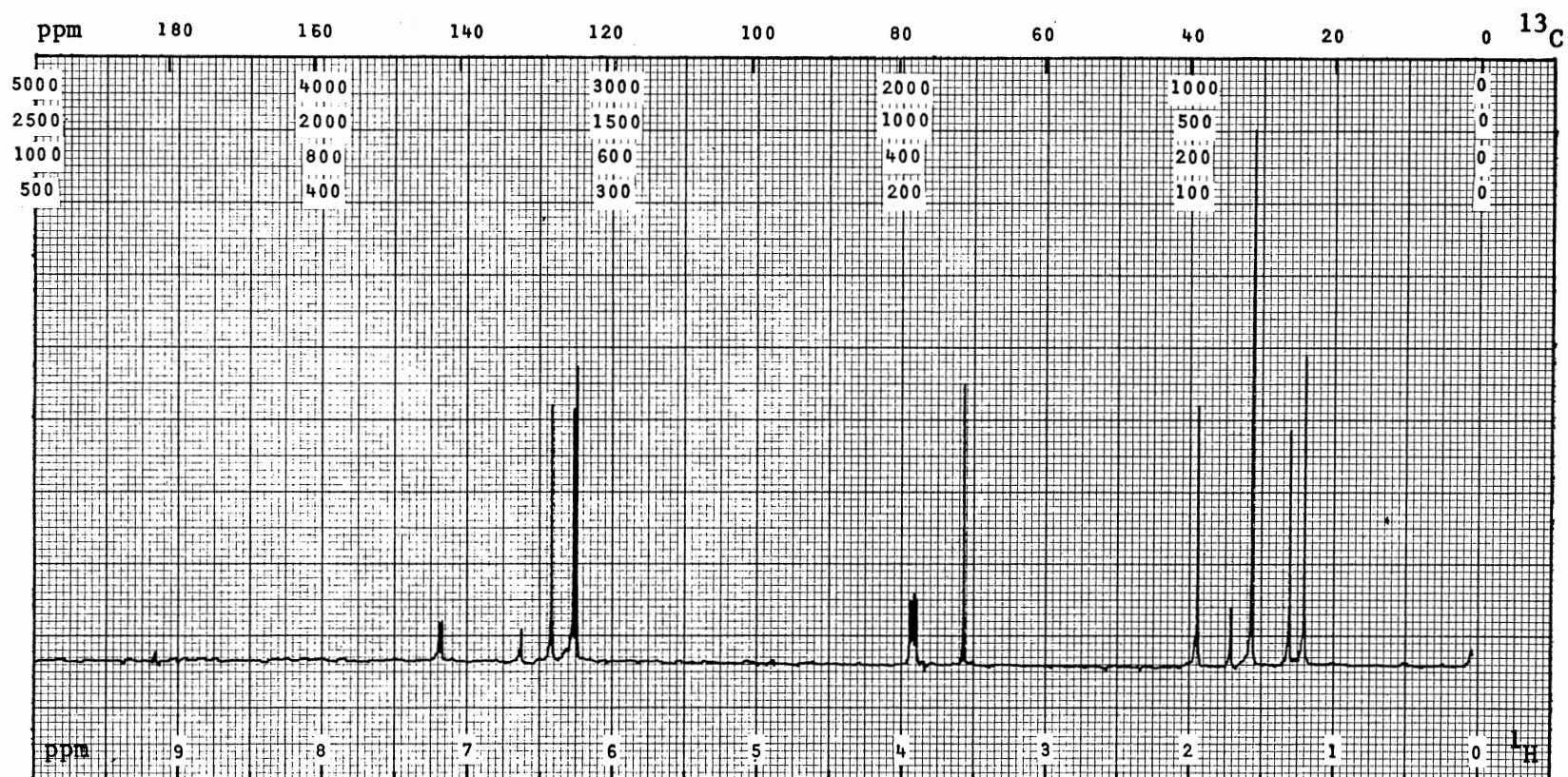
PLATE XIII



^{13}C NMR Spectrum of 31a

PFT _ CW X ; Solvent. . CDCl_3 ; SO. . 85771 Hz; PW. . 1000 Hz; T. . 30 °C; Acq/SA. .
 Size. . K; P2/RF. . 60 $\mu\text{s/dB}$; SF. . 100.1 Hz; FB. . 2 Hz; Lock. . ^2H ; D5/ST. . 250 s
 DC. . ; Gated Off. . ; Offset. . Hz; RF. . W/dB; NBW. . Hz

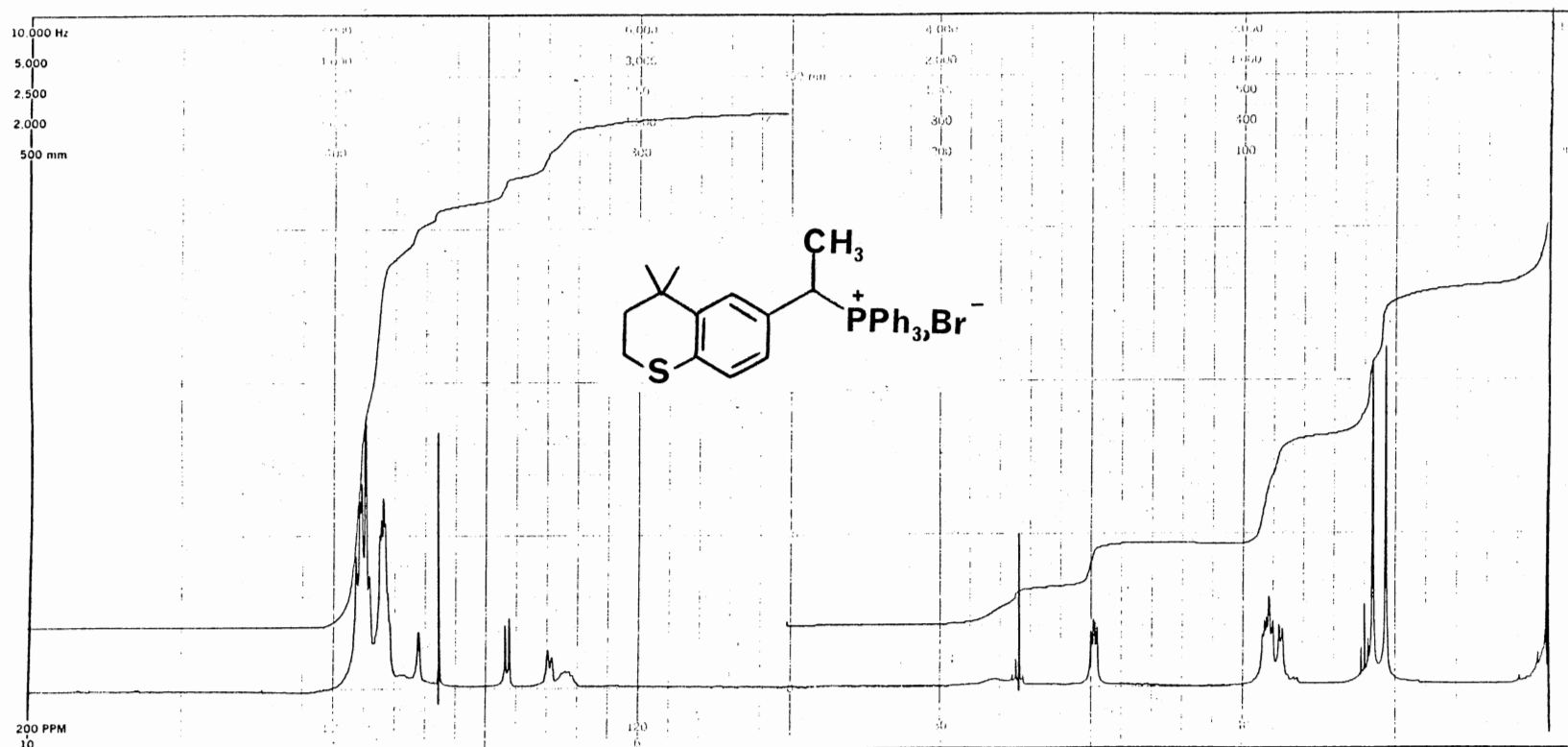
PLATE XIV



^{13}C NMR Spectrum of 3la

PFT X CW ; Solvent. . CDCl_3 ; SO. . Hz; PW. . 20000 Hz; T. . 25 °C; Acq/SA. . 140
 Size. . K; P2/RF. . 12 $\mu\text{s}/\text{dB}$; SF. . 75.4 Hz; FB. . Hz; Lock. . ^2H ; D5/ST. . 5 s
 DC. . ^1H ; Gated Off. . ; Offset. . Hz; RF. . W/dB; NBW. . Hz

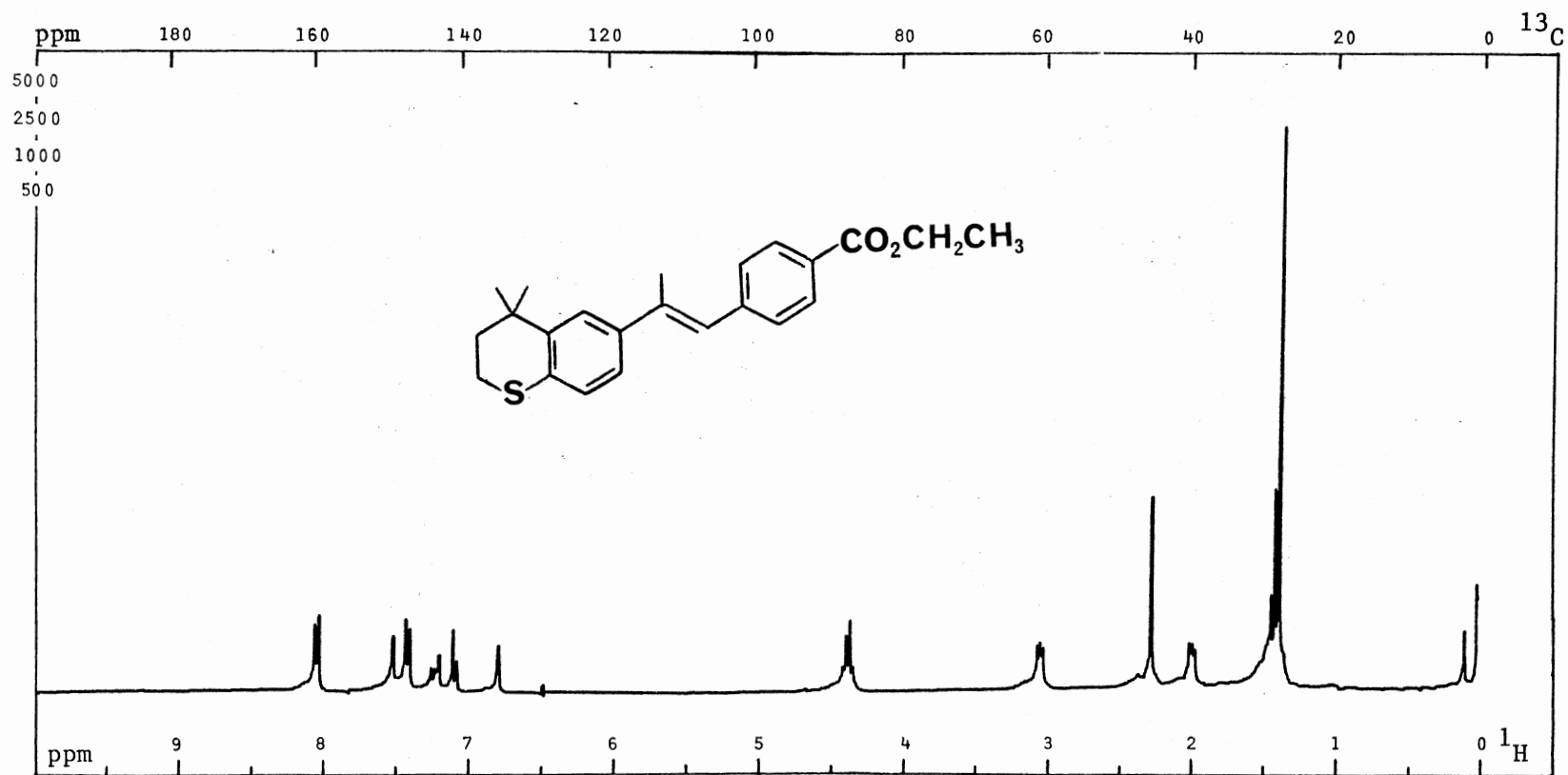
PLATE XV



^1H NMR Spectrum of 32a

PFT X CW ; Solvent. . CDCl_3 ; SO. . Hz; PW. . 4000 Hz; T. . 25 °C; Acq/SA. . 16
 Size. . K; P2/RF. . 3 $\mu\text{s}/\text{dB}$; SF. . 299.9 Hz; FB. . Hz; Lock. . ^2H ; D5/ST. . 1 s
 DC. . ; Gated Off. . ; Offset. . Hz; RF. . W/dB; NBW. . Hz

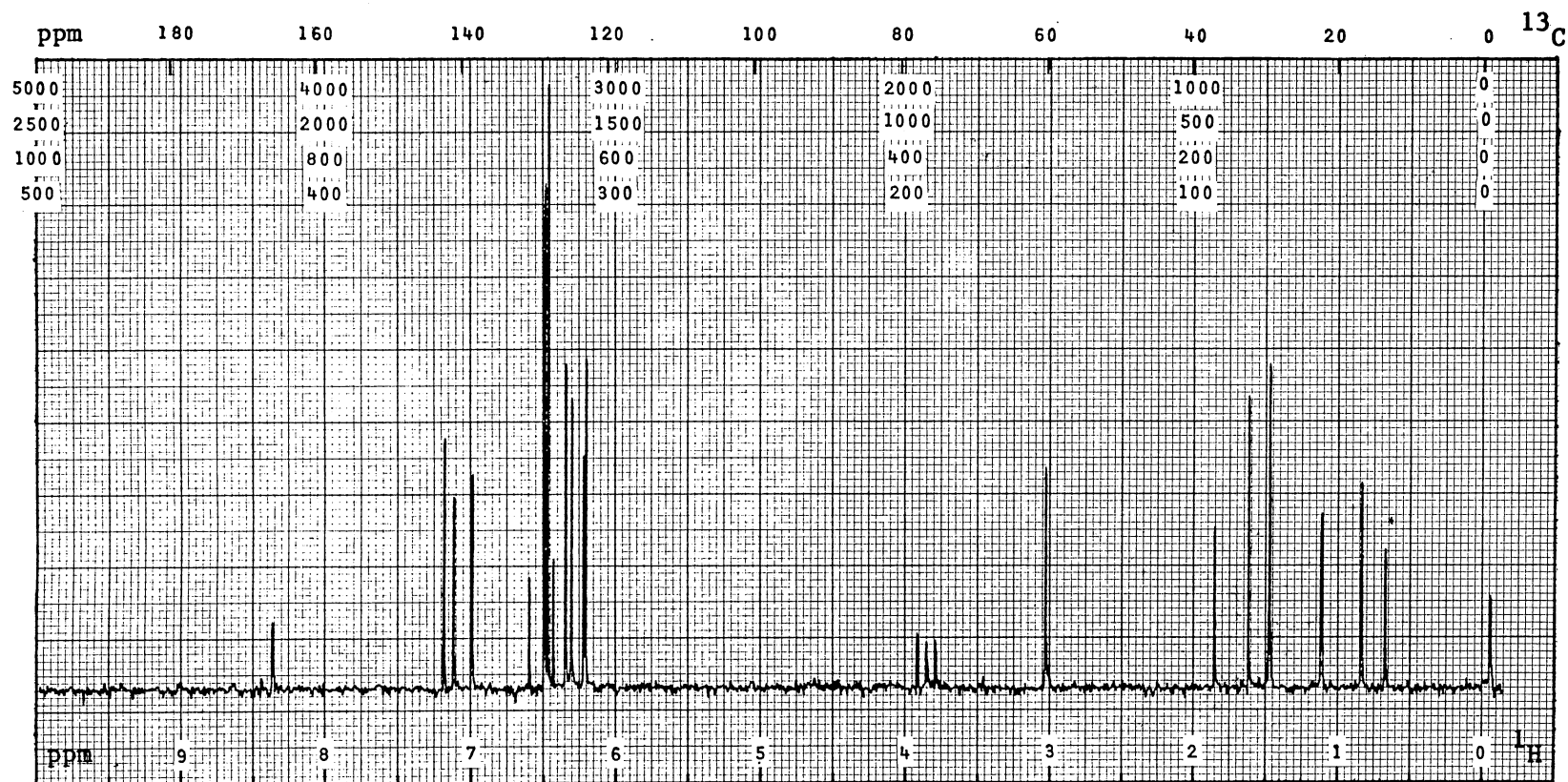
PLATE XVI



^1H NMR Spectrum of 22a

PFT X CW _ ; Solvent. . CDCl_3 ; SO. . Hz; PW. . 4000 Hz; T. . 25 °C; Acq/SA. .16
 Size. . K; P2/RF. . 3 $\mu\text{s}/\text{dB}$; SF. . 299.9 Hz; FB. . Hz; Lock. . ^2H ; D5/ST. . 1 s
 DC. . ; Gated Off. . ; Offset. . Hz; RF. . W/dB; NBW. . Hz

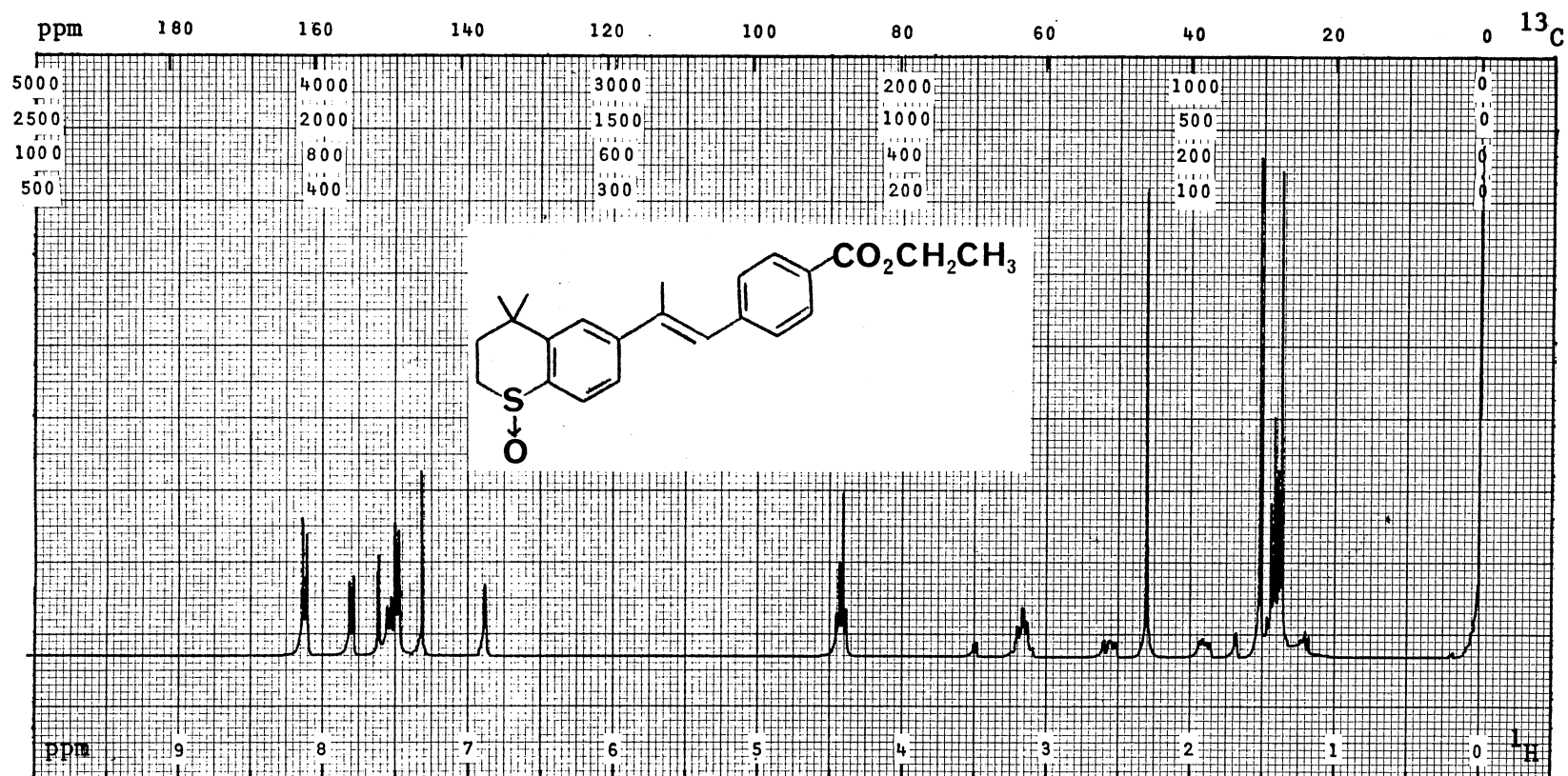
PLATE XVII



^{13}C NMR Spectrum of 22a

PFT X CW ; Solvent. . CDCl_3 ; SO. . 35101 Hz; PW. . 5000 Hz; T. . 30 °C; Acq/SA. . 500
 Size. . 8 K; P2/RF. . 10 $\mu\text{s/dB}$; SF. . 25.2 Hz; FB. . Hz; Lock. . ^2H ; D5/ST. . 5 s
 DC. . ^1H ; Gated Off. . ; Offset. . 45051 Hz; RF. . 9 W/dB; NBW. . Hz

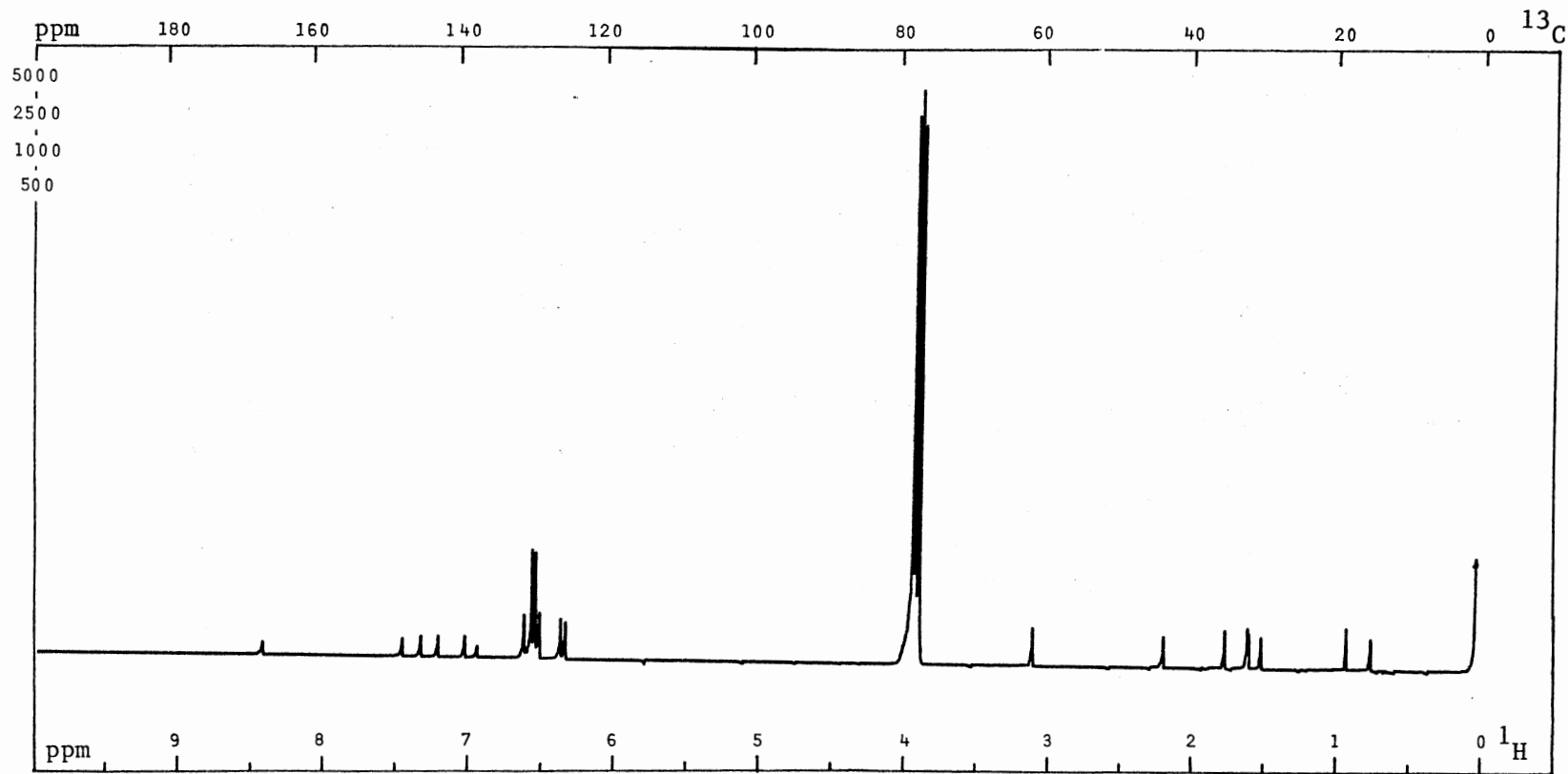
PLATE XVIII



¹H NMR Spectrum of 22d

PFT X CW ; Solvent. . CDCl₃ ; SO. . Hz; PW. . 4000 Hz; T. . 25 °C; Acq/SA. . 16
 Size. . K; P2/RF. . 3 μs/dB; SF. . 299.9 Hz; FB. . Hz; Lock. . ²H ; D5/ST. . 1 s
 DC. . ; Gated Off. . ; Offset. . Hz; RF. . W/dB; NBW. . Hz

PLATE XIX



^{13}C NMR Spectrum of 22d

PFT X CW _ ; Solvent. . CDCl_3 ; SO. . Hz; PW. .20000 Hz; T. . 25 °C; Acq/SA. .2000
 Size. . K; P2/RF. . 12 $\mu\text{s}/\text{dB}$; SF. . 75.4 Hz; FB. . Hz; Lock. . ^2H ; D5/ST. . 5 s
 DC. . ^1H ; Gated Off. . ; Offset. . Hz; RF. . W/dB; NBW. . Hz

PLATE XX

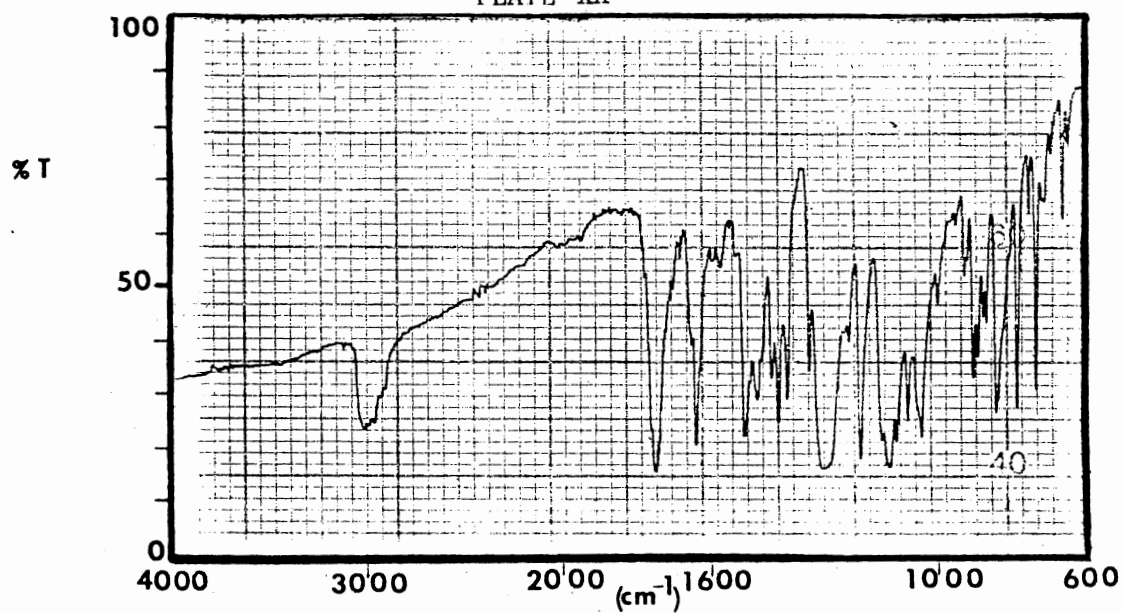
IR Spectrum of 22a

PLATE XXI

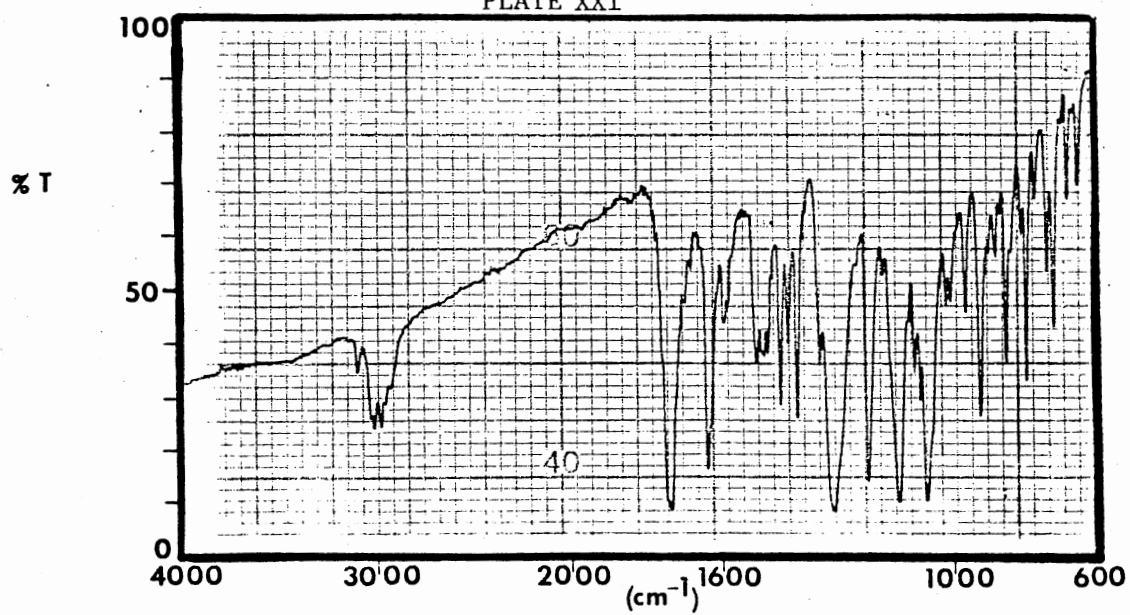
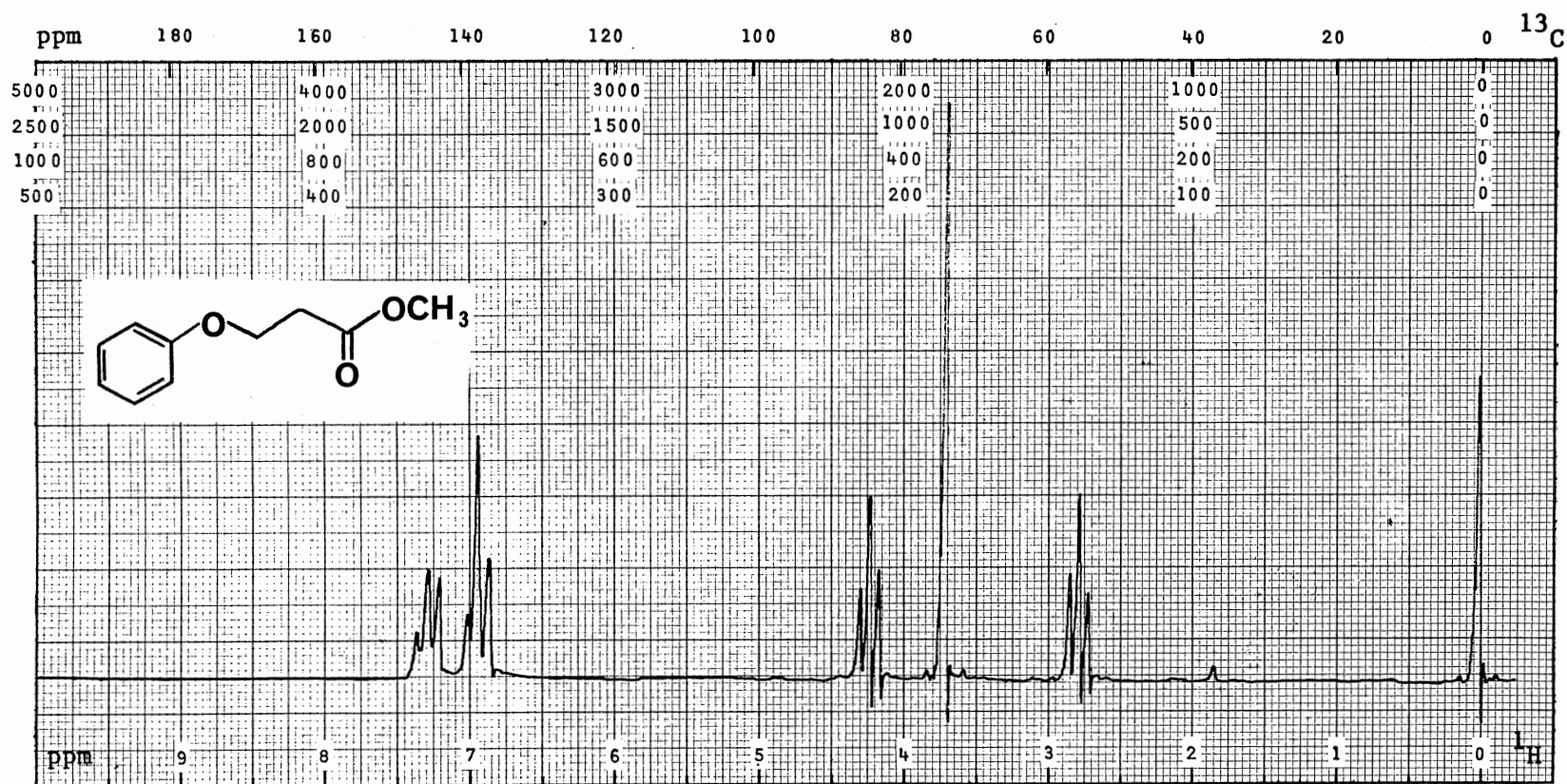
IR Spectrum of 22d

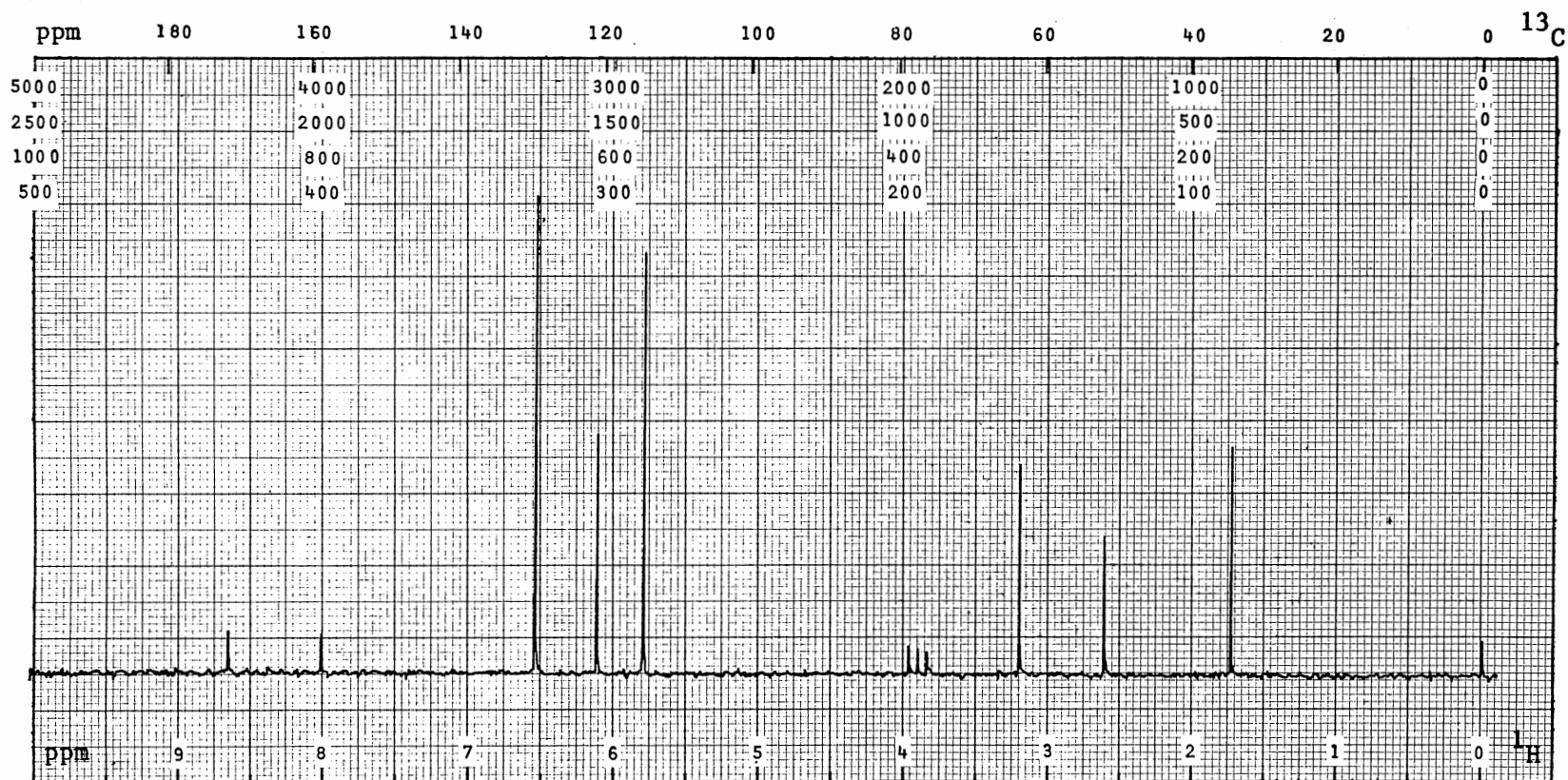
PLATE XXII



^1H NMR Spectrum of 26b

PFT _ CW X ; Solvent. . CDCl_3 ; SO. . 85771 Hz; PW. . 1000 Hz; T. . 30 °C; Acq/SA. .
 Size. . K; P2/RF. . 58 $\mu\text{s}/\text{dB}$; SF. . 100.1 Hz; FB. . 2 Hz; Lock. . ^2H ; D5/ST. . 250 s
 DC. . ; Gated Off. . ; Offset. . Hz; RF. . W/dB; NBW. . Hz

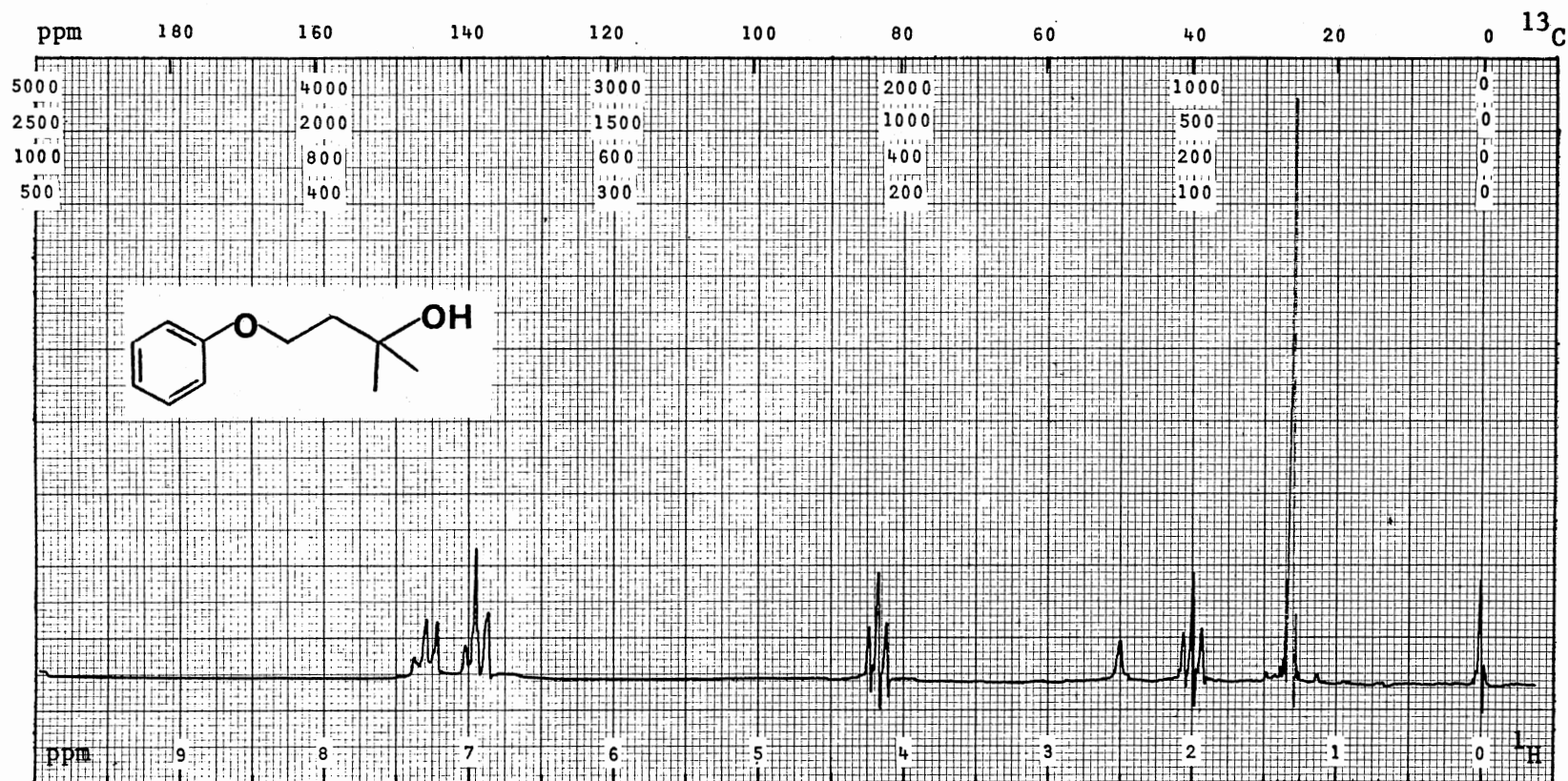
PLATE XXIII



^{13}C NMR Spectrum of 26b

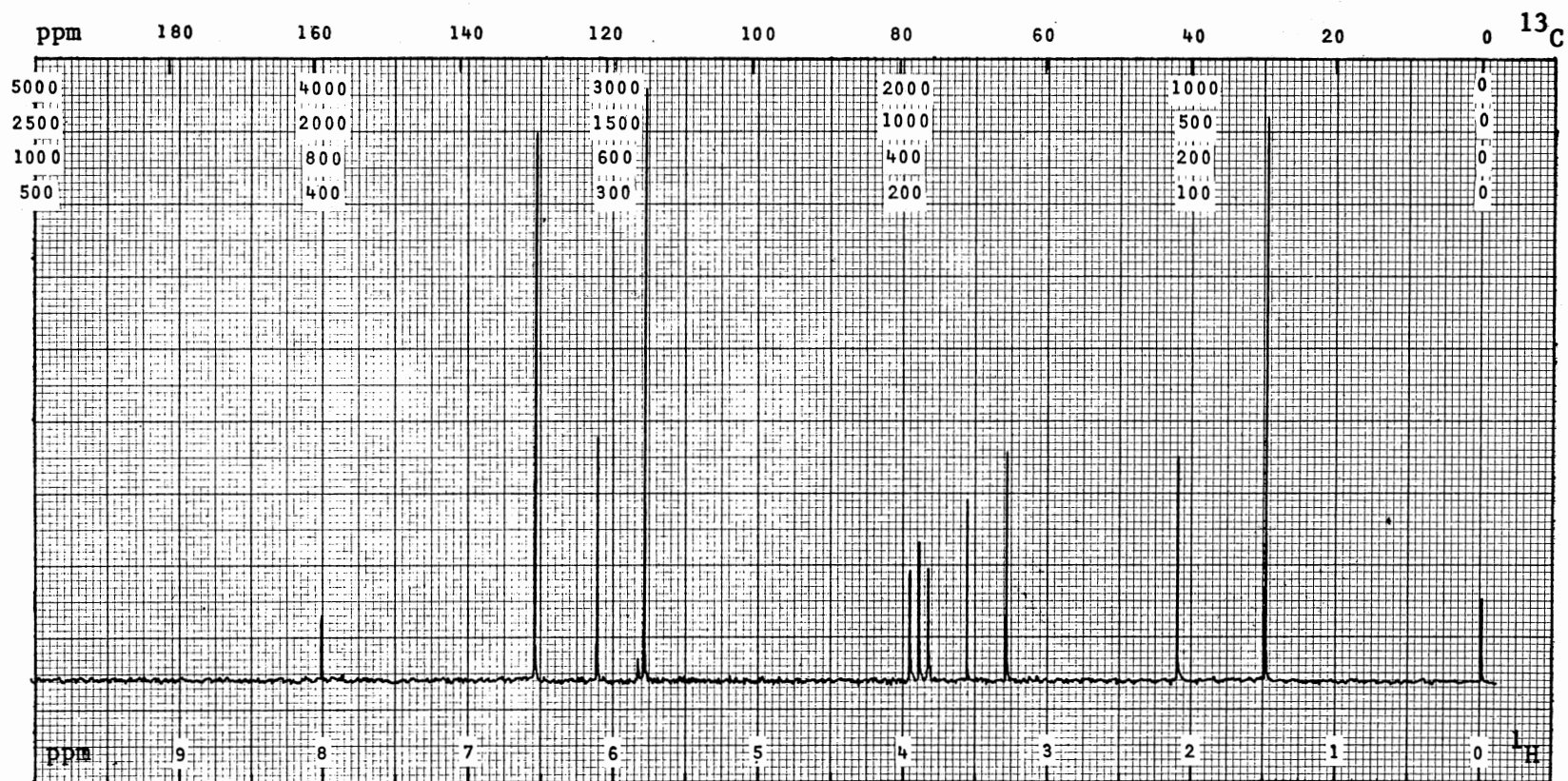
PFT X CW _; Solvent. . CDCl_3 ; SO. . 35101 Hz; PW. . 5000 Hz; T. . 30 °C; Acq/SA. . 400
 Size. . 8 K; P2/RF. . 10 $\mu\text{s/dB}$; SF. . 25.2 Hz; FB. . Hz; Lock. . ^2H ; D5/ST. . 5 s
 DC. . ^1H ; Gated Off. . ; Offset. . 45051 Hz; RF. . 9 W/dB; NBW. . Hz

PLATE XXIV



¹H NMR Spectrum of 27b
 PFT _ CW X; Solvent. . CDCl₃ ; SO. . 85771 Hz; PW. . 1000 Hz; T. . 30 °C; Acq/SA. .
 Size. . K; P2/RF. . 65 μs/dB; SF. . 100.1 Hz; FB. . 2 Hz; Lock. . ²H ; D5/ST. . 250 s
 DC. . ; Gated Off. . ; Offset. . Hz; RF. . W/dB; NBW. . Hz

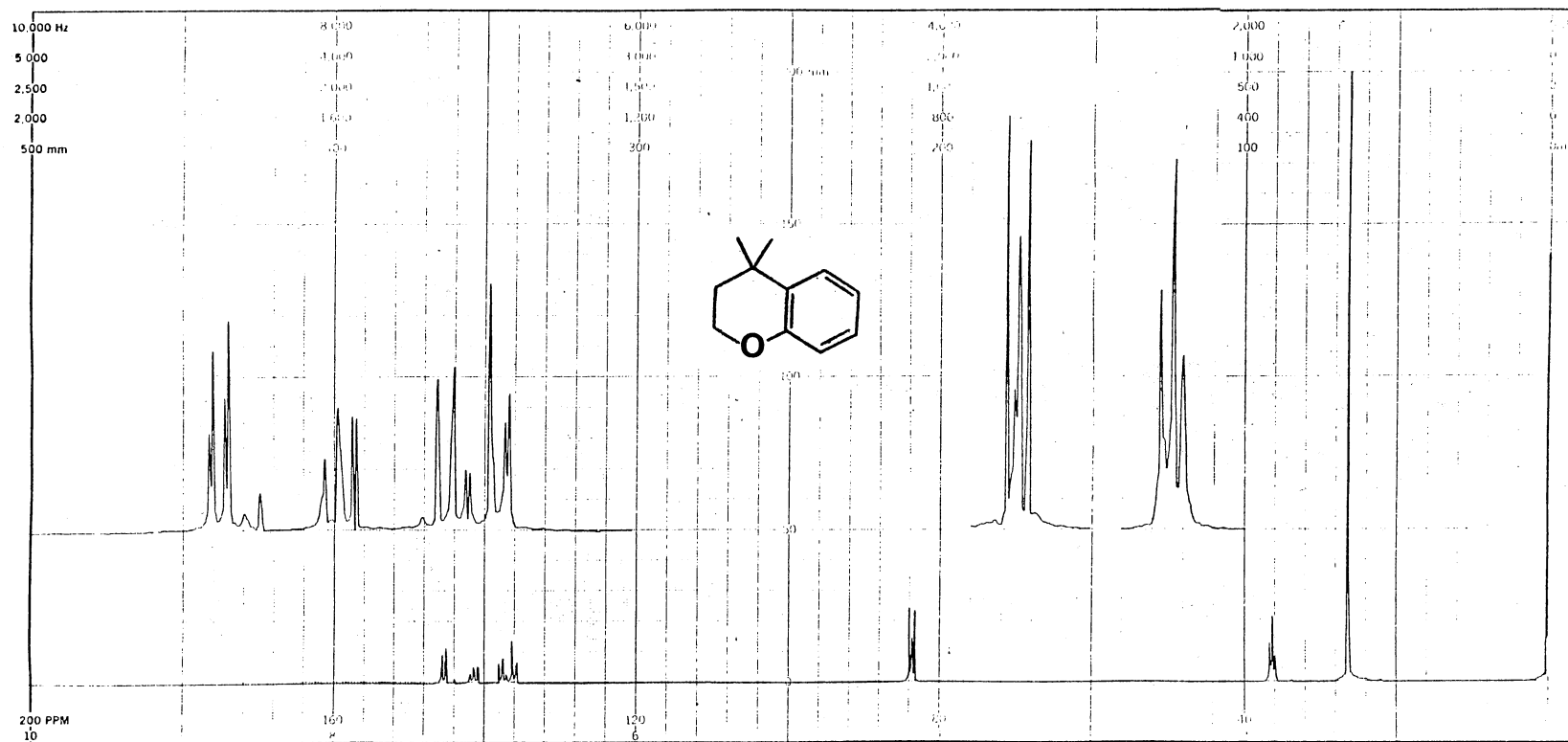
PLATE XXV



^{13}C NMR Spectrum of 27b

PFT X CW _ ; Solvent. . CDCl_3 ; SO. . 35101 Hz; PW. . 5000 Hz; T. . 30 °C; Acq/SA. . 500
 Size. . 8 K; P2/RF. . 10 $\mu\text{s/dB}$; SF. . 25.2 Hz; FB. . Hz; Lock. . ^2H ; D5/ST. . 5 s
 DC. . ^1H ; Gated Off. . ; Offset. . 45051 Hz; RF. . 9 W/dB; NBW. . Hz

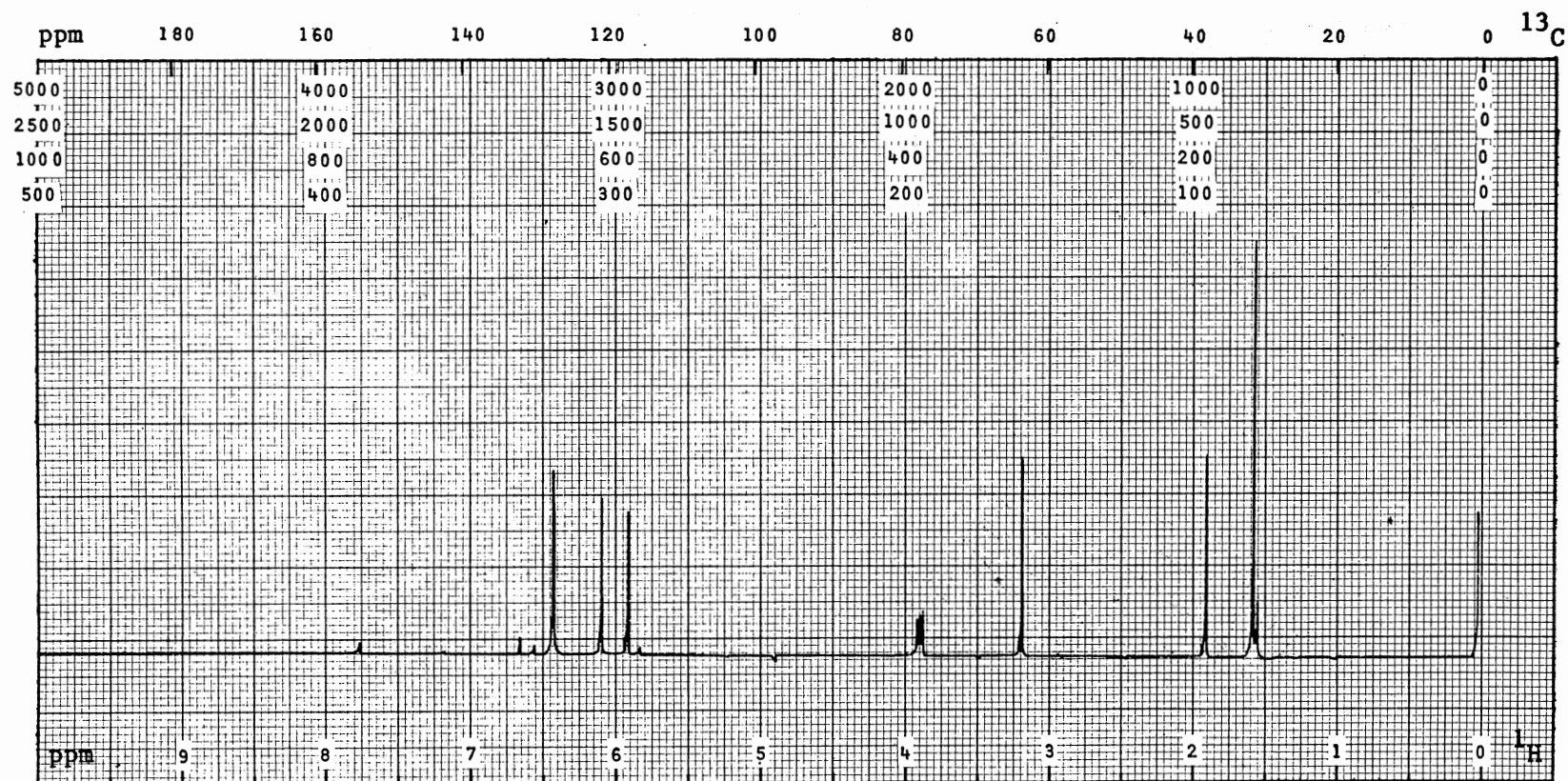
PLATE XXVI



¹H NMR Spectrum of 29b

PFT X CW _; Solvent. . CDCl₃ ; SO. . Hz; PW. .4000 Hz; T. . 25 °C; Acq/SA. .16
 Size. . K; P2/RF. . 3 μs/dB; SF. . 299.9 Hz; FB. . Hz; Lock. . ²H ; D5/ST. . 1 s
 DC. . ; Gated Off. . ; Offset. . Hz; RF. . W/dB; NBW. . Hz

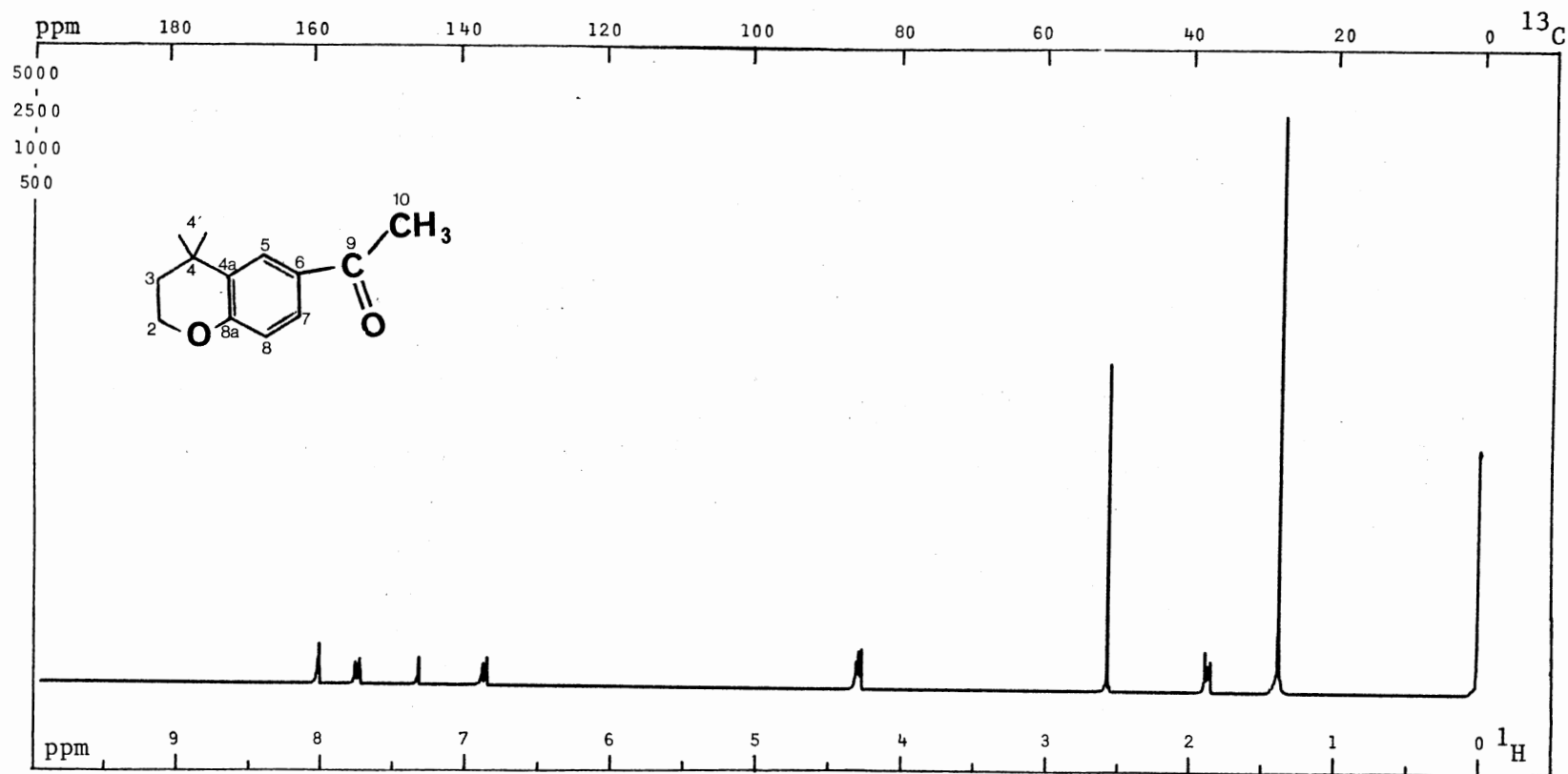
PLATE XXVII



^{13}C NMR Spectrum of 29b

PFT X CW _; Solvent. . CDCl_3 ; SO. . Hz; PW. . 20000 Hz; T. . 23 °C; Acq/SA. . 200
 Size. . K; P2/RF. . 12 $\mu\text{s/dB}$; SF. . 75.4 Hz; FB. . Hz; Lock. . ^2H ; D5/ST. . 5 s
 DC. . ^1H ; Gated Off. . ; Offset. . Hz; RF. . W/dB; NBW. . Hz

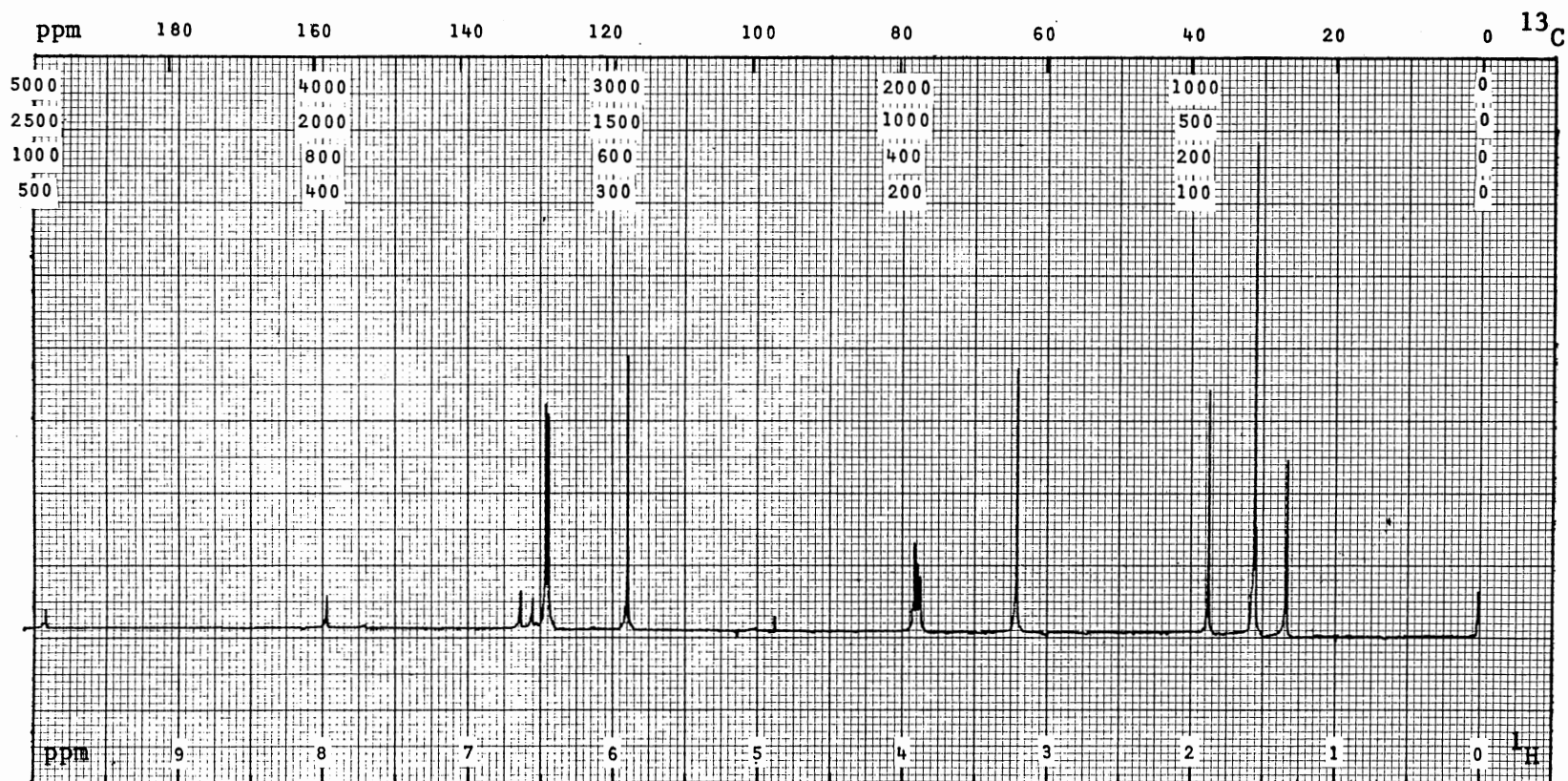
PLATE XXVIII



^1H NMR Spectrum of 30b

PFT X CW ; Solvent. . CDCl_3 ; SO. . Hz; PW. . 4000 Hz; T. . 25 °C; Acq/SA. .16
 Size. . K; P2/RF. . 3 $\mu\text{s}/\text{dB}$; SF. . 299.9 Hz; FB. . Hz; Lock. . ^2H ; D5/ST. . 1 s
 DC. . ; Gated Off. . ; Offset. . Hz; RF. . W/dB; NBW. . Hz

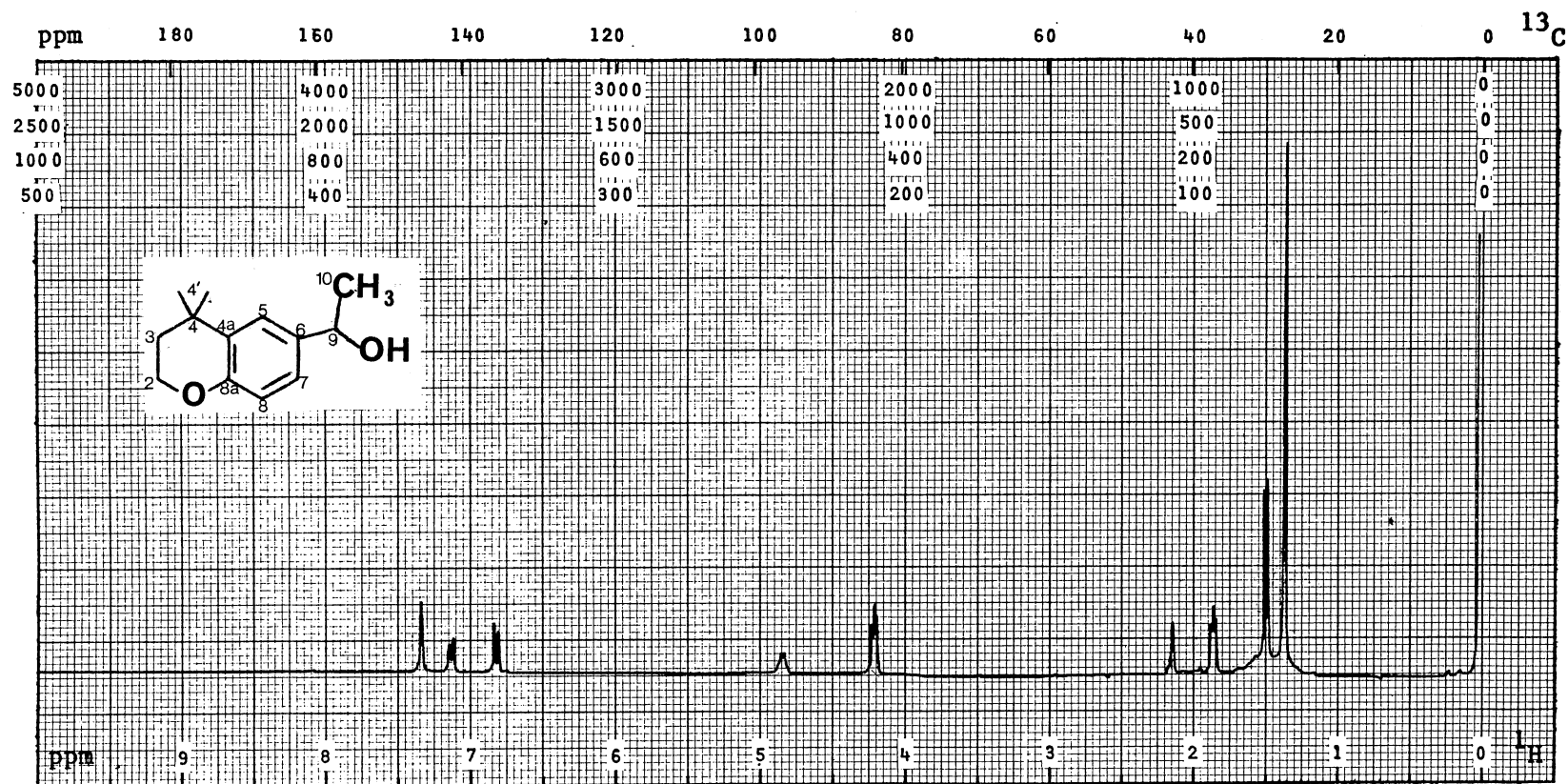
PLATE XXIX



^{13}C NMR Spectrum of 30b

PFT X CW _ ; Solvent. . CDCl_3 ; SO. . Hz; PW. . 20000 Hz; T. . 25 °C; Acq/SA. . 180
 Size. . K; P2/RF. . 12 $\mu\text{s}/\text{dB}$; SF. . 75.4 Hz; FB. . Hz; Lock. . ^2H ; D5/ST. . 5 s
 DC. . ^1H ; Gated Off. . ; Offset. . Hz; RF. . W/dB; NBW. . Hz

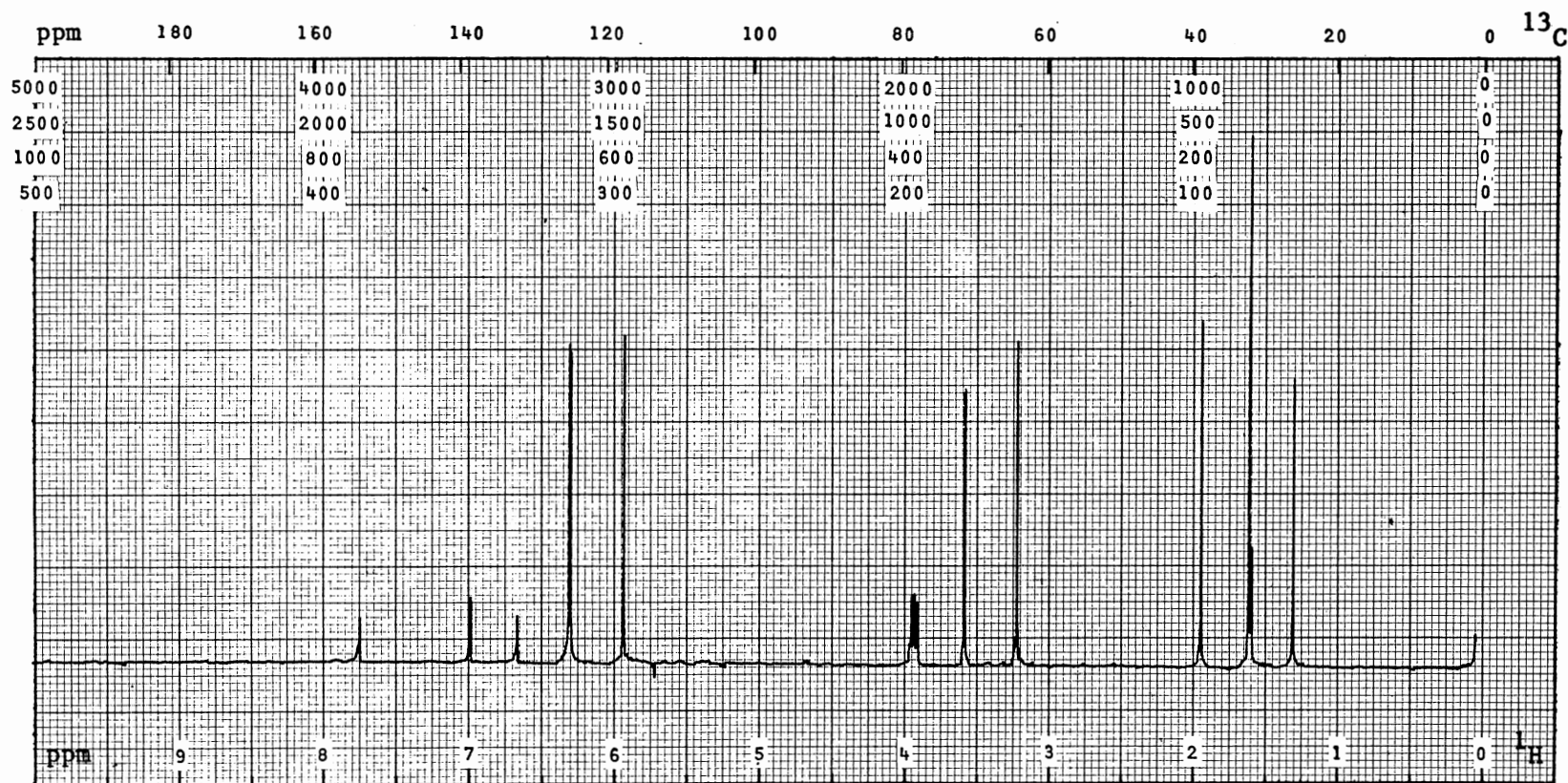
PLATE XXX



^1H NMR Spectrum of 31b

PFT X CW ; Solvent. . CDCl_3 ; SO. . Hz; PW. . 4000 Hz; T. . 25 °C; Acq/SA. . 16
 Size. . K; P2/RF. . 3 $\mu\text{s}/\text{dB}$; SF. . 299.9 Hz; FB. . Hz; Lock. . ^2H ; D5/ST. . 1 s
 DC. . ; Gated Off. . ; Offset. . Hz; RF. . W/dB; NBW. . Hz

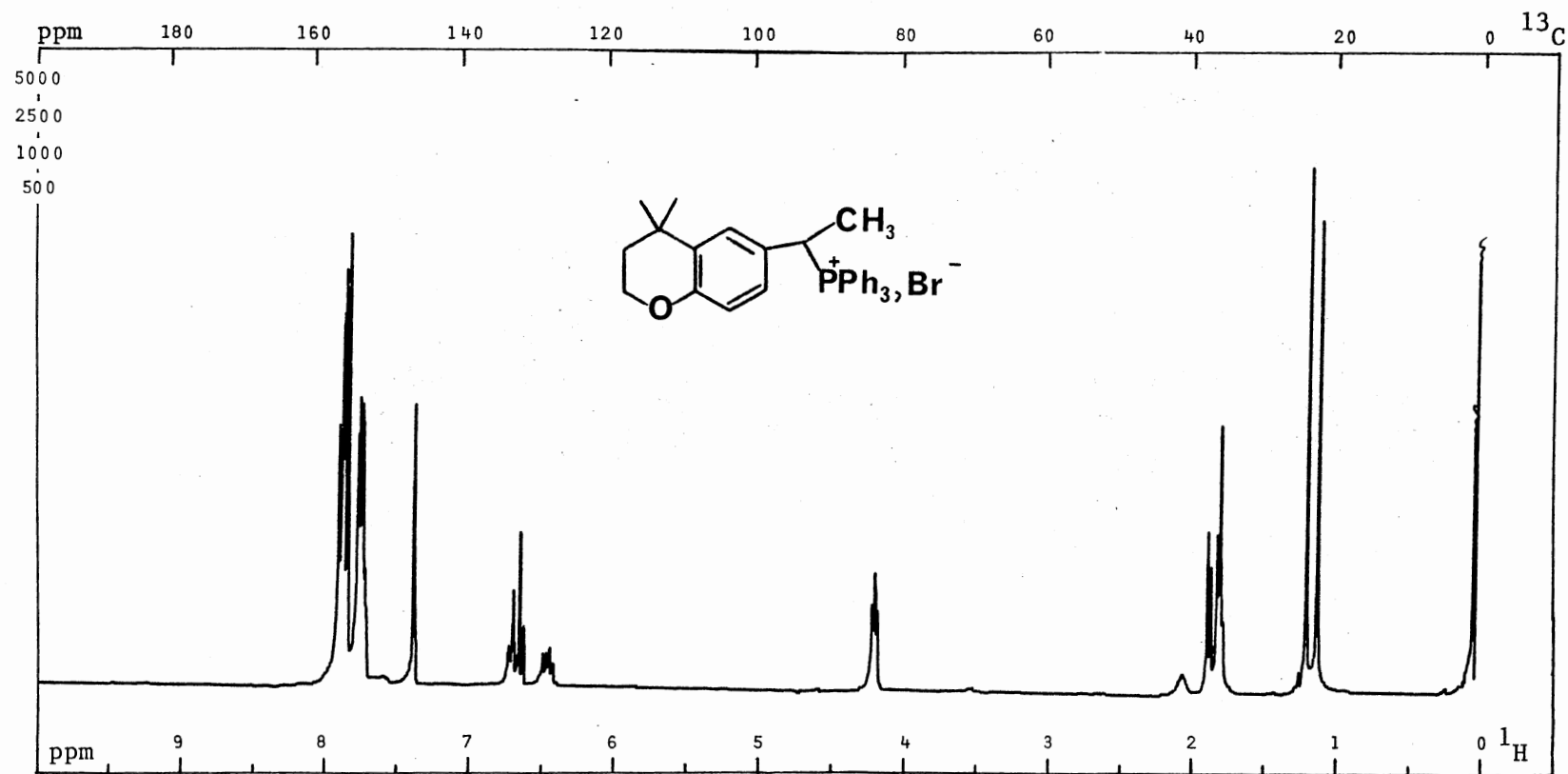
PLATE XXXI



^{13}C NMR Spectrum of 31b

PFT X CW _; Solvent. . CDCl_3 ; SO. . Hz; PW. . 20000Hz; T. . 25 °C; Acq/SA. . 160
 Size. . K; P2/RF. . 12 μs /dB; SF. . 75.4 Hz; FB. . Hz; Lock. . ^2H ; D5/ST. . 5 s
 DC. . ^1H ; Gated Off. . ; Offset. . Hz; RF. . W/dB; NBW. . Hz

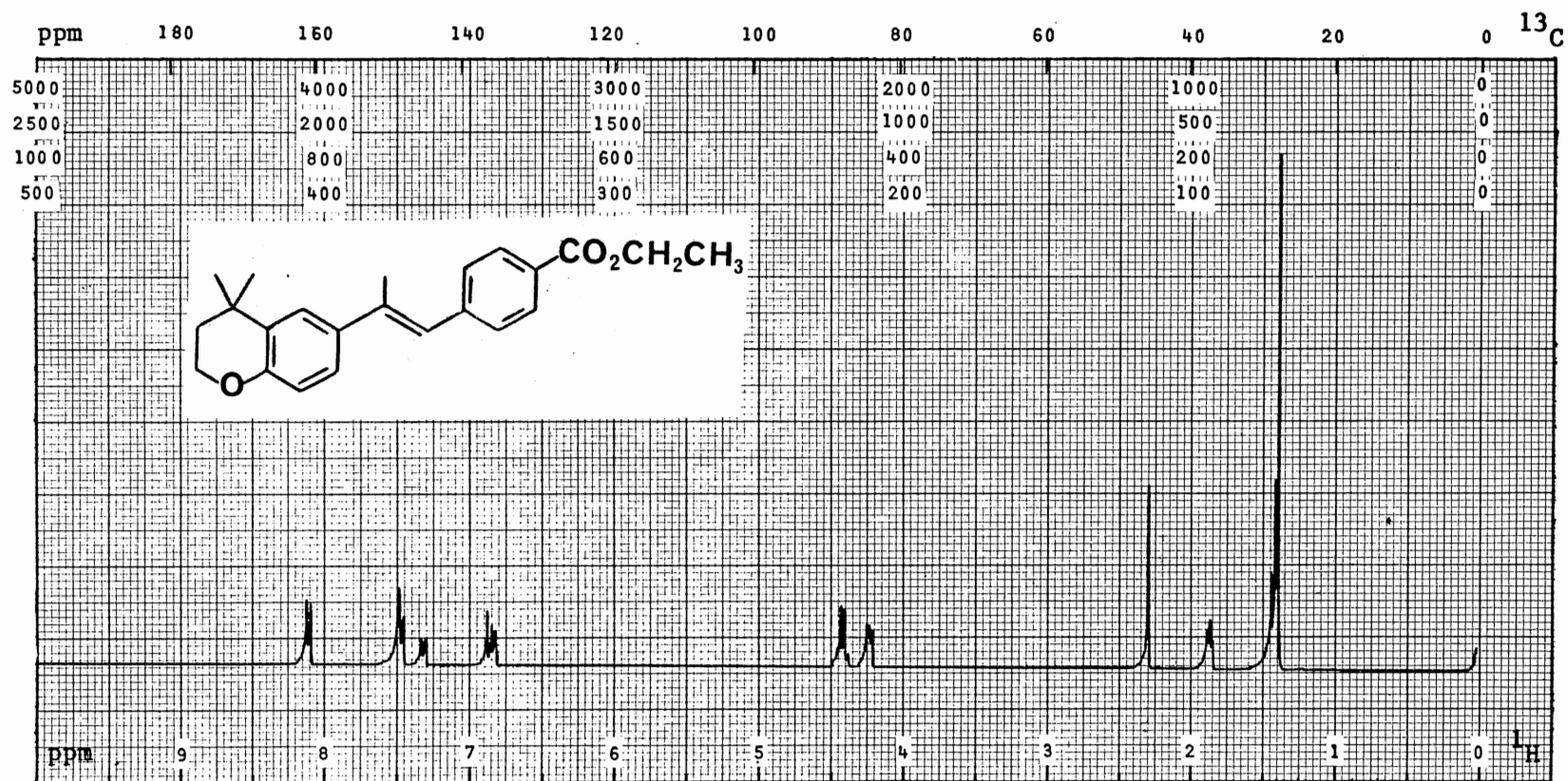
PLATE XXXII



^1H NMR Spectrum of 32b

PFT X CW _ ; Solvent. . CDCl_3 ; SO. . Hz; PW. . 4000 Hz; T. . 25 °C; Acq/SA. . 16
 Size. . K; P2/RF. . 3 $\mu\text{s/dB}$; SF. . 299.9 Hz; FB. . Hz; Lock. . ^2H ; D5/ST. . 1 s
 DC. . ; Gated Off. . ; Offset. . Hz; RF. . W/dB; NBW. . Hz

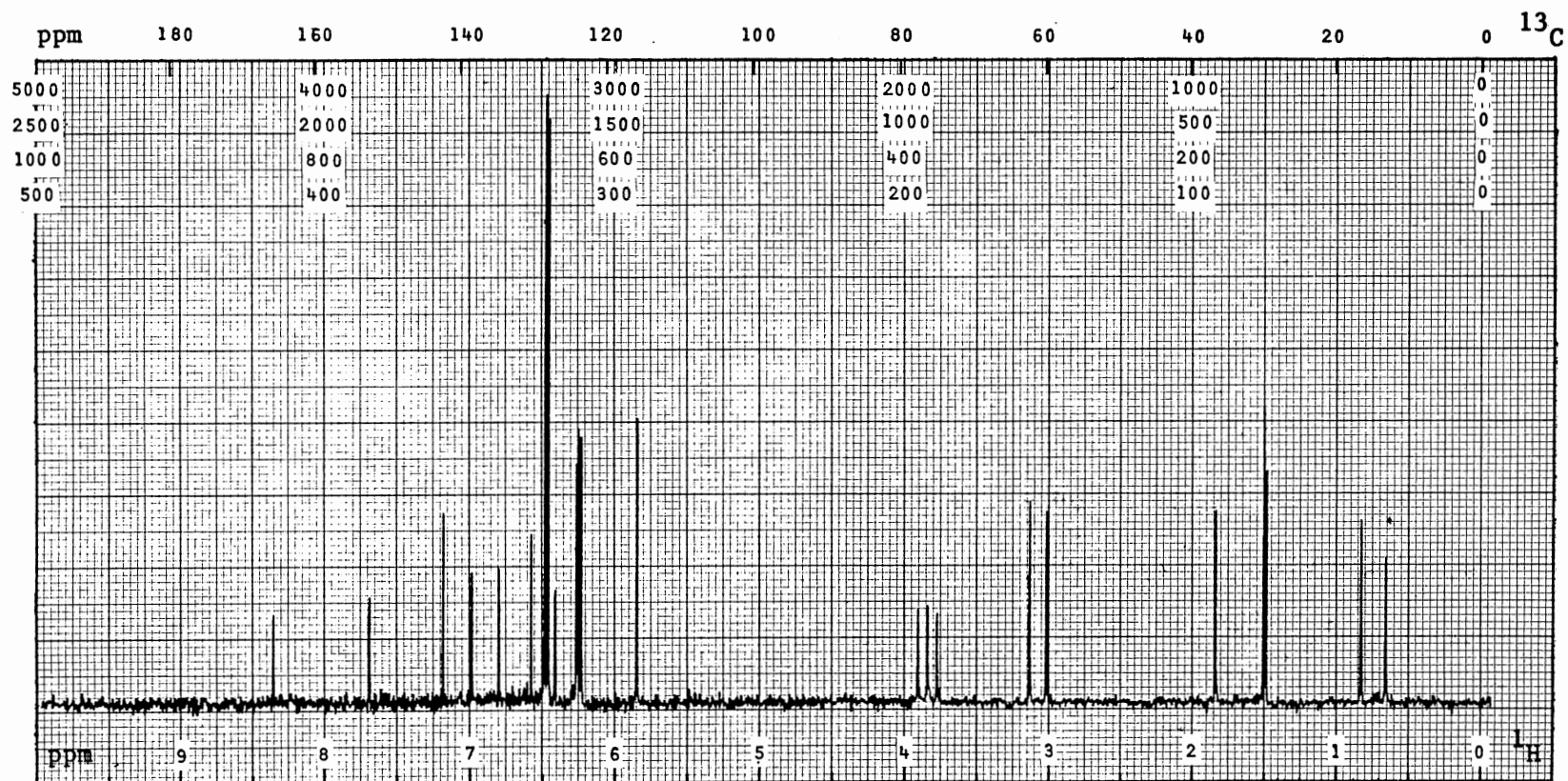
PLATE XXXIII



^1H NMR Spectrum of 22b

PFT X CW ; Solvent. . CDCl_3 ; SO. . Hz; PW. . 4000 Hz; T. . 25 °C; Acq/SA. . 16
 Size. . K; P2/RF. . 3 $\mu\text{s}/\text{dB}$; SF. . 299.9 Hz; FB. . Hz; Lock. . ^2H ; D5/ST. . 1 s
 DC. . ; Gated Off. . ; Offset. . Hz; RF. . W/dB; NBW. . Hz

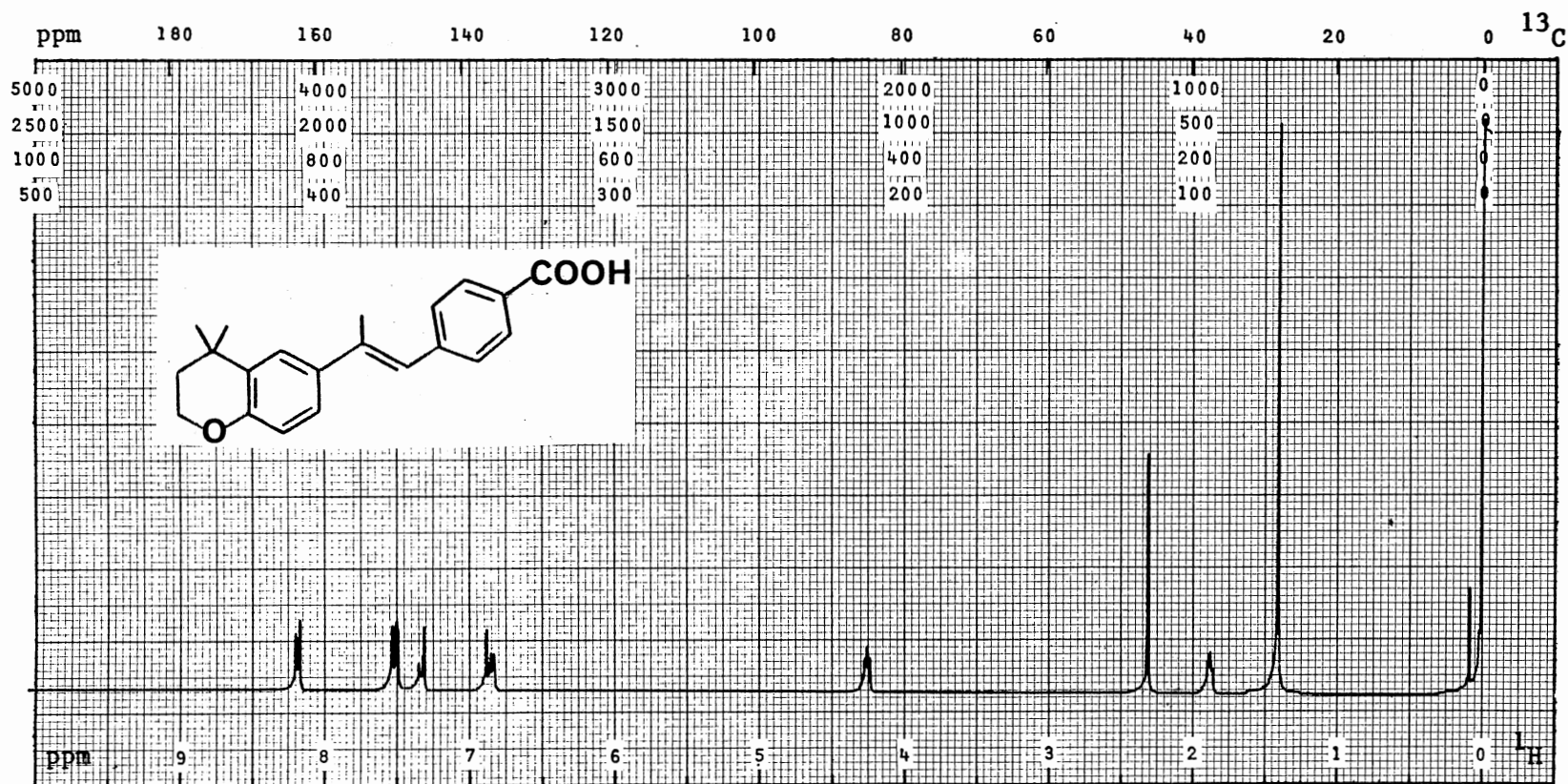
PLATE XXXIV



^{13}C NMR Spectrum of 22b

PFT X CW _ ; Solvent . . CDCl_3 ; SO . . 35101 Hz; PW . . 5000 Hz; T . . 30 °C; Acq/SA . . 400
 Size . . 8 K; P2/RF . . 10 $\mu\text{s}/\text{dB}$; SF . . 25.2 Hz; FB . . Hz; Lock . . ^2H ; D5/ST . . 5 s
 DC . . ^1H ; Gated Off . . ; Offset . . 45051 Hz; RF . . 9 W/dB; NBW . . Hz

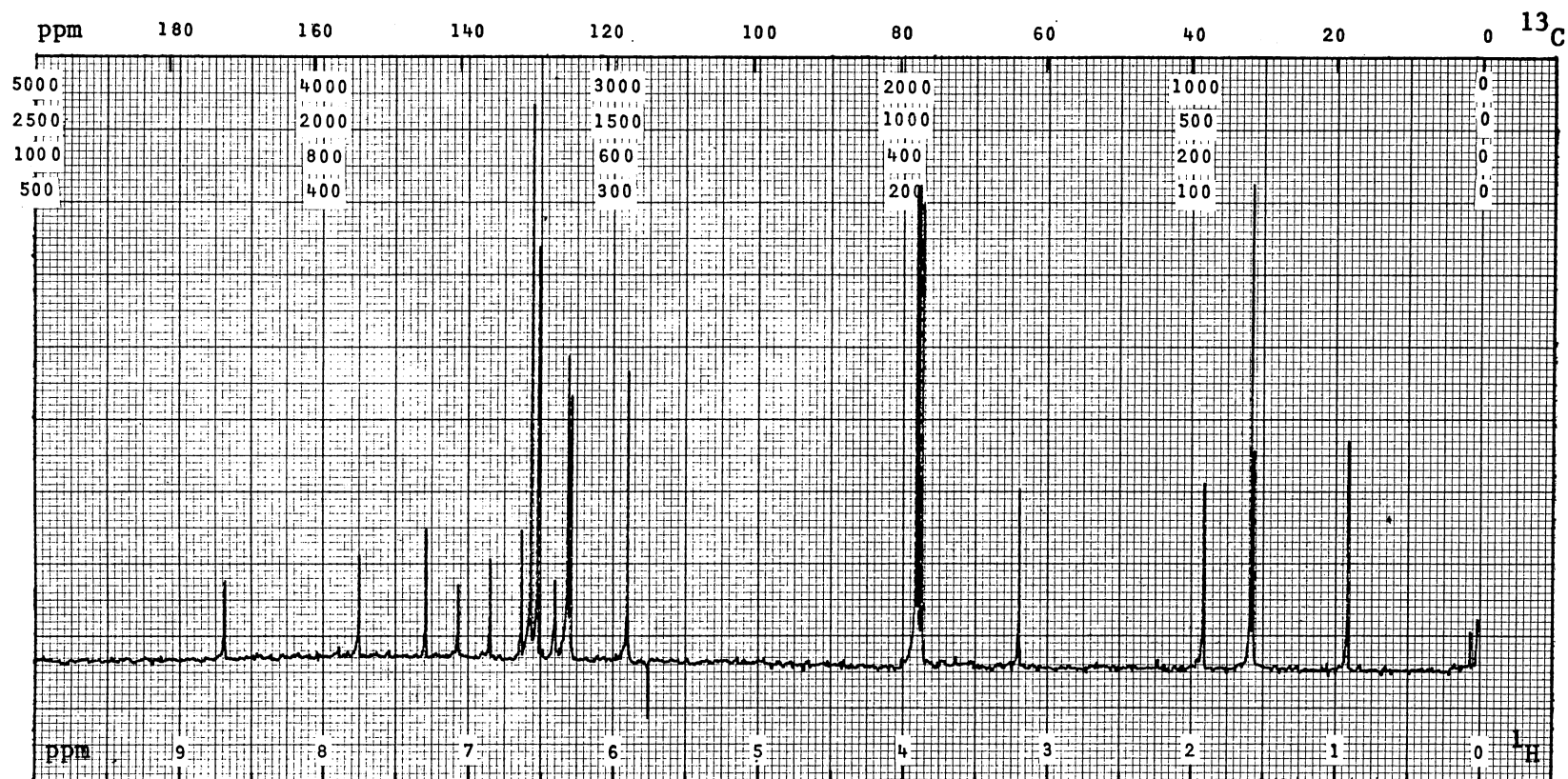
PLATE XXXV



^1H NMR Spectrum of 22c

PFT X CW ; Solvent. . CDCl_3 ; SO. . Hz; PW. . 4000 Hz; T. . 25 °C; Acq/SA. . 16
 Size. . K; P2/RF. . 3 $\mu\text{s}/\text{dB}$; SF. . 299.9 Hz; FB. . Hz; Lock. . ^2H ; D5/ST. . 1 s
 DC. . ; Gated Off. . ; Offset. . Hz; RF. . W/dB; NBW. . Hz

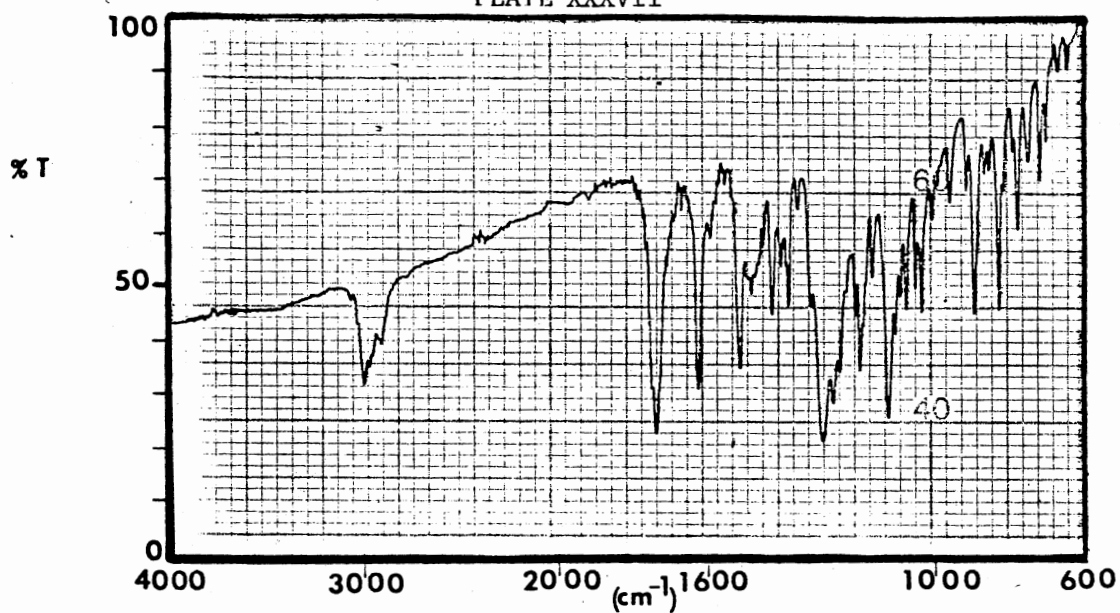
PLATE XXXVI



^{13}C NMR Spectrum of 22c

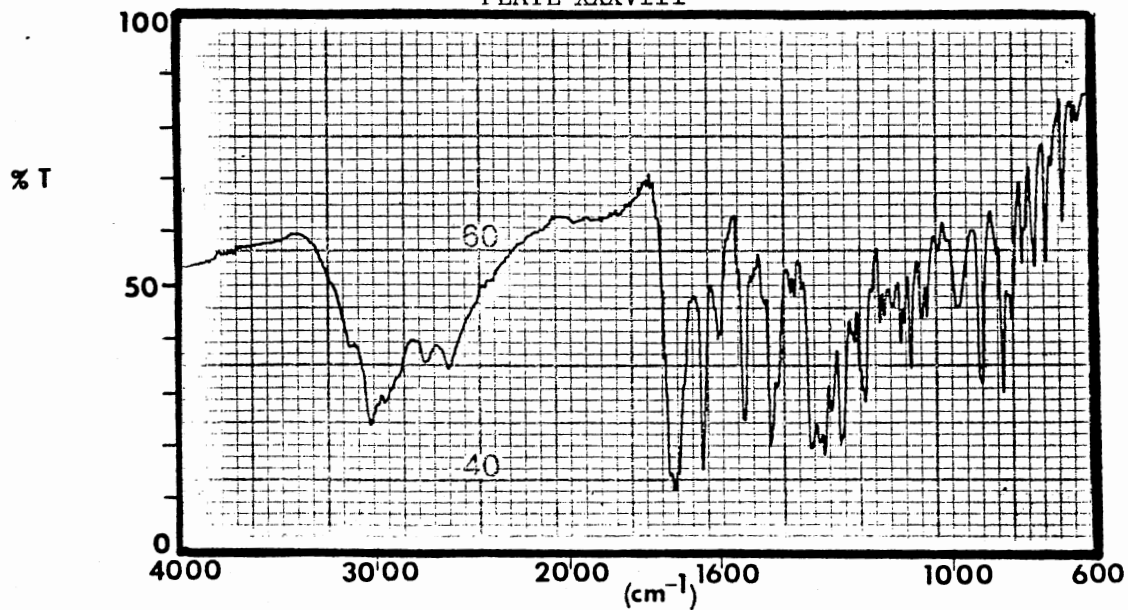
PFT X CW _ ; Solvent. . CDCl_3 ; SO. . Hz; PW. 20000 Hz; T. . 25 °C; Acq/SA. . 120
 Size. . K; P2/RF. . 12 $\mu\text{s}/\text{dB}$; SF. . 75.4 Hz; FB. . Hz; Lock. . ^2H ; D5/ST. . 5 s
 DC. . ^1H ; Gated Off. . ; Offset. . Hz; RF. . W/dB; NBW. . Hz

PLATE XXXVII



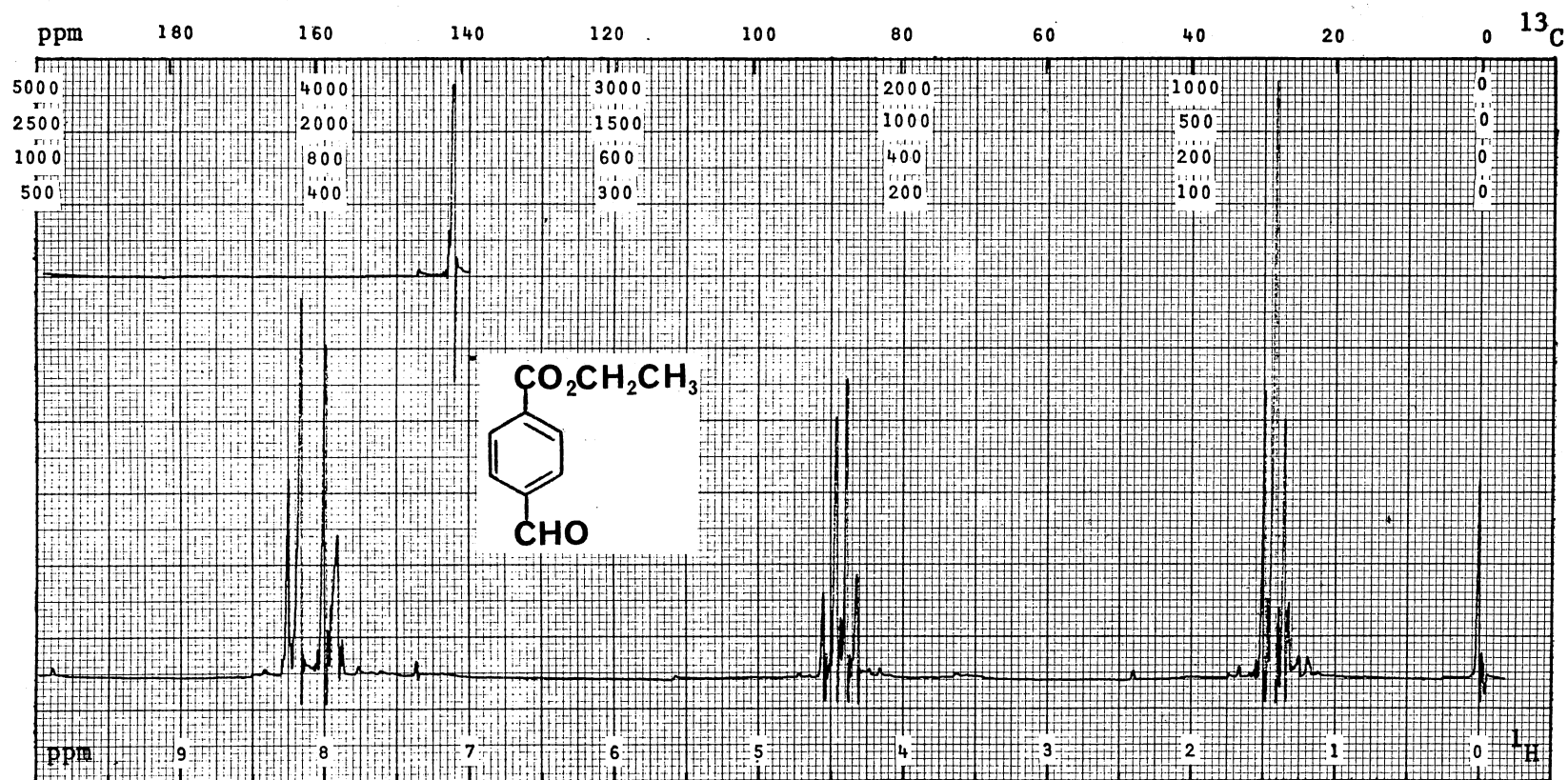
IR Spectrum of 22b

PLATE XXXVIII



IR Spectrum of 22c

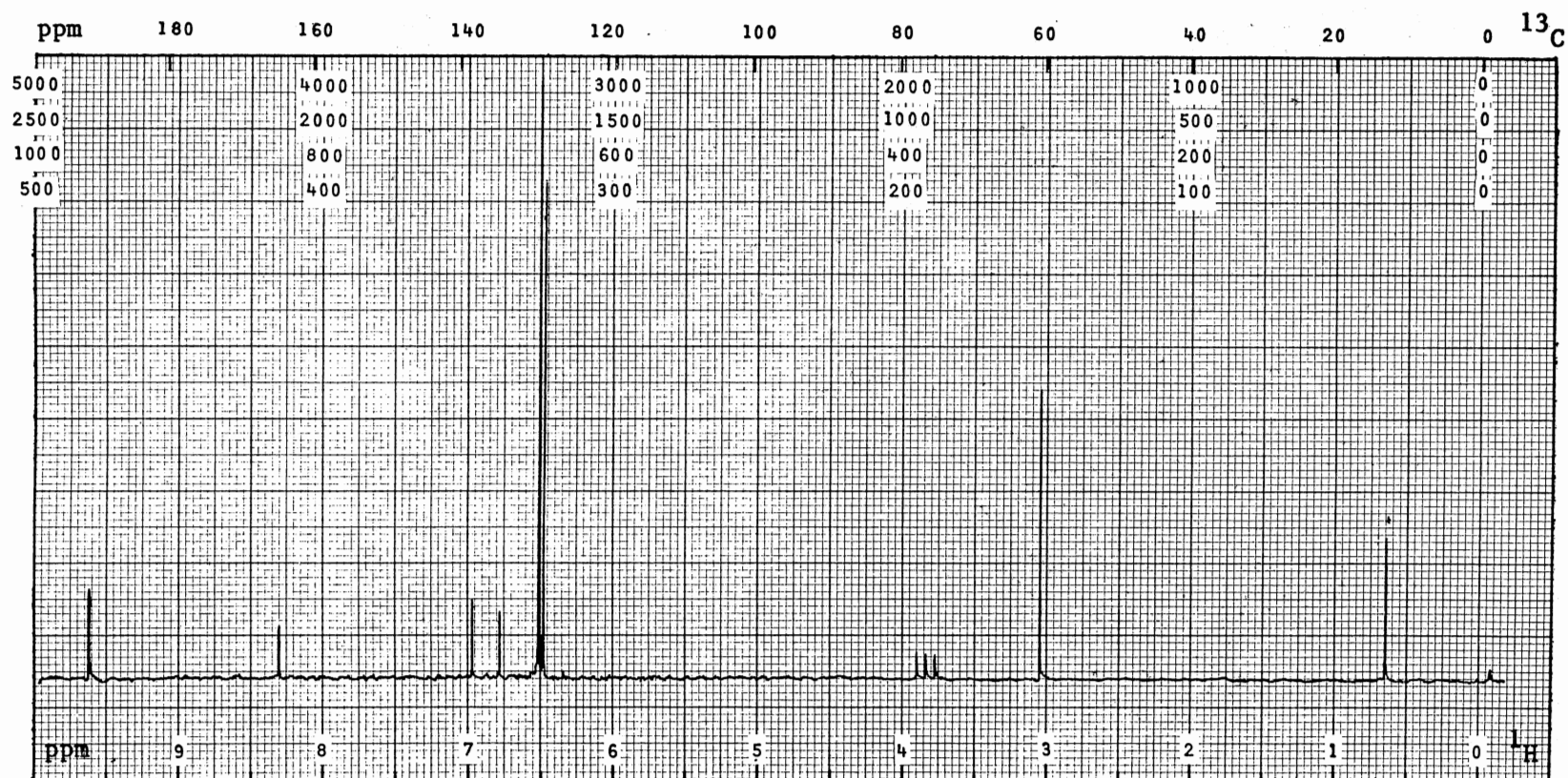
PLATE XXXIX



^1H NMR Spectrum of 33

PFT _ CW X ; Solvent . . CDCl_3 ; SO . . 85771 Hz; PW . 1000 Hz; T . . 30 °C; Acq/SA . .
 Size . . K; P2/RF . . 55 $\mu\text{s}/\text{dB}$; SF . . 100.1 Hz; FB . . 2 Hz; Lock . . ^2H ; D5/ST . . 250 s
 DC . . ; Gated Off . . ; Offset . . Hz; RF . . W/dB; NBW . . Hz

PLATE XXXX



^{13}C NMR Spectrum of 33

PFT X CW _ ; Solvent. . CDCl_3 ; SO. . 35101 Hz; PW. . 5000 Hz; T. . 30°C; Acq/SA. . 600
 Size. . 8 K; P2/RF. . 10 $\mu\text{s}/\text{dB}$; SF. . 25.2 Hz; FB. . Hz; Lock. . ^2H ; D5/ST. . 5 s
 DC. . ^1H ; Gated Off. . ; Offset. . 45101 Hz; RF. . 9 W/dB; NBW. . Hz

BIBLIOGRAPHY

1. Arens, J. F.; van Dorp, D. A. Nature (London), 1946, 157, 190-191.
2. Berkow, R., Ed., "The Merck Manual", 13th ed., Merck and Co., Rahway, N.J., 1977, pp. 1151-1153.
3. Bollag, W. Experientia, 1971, 27, 90-92.
4. Bollag, W. Eur. J. Cancer, 1974, 10, 731-737.
5. Brownbridge, P.; Warren, S. J. Chem. Soc. Perkins Trans. I, 1977, 2272-2285.
6. Butsugan, Y.; Tsukamoto, H.; Morito, N.; Bito, T. Chem Lett., 1976, 523-524.
7. Chopra, D. P.; Wilkoff, L. J. Proc. Am. Assoc. Cancer Res., 1975, 16, 35.
8. Colonge, J.; Le Sech, E.; Marey, R. Bull. Soc. Chim. France, 1957, 776-779.
9. Delisle, A. Annalen, 1890, 260, 250.
10. Euler, B. V.; Euler, H. V.; Karrer, P. Helv. Chim. Acta, 1929, 12, 278-285. Chem. Abstr., 1929, 23, 3254.
11. Euler, H. V.; Karrer, P. Helv. Chim. Acta, 1931, 14, 1040-1044.
12. Fleming, I.; Paterson, I.; Pearce, A. J. Chem. Soc. Perkins Trans. I, 1981, 256-262.
13. Fujimaki, Y. J. Cancer Res., 1926, 10, 469-477.
14. Gander, R. J. Brit. UK Patent Appl. 2,026,493; February 6, 1980. Chem. Abstr., 1981, 94, 30960w.
15. Gatti, J. C.; Cardama, J. E.; Gabrielli, M.; Cabrera, H. in "Retinoids: Advances in Basic Research and Therapy", Orfanos, C. E., et al. (Ed.); Springer-Verlag, New York, 1981, pp. 185-192.
16. Gray, G. A. Varian Instrument Applications, 1982, 16, 11-12.

17. Hanze, A. R.; Conger, T. W.; Wise, E. C.; Weisblat, D. I. J. Am. Chem. Soc., 1948, 70, 1253-1256.
18. Hauptmann, S.; Brandes, F.; Brauer, E.; Gabler, W. J. Prakt. Chem., 1964, 25, 56-58. Chem. Abstr., 1964, 61, 13225b.
19. Isler, O.; Ronco, R.; Guex, W.; Hindley, N. C.; Huber, W.; Dialer, K.; Kofler, M. Helv. Chim. Acta, 1949, 32, 489-505.
20. Isler, O. in "Carotenoids", Isler, O., Ed., Birkhauser Verlag, Basel, 1971, pp. 11-27.
21. Iwai, K.; Kosugi, H.; Miyazaki, A.; Uda, H. Syn. Commun. 1976, 6, 357-363.
22. Jablonska, S.; Wolska, H.; Dabrowski, J.; Haftek, M.; Groniowska, M.; Jarzabek-Chorzelska, M. in "Retinoids" Advances in Basic Research and Therapy", Orfanos, C. E., et al. (Ed.); Springer-Verlag, New York, 1981, pp. 165-173.
23. Jones, D. H.; Cunliffe, W. J.; Cove, J. H. in "Retinoids: Advances in Basic Research and Therapy", Orfanos, C. E., et al. (Ed.); Springer-Verlag, New York, 1981, pp. 255-258.
24. Karrer, P.; Helfenstein, A.; Wehrli, H.; Wettstein, A. Helv. Chim. Acta, 1930, 13, 1084-1099.
25. Karrer, P.; Morf, R.; Schopp, K. Helv. Chim. Acta, 1931, 14, 1036-1040, 1431-1436. Chem. Abstr., 1932, 26, 4359.
26. Kligman, A. M. U.S. Patent 3,729,568; April 24, 1973.
27. Lasnitzki, I. Brit. J. Cancer, 1955, 9, 434-441.
28. Lee, K. H. U.S. Patents 3,882,244; May 6, 1975; 3,966,967; June 29, 1976.
29. Lee, K. H. U.S. Patents 3,934,028; January 20, 1976; 4,021,573; May 3, 1977.
30. Loeliger, P.; Bollag, W.; Mayer, H. Eur. J. Med. Chem.-Chim. Ther., 1980, 15, 9-15.
31. Lovey, A. J.; Pawson, B. A. J. Med. Chem., 1982, 25, 71-75.
32. Montanari, F.; Daniel, R.; Hogeveen, H.; Maccagnani, G. Tetrahedron Lett., 1964, 2685-2689.
33. Moore, T. Biochem. J., 1930, 24, 692-702.
34. Moore, T. "Vitamin A", Elsevier Publishing Co., New York, 1957.
35. Morris, G. A.; Freeman, R. J. Am. Chem. Soc., 1979, 101, 760.

36. Morton, R. A. Nature (London), 1944, 153, 69-71.
37. Morton, R. A.; Goodwin, T. W. Nature (London), 1944, 153, 405-406.
38. Newton, D. L.; Henderson, W. R.; Sporn, M. B. Cancer Res., 1980, 40, 3413-3425.
39. Orfanos, C. E.; Brawn-Falco, O.; Farber, E. M.; Grupper, C.; Polano, M. K.; Schuppli, R. "Retinoids: Advances in Basic Research and Therapy", Springer-Verlag, New York, 1981.
40. Pawson, B. A.; Ehmann, C. W.; Itri, L. M.; Sherman, M. I. J. Med. Chem., 1982, 25, 1269-1277.
41. Peck, S. M.; Chargin, L.; Sobotka, H. Arch. Dermatol. Syphilol., 1941, 43, 223-229. Chem. Abstr., 1941, 35, 2934.
42. Plewig, G.; Wagner, A.; Nikolowski, J.; Landthaler, M. in "Retinoids: Advances in Basic Research and Therapy", Orfanos, C. E., et al. (ed.); Springer-Verlag, New York, 1981, pp. 219-235.
43. Porter, A. D.; Godding, E. W. Brit. J. Dermatol., 1945, 57, 197-200. Chem. Abstr., 1947, 41, 2466.
44. Saffioti, U.; Montesano, R.; Sallakumar, A. R.; Borg, S. A. Cancer, 1967, 20, 857-864.
45. Sadano, C. S. "Vitamins: Synthesis, Production and Use", Noyes Data Corp., Park Ridge, N. J.; 1978, pp. 2-33.
46. Sporn, M. B.; Dunlop, N. M.; Newton, D. L.; Henderson, W. R. Nature, 1976, 263, 110-113.
47. Sporn, M. B.; Dunlop, N. M.; Newton, D. L.; Smith, J. M. Federation Proc., 1976, 35, 1332-1338.
48. Stepp, W. Biochem. Z., 1909, 22, 452-460. Chem. Abstr., 1910, 485.
49. Stepp, W. Z. Biol., 1911, 57, 135-171. Chem. Abstr., 1912, 6, 103.
50. Van Scott, E. J.; Yu, R. J. U.S. Patent 3,932,665; January 13, 1976.
51. Wald, G. J. Gen. Physiol., 1935, 18, 905-915.
52. Wald, G. J. Gen. Physiol., 1935, 19, 351-371.
53. Welch, S. C.; Gruber, J. M. J. Med. Chem., 1979, 22, 1532-1534.

54. Welch, S. C.; Gruber, J. M.; Rao, A. S. C. P. J. Med. Chem., 1982, 25, 81-84.
55. Wolbach, S. B.; Howe, P. R. J. Exp. Med., 1925, 42, 753-778.
56. Wolbach, S. B.; Maddock, C. L. Proc. Soc. Exp. Biol. Med., 1951, 77, 825-829.
57. Yu, R. J.; Van Scott, E. J. U.S. Patent 3,932,665; January 13, 1976.

VITA

Kristy Marie Waugh

Candidate for the Degree of

Doctor of Philosophy

Thesis: Part I. SYNTHESSES AND NMR ANALYSES OF SELECTED
 ω -(2-ANTHRYL)SUBSTITUTED FATTY ESTERS.

Part II. SYNTHESSES AND CHARACTERIZATIONS OF SELECTED
HETEROAROTINOIDS

Major Field: Chemistry

Biographical:

Personal Data: Born in Lawton, Oklahoma on June 28, 1956, the
daughter of Mr. and Mrs. Bud Waugh.

Education: Graduated from Eisenhower High School, Lawton, Okla-
homa, in May, 1974; received Bachelor of Science degree in
Chemistry from Cameron University, Lawton, Oklahoma in May,
1978; completed requirements for the Doctor of Philosophy
degree at Oklahoma State University in July, 1983.

Professional Experience: Undergraduate research assistant,
Oklahoma State University, summer of 1977; Chemist, Halli-
burton Services, October, 1978 to August, 1979; graduate
teaching assistant, Oklahoma State University, 1979-1983.